THE POTENTIAL OF MODULATING Na^+ K^+ ATPASE PUMPS AND K_{ATP} CHANNELS IN THE DEVELOPMENT OF A NEW THERAPY TO TREAT HYPERKALEMIC PERIODIC PARALYSIS

By

Tarek Ammar

A thesis submitted to the Faculty of Graduate and Postdoctoral Studies in partial fulfillment for the requirements of Ph.D. degree in Cellular and Molecular Medicine.

Department of Cellular and Molecular Medicine
Faculty of Medicine
University of Ottawa

ABSTRACT

Hyperkalemic periodic paralysis (HyperKPP) is characterized by myotonic discharges and weakness/paralysis. It is a channelopathy that is caused by mutation in the SCN4A gene that encodes for the skeletal muscle Na^+ channel isoform (Nav1.4) α-subunit. Limb muscles are severely affected while breathing musculature is rarely affected even though diaphragm expresses the Nav1.4 channel. The objective of this study was to investigate the mechanism(s) that render the HyperKPP diaphragm asymptomatic in order to find a novel long lasting therapeutic approach, to treat HyperKPP symptoms. A HyperKPP mouse model carrying the M1592V mutation was used because it has a similar phenotype to that of patients carrying the same mutation. HyperKPP diaphragm, the limb muscles soleus and EDL all had a higher tetrodotoxin (TTX) sensitive Na^+ influx than wild type (WT), but only the soleus and EDL had a depolarized resting potential, lower force and greater K^+-induced force loss when compared to WT. The lack of a membrane depolarization in HyperKPP diaphragm was because of greater electrogenic contribution of the Na^+ K^+ ATPase pump compared to WT while such increase was not observed in EDL and soleus. HyperKPP diaphragm also had greater action potential amplitude than EDL and soleus possibly because of higher Na^+ K^+ ATPase pump maintaining a low $[Na^+]_i$. An inhibition of PKA, but not of PKC, increased the sensitivity of the HyperKPP diaphragm to the K^+-induced force depression. So, HyperKPP soleus was exposed to forskolin to increase cAMP levels in order to activate PKA to document whether greater activity of PKA will alleviate HyperKPP symptoms. At 4.7 mM K^+, forskolin increased force production, but worsened the decrease in force at 8 and 11 mM K^+. Forskolin also did not improve membrane excitability. Pinacidil a K_{ATP} channel opener, improved force production at all $[K^+]_e$ by causing a hyperpolarization of resting EM which then allowed for greater action potential amplitude and more excitable fibers. It is concluded that the development

of a better therapeutic approach to treat HyperKPP can include a mechanism which activates Na^+ K^+ ATPase pumps and K_{ATP} channels.

TABLE OF CONTENTS

LIST OF FIGURES

LIST OF TABLES

LIST OF ABBREVIATIONS

$[Ca^{2+}]_e$	Extracellular Ca^{2+}concentration
$[Ca^{2+}]_i$	Intracellular Ca^{2+} concentration
$[cAMP]_e$	Extracellular cAMP concentration
$[cAMP]_i$	Intracellular cAMP concentration
$[Cl^-]$	Cl^- concentration
$[Cl^-]_e$	Extracellular Cl^- concentration
$[K^+]_e$	Extracellular K^+ concentration
$[K^+]_i$	Intracellular K^+ concentrations
$[Na^+]$	Na^+ concentration
$[Na^+]_e$	Extracellular Na^+ concentration
$[Na^+]_i$	Intracellular Na^+ concentration
AP	Action potentials
cAMP	Cyclic adenosine monophosphate
Cav1.1 channel	Voltage gated L-type Ca^{2+} channel
EDL	Extensor digitorum longus
E_{ion}	Equilibrium potential for an ion
E_{Cl}	Equilibrium potential for Cl^-
E_K	Equilibrium potential for K^+
E_{Na}	Equilibrium potential for Na^+
EM	Membrane potential
EMG	Electromyography
FDB	Flexor digitorum brevis

G_{Cl}	Cl^- conductance
G_K	K^+ conductance
G_m	Membrane conductance
G_{Na}	Na^+ conductance
I_{gp}	Gating pore current
HyperKPP	Hyperkalemic periodic paralysis
HypoPP	Hypokalemic periodic paralysis
I_{Kir}	Inward rectifier current
I_{Kv}	Voltage sensitive K^+ channel current
K_{ATP} channel	ATP sensitive K^+ channel
Kir channel	K^+ inward rectifier channel
K_V channel	Voltage sensitive K^+ channel
MC	Myotonia congenita
MRP	Multidrug resistance protein
Nav channel	Voltage sensitive Na^+ channel
NCX	Na^+ Ca^{2+} exchanger
NKA pump	Na^+ K^+ ATPase pump
PAM	Potassium aggravated myotonia
PKA	Protein kinase A
PKC	Protein kinase C
PLM	Phospholemman
PMC	Paramyotonia congenita
SCM	Sodium channel myotonia

SOCE	Store operated Ca^{2+} entry
SUR2	Sulfonylurea receptor 2
TPP	Thyrotoxic hypokalemic periodic paralysis
t-tubules	Transverse tubules
TTX	Tetrodotoxin
WT	Wild type

ACKNOWLEDGMENTS

I would like to express my sincere gratitude to my supervisor Prof. Jean Marc Renaud for his continuous support, guidance, patience and motivation during my PhD study. His mentorship and valuable comments were crucial in helping me complete my degree.

I would like to thank my thesis advisory committee members: Prof. Anthony Krantis, Dr. Pierre Fortier and Dr. Michael Jonz for their insightful comments and encouragement.

Many thanks go to Dr. Wei Lin for his continuous technical help and troubleshooting. I would also like to thank all my current and previous lab mates especially Hind, Erik, Amanda, Kyle and Shiemaa for their help and encouragement.

Finally, I would like to thank my late father Prof. Elsayed Ammar and my mother Prof. Ahdab Elmorshedy for their love, endless support and encouragement throughout my life. I also thank my brothers Mohammed, Moataz and Amr for their continuous help and motivation.

GENERAL INTRODUCTION

Muscle contraction is initiated by action potentials (APs) that start at the neuromuscular junction where motor neurons innervate fibers. An AP is generated by Na^+ influx through voltage sensitive Na^+ (Nav) channels, allowing for a depolarization of resting membrane potential (resting EM) from -80 mV to +30 mV followed by opening of voltage sensitive K^+ (K_V) channels to allow for K^+ efflux and repolarization back to -80 mV. AP then propagates along the sarcolemma and transverse tubules (t-tubules), the latter being deep invagination of the cell membrane associated with the sarcoplasmic reticulum (MacIntosh *et al.*, 2012). As the APs propagate down t-tubules, voltage gated L-type Ca^{2+} channels (also called Cav1.1 or dihydropyridine receptor) detect the depolarization causing them to undergo a conformational change. This change allows for the activation of Ca^{2+} release channels (also known as ryanodine receptors) in the sarcoplasmic reticulum. Once released, Ca^{2+} diffuses into the sarcomere, which is the muscle contractile unit. Sarcomeres are composed of two filaments; i) the thick filament, which contains myosin and ii) and the thin filament which contains actin, troponin and tropomyosin. At rest, tropomyosin blocks the myosin binding sites on actin. When myoplasmic $[Ca^{2+}]$ ($[Ca^{2+}]_i$) increases, Ca^{2+} binds to troponin causing a conformational change that removes tropomyosin from the myosin binding sites on actin. The binding of myosin to actin then allows for force generation and sarcomere shortening (MacIntosh *et al.*, 2012).

Normal muscle function depends in part on the proper action potential generation and maintenance of membrane excitability. This maintenance first depends on the regulation of resting EM that is modulated by ClC-1 Cl^- channels (Pedersen *et al.*, 2009*a*, 2009*b*), K^+ inward rectifier channels (Kir2.1) and ATP sensitive K^+ channels (K_{ATP}) (Leech & Stanfield, 1981; Lindinger *et al.*, 2001; Nielsen *et al.*, 2003; Hibino *et al.*, 2010). It also depends on the regulation of Nav and

Kv channels that generate APs. Mutation in genes encoding for ion channels can result in either loss of membrane excitability giving rise to paralysis or increased membrane excitability resulting in myotonia. This group of diseases are called channelopathies.

Hyperkalemic periodic paralysis (HyperKPP) is one of these diseases in which patients suffer from both myotonia and paralysis (Miller *et al.*, 2004; Cannon, 2006). It is an autosomal dominant disease caused by mutations in the SCNA4 gene that encodes for the skeletal muscle Nav1.4 Na^+ channel (Cannon, 2006). HyperKPP patients experience myotonic discharge before and between paralytic attacks (Bradley *et al.*, 1990; Miller *et al.*, 2004). The disease mainly affects limb muscles with more than 80% of the patients complaining of stiffness and weakness in limbs during and between paralytic attacks. Durations of attacks vary between patients and they can last from hours to days or even months (Bradley *et al.*, 1990; Miller *et al.*, 2004). As the patients grow older the attacks frequency decrease but they develop progressive myopathy and some patients become bedridden (Bradley *et al.*, 1990). Available treatments to prevent attack frequency or severity are not fully effective; and often lose effectiveness over time and do not address the later development of fixed myopathy (Clausen *et al.*, 1980; Miller *et al.*, 2004).

Notably, only 26% of patients report affected breathing musculature (Charles *et al.*, 2013), consequently, patients do not suffer of respiratory distress. This is an interesting fact because human diaphragm expresses the skeletal Nav1.4 isoform as do hindlimb muscles (Zhou & Hoffman, 1994), the most affected muscles by the disease (Hayward *et al.*, 2008; Clausen *et al.*, 2011; Khogali *et al.*, 2015). So, the overall objective of this PhD study is to understand the mechanism that spares HyperKPP diaphragm from the disease symptoms and to establish whether activation of some of these mechanisms in hindlimb muscles can offer a new therapeutic approach to treat HyperKPP patients.

REGULATION OF MEMBRANE EXCITABILITY

As mentioned above, normal function of skeletal muscles depends on the proper functioning of the cell membrane excitability, i.e. its capacity to generate AP. Such regulation does not involve just the regulation of the Nav and Kv channel activity but also involves regulation of resting EM because changes in resting EM affects the activation of Nav channel and thus membrane excitability. So, in this section, the objective is to review how resting EM is generated and regulated by various ion channels in healthy skeletal muscle fiber.

IMPACT OF ION GRADIENTS AND PERMEABILITY ON MEMBRANE POTENTIALS

EM is a function of ion gradients, ion channel and transporter activities. Na^+ concentration ($[Na^+]$) and Cl^- concentration ($[Cl^-]$) are higher on the extracellular side while the opposite is observed for K^+. The concentration gradient for Na^+ and K^+ is maintained by Na^+ K^+ ATPase pump (NKA pump) which constantly pumps Na^+ out and K^+ in (as further discussed in the section entitled 'Na^+ K^+ ATPase pump'). The concentration gradient for Cl^- is in part maintained because cell membrane potential is more negative inside forcing Cl^- out of the fiber. As a result of these concentration gradients, ions flow down their concentration gradients. However, there is an electrical gradient too, as the membrane potential is more negative at rest on the inside it attracts Na^+ and K^+ ions, while Cl^- ions will move to the more positive extracellular side of the fiber. The final net ion fluxes are then a function of the difference in concentration and electrical gradient.

The equilibrium potential of an ion (E_{ion}) is the potential at which both electrical and chemical gradients are balanced resulting in no net movement of the ion across the cell membrane. The equilibrium potential for K^+ (E_K) is -95 mV and for Na^+ (E_{Na}) is +60 mV. For Na^+ the concentration gradient as well as the electrical gradient favours an influx. As Na^+ enters the myoplasm it depolarizes resting EM bringing it toward E_{Na}. K^+ also tries to reach its equilibrium

potential, so the opposite is observed for K^+, because for EM to move toward E_{K^+}, K^+ ions must diffuse out of the fiber to hyperpolarize resting EM. In mammalian hindlimb muscle, E_{Cl} is -66 mV at 37 °C (Dulhunty, 1978), and as a consequence there is a constant Cl^- efflux that depolarizes resting EM. The net balance between these ion fluxes sets the resting EM at values ranging from -70 to -85 mV in mammalian skeletal muscles (Light *et al.*, 1994; Yensen *et al.*, 2002; Cairns *et al.*, 2003; Pedersen *et al.*, 2005; Clausen *et al.*, 2011).

A single action potential does not cause a substantial change in intracellular Na^+ concentration ($[Na^+]_i$), and extracellular Na^+ concentration ($[Na^+]_e$) or intracellular K^+ concentrations ($[K^+]_i$) and extracellular K^+ concentrations ($[K^+]_e$). However, during prolonged muscle activity a large number of AP are generated leading to large Na^+ and K^+ fluxes. For example, during exercise, interstitial $[K^+]$ increases from 4 to 10-11 mM (Nielsen *et al.*, 2004; Mohr *et al.*, 2004), while $[K^+]_i$ decreases from 168-182 mM to 130-136 mM (Sjøgaard *et al.*, 1985; Juel, 1986). Such changes in K^+ gradient makes E_K less negative resulting in a depolarization of resting EM by up to 20 mV (Cairns *et al.*, 1995, 1997; Yensen *et al.*, 2002). Also during exercise, interstitial $[Na^+]$ slightly decreases from 140 to 130 mM (Street *et al.*, 2005), while intracellular $[Na^+]$ $[Na^+]_i$ increases from 10-13 to 23-24 mM (Sjøgaard *et al.*, 1985; Juel, 1986). The resulting decrease in $[Na^+]$ gradient reduces AP overshoot from +30 to +10 mV (Cairns *et al.*, 2003).

The extent to which an ion modulates resting EM also depends on membrane permeability which in turn depends on the activity of its own channels because it is the major mechanism by which an ion creates a current through cell membrane, large enough to generate significant potential. At rest, Cl^- and K^+ are the two most important ions in the regulation of resting EM. Cl^- conductance (G_{Cl}) through ClC-1 channels represents 80-90 % of total membrane conductance (G_m) (Pedersen *et al.*, 2009*a*, 2009*b*). The remaining G_m is K^+ conductance (G_K), which involves

two K^+ channels: the K_{ATP} and Kir2.1 channel (Leech & Stanfield, 1981; Lindinger *et al.*, 2001; Nielsen *et al.*, 2003). So, this is why changes in $[K^+]_e$ occurring during muscle activity described above has a significant impact on resting EM depolarizing it by up to 20 mV. On the other hand, Nav1.4 Na^+ channels are closed at rest so they have a very little effect on resting EM, while they have an impact when Nav1.4 channels open lowering AP amplitude. However, when they open during an AP they allow for large Na^+ current that underlies the upstroke of AP.

To best understand how membrane excitability is regulated the electrophysiological properties and function of Na^+, K^+ and Cl^- channels will now be reviewed.

ION CHANNELS REGULATING AP

There are two channels that are important in generating AP. The first is the Nav channel, which is responsible for the depolarization phase bringing EM from resting EM to +30 mV. The second channel, is Kv channel, which returns EM back to resting EM.

Nav1.4 channel

Nav channels constitute a family of voltage-gated channels that plays a critical role in action potential initiation and propagation in excitable tissues. For Nav channels, ten genes expressing different isoforms have been identified (Goldin *et al.*, 2000; Goldin, 2001). Nav1.1-1.3 and Nav1.6 are expressed in the neurons of the central nervous system while Nav1.7-1.9 are expressed in the peripheral nervous system. Nav1.5 is expressed in the heart and in neonatal skeletal muscle while Nav1.4 is expressed in skeletal muscles.

At rest, the opening probability of voltage gated Na^+ channels is extremely low and very few channels are open. When resting EM depolarizes, the channels open allowing for a transient inward Na^+ current (Fig. 1.1A). It is important to note that the Na^+ current rapidly returns to zero

before EM is returned to the pre-test potential because Nav channels inactivate; i.e. the channel has two gating components: activation and inactivation which will now be discussed.

Activation gate

Plotting Na^+ current (I) versus EM (V) shows that Nav1.4 channels start to activate at -60 mV (Fig. 1.1B) which is in agreement with the fact that AP is triggered when resting EM reaches a threshold of -55 mV (Sheets & Hanck, 1999). As EM depolarizes beyond -20 mV Nav current starts to decrease because as E_M approaches E_{Na} the Na^+ current returns to zero. Plotting normalized Nav channel conductance versus EM shows $V_{1/2}$ of -40 mV and Vmax -20 mV (Fig. 1.1C). The activation time constant of the channels is also voltage sensitive ranging from 0.2 ms at -80 mV to 0.14 ms at a depolarization at +30 mV (Hodgkin & Huxley, 1952). As the Na^+ channel activation gate remains open at a depolarized EM, another gate must close the channel to allow for repolarization, this gate is known as the fast inactivation gate.

Fast inactivation

Nav channels inactivate rapidly within 1-2 ms after a depolarization (Hodgkin & Huxley, 1952b), and this is observed by the rapid decrease in Na^+ current while EM is still depolarized (Fig. 1.1A). This process is required for repetitive firing of AP and control of muscle excitability (Catterall, 2014). It also creates a refractory period allowing for a unidirectional propagation of the action potential thus preventing it from backward propagation. Steady state fast inactivation starts at -85 mV and reaches complete inactivation at -50 mV with $V_{1/2}$ of -76 mV (Fig. 1.2) (Chahine *et al.*, 1996). The time constant for fast inactivation ranges from 8 ms at -80 mV to 0.3 ms at +30 mV while recovery from fast inactivation time constant is 3.5 ms at -20 mV (Chahine *et al.*, 1996; Featherstone *et al.*, 1996). It is noted that fast inactivation time constant is

FIGURE 1.1

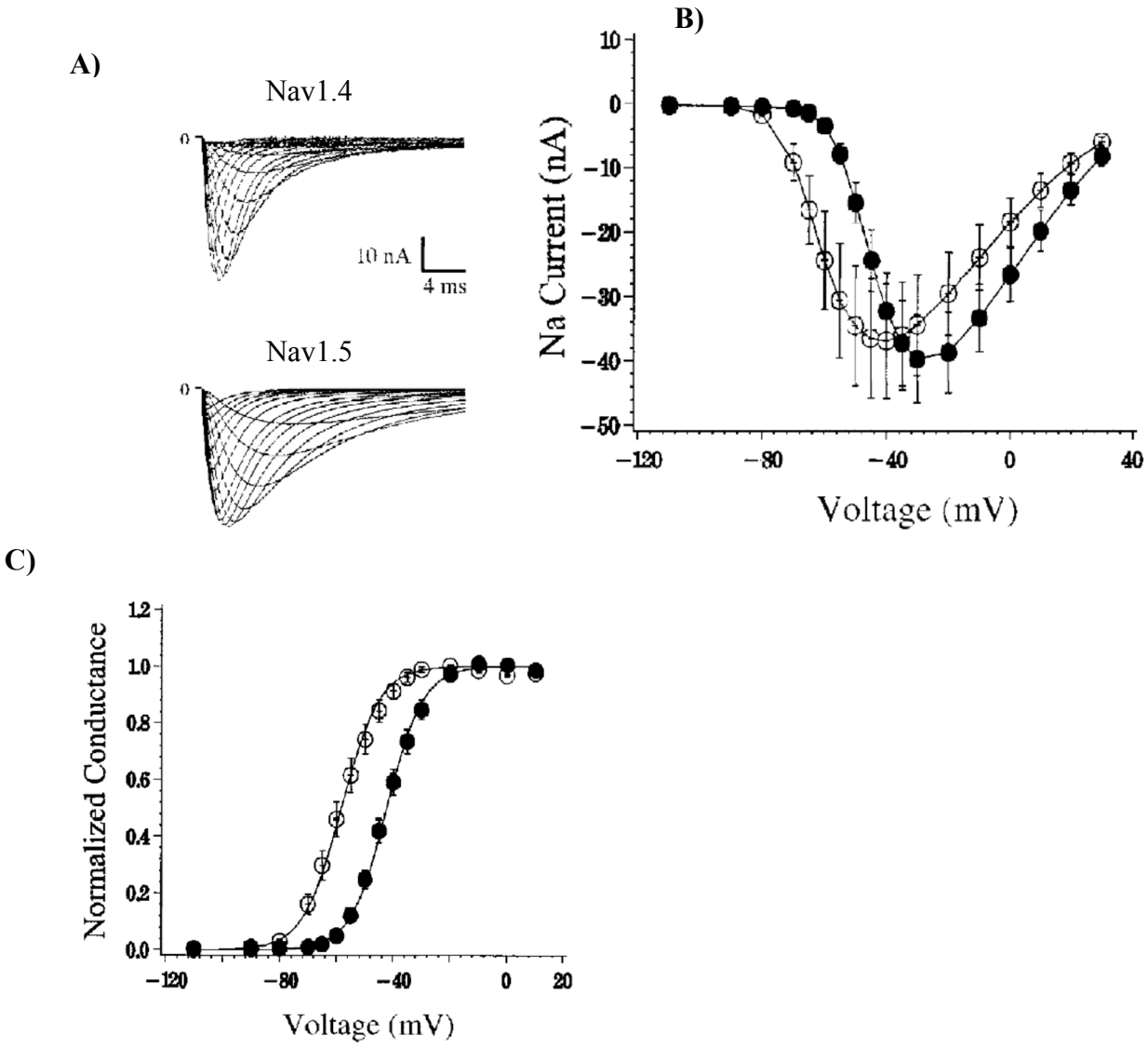

Figure 1.1 Current voltage (I-V) curve for Nav1.4 the (adult isoform) and the Nav1.5 (neonatal and cardiac isoform) expressed in HEK 293 cells. A) A family of currents recorded from HEK 293 cells expressing Nav1.4 and Nav1.5 channels in response to series of voltage steps depolarizations between −70 and +30 mV from a holding potential of -150 mV. B) I-V relationship for Nav1.4 and Nav1.5 C) Normalized conductance voltage relationships for the same cells as in B with the values for each cell normalized to the maximum conductance value of each cell. Symbols: ●, Nav1.4; ○, Nav1.5 (from Sheets & Hanck, 1999).

FIGURE 1.2

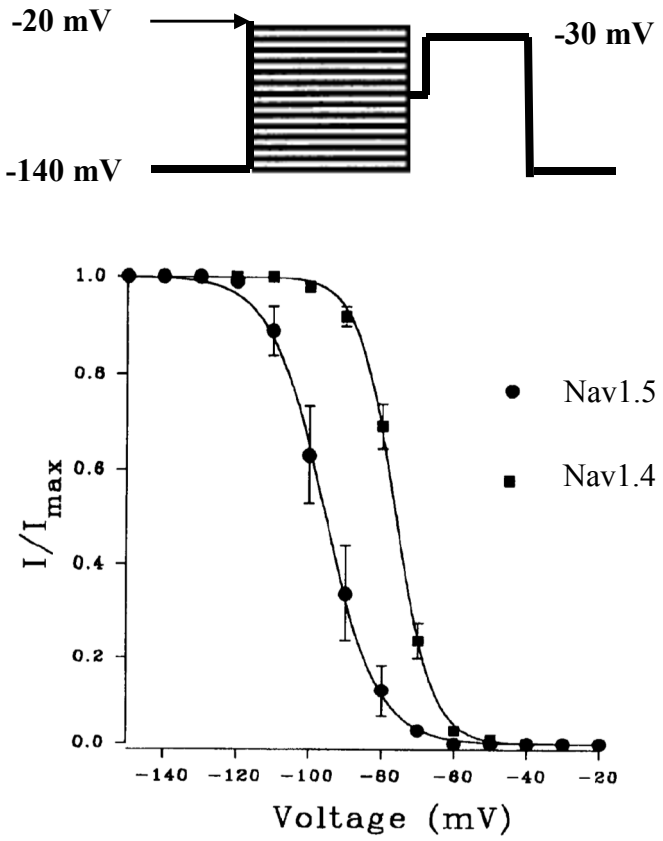

Figure 1.2. Voltage dependence for steady state fast inactivation for Nav1.4 and Nav1.5 expressed in HEK293 cells. Steady state inactivation was studied by a two-pulse protocol with 500 ms depolarizing pre-pulses from a holding potential of -140 mV stepped from -140 to -20 mV in 10 mV increments, during which Nav channels became fast inactivated, followed by a -30 mV test pulse. The current amplitude during the test pulse was normalized to the one obtained at -140 mV conditioning pulse and plotted against the voltage. Symbols: ■, Nav1.4; ●, Nav1.5 (from Chahine et al., 1996).

longer than the time constant for activation. The importance of that is to allow for Nav channel to open long enough to allow for Na^+ influx and depolarization of resting EM before it inactivates.

Slow inactivation

There is a second type of inactivation called slow inactivation. While fast inactivation occurs over ms, slow inactivation occurs over a range of hundred millisecond to minutes (Adelman & Palti, 1969; Rudy, 1978; Simoncini & Stühmer, 1987). It has been proposed that the function of slow inactivation is to modulate the number of available Nav channels on the sarcolemma limiting their ability to generate repetitive action potentials for extended periods. Steady state slow inactivation starts at -80 mV and reach maximal inactivation at -20 mV with a $V_{1/2}$ of -62 mV (Hayward *et al.*, 1997). The time constant for slow inactivation ranges from 24 sec at -80 mV to 1 sec at +30 mV (Featherstone *et al.*, 1996). Recovery time constant from slow inactivation is 0.54 sec at -10 mV which is much longer than that for fast inactivation (Hayward *et al.*, 1997).

Kv channel

Kv channels constitute a superfamily of voltage sensitive K^+ channels. In skeletal muscles, Kv channels are equally distributed between the t-tubules and sarcolemma with 70 % of Kv current (IKv) arising from the t-tubules (DiFranco *et al.*, 2012). Like Nav channels, Kv channels are typically closed at resting EM but open upon membrane depolarization. Opening of Kv channels results in K^+ efflux upon membrane depolarization. The K^+ efflux helps repolarize the membrane during the action potential (Wulff *et al.*, 2009).

A small IKv current is observed at +10 mV reaching a peak at 7 ms while a large current is observed at 110 mV reaching a peak at 4 ms (Fig. 1.3A). On an average basis, the steady state activation curve demonstrate that IKv channels become activated at -20 mV, increasing with further membrane depolarization (Fig. 1.3B). DiFranco et al. noticed that the I-V relationship was

FIGURE 1.3

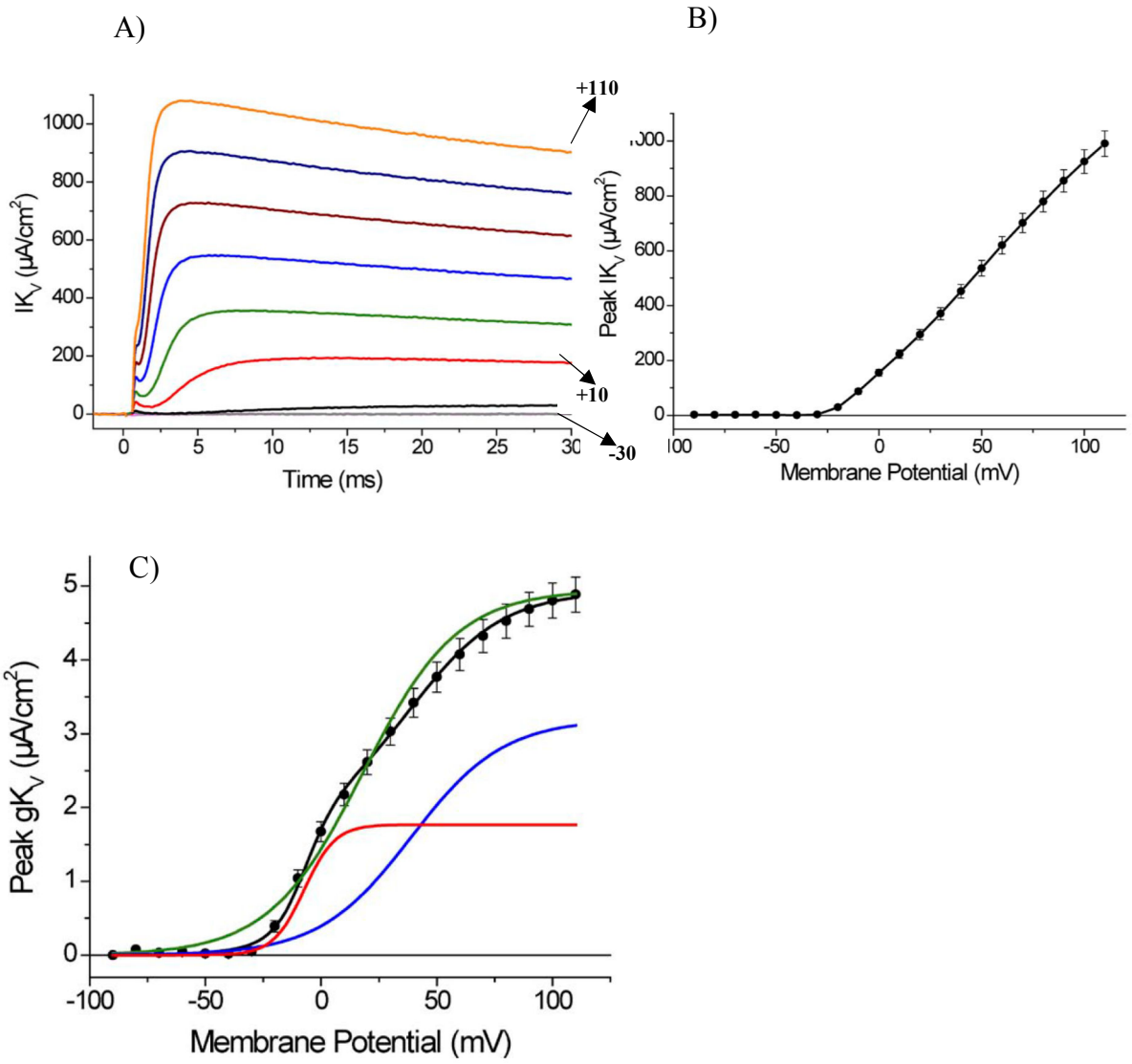

Figure 1.3. Delayed rectifier K^+ currents in FDB fibers. (A) IKv recorded in response to depolarizations from a holding potential of -90 mV to membrane potential as indicated. (B) Steady sate I-V relationship of Kv channels between -90 and 110 mV in 10 mV steps. (C) Voltage dependence of the mean peak gKV (circles), calculated from the data in B. The green trace is a single Boltzmann fit to the data. The black trace is a double Boltzmann fit to the data. The red and blue traces are the independent components of the double Boltzmann function representing the low and high threshold channels respectively (from DiFranco et al., 2012).

not linear as a small shoulder could be observed near 10-20 mV. This shoulder became more evident when peak conductance (G_{KV}) was calculated (Fig. 1.3C). The voltage dependence of (G_{KV} was better explained using a double Boltzmann equation indicating that the presence of two different Kv channels:. i) one Kv channel with a low threshold and steep voltage-dependence with a $V_{1/2}$ of -10 mV contributing about 31% of $G_{KV,}$ ii) a second Kv channel with a high threshold and a shallower dependence with a $V_{1/2}$ of 40 mV. (DiFranco *et al.*, 2012). Finally, the presence of two Kv channels was further confirmed using Western blotting analysis for the presence of Kv1.4 and Kv3.4 channels. The authors, however, did not link which electrophysiological characteristics belong to each of Kv1.4 and Kv3.4.

ION CHANNELS REGULATING RESTING EM

Regulation of resting EM is crucial for the proper generation of AP; i.e. maintenance of proper membrane excitability. This is because as discussed above a chronic depolarization of resting EM increases the extent of Nav channel inactivation resulting in lower AP amplitude, which then reduces Ca^{2+} release and capacity of muscles to contract. Three major ion channels are involved in regulation of resting EM: i) ClC-1 Cl^- channels, ii) Kir2.1 and iii) K_{ATP} channels. Furthermore two of them (ClC-1 Cl^- and K_{ATP} channels) can directly modulate AP kinetics by providing outward currents. The electrophysiological characteristics of the three channels and how they regulate resting EM and modulate AP kinetics will now be discussed.

ClC-1 Cl^- channel

ClC is a family of voltage gated Cl^- channels. The ClC-1 channel is the major Cl^- channel expressed in skeletal muscles (Steinmeyer *et al.*, 1991; Koch *et al.*, 1992). These channels are

responsible for stabilizing resting EM providing 80-90 % of total G_m at rest (Pedersen *et al.*, 2009*a*, 2009*b*, 2016). ClC-1 Cl^- channels are localized on the sarcolemmal membrane (Gurnett *et al.*, 1995; Lueck *et al.*, 2010) and in the t-tubular system (DiFranco *et al.*, 2011). One major function of Cl^- is to clamp resting EM (Lipicky *et al.*, 1971; Furman & Barchi, 1978; Pedersen *et al.*, 2016). This is evident by the fact that reduction of extracellular Cl^- ($[Cl^-]_e$) from 128 to 10 mM causes resting EM to depolarize at 9 mM $[K^+]_e$ by 5 mV (Cairns *et al.*, 2004). Similarly, replacing Cl^- at 60 mM $[K^+]_e$ with sulphate as the major external anion at 65 mM $[K^+]_e$ resulted in a greater depolarization by 10 mV (Dulhunty, 1978). During trains of AP, complete removal of $[Cl^-]_e$ results in a depolarizations by 15 mV compared to that at 127 mM $[Cl^-]_e$ (de Paoli *et al.*, 2013). Thus, Cl^- reduces the extent of depolarization when $[K^+]_e$ increases during exercise or during AP tarins.

ClC-1 channels are voltage dependent being activated when the membrane potential depolarizes from -85 mV, while hyperpolarization to more negative values deactivate ClC-1 channels (Fig. 1.4) (Fahlke & Rüdel, 1995). However, the activation kinetics are much slower compared to Nav and Kv, as ClC-1 channels have an activation time constant of 400 ms (Fahlke & Rüdel, 1995). Thus, there is no change in the number of opened channels during a 2 ms long AP. However, 20% of ClC-1 channels are open at rest. So, during an action potential, they allow for Cl^- influx that counteracts the Na^+ induced depolarization and contributes to the K^+ induced-repolarization phase (Heiny *et al.*, 1990).

ClC-1 channels play an important role in regulating muscle excitability during exercise. When EDL fibers were repeatedly stimulated with 3.5 sec trains of action potentials every 7 sec, G_{Cl} decreased by 70% within 40 sec and remained constant for about 200 sec; this period was defined as phase 1 and represents changes in G_{Cl} at the onset of exercise. As the stimulation

FIGURE 1.4

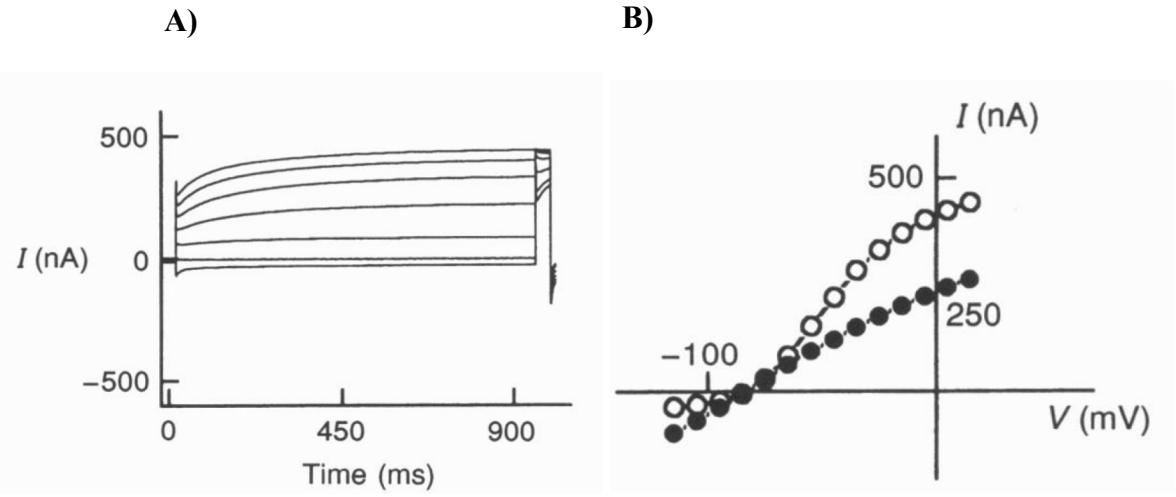

Figure 1.4. Voltage dependence of the muscle ClC-1 channels in rat psoas major single fibers. A) Current responses to test pulses from a holding potential of -85 mV to test potential ranging from -115 to +5 mV in 20 mV steps. Each test pulse was followed by a step lasting 40 ms to +5 mV. B) I-V relationship for the instantaneous current observed immediately after the step change potential (●) and late current (○) at the end of test voltage pulse (from Fahlke & Rüdel, 1995).

continued beyond 250 sec and the number of APs generated exceeded 1800, G_m suddenly increased above pre-stimulation levels as K_{ATP} and ClC-1 channels were activated concomitantly by 14- and 3- folds above pre-stimulation levels, respectively. This period during which G_m increased was defined as phase 2 (Pedersen *et al.*, 2009*b*). Notably, only phase 1 was observed when similar experiment were repeated with soleus, a more oxidative and fatigue resistant muscle (Pedersen *et al.*, 2009*a*).

The physiological significance of the reduction in G_{Cl} at the onset of exercise during phase 1 is to prevent loss of excitability caused by increases in $[K^+]_e$. At 4.7 mM K^+ the Cl^- conductance basically has a very small influence on action potential magnitude (Cairns *et al.*, 2004), because the Na^+ conductance (G_{Na}) largely exceeds G_{Cl}, However, When $[K^+]_e$ increases and resting EM depolarizes by about 20 mV as discussed above, Nav1.4 channels become inactivated reducing the number of available channels for AP depolarization (Ruff *et al.*, 1988). Consequently, AP amplitude decreases leading to less Ca^{2+} release and force development (Cairns *et al.*, 1997; Yensen *et al.*, 2002). A reduction in G_{Cl} have been shown to improve excitability and force generation at high $[K^+]_e$ (Pedersen *et al.*, 2005; de Paoli *et al.*, 2010, 2013). One mechanism involves a reduction in outward current allowing for an increase in AP amplitude. The reduced G_{Cl} also facilitates membrane depolarization to threshold allowing for an increase in number of excitable fibers (Pedersen *et al.*, 2005).

A second mechanism is an effect on resting EM. While a reduction in G_{Cl} increases the K^+ induced depolarization, it can also decrease the depolarization linked to the fact that E_{Cl} is less negative then EM (Dulhunty, 1978; Aickin *et al.*, 1989). The net result is hyperpolarization when skeletal muscles are at 37°C (Higgins and Renaud, unpublished results). Taking all these mechanisms, a partial decrease in $[Cl^-]_e$ to decrease G_{Cl} will increase excitability and force

generation while complete removal of Cl^- to completely abolish G_{Cl} worsen the K^+-induced reduction in membrane excitability and force generation (Cairns *et al.*, 2004; de Paoli *et al.*, 2013). Using 9-AC a ClC-1 channel inhibitor, it has been shown that 70% reduction in G_{Cl} was optimum in improving force generation at high $[K^+]_e$ (Higgins and Renaud, unpublished results).

The increase in G_{Cl} during phase 2 has been suggested to be an important trigger for muscle fatigue. It is now believed that fatigue is a protective mechanism which involves a transient and recoverable decline in muscle force with repeated or continuous muscle contractions (McKenna *et al.*, 2008); i.e. one expects that phase 2 is triggered when a metabolic stress develops. Indeed, the development of phase 2 in EDL was accelerated either with when the stimulation frequency was increased or when glucose was removed from the physiological solution in EDL. Phase 2 never developed in the fatigue resistant oxidative soleus muscle even after 15000 APs (Pedersen *et al.*, 2009*a*, 2009*b*). As discussed in the next section, K_{ATP} channels are activated during metabolic stress, so its activation with ClC-1 in phase 2 is further evidence for an increase in metabolic stress during this condition. Finally, ClC-1 channels are also regulated by ATP as high ATP levels shift the voltage gating to more positive potentials, i.e. ClC-1 channels are ATP sensitive and a decrease in intracellular ATP increases ClC-1 channel activity (Bennetts *et al.*, 2005).

The effect of increasing G_{Cl} on force has so far not been studied because of a lack of a ClC-1 channel opener. However, if a decrease in G_{Cl} improves force at elevated $[K^+]_e$ then one can assume that an increase in G_{Cl} has the opposite effect. This is in fact supported by the fact that while AP amplitude is well maintained during phase 1, it actually decreases during phase 2 as G_{Cl} and G_K increases (Pedersen *et al.*, 2009*b*). So, a regulation of ClC-1 channels during muscle activity is crucial in regulating membrane excitability and force generation; at the onset of exercise G_{Cl} decreases to prevent K^+ induced loss of excitability while when metabolic stress starts then G_{Cl}

increases to reduce excitability and trigger fatigue; the ultimate goal being a decrease in ATP demand to prevent a metabolic catastrophe (MacIntosh *et al.*, 2012)

Kir2.1 and K_{ATP} channels (Kir6.2)

The remaining 10-20% of G_m at rest depend on K^+ conductance (G_K), which involves two K^+ channels: the K_{ATP} and Kir2.1 channels (Leech & Stanfield, 1981; Lindinger *et al.*, 2001; Nielsen *et al.*, 2003). Both channels are members of the superfamily of K^+ inward rectifier channels (Kir1.x-7.x) (Hibino *et al.*, 2010). Kir2.1 are strong inward rectifier channels that are expressed in the sarcolemma and in t-tubules (DiFranco *et al.*, 2015*b*). Kir2.1 channels have a higher permeability for K^+ influx than for K^+ efflux allowing K^+ to move more easily into rather than out of the cell (Matsuda *et al.*, 1987; Hibino *et al.*, 2010). This is clearly evident from the I-V relationship where at EM negative to E_K strong inward currents are observed whereas at potentials less negative to E_K, only a small outward current occurred becoming zero at -20 mV (Fig. 1.5) (Dhamoon *et al.*, 2004; Bendahhou *et al.*, 2005). The closing of Kir2.1 channels by membrane depolarization is due to voltage dependent blockade of the channel by Mg^{2+} and polyamines (Matsuda *et al.*, 1987; Lopatin *et al.*, 1994).

At rest, enough channels are open to allow for a K^+ efflux to contribute to the negative resting EM where K^+ is shifting it toward E_K of -95 mV. Loss of outward current upon membrane depolarization is crucial in preventing K^+ efflux during the AP depolarization phase. It has also been proposed that Kir2.1 channel has an important role in K^+ homeostasis during muscle activity. Due to the small size of t-tubules, it is believed that $[K^+]_e$ in t-tubules renders E_K less negative than resting EM favouring K^+ influx from t-tubules into the myoplasm (Wallinga *et al.*, 1999; Kristensen *et al.*, 2006). So, Kir2.1 channel maybe important in returning K^+ from t-tubules to

FIGURE 1.5

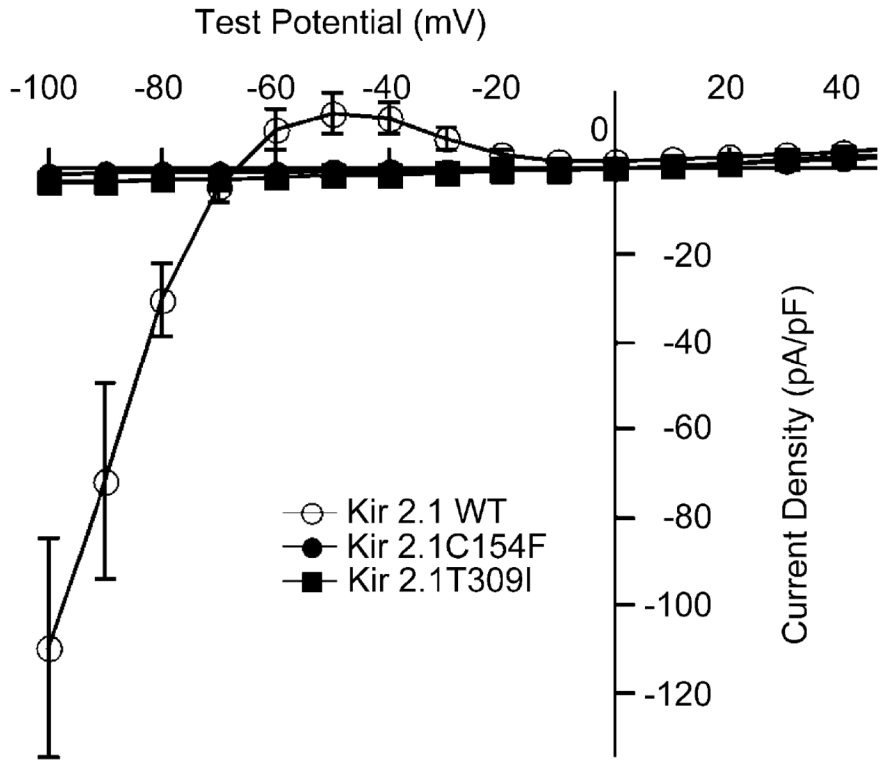

Figure 1.5. Whole-cell currents in COS-7 cells after transfection with Kir2.1 DNA. Cells were held at -80 mV, then depolarized to various test potentials (-100 to +50 mV) for 200 ms duration in 10 mV increments. Kir2.1C154F and KirT309I are two mutations causing Andersen's syndrome. Each value represents the average of 8 cells. Symbols: ○, Kir2.1 WT; ●, Kir2.1C154F; ■, KirT309I (from Bendahhou et al., 2005).

myoplasm between contractions reducing the depolarizing effect of increasing $[K^+]_e$.

K_{ATP} channel is an ATP sensitive channel that closes upon binding of ATP to its intracellular side (Noma, 1983). In skeletal muscle K_{ATP} channel is composed of two proteins encoded by two different genes. One protein is Kir.6.2 which is the pore forming subunit and the other is sulfonylurea receptor 2 (SUR2) regulatory subunit containing Walker A and Walker B motifs. These motifs are involved in the activation of the K_{ATP} channel by MgADP (Allard & Lazdunski, 1992; Ashcroft, 2000; Flagg *et al.*, 2010). Kir and SUR subunits co-assemble in a 4:4 stoichiometry to form an octameric channel complex (Clement *et al.*, 1997). Contrary to Kir2.1, Kir6.2 are weaker inward rectifier; that is K_{ATP} have much greater outward conductance than Kir2.1 inward rectifiers (Fig. 1.6) (Bollensdorff *et al.*, 2004). It is still not clear whether K_{ATP} channels are active at rest. This is because the channels are inactive at rest in vitro (Standen *et al.*, 1992, Hesse and Renaud, unpublished), while there is evidence that in vivo they largely contribute to K^+ efflux at rest as the K_{ATP} channel inhibitor, glibenclamide, completely abolished the K^+ efflux while reducing interstitial $[K^+]$ from 4.5 to 4.0 mM (Lindinger *et al.*, 2001; Nielsen *et al.*, 2003).

K_{ATP} channels are activated by changes in metabolites that occur during various metabolic stresses. That is they are activated by decreases in intracellular ATP, increases in intracellular ADP and reduction of intracellular pH (Noma, 1983; Davies, 1990; Vivaudou *et al.*, 1991). Thus, K_{ATP} channel acts as energy sensor linking the sarcolemmal excitability to the metabolic state of muscle fiber. Several studies have now documented severe fiber damage and muscle dysfunction during fatigue in the absence of K_{ATP} channel activity (Thabet *et al.*, 2005; Cifelli *et al.*, 2007, 2008). Two mechanisms have been elucidated for the myoprotective effects of K_{ATP} channels. The first mechanism involves a decrease in AP amplitude because contrary to Kir2.1 channels, Kir6.2

FIGURE 1.6

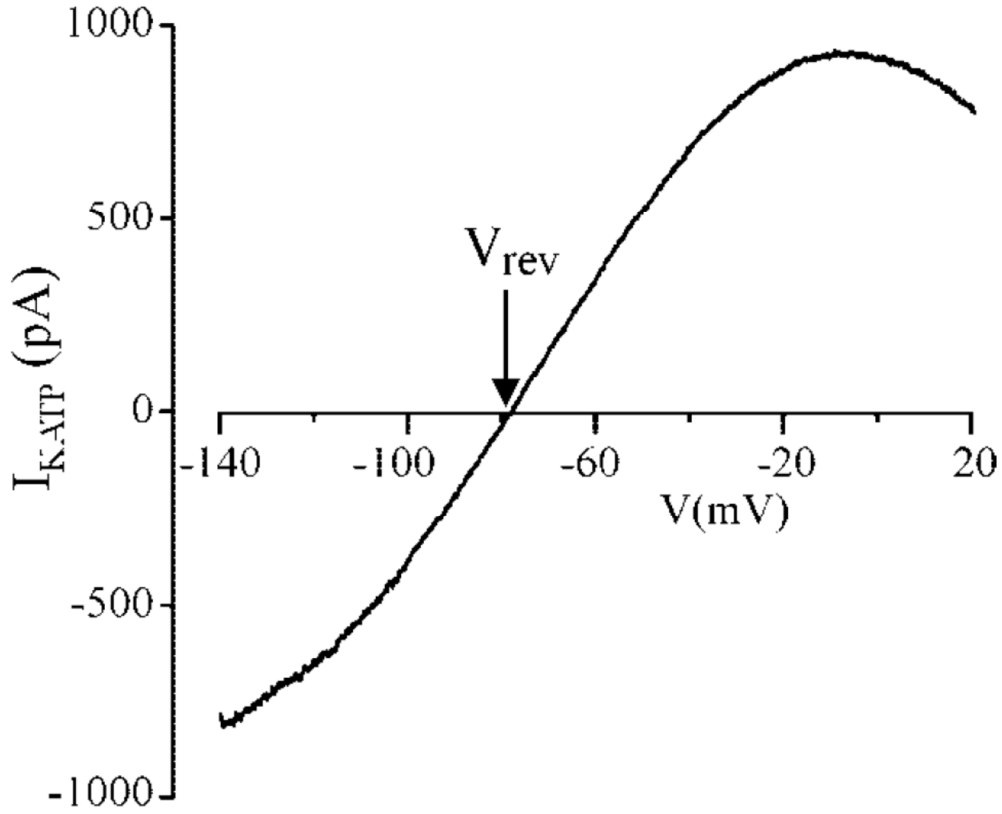

Figure 1.6. I-V relationship KATP channels in oocytes. In excised patches, macroscopic currents were recorded by applying voltage ramps (slope 0.16 V/sec) applied every 2 sec. Measurements were started after the K_{ATP} current (IK_{ATP}) initial rundown was finished and IK_{ATP} had an approximately constant amplitude (Bollensdorff et al., 2004).

channels produce a significant outward current at depolarized resting EM. This outward current decreases the extent of the Na^+ induced depolarization (Noma, 1983; Gong *et al.*, 2003), and prevents excessive depolarization during fatigue (Cifelli *et al.*, 2008). As a consequence of reduced AP amplitude, less Ca^{2+} is released and less force is generated (Matar *et al.*, 2001; Gong *et al.*, 2003; Zhu *et al.*, 2014). The physiological significance of the decrease in Ca^{2+} release associated with K_{ATP} channel activity is the reduction of the activity of Ca^{2+} ATPase pump and myosin ATPase activity reducing ATP demand in order to dampen ATP depletion. The second mechanism is a better maintenance of resting EM preventing excessive depolarizations during fatigue which can reach 50 mV in absence of K_{ATP} channel activity (Cifelli *et al.*, 2008).

Na^+ K^+ ATPase pump (NKA pump)

As Na^+ constantly enters myoplasm while K^+ moves out, especially during AP, a mechanism is necessary to reverse the fluxes. This is accomplished by the NKA pump which is a primary active pump, pumping 3 Na^+ out of the cell and 2 K^+ into the cell (i.e it is crucial to maintain proper Na^+ and K^+ concentration gradients for AP generation). As a consequence of the difference in Na^+ and K^+ movement one positive charge is transported by NKA pump generating an outward current that also contributes in hyperpolarizing resting EM (Clausen, 2003, 2013; McKenna *et al.*, 2008). Three NKA isoforms α1, α2 and α3 are expressed in skeletal muscles (Hundal *et al.*, 1994; Murphy *et al.*, 2006), with α1 and α2 having known functions in skeletal muscles. α1 is mainly expressed on the sarcolemma while α2 expression is enhanced in t-tubules (Williams *et al.*, 2001; Radzyukevich *et al.*, 2013). In WT rat diaphragm, α1 contributes ≈14 mV to resting EM while the α2 contributes ≈ 4 mV (Chibalin *et al.*, 2012; Radzyukevich *et al.*, 2013). The small 4 mV contribution of α2 is also seen in EDL despite the fact that α2 forms 87% of the pumps and α1 only 13% (He *et al.*, 2001; Radzyukevich *et al.*, 2013).

α1 isoform is ubiquitously expressed in all tissues and is believed to be responsible for the basic pumping activities of Na^+ and K^+ in resting cells (Radzyukevich *et al.*, 2004, 2013; Blanco, 2005). There is now evidence for an important role of α2 in exercise. α2 knockout mice have reduced exercise capacity, produce significantly less tetanic and twitch force and are more susceptible to fatigue than WT indicating that α2 activity is critical during exercise to help muscles maintain membrane excitability (Radzyukevich *et al.*, 2013). As it is the main isoform in t-tubules, the greater susceptibility to fatigue of α2 knockout is because they are unable to clear K^+ from the t-tubules during muscle activity, consequently resting EM depolarizes and Nav channels inactivate and excitability is reduced. A later study showed that α2 operates below its maximum activity at resting $[K^+]_e$, while during action potential activity α2 activity increases in proportion to the increase in $[K^+]_e$ (DiFranco *et al.*, 2015*a*).

CHANNELOPATHIES

Channelopathies are a group of diseases caused by mutations in genes encoding for ion channels. In regard to skeletal muscles the following channels have been found to be involved: ClC-1, Nav1.4, Cav1.1, Kir2.1 and Kir2.6 (Cannon, 2006, 2015). These channels are expressed only in skeletal muscles, except Kir2.1 which is also expressed in other tissues. So, except for Kir2.1 mutations, symptoms are limited to skeletal muscles. Channelopathies span a spectrum of symptoms with two extremes. At one end, there is myotonia in which patients suffer from paroxysmal attacks of muscle stiffness resulting from enhanced muscle excitability. At the other end, there is intermittent failure of excitability resulting in severe weakness described as periodic paralysis as the membrane becomes inexcitable (Fig. 1.7) (Cannon, 2006, 2015). Myotonia is normally observed following contractions when muscle fibers generate themselves a sustained

FIGURE 1.7

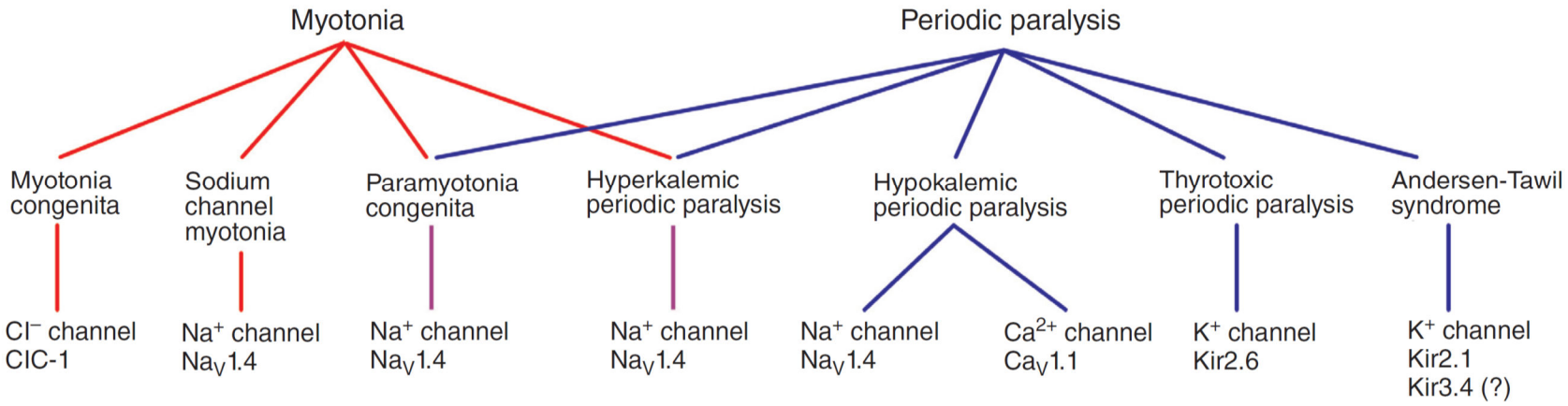

Figure 1.7. Clinical spectrum of the nondystrophic myotonias. Myotonia predominates in disorders further to the left in this spectrum, whereas periodic paralysis is the major symptom for those toward the right. The underlying molecular genetic defects in each of these disorders are mutations in voltage-gated ion channel genes (bottom row) (from Cannon, 2015).

burst of action of potentials that can persist several seconds causing a delay in muscle relaxation. Paralysis are attacks of weakness that can last from minutes to days during which the muscle fibers become electrically inexcitable (Cannon, 2006).

CHANNELOPATHIES ASSOCIATED WITH ClC-1 MUTATIONS

Myotonia congenita (MC) is caused by loss of function due to mutations of the CLCN1 gene which encodes for ClC-1 Cl^- channels in skeletal muscles (Koch *et al.*, 1992; Pusch, 2002; Cannon, 2006; Pedersen *et al.*, 2016). Some mutations are autosomal dominant while others are recessive. Patients suffer from myotonic stiffness during childhood. Legs are the most commonly affected (Trivedi *et al.*, 2013). Attacks can be triggered by cold and sudden forceful movements after rest (Drost *et al.*, 2001; Trivedi *et al.*, 2013). Relief of muscle stiffness occurs with repeated low muscular activity (warm up) in most patients.

Most mutations will cause complete or near complete loss of function of ClC-1 channels (Lossin & George, 2008). The defect in F413C and A531V mutations result in poor expression of the channel on the plasma membrane due to defective export from endoplasmic reticulum to Golgi elements (Papponen *et al.*, 2008). D136G results in an inverted voltage dependence of activation, such that the mutant channel opens only at voltages negative to E_{Cl} in contrast to WT channels which exhibit deactivation at this potential. Consequently, the probability of opening at voltage positive to E_{CL} is very low (Fahlke *et al.*, 1995). Many mutations with dominant effects shift the voltage dependence to depolarized voltages and exerts dominant effect even when expressed with WT gene because they form mutant/WT hetero-oligomeric channels (Pusch *et al.*, 1995; Kubisch *et al.*, 1998). The V236L mutation is recessive because while the voltage dependence is also shifted to depolarized potentials, WT currents are observed when mutant channels are co-expressed with WT (Kubisch *et al.*, 1998).

As discussed earlier, G_{Cl} through ClC-1 channels plays an important role in clamping resting EM by preventing large depolarization when $[K^+]_e$ increases and contributes to repolarization from AP (Adrian & Bryant, 1974). So in the absence of ClC-1 channel activity, EM is often destabilized resulting in EM reaching threshold for AP generation especially after contractions resulting in hyperexcitability and myotonia (Cannon, 2015).

CHANNELOPATHIES ASSOCIATED WITH Kir2.1 MUTATIONS

Andersen-Tawil syndrome is a periodic paralysis caused by mutations in the KCNJ2 gene that encodes for the Kir2.1 channels inward rectifier K^+ channels (Plaster *et al.*, 2001; Bendahhou *et al.*, 2005). It is a multisystem disorder in which patients suffer from K^+ sensitive periodic paralysis, ventricular arrhythmias and dysmorphic features (Tawil *et al.*, 1994). Most of the time weakness is associated with hypokalemia, however, hyper and normokalemia have been reported (Sansone *et al.*, 1997; Davies *et al.*, 2005).

Functional Kir channels are composed of four subunits which bind together to form a channel (Hibino *et al.*, 2010). The four subunits form a homo-tetramer when all four subunits are from the same gene while they form hetero-tetramers when they are formed by different subunits formed by different genes within the subfamily (ex. among Kir2.x subunits). Kir2.1 mutations have a dominant negative effects (Plaster *et al.*, 2001; Bendahhou *et al.*, 2005). Consequently, channels become non-functional when one or more subunits are mutant (Plaster *et al.*, 2001; Tristani-Firouzi *et al.*, 2002).

Myotubes obtained from patients lack the Ba^{2+} sensitive inward rectifying currents and have a depolarized resting EM (Sacconi *et al.*, 2009). Andersen Tawil syndrome patients also show a decrease in compound action potential amplitude during rest after long exercise which indicates a decrease in skeletal muscle excitability (Bendahhou *et al.*, 2005). The decrease in excitability is

most likely linked to a depolarized resting EM that inactivates Nav channels. It is proposed that in cardiac muscles reduction of Kir2.1 prolongs the cardiac action potential and QT interval by reducing the repolarizing current in the terminal phase of action resulting in tachycardia (Plaster *et al.*, 2001).

CHANNELOPATHIES ASSOCIATED WITH Kir2.6 MUTATIONS

Thyrotoxic hypokalemic periodic paralysis (TPP) is another periodic paralysis. Its name comes from the fact that paralysis and hypokalemia occurs in the setting of hyperthyroidism especially in males being more affected than females (Ober, 1992). TPP is linked to mutations in the KCJN18 gene encoding for the Kir2.6 inward rectifier in skeletal muscles which is transcriptionally regulated by thyroid hormone (Ryan *et al.*, 2010). Resting EM is reported to be depolarized in TPP (Puwanant & Ruff, 2010). After prolonged exercise compound action potential amplitude first increase, then this is followed by a time during which there is gradual decline indicating that there is a hyperexcitability followed by lower excitability (Arimura *et al.*, 2007).

Different mechanisms have been proposed for TTP. One mutation (V168M) results in decreased channel opening probability and exerts a dominant negative on both WT Kir2.6 and 2.1 channels because its expression with WT reduces outward and inward Kir2.6 currents (Cheng *et al.*, 2011). Another TPP mutation (I144F) renders the channels non-functional, which is proposed to depolarize resting EM causing inactivation of Nav channel and weakness. For the T354M mutation, the open probability of the channel is not altered by PKC phosphorylation as it is for the WT channels; i.e., PKC phosphorylation fails to reduce the open probability of the channels (Ryan *et al.*, 2010). In this case, the mutation causes hyperpolarization of resting EM and make it harder to reach AP threshold to trigger AP.

CHANNELOPATHIES ASSOCIATED WITH Cav1.1 MUTATIONS

Mutations in the CACNA1S gene, which encodes for the Cav1.1 channels (also known as L-type Ca^{2+} channels) are the major cause for hypokalemic periodic paralysis (hypoPP) representing 70% of all cases (Sternberg *et al.*, 2001). It is an autosomal dominant channelopathy with incomplete penetrance in females (Wu *et al.*, 2012). Patients experience paralysis that is associated with low serum $[K^+]$. Attacks are triggered by carbohydrate ingestion, which in response to rising glucose and insulin levels promotes K^+ uptake by the muscle, or by rest after exercise (Cannon, 2006, 2015). After period of long exercise HypoPP patients show a reduction in compound action potential amplitude indicating a decrease in muscle excitability (Fournier *et al.*, 2004). Patients develop late onset permanent proximal weakness with vacuolar myopathy (Links *et al.*, 1990).

Six out of seven known HypoPP Cav1.1 mutations involve one of the arginine residues the voltage sensor; i.e. in segment 4 of domains II, III or IV (Matthews *et al.*, 2009; Cannon, 2010). It is believed that these mutations generate a gating pore, which is separate from the channel selective pore and serves as a pathway for ion conduction. Measurements from fibers from mice carrying R528H mutations revealed that the current through the gating pore (I_{gp}) is voltage dependent creating an inward current upon hyperpolarization (Wu *et al.*, 2012).

At 4.5 mM K^+ the impact of I_{gp} on resting EM is small causing only a depolarization of 3 mV (Struyk & Cannon, 2008; Cannon, 2010, 2015). In WT, reduction of $[K^+]_e$ from 4 to 2 mM results in resting EM hyperpolarization, while further decreases to 1.5 mM causes EM to depolarize to ≈ -66 mV (Cannon, 2010). The depolarization is caused as the contribution of inward rectifier current (I_{Kir}) diminishes as $[K^+]_e$ is decreased. For HypoPP fibers, similar depolarization at lower $[K^+]_e$ start at 3 mM (Cannon, 2010). Further decreases in $[K^+]_e$ worsened the

depolarization. For example, at 2.5 mM $[K^+]_e$ HypoPP fibers depolarize by 16 mV while normal fiber hyperpolarize by 5 mV (Puwanant & Ruff, 2010). It has been suggested that the depolarization occurs at higher $[K^+]_e$ in HypoPP than WT fibers because as $[K^+]_e$ is lowered, the decreased outward I_{Kir} becomes overwhelmed by the inward gating current. Consequently, resting EM depolarizes until delayed rectifier K^+ channel is activated and current balance of zero mV is established at a resting EM of -65 mV. Consequently, Nav channels inactivate causing loss of excitability and paralysis (Cannon, 2010, 2015).

HypoPP fibers have also reduced K_{ATP} channel activity and administration of insulin further reduced the outward I_{Kir} contributing to EM depolarization (Tricarico *et al.*, 1999; Ruff, 1999). The attacks of weakness triggered by high carbohydrate ingestion may be explained by an increase of [ATP]/[ADP] ratio which would inhibit K_{ATP} channels (Cannon, 2010). Insulin also activates NKA pump lowering $[K^+]_e$ (Clausen, 2003), and it lowers I_{Kir} in HypoPP (Ruff, 1999). Taken together, these effects combined will contribute to depolarization and weakness (Cannon, 2010).

CHANNELOPATHIES ASSOCIATED WITH Nav1.4 MUTATIONS

While mutations of ClC-1, Kir2.1, Kir2.6 and Cav.1. lead to either myotonia or paralysis, mutations in Nav1.4 result in a spectrum of diseases ranging from myotonia to paralysis (Cannon, 2006, 2015). They include sodium channel myotonia (SCM), paramyotonia congenita (PMC), HypoPP and HyperKPP. The final phenotype of the disease depends on whether the mutation affects activation, fast or slow inactivation. For this reason, Nav1.4 channel structure activity relationship will first be discussed.

Nav structure activity relationship

Like all voltage sensitive cation channels, Nav1.4 channel structure consists of two subunits an α and one or more β subunits (Kraner *et al.*, 1985; Roberts & Barchi, 1987; Catterall & Swanson, 2015). The largest one is the α subunit with a molecular weight of 260 kDa while the β-subunit is smaller with a molecular weight of 38 kDa.

Nav1.4 channel α subunit structure consists of four domains, each one is composed of six segments that are capable of forming membrane spanning helices (Figure 1.8), (Barchi, 1995; Ashcroft, 2000). The first three segments S1, S2, S3 have several charged residues and are weakly amphipathic (Stühmer *et al.*, 1989; Barchi, 1995). S4 segments of each domain make the voltage sensor as they are composed of 4-8 positively charged amino acid residue (usually arginine) separated by 2 hydrophobic ones. The gating charges are believed to be stabilized by forming ion pairs with neighbouring negatively charged and hydrophilic residues in other transmembrane segments (Catterall & Swanson, 2015). When the membrane depolarizes, the voltage driven outward movement of the gating charge in the S4 segments initiate conformational changes that lead to pore opening. Segments 5 and 6 line up the channel pore. The loop that links segments 5 and 6 in each domain forms the selectivity barrier, they contain the 4 amino acids; glutamic acid, aspartic acid, lysine and alanine forming a ring through which Na^+ ions enter the pore (Noda *et al.*, 1989; Pusch *et al.*, 1991; Terlau *et al.*, 1991; Heinemann *et al.*, 1992; Ashcroft, 2000; Lipkind & Fozzard, 2008). Inactivation results from the movement of a protein particle that blocks the pore (Armstrong, 1977). There is an evidence that the cytoplasmic loop connecting domain 3 and 4 (Fig. 1.8) plays a role in fast inactivation as antibodies directed against this loop slowed inactivation rates (Vassilev *et al.*, 1988). More specifically, a cluster of three hydrophobic amino isoleucine-phenylalanine-methionine (IFM) at positions 1488-1490 have been shown to be

necessary for fast inactivation (West *et al.*, 1992). Based on these findings it was proposed that the hydrophobic residues stabilized the inactivated state of Na^+ channel in hinged lid mechanism in which the inactivation gate serves as intracellular blocking particle that folds into the channel structure and blocks the pore during inactivation.

Slow inactivation mechanism involves conformational change in the selectivity filter in the pore (Balser *et al.*, 1996; Todt *et al.*, 1999; Vilin *et al.*, 2001; Hilber *et al.*, 2005) and the S6 segment (O'Reilly *et al.*, 2001; Zhao *et al.*, 2004; Chen *et al.*, 2006). The proposed mechanism is that the selectivity filter, central cavity and intracellular activation gate are "all modified by an asymmetric pore collapse in which two of the S6 segments move toward the central axis of the pore and two move away". "This pore collapse is responsible for the stability of the slow inactivated state and the long time required for recovery from slow inactivation" (Payandeh *et al.*, 2012; Catterall, 2014).

HypoPP

While 70% of cases of HypoPP are linked to mutations in the CACNA1S gene which encode for the Cav1.1, 10% of cases are caused by mutation in SCN4A gene (Sternberg *et al.*, 2001). Similar to Cav1.1 mutations, the Nav1.4 mutations cause HypoPP and are located at the arginine residues in the S4 segments (Fig. 1.9) (Cannon, 2010, 2015; Wu *et al.*, 2011). The mutation also causes a gating pore current which is the source of the aberrant depolarization at hypokalemia (Cannon, 2010, 2015; Wu *et al.*, 2011). While most symptoms are similar to Cav1.1 HypoPP, there are two major differences i) Nav1.4 mutations do not cause vacuolar myopathy and ii) the penetrance is equal in males and females (Wu *et al.*, 2011).

FIGURE 1.8

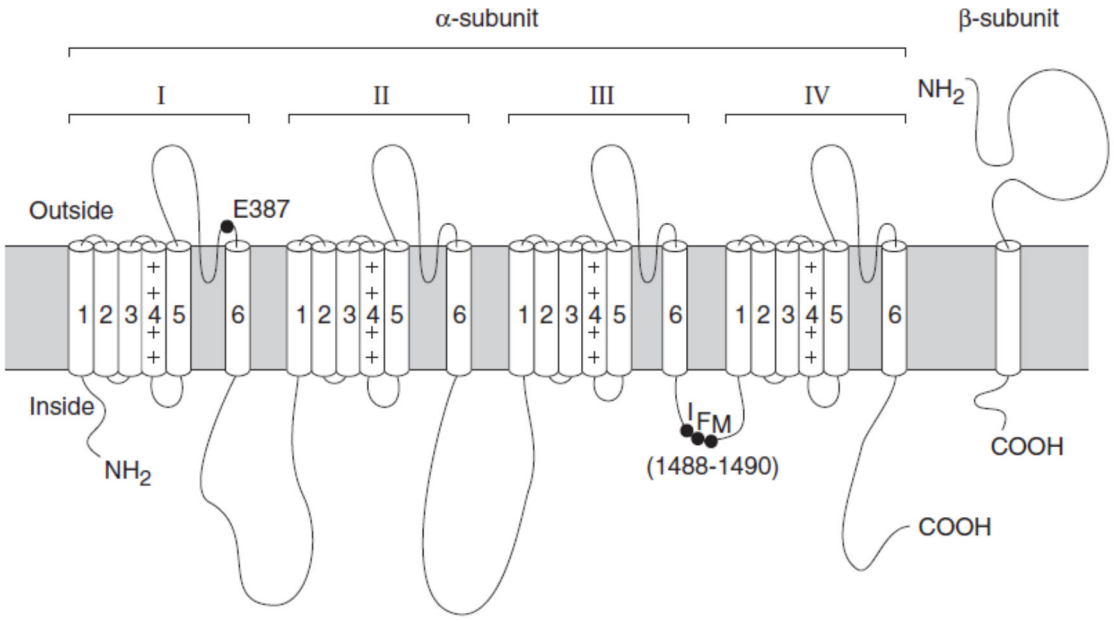

Figure 1.8. Putative topology of the voltage-gated Nav channel. Note the 1) positively charged residues in S4 that make up the voltage sensor; 2) extracellular P loops between transmembrane spans 5 and 6 of each domain lining the pore and contributing to the selectivity filter; and 3) the intracellular loop between III and IV with the IFM "particle" associated with fast-inactivation (from Ashcroft, 2000).

FIGURE 1.9

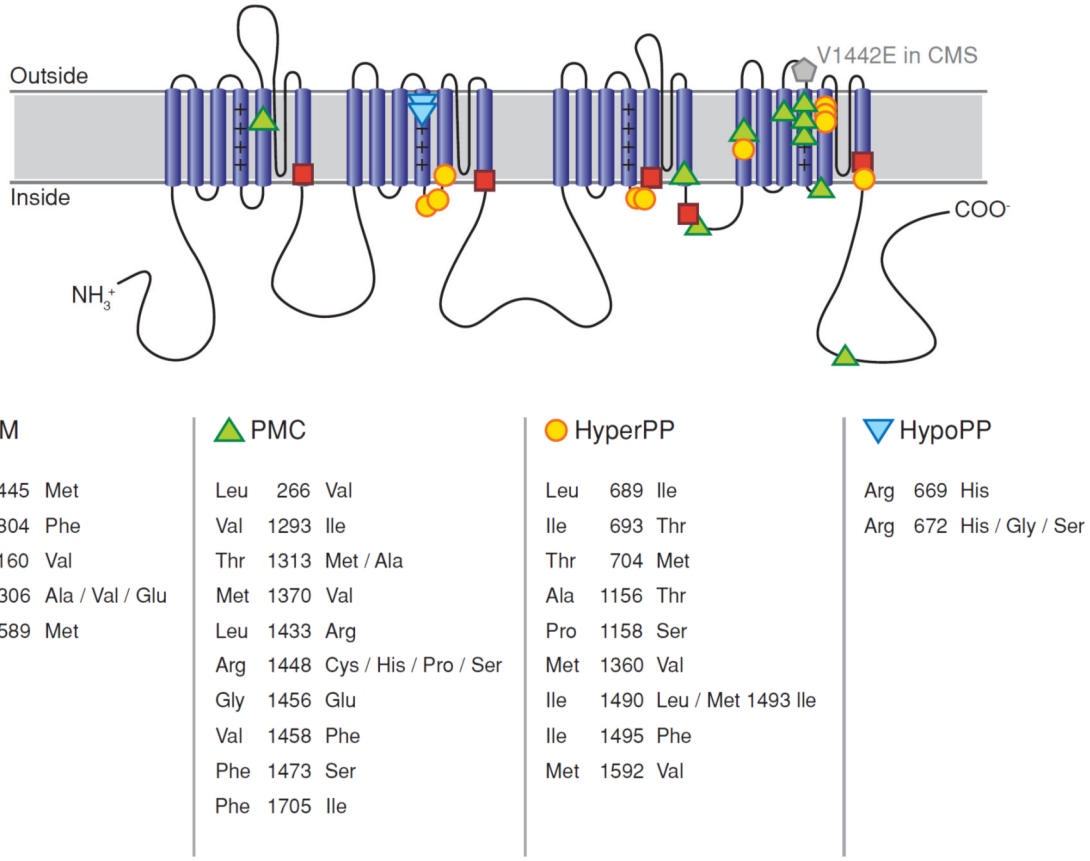

Figure 1.9. Missense mutations in Nav1.4 associated with disorders of muscle excitability. The schematic diagram for the membrane-folding structure of Nav1.4 shows the relative locations of missense mutations associated with PAM which is classified under SCM in a later review (Cannon, 2015), PMC, HyperPP and HypoPP (from Cannon, 2006).

Myotonia

In PMC, myotonia worsens by cooling or with repeated muscle activity. The latter is in contrast to MC for which the myotonia decreases with muscle activity, and hence the name paramyotonia (Cannon, 2006, 2015). In PMC resting EM is normal at 37°C but depolarizes by up to 40 mV upon cooling to 27°C (Lehmann-Horn *et al.*, 1981).

Mutations such T1306M in the rat (corresponding to the human T1313M) associated with PMC disrupt fast inactivation by shifting the steady state I-V curve to depolarized EM (Fig. 1.10) resulting in a large persistent Na^+ current (Hayward *et al.*, 1996, 1997). Studies of several mutations causing PMC showed that they also increase the time constant of inactivation by three to five folds, while they shorten recovery from fast inactivation time constant (Yang *et al.*, 1994). Consequently, during AP more Nav channels remain available as they do not all inactivate resulting in myotonic runs that are triggered after the termination of neural stimulation. Slower rate of inactivation also increases the AP duration allowing more K^+ efflux per spike into t-tubules augmenting the depolarization that triggers the next spike. Paralysis occurs when the depolarization is large enough to inactivate Nav channels.

SCM is characterized by myotonia without periodic paralysis (Cannon, 2015). One example of SCM is potassium aggravated myotonia (PAM), which is aggravated by ingesting K^+ rich food and also by cold (Heine *et al.*, 1993). Mutations causing SCM such as rat G1299E (corresponding to human G1306E) shift fast inactivation IV curve to a depolarized EM (Fig. 1.10) and also increases the time constant of fast inactivation causing myotonia by a mechanism similar to PMC (Hayward *et al.*, 1996, 1997). However, the extent of symptoms in SCM are lesser

FIGURE 1.10

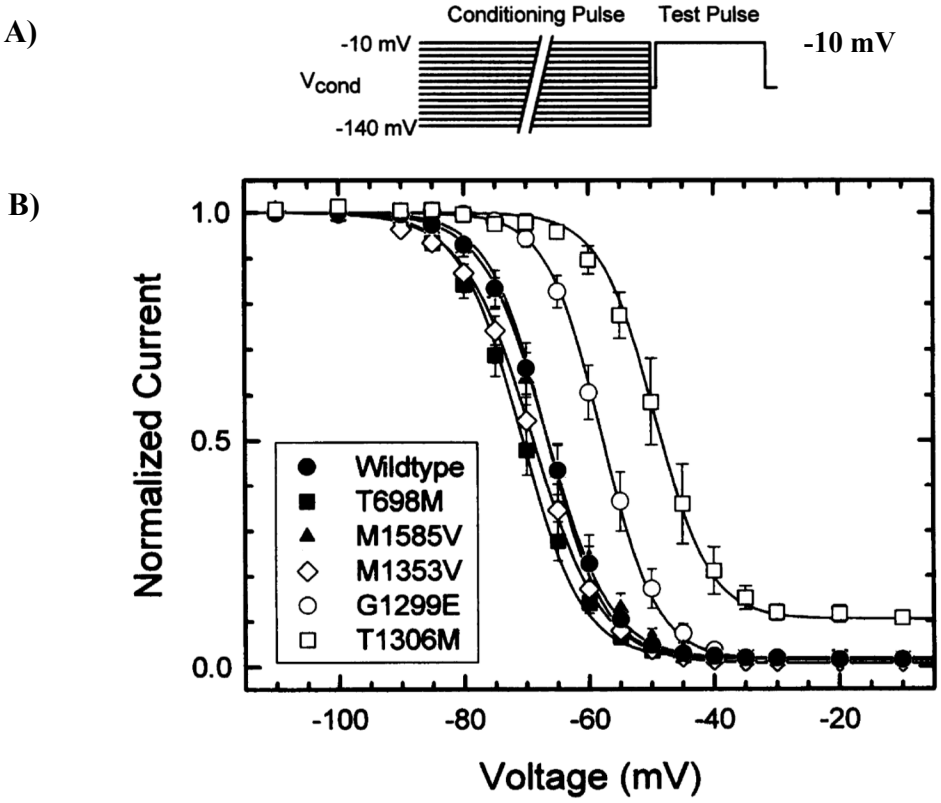

Figure 1.10. Voltage dependence of fast inactivation of mutant rat Nav1.4 channel. A) Schematic of the pulse protocol involving depolarization to -10 mV, after a conditioning pre-pulse of 300 ms at potentials from -140 to -10 mV and a 0.2-ms gap to -80 mV to deactivate channels before application of the test pulse for fast inactivation. The current was normalized to the current after a conditioning pulse at -140 mV. B) Steady state I-V relationship. Human (h) Nav1.4 mutations were expressed at the corresponding position in rat (r) Nav1.4 as described below. The rG1299E (hG1306E) mutation causes a form of sodium channel myotonia associated with severe myotonia but no paralysis. rT1306M (hT1313M) mutation causes paramyotonia congenital. rT698M (hT704M) and rM1585V (hM1592V) are two mutations that cause HyperKPP with severe episodic weakness. rM1353V (hM1360V) mutation causes a variant of HyperKPP with muscle stiffness in addition to weakness (from Hayward et al., 1997).

compared to PMC (Hayward *et al.*, 1996). This is because SCM rat G1299E mutation (human G1306E) slows fast inactivation only two folds compared to WT. While the PMC rat T1306M (human T1313M) slows inactivation 20 folds. In addition, $V_{1/2}$ of steady state fast inactivation curve is shifted to depolarized potentials by 10 mV in SCM compared to 17 mV in PMC. Consequently, there is larger persistent Na^+ current in PMC than SCM which predisposes to paralysis in PMC but not in SCM.

A final channelopathy that associates with SCNA4 gene mutations is HyperKPP which will now be fully discussed in greater details as it is the main subject of this thesis.

HYPERKPP

HyperKPP is an autosomal dominant channelopathy disease that results in both myotonia and paralysis with nearly complete penetrance (Gamstorp *et al.*, 1957; Pearson, 1964; Bradley *et al.*, 1990). Patients experience episodes of myotonic discharge during and between paralytic attacks (Jurkat-Rott & Lehmann-Horn, 2007). Weakness mainly affects the limbs in 85% of patients (Gamstorp *et al.*, 1957; Clausen *et al.*, 1980; Charles *et al.*, 2013). The duration of attacks differs from one person to another and from one mutation to another. Attacks are of short duration during childhood and become longer and more severe during adolescence (Gamstorp *et al.*, 1957; Bradley *et al.*, 1990). From adolescence the attacks range from minutes to hours or even days (Miller *et al.*, 2004; Fontaine, 2008). In some cases, paralysis is associated with increase in serum K^+ from 4 to 6-8 mM (Gamstorp *et al.*, 1957; Lehmann-Horn *et al.*, 1983; Bradley *et al.*, 1990), while in other cases no increase in serum K^+ is reported (Poskanzer & Kerr, 1961; Chinnery *et al.*, 2002). Paralytic attacks are constantly triggered by ingestion of high K^+ salts because HyperKPP muscles have a greater to sensitivity to K^+-induced force depression. Rest after

exercise (80% of cases), cold exposure (54% of cases) and fasting (25% of cases) constitute other triggers (Wang & Clausen, 1976; Miller *et al.*, 2004; Jurkat-Rott & Lehmann-Horn, 2007). Later in life attacks may decrease in frequency but patients suffer from chronic muscle weakness due to vacuolar myopathy and fiber damage. Some patients eventually become bedridden by the fifth decade of life (Bradley *et al.*, 1990; Miller *et al.*, 2004).

Ingestion of calcium gluconate partially decreases the severity of symptoms (Gamstorp *et al.*, 1957; Pearson, 1964), while acetazolamide, a carbonic anhydrase inhibitor, reduces the frequency of attacks, but becomes ineffective over time (Lehmann-Horn *et al.*, 1983). Furthermore, not all patients show an initial response to acetazolamide (Miller *et al.*, 2004). Salbutamol, a β_2 adrenergic agonist, originally used to treat bronchial asthma alleviates hyperkalemia and paralysis in HyperKPP patients but it also eventually becomes ineffective in some patients over prolonged use (Wang & Clausen, 1976; Clausen *et al.*, 1980). So, there is a need for a more effective long lasting treatment.

HyperKPP is caused by mutations in SCN4A gene that encodes for the Nav1.4 channel, (Fontaine *et al.*, 1990; Rojas *et al.*, 1991; Cannon, 2006). Two mutations: methionine to valine (M1592V) and threonine to methionine (T704M) together are responsible for 75% of cases while the other 7 mutations are responsible for the remaining 25% (Fig 1.9) (Miller *et al.*, 2004). Some differences in phenotype exist between mutations. T704M patients suffer their first attack before the age of 1 year while for M1592V patients it starts by the age of 5 years. T704M patients experience an average of 28 attacks per months with a mean of 8 hours while the values for M1592V patients are 3 attacks of 89 hours each.

Electrophysiological studies in both human Met1592V and T704M Nav1.4 channels or their equivalent mutation in rat at positions 1585 and 698, respectively, showed three major defects

in the Nav1.4 channel. First, the steady state activation curve is shifted toward more negative EM with $V_{1/2}$ being -27 mV in HyperKPP M1592V and T698M compared to -17 mV in WT (Fig. 1.11) (Cummins *et al.*, 1993; Rojas *et al.*, 1999). The shift lowers AP threshold. Secondly, while the steady state fast inactivation is not affected (Fig. 1.10), the steady state slow inactivation curve is shifted toward less negative EM (Fig 1.12) and recovery from slow activation is accelerated for both M1592V and T704M mutations (Hayward *et al.*, 1997). $V_{1/2}$ of steady state slow inactivation were -50 and -34 mV in M1585V and T698M, respectively, compared to -62 mV in WT cells. Because of this defect Nav1.4 channel opening probability increases during resting state. Finally, mutant channels, also enter a non-inactivation mode upon membrane depolarization at elevated $[K^+]_e$, an effect not observed in normal channels (Cannon *et al.*, 1991).

As a consequence of the defects in activation and slow inactivation, more Nav1.4 channels appear to be opened at rest (Fig 1.13). HyperKPP muscles have a large Na^+ influx at rest that can be blocked by tetrodotoxin (TTX), a Nav1.4 channel blocker. This TTX sensitive Na^+ influx is 6-folds higher in HyperKPP than in normal muscles (Clausen *et al.*, 2011). TTX also prevents the 16 mV depolarization observed in HyperKPP muscles compared to WT, which suggests that the depolarization is linked to the increased Na^+ influx (Lehmann-Horn *et al.*, 1987; Clausen *et al.*, 2011; Khogali *et al.*, 2015). APs are often generated because the threshold is lowered by the shift in the activation curve and are the cause of myotonia and stiffness reported by patients. The K^+ efflux associated with AP then increases $[K^+]_e$. An increase in $[K^+]_e$ from 3.5 to 10 mM K^+ normally depolarizes control muscle fibers by 15 mV whereas it reaches 30 mV in HyperKPP fibers, as a result of such large depolarization, resting EM can reach -50 mV (Lehmann-Horn *et al.*, 1987). As a result of this depolarization Nav channels inactivate and excitability is lost.

FIGURE 1.11

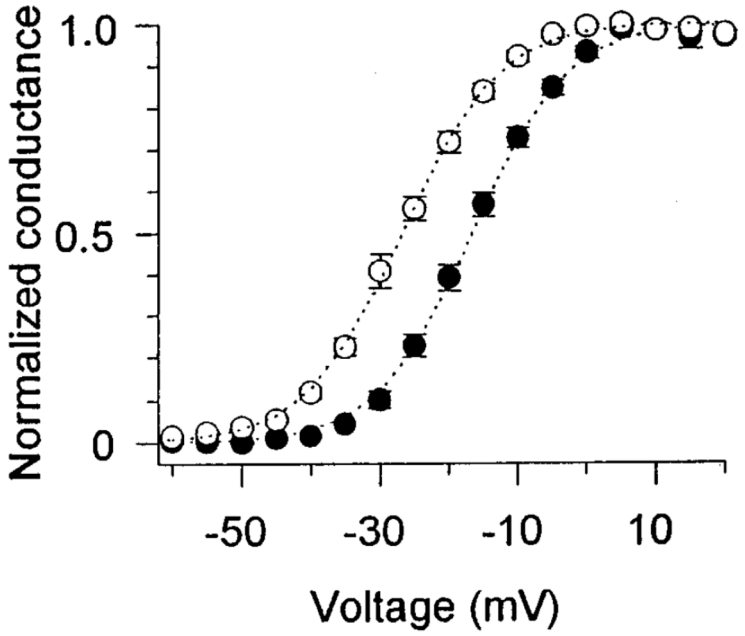

Figure 1.11. Steady state activation of wild-type and HyperKPP M1592V mutant Na^+ currents recorded by cut-open voltage-clamp in Xenopus oocyte. "Currents were elicited by test depolarizations from -70 to 25 mV in 5-mV steps. Holding potential was set at -110 mV. The activation curves were calculated with the equation G = I/(Vtest - Vrev), where G is the conductance, I is the measured peak current, Vtest is the test potential, and Vrev is the reversal potential calculated by extrapolation from I-V plots to zero-current level". Symbols: ●, WT; ○, M1592V (from Rojas et al., 1999).

FIGURE 1.12

A)

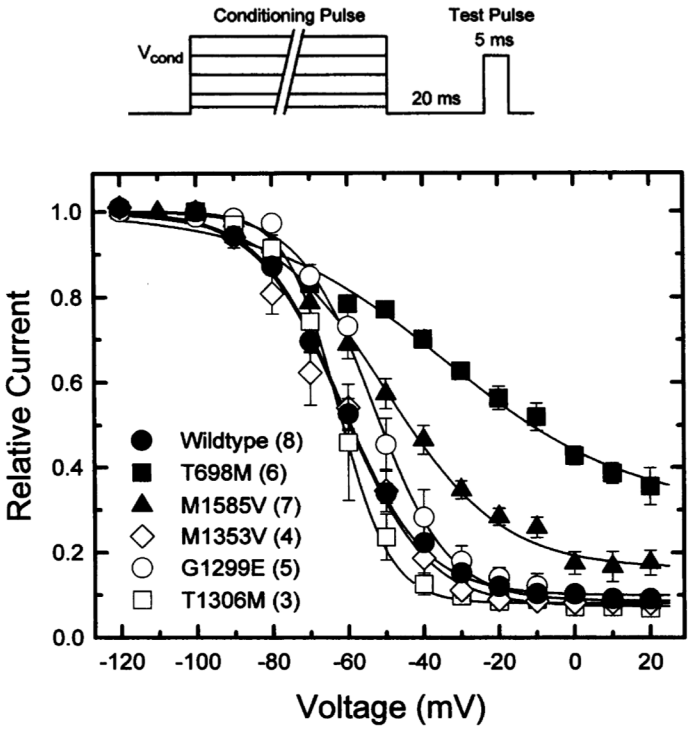

Figure 1.12. Steady-state voltage dependence of slow inactivation of mutant rat Nav1.4 channel. Peak. A) Schematic of pulse protocol involving a depolarization to -10 mV from a holding potential of -100 mV after a 60 sec conditioning pulse. The conditioning and test pulses were separated by a 20-ms hyperpolarization to -100 mV to allow channels to recover from fast inactivation. The current was normalized to the peak current elicited from a holding potential of -100 mV. B) Steady state I-V relationship. Human Nav1.4 (h) mutations were expressed at the corresponding position in rat Nav1.4 (r) as described below. rT698M (hT704M) and rM1585V (hM1592V) are two mutations that cause HyperKPP with severe episodic weakness. rM1353V (hM1360V) mutation causes a variant of HyperKPP with muscle stiffness in addition to weakness. The rG1299E (hG1306E) mutation causes a form of sodium channel myotonia associated with severe myotonia but no paralysis. rT1306M (hT1313M) mutation causes paramyotonia congenita mutation (from Hayward et al., 1997).

FIGURE 1.13

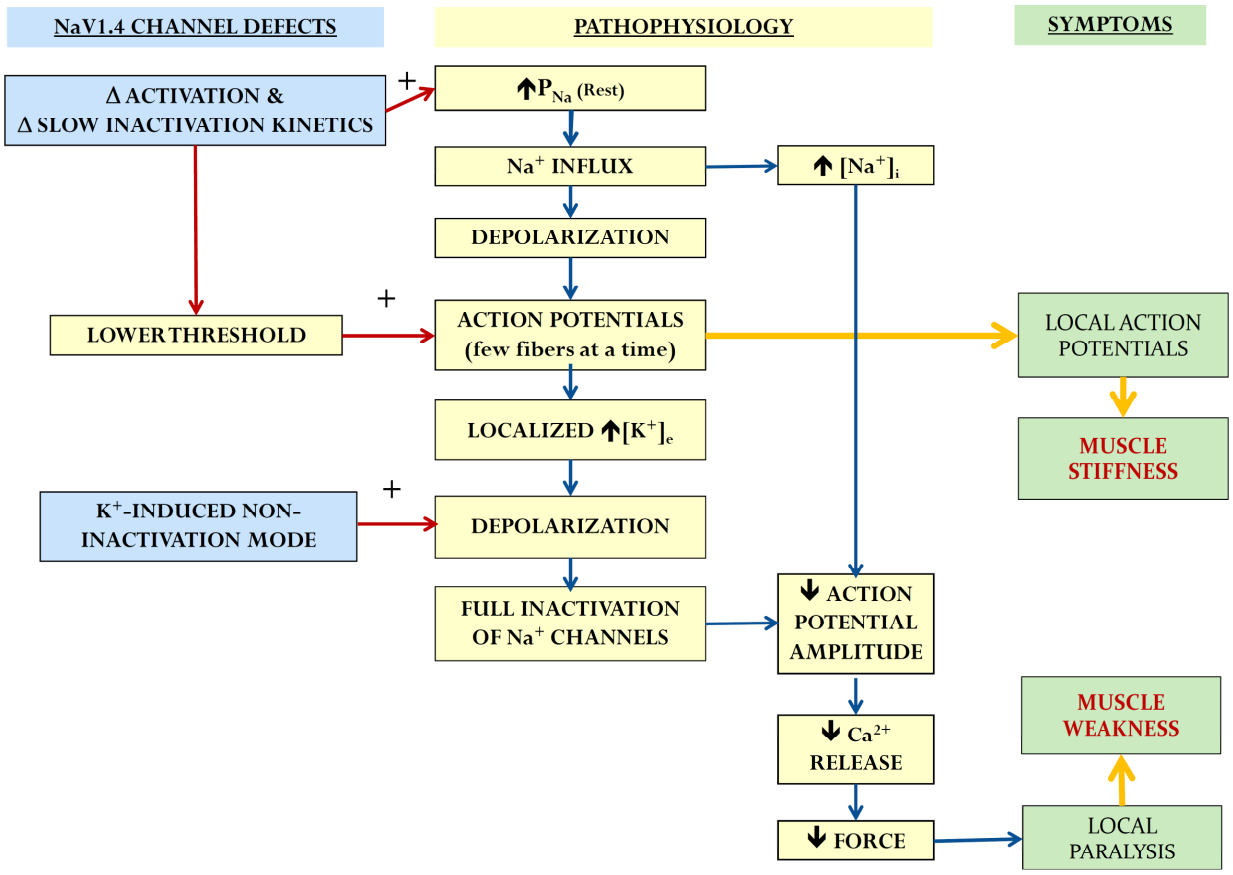

Figure 1.13. Diagram showing the mechanism by which an increase in Na^+ influx in HyperKPP results in both stiffness (myotonia) and paralysis.

Although one can argue that testing HyperKPP a 10 mM $[K^+]_e$ is too high as serum $[K^+]$ does not exceed 8 mM during an attack (Gamstorp *et al.*, 1957; Lehmann-Horn *et al.*, 1983), it is known that during exercise interstitial K^+ reaches concentrations 4-5 mM higher than serum levels (Nielsen *et al.*, 2004); i.e interstitial and t-tubular $[K^+]$ may well reach 10 mM during an attack. According to steady state fast and slow inactivation curves (Fig 1.10 and 1.12), Nav channels are nearly completely inactivated at -55 mV. In fact no force is generated in WT muscles when EM reaches -55 mV (Cairns *et al.*, 1997). Resting EM depolarization also reduces AP amplitude (Yensen *et al.*, 2002). So, the large depolarization is most likely the mechanism that causes the loss of excitability and paralysis. A final factor to consider is the increase in $[Na^+]_i$ linked to the large Na^+ influx (Lehmann-Horn *et al.*, 1987; Clausen *et al.*, 2011; Khogali *et al.*, 2015). It is expected that increases in $[Na^+]_i$ itself lower AP overshoot as observed with reduction in $[Na^+]$ gradient (Cairns *et al.*, 2003), which further contributes to loss of excitability. So in HyperKPP when the depolarization eventually becomes large enough to inactivate enough Nav channels and AP can no longer be generated, excitability is lost resulting in a decrease in Ca^{2+} release and tetanic force production and paralysis (Fig. 1.13).

Mouse model

A mouse model of HyperKPP Met1592Val mutation has been successfully generated (Hayward *et al.*, 2008), and helped us understand the phenotype associated with this mutation. Muscles from these mice demonstrate all the hallmarks of HyperKPP defects; that is increased Na^+ influx, resting EM depolarizations, increased sensitivity to the K^+-induced force depression and fiber type switch to more oxidative type (Hayward *et al.*, 2008; Clausen *et al.*, 2011; Khogali *et al.*, 2015). Studying the progression of the disease in these mice versus the changes in Nav1.4 channel protein first showed that all physiological defects did not worsen beyond the age of 4

weeks, the time at which channel content reaches maximum as in WT muscles (Appendix 1; Khogali *et al.*, 2015). This suggests that the symptoms may well be solely related to the defects caused by mutated channels.

Patients from a family suffering from HyperKPP who was later found to carry the M1592V mutation (Poskanzer & Kerr, 1961; Chinnery *et al.*, 2002), suffer mainly of muscle stiffness with no myotonia except upon penetration of EMG needle in the muscle. In a different study, M1592V patients were reported to experience myotonia but it was not clear if it was only triggered on needle penetration or not (Miller *et al.*, 2004). M1592V patients also suffer from muscle weakness ranging from 3 to 4 days, but rarely suffer from full paralysis forcing them to remain in bed; in fact, such attacks occur only one to three times per year (Poskanzer & Kerr, 1961; Chinnery *et al.*, 2002).

Similar to the phenotype in humans, needle movements increased myotonia during EMG measurements in muscles of the M1592V mouse model (Hayward *et al.*, 2008). Myotonia is defined clinically as sustained burst of AP originating from muscle fiber and persisting for several seconds after neural stimulation has stopped (Cannon, 2006). So while HyperKPP muscles have higher EMG activity than WT suggesting that HyperKPP generate greater APs than WT, sudden contractions were observed in absence of any electrical or neuronal stimulation such as during muscle dissection and between electrically elicited tetanic contractions. Also when mice were free to move, a sustained series of EMG peaks as expected for a myotonic run were only observed in one mouse and lasted for 9 sec only (Khogali *et al.*, 2015). This suggests that myotonic discharge is not a key feature of M1592V and it was proposed that there are periods of hyperexcitability during which HyperKPP fibers randomly generate APs in absence of any stimuli and the resulting contractions are the cause of the muscle stiffness reported by patients.

Similarly, to human patients, full paralytic attacks were rarely observed in the M1592V HyperKPP mouse. Prolonged periods of hindlimb immobility in mice were rarely seen in their cages and it lasted less than 60 sec. This was further supported by EMG measurements for which only periods of reduced EMG activity were observed only 3% of time with a mean duration of 3 sec during a 4 hr EMG measurement (Khogali *et al.*, 2015). Instead, HyperKPP EDL and soleus muscles produced less force than WT muscles even at normal $[K^+]_e$ (Hayward *et al.*, 2008; Clausen *et al.*, 2011; Khogali *et al.*, 2015). It was proposed that few fibers become hyperexcitable and the resulting APs cause a local increase in interstitial $[K^+]$. As HyperKPP fiber have higher K^+-induced force sensitivity, only fibers exposed to the high $[K^+]$ will have reduced force production at normal $[K^+]_e$ resulting in muscle weakness instead of full paralysis. Collectively these findings indicate that the M1592V mouse model successfully reproduce the symptoms reported in patient with the same mutation.

THE ASYMPTOMATIC DIAPHRAGM

A study of 94 HyperKPP patients reported that only 26% of them suffer of breathing difficulties while 85% report that limb muscles are affected (Charles *et al.*, 2013). For the family with the M1592V mutations none of the patients reported respiratory stress (Poskanzer & Kerr, 1961; Chinnery *et al.*, 2002). This is interesting because human diaphragm expresses the Nav1.4 channel mRNA (Zhou & Hoffman, 1994). In rats, the Nav1.4 protein content of the diaphragm is 75% of the content in hindlimb EDL muscle and 2-fold greater than in soleus (Bay & Strichartz, 1980), two muscles that are severely affected by the disease (Hayward *et al.*, 2008; Clausen *et al.*, 2011; Khogali *et al.*, 2015). A first indication that the diaphragm of M1592V mouse is asymptomatic comes from the fact that up to the age of 12 months fiber type composition remains unchanged and is similar to that of the WT. This is important as a major shift in fiber type toward

type IIA occur in HyperKPP EDL and toward type I in HyperKPP soleus (Khogali *et al.*, 2015). It is believed that the shift is associated with chronic increases in $[Ca^{2+}]_i$ due to spontaneous AP generation responsible for stiffness (Hayward *et al.*, 2008; Khogali *et al.*, 2015) for which Ca^{2+} may modulate myosin isoform expression (Chin *et al.*, 1998; Dunn *et al.*, 1999). So, the absence of any change in fiber type in HyperKPP diaphragm suggests it does not suffer of spontaneous AP generation or stiffness which normally precede weakness or paralysis (Fig 1.13).

Considering the likelihood that diaphragm is asymptomatic and considering that the present treatments are not fully effective or lose effectiveness over time, then studying the mechanisms that protect the diaphragm is crucial because it will help us identify potential targets for which the activity can be modulated for the development of long term effective treatment.

OBJECTIVES

The overall objective of the PhD study is to understand the mechanism(s) responsible for the different phenotype among EDL, soleus, diaphragm muscles in order to identify targets for the development of a new effective and long lasting pharmacological therapy.

Three major studies were carried out to achieve this objective:

1- To characterize the differences in the extent of symptoms between the diaphragm and three hindlimb muscles: EDL, soleus and FDB.

2- To document that nature of the mechanisms that render the HyperKPP diaphragm asymptomatic.

3- To study the therapeutic potential of increasing protein kinase A (PKA) and protein kinase C (PKC) activity in hindlimb muscles.

CHAPTER 2

CONTRACTILE ABNORMALITIES OF MOUSE MUSCLES EXPRESSING HYPERKALEMIC PERIODIC PARALYSIS MUTANT NAV1.4 CHANNELS DO NOT CORRELATE WITH NA^+ INFLUX OR CHANNEL CONTENT

Brooke Lucas,*[1] **Tarek Ammar,*[1]** Shiemaa Khogali,*[1] Danica DeJong,[1] Michael Barbalinardo, [1]Cameron Nishi,[1] Lawrence J. Hayward,[2] and Jean-Marc Renaud,[1]

* B. Lucas, T. Ammar and S. Khogali contributed equally to this work.

[1]Department of Cellular and Molecular Medicine, University of Ottawa, Ottawa, Ontario, Canada; and [2]Department of Neurology, University of Massachusetts Medical School, Worcester, Massachusetts

Physiological Genomics 46: 385–397, 2014.

AUTHORS CONTRIBUTION

- Ammar: Fig 2.1, 2.2, 2.8, 2.9, 2.10
- Lucas: Fig. 2.4
- Khogali: Fig. 2.7
- DeJong: Fig. 2.6
- Barbalinardo: Fig. 2.3 and 2.5
- Nishi: Fig 2.6

ABSTRACT

Hyperkalemic periodic paralysis (HyperKPP) is characterized by myotonic discharges that occur between episodic attacks of paralysis. Individuals with HyperKPP rarely suffer respiratory distress even though diaphragm muscle expresses the same defective Na^+ channel isoform (Nav1.4) that causes symptoms in limb muscles. We tested the hypothesis that the extent of the HyperKPP phenotype (low force generation and shift toward oxidative type I and IIA fibers) in muscle is a function of *1*) the Nav1.4 channel content and *2*) the Na^+ influx through the defective channels [i.e., the tetrodotoxin (TTX)-sensitive Na^+ influx]. We measured Nav1.4 channel protein content, TTX-sensitive Na^+ influx, force generation and myosin isoform expression in four muscles from knock-in mice expressing a Nav1.4 isoform corresponding to the human M1592V mutant. The HyperKPP flexor digitorum brevis muscle showed no contractile abnormalities, which correlated well with its low Nav1.4 protein content and by far the lowest TTX-sensitive Na^+ influx. In contrast, diaphragm muscle expressing the HyperKPP mutant contained high levels of Nav1.4 protein and exhibited a TTX-sensitive Na^+ influx that was 22% higher compared with affected extensor digitorum longus (EDL) and soleus muscles. Surprisingly, despite this high burden of Na^+ influx, the contractility phenotype was very mild in mutant diaphragm compared with the robust abnormalities observed in EDL and soleus. This study provides evidence that HyperKPP phenotype does not depend solely on the Nav1.4 content or Na^+ influx and that the diaphragm does not depend solely on Na^+ K^+ pumps to ameliorate the phenotype.

INTRODUCTION

Hyperkalemic periodic paralysis (HyperKPP) is an autosomal dominant disease with complete or nearly complete penetrance caused by mutant variants of the skeletal muscle Na^+ channel, Nav1.4 (Gamstorp *et al.*, 1957). Muscles in HyperKPP often exhibit paralytic attacks during a resting period that follows strenuous exercise, fasting and potassium ingestion (Lehmann-Horn *et al.*, 1983; Bradley *et al.*, 1990; Miller *et al.*, 2004; Jurkat-Rott & Lehmann-Horn, 2007). Affected individuals generally do not complain of muscle stiffness, but myotonic discharges are detected in 75% of cases (Miller *et al.*, 2004). Weakness during attacks is prominent in the limbs (Gamstorp *et al.*, 1957; Bradley *et al.*, 1990), and can incapacitate patients such that they are confined to bed. The attacks may be short and frequent in childhood and can become longer and more severe during adolescence (Gamstorp *et al.*, 1957; Lehmann-Horn *et al.*, 1983; Bradley *et al.*, 1990). Although paralysis is typically associated with increased plasma $[K^+]$ $(6-8$ mM), some individuals may be normokalemic during attacks (Gamstorp *et al.*, 1957; Lehmann-Horn *et al.*, 1983; Miller *et al.*, 2004). Available treatments to reduce attack frequency or severity are either not always or not fully effective; they may also lose effectiveness over time and do not address the later development of fixed myopathy (Clausen *et al.*, 1980; Miller *et al.*, 2004).

It is now well established that HyperKPP is linked to missense mutations in the SCN4A gene that encodes for the α-subunit of Nav1.4, the Na^+ channel isoform expressed in skeletal muscle (Goldin *et al.*, 2000; Miller *et al.*, 2004). Other excitable tissues, such as cardiac muscle and neurons, are not affected by mutations of the SCN4A gene because they express other Nav isoforms; i.e., cardiac muscles express Nav1.5, while neurons express Nav1.1-Nav1.3 and Nav1.6-Nav1.9 (Goldin *et al.*, 2000). Most (~70%) of the HyperKPP cases result from two

mutations: threonine to methionine (T704M) and methionine to valine (M1592V); the remaining cases (~30%) are due to seven other mutations (Miller *et al.*, 2004). In one retrospective study, patients with the T704M mutation usually suffered their first paralytic attack before the age of 1 yr, and the frequency varied from 8 to 42 attacks per month. In comparison, patients with the M1592V mutation suffered their first attack later (≈5 yr old) and less frequently (5–6 attacks per month). The mean duration of the paralysis was about 10 times longer for the M1592V mutation than for the T704M (89 vs. 8 h), with maximum duration as long as 7 days for both mutations (Miller *et al.*, 2004).

The T704M and M1592V mutations shift the steady-state activation curve of the Nav1.4 channel toward a more negative membrane potential and also shift the steady-state slow inactivation curve toward a less negative membrane potential (Cummins *et al.*, 1993; Hayward *et al.*, 1999). The mutated Nav1.4 channels also enter a non-inactivating mode upon membrane depolarization at elevated extracellular K^+ concentration ($[K^+]_e$) (Cannon *et al.*, 1991). As a result of these perturbations, resting HyperKPP muscles have a more depolarized membrane potential and greater Na^+ influx compared with wild-type muscles (Jurkat-Rott & Lehmann-Horn, 2007; Clausen *et al.*, 2011). The membrane depolarization associated with the shift in steady-state activation and slow inactivation curve increases the possibility of action potentials being generated in the absence of motor neuron activation leading to myotonic discharges (Lehmann-Horn *et al.*, 1983). The K^+ efflux associated with action potentials then increases $[K^+]_e$; i.e., it causes the hyperkalemia characteristic of this disease. In normal muscles, a doubling of $[K^+]_e$ depolarizes the cell membrane by 10 mV, whereas in HyperKPP muscles the depolarization can be as high as 30 mV (Jurkat-Rott & Lehmann-Horn, 2007), and appears to be high enough to inactivate enough Na^+ channels to cause paralysis.

HyperKPP patients rarely suffer from respiratory distress (Bradley *et al.*, 1990), which would be expected to occur if the diaphragm also developed paralytic attacks. There are, however, a few cases of respiratory distress (Creutzfeldt *et al.*, 1963; Bradley *et al.*, 1990). This is rather surprising because the diaphragm expresses Nav1.4 channels (Zhou & Hoffman, 1994), to levels that are almost as high as in extensor digitorum longus (EDL) muscle and more than twofold greater than in soleus (Bay & Strichartz, 1980), two muscles that suffer from HyperKPP symptoms in terms of increased Na^+ influx, membrane depolarization, and low force generation, especially at elevated $[K^+]_e$ (Hayward *et al.*, 2008; Clausen *et al.*, 2011). To fully characterize the disease mechanisms and to be able to develop more effective pharmacological treatments for HyperKPP, we need to understand how the disease differentially affects various muscle subtypes and especially why some are spared from episodic attacks.

It is now established that significant changes in gene expression occur in HyperKPP compared with wild-type muscles such as the shift toward greater expression of myosin IIA (Hayward *et al.*, 2008). We hypothesized that either the expression of the Nav1.4 channel or the Na^+ influx is altered in HyperKPP diaphragm compared with limb muscles, in a manner that may protect from symptoms. To test this hypothesis, we measured Nav1.4 protein content, Na^+ influx, contractility in vitro and expression of myosin isoforms (assuming that the more affected a muscle is, the greater the changes in myosin isoform expression). Four muscles were examined: EDL, soleus, diaphragm, and flexor digitorum brevis (FDB). The latter muscle was included because in the course of our experiments it became evident that this muscle was even less affected than diaphragm. The results show that indeed the lack of symptoms in FDB was related to lower Nav1.4 channel content and Na^+ influx compared with other muscles. However, this explanation did not apply to HyperKPP diaphragm.

METHODS AND MATERIALS

ANIMALS, MUSCLE BUNDLE, AND SINGLE FIBER PREPARATION

HyperKPP mice [strain FVB.129S4(B6)-*Scn4a*$^{tm1.1Ljh}$/J, Jackson Laboratory #011033] were generated by knocking in the equivalent of human missense mutation M1592V into the mouse genome; i.e., at position 1585 (Hayward *et al.*, 2008). The homozygous mutants generally do not survive beyond postnatal day 5, so knock-in mice were maintained as heterozygotes by crossbreeding with FVB mice for 10 generations. Mice were fed ad libitum and housed according to the guidelines of the Canadian Council for Animal Care. The Animal Care Committee of the University of Ottawa approved all experimental procedures used in this study. Prior to muscle excision, 1 to 4 mo old mice were anesthetized with a single intraperitoneal injection of 2.2 mg ketamine/0.4 mg xylazine/0.22 mg acepromazine per 10 g of animal body wt and killed by cervical dislocation.

For Western blots, EDL, soleus, FDB, and whole diaphragm muscles were used. For Na^+ influx and contractility measurements, FDB fiber bundles controlling the 4th digit were dissected as described by Cifelli et al. (Cifelli *et al.*, 2007) ; whole EDL and soleus and 5–7 mm wide diaphragm strips were used. For myosin immunohistochemistry, diaphragm strips and whole EDL, soleus and FDB were used. Some experiments were also conducted on single FDB muscle fibers that were dispersed by trituration following a collagenase treatment as described by Cifelli et al. (Cifelli *et al.*, 2007).

GENOTYPING

A 2 mm tail piece was incubated overnight with 500 µl tail digestion buffer (0.2 mM Na_2EDTA and 25 mM NaOH, pH 12.3) and 50 µl Proteinase K (1 mg/ml) at 56°C. DNA extraction involved the addition of 650 µl of 1:1 phenol-CIA [chloroform-isoamyl alcohol

(24:1 vol/vol)] and centrifugation at 12,000 *g* for 10 min. Twice we added 650 µl of CIA to the pellet and centrifuged it before suspending the resulting pellet in 750 µl of isopropyl alcohol. After 10 min, the solution was centrifuged 15 min at 15,000 *g*. The alcohol was removed, and the pellet suspended in 750 µl 70% ethanol and centrifuged. After the alcohol was removed, the pellet was let to dry 30 min prior to addition of 200 µl TE buffer (10 mM Tris, 1 mM EDTA, pH 8.0) and incubated at 65°C for 2 h. PCR was then completed with the previously extracted DNA and the following primers: NC1F (forward): 5' TGT CTA ACT TCG CCT ACG TCA A 3'; NC2R (reverse): 5' GAG TCA CCC AGT ACC TCT TTG G 3'. PCR products were digested for 6 h with the restriction digest enzyme *Nsp*I. The mutation that is knocked in to the HyperKPP mice causes the removal of one *Nsp*I cut site that is easily detected by agarose gel electrophoresis; two bands were visualized for wild-type mice, which carry the cut site on both alleles, and three bands were seen for heterozygous HyperKPP mice harboring one normal allele and one mutant allele.

WESTERN BLOTS OF Nav1.4 CHANNELS

Muscles were homogenized in buffer containing (in mM): 50 Tris,150 NaCl, 1% Triton X-100, 0.5% sodium deoxycholate, 0.1% SDS, and protease inhibitor cocktail, pH 8.0. Homogenates were kept 10 min on ice and then centrifuged for 15 min at 16,000 *g* and 4°C. Protein concentration was determined in supernatants by the BC assay method (Thermo Scientific). We resolved 40 µg of proteins on a 6% of acrylamide gel at 100 V and then transferred that onto nitrocellulose membranes (Bio-Rad Laboratories Miniprotean III apparatus). Total protein contents on membrane were verified with Ponceau S (MP Biomedicals). Membranes were blocked overnight at 4°C with 5% skim milk powder in phosphate-buffered solution (PBS) containing 0.1% Tween, washed three times (10 min each)

with PBS, and incubated 2 h with rabbit anti-NaV1.4 (1:200 dilution, Alomone Labs, Jerusalem, Israel) in the presence of 5% skim milk, 1% bovine serum albumin (BSA) in PBS. Membranes were washed three times (10 min each) with PBS and incubated 1 h with horseradish peroxidase-conjugated goat anti-rabbit antibody (Jackson ImmunoResearch Laboratories) diluted 1:10,000 in 5% skim milk in PBS. Bands were visualized by chemiluminescence using the ECL kit (PerkinElmer) on Cl-X Posure film (Thermo Scientific). Films (Cl-XPosure film, Thermoscientific) were scanned (MP 600 Cannon PIXMA) and quantified using Image J (US National Institutes of Health). Normalizing the Nav1.4 protein content to the β-actin content is not feasible when measuring differences between muscles. However, as stated in the DISCUSSION, the relative differences between all four wild-type muscles were as expected from other studies in which the Na^+ channel density was measured with radioactive tracers or current measurements. So, none of the measurements of Nav1.4 protein content were normalized to β-actin protein content.

PHYSIOLOGICAL MEASUREMENTS SOLUTIONS.

Control solution contained (in mM): 118.5 NaCl, 4.7 KCl, 1.3 $CaCl_2$, 3.1 $MgCl_2$, 25 $NaHCO_3$, 2 NaH_2PO_4 and 5.5 D-glucose. Solutions 8–11 mM K^+, 2.4 mM Ca^{2+}, or 5 mM Ni^{2+} were prepared by the addition of the appropriate amount of KCl, $CaCl_2$, or $NiCl_2$, respectively. We prepared tetrodotoxin (TTX, a Na^+ channel blocker) and ouabain (Na^+-K^+ pump inhibitor, Sigma) by adding them directly in the control solution. BTP-2, (a blocker of store-operated Ca^{2+} entry or SOCE blocker, Sigma) was first dissolved in 100% DMSO and sonicated 5 min before being added to the physiological solution, which was also sonicated 5 min to make sure BTP-2 remains in solution; the final concentrations of BTP-2 and DMSO were, respectively, 20 μM

and 0.1% (vol/vol). All solutions were continuously bubbled with 95% O_2/5% CO_2 to maintain a pH of 7.4. Experimental temperature was 37°C.

$^{22}Na^+$ INFLUX.

Muscles were mounted vertically into chambers consisting of methyl acrylate cuvettes. Muscles were equilibrated 30 min in 2 ml physiological solution before being incubated 10 min with 2 μCi/ml $^{22}Na^+$. Extracellular $^{22}Na^+$ was washout out as described by Clausen et al. (Clausen *et al.*, 2011). In brief, muscles were bathed once for 5 min and three times for 15 min in Na^+-free solutions containing (in mM) 10 mM HEPES, 280 mM sucrose, 500 nM TTX, pH 7.4. TTX was added to prevent loss of intracellular $^{22}Na^+$ during washout, especially in HyperKPP muscles. The washing period consisted of three 15 min long washes, which was long enough to remove all extracellular ^{14}C-sucrose in another experiment (data not shown). $^{22}Na^+$ was counted with an LKB Wallac gamma counter (1282 Compugamma).

Force measurement. Muscles were positioned horizontally in a Plexiglas chamber. One end of the muscle was attached to a force transducer (model #400A, Aurora Scientific), while the other end was fixed to a stationary hook. Flow of physiological solution below and above muscles was maintained at a total of 15 ml/min. Muscle length was adjusted to give maximal tetanic force. Electrical stimulations were applied across two platinum wires (4 mm apart) located on opposite sides of the fibers. They were connected to a Grass S88 stimulator and a Grass SIU5 isolation unit (Grass Technologies/Astro- Med). Tetanic contractions were elicited with 200 ms trains of 0.3 ms, 10 V (supramaximal voltage) pulses. Stimulation frequencies were set to give maximum peak tetanic force, being 140 Hz for soleus and 200 Hz for EDL, FDB, and diaphragm. For all experiments, tetanic contractions were elicited every 100 s. Force transducers were connected to a KCP13104 data acquisition system (Keithle), and data

were recorded at 5 kHz. Parameters of the tetanic contraction were later analyzed with a computer. Peak tetanic force was defined as the maximal force developed while muscles were electrically stimulated and was calculated as the difference between the maximum force during a contraction and the baseline force measured 5 ms before stimulation.

$[Ca^2]_i$ AND SARCOMERE LENGTH.

Intracellular Ca^{2+} concentration ($[Ca^{2+}]_i$) and sarcomere length were measured in single FDB muscle fibers. Fibers were loaded with Fura-2 by exposure for 30 min at 37°C to 5 μM Fura-2AM (Molecular Probes) dissolved in culture minimum Earl's medium (Invitrogen) containing 0.1% (vol/vol) DMSO. After transferring coverslips to a chamber (model RC-25, Warner Instru-ments), we superfused fibers with saline solution at a rate of 2–3 ml/min, while temperature was maintained with a dual-channel heater (model TC-344B, Warner Instruments), one channel heating the incoming fluid and the other heating the chamber itself. $[Ca^{2+}]_i$ and sarcomere length was measured with a fluorescent and contractility device (IonOptix). We monitored $[Ca^{2+}]_i$ by illuminating fibers alternately 340 and 380 nm and measuring fluorescence at 505 nm at a sampling rate of 200 Hz. Sarcomeres were visualized with a Digital CCD video (MyoCam-S), and light intensities of the A and I bands were monitored along the length of the fiber. Using a Fourier analysis, we transformed light intensities into a power spectrum, which gave a major peak; from the frequency of that peak and using a calibration, we measured changes in sarcomere length at a sampling rate of 250 Hz.

Myosin Immunohistochemistry.

Immunohistochemical analysis was used to determine the expression of the different myosin isoforms. Serial cross sections were double-stained with rabbit anti-laminin antibody (Sigma) and one of mouse monoclonal anti-MHC I (A4.840), IIA (SC-71), IIB (BF-F3), or IIX

(6H1) antibodies (Developmental Studies Hybridoma Bank). Anti-laminin antibody was used to better identify boundaries between individual fibers. For myosin MHC-I, MHC-IIA, and MHC-IIB staining, slides were placed 15 min at 37°C on a slide dryer before being rinsed 3 min in PBS. Sections were blocked 1 h in a humid chamber with 0.5% BSA in PBS before being exposed 2 h to primary antibodies in a humid chamber. Sections were rinsed in PBS three times (5 min each time) before a 45 min incubation at 37°C in a humid chamber for 2 h with secondary antibodies diluted in Triton-X 100. Secondary antibodies were: rhodamine-conjugated goat anti-rabbit IgG for laminin, FITC-conjugated goat anti-mouse IgG for myosin IIA, and IgM for myosin I and IIB. Sections were rinsed three times in PBS, mounted with antifade reagent, and stored at -80°C until viewed. Control sections were also stained without the primary antibody to test for nonspecific secondary antibody binding.

For MHC-IIX, the staining protocol was slightly modified to enhance primary antibody binding and block nonspecific binding. After sections were thawed on the slide dryer, they were fixed in 100% ethanol for 5 min and then rinsed in PBS that was kept at pH of 7.4. Sections were blocked with 5% horse serum (HS) in PBS and incubated overnight at 4°C with anti-myosin IIX. Sections were rinsed three times in PBS (5 min each time) and incubated 1 h with FITC-conjugated goat anti-mouse IgM diluted in 5% HS blocking solution. Sections were rinsed in PBS, mounted with antifade reagent, and kept at - 80°C until viewed.

STATISTICAL ANALYSIS

Data are presented as means ±SE. ANOVA was used to determine significant differences. Split plot ANOVA designs were used when muscles were tested at all-time levels. ANOVA calculations were made with version 9.2 General Linear Model procedures of the Statistical Analysis Software (SAS Institute, Cary, NC). When a main effect or an interaction was

significant, the least square difference was used to locate the significant differences (Steel & Torrie, 1980). The word “significant” refers only to a statistical difference ($P < 0.05$).

RESULTS

Nav1.4 CONTENT

Skeletal muscles from heterozygous HyperKPP mice harboring one normal and one mutant *SCN4A* allele previously were shown to express mRNAs encoding both normal and mutant Nav1.4 channels (Hayward *et al.*, 2008). However, the absence of antibodies or toxins specific for the mutant channel precludes a direct measurement of the normal vs. mutant Nav1.4 channel contents. Alternatively, we sought to *1*) determine whether the presence of the mutant channel alters the total Nav1.4 content and *2*) define the relative differences in Na channel contents between muscles. HyperKPP EDL, soleus, diaphragm and FDB all had significantly lower Nav1.4 protein content compared with their wild-type counterpart, the content in HyperKPP muscles varying between 54 and 73% of the content in wild-type muscles (Fig. 2.1). Of all four muscles, both wild-type and HyperKPP EDL had the largest Nav1.4 channel protein content (Fig. 2.2). The content in diaphragm was 71% of EDL for wild-type and 76% for HyperKPP. Soleus and FDB had the lowest content, being, respectively, 31 and 25% of the EDL for wild-type and 32 and 24% for HyperKPP. So, while HyperKPP muscles contained fewer Nav1.4 channels than wild-type muscles, the differences in Nav1.4 channel contents are of the same order for wild-type and HyperKPP muscles; i.e., EDL > diaphragm >> soleus ~ FDB.

Na^+ INFLUX

A major physiological consequence of the M1592V mutation is a significant increase in TTX-sensitive Na^+ influx even when muscles are at rest (Clausen *et al.*, 2011). We therefore measured the extent to which that mutation affects Na^+ influx at rest to best understand how

FIGURE 2.1

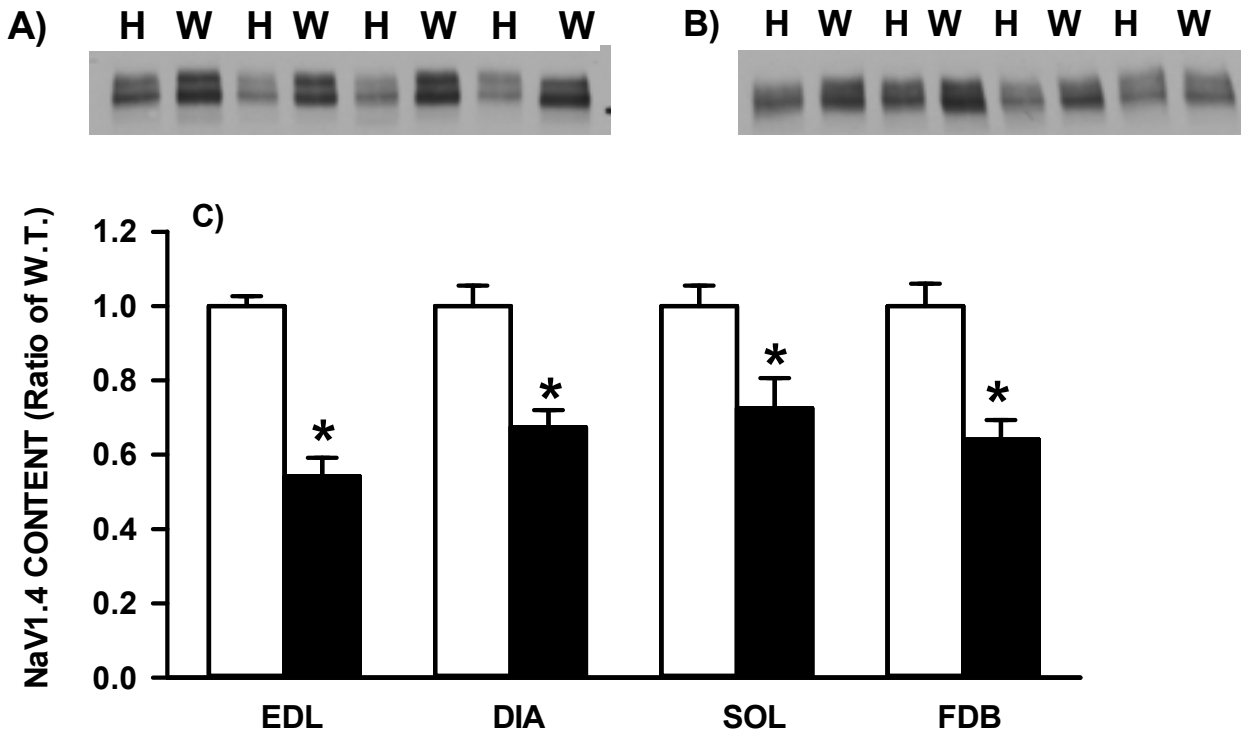

Figure 2.1. The Nav1.4 channel protein content was significantly lower in hyperkalemic periodic paralysis (HyperKPP) than in wild-type muscles. Representative Western blots from extensor digitorum longus (EDL) (A) and diaphragm (B) comparing Nav1.4 channel protein content between wild-type (W) and HyperKPP (H) muscles. Nav1.4 content was normalized to wild-type muscle content. Open columns, wild type; filled columns, HyperKPP. Vertical bars represent the SE of 7–8 muscles. *Significantly different from wild type, ANOVA, and least significant difference (LSD), $P < 0.05$.

FIGURE 2.2

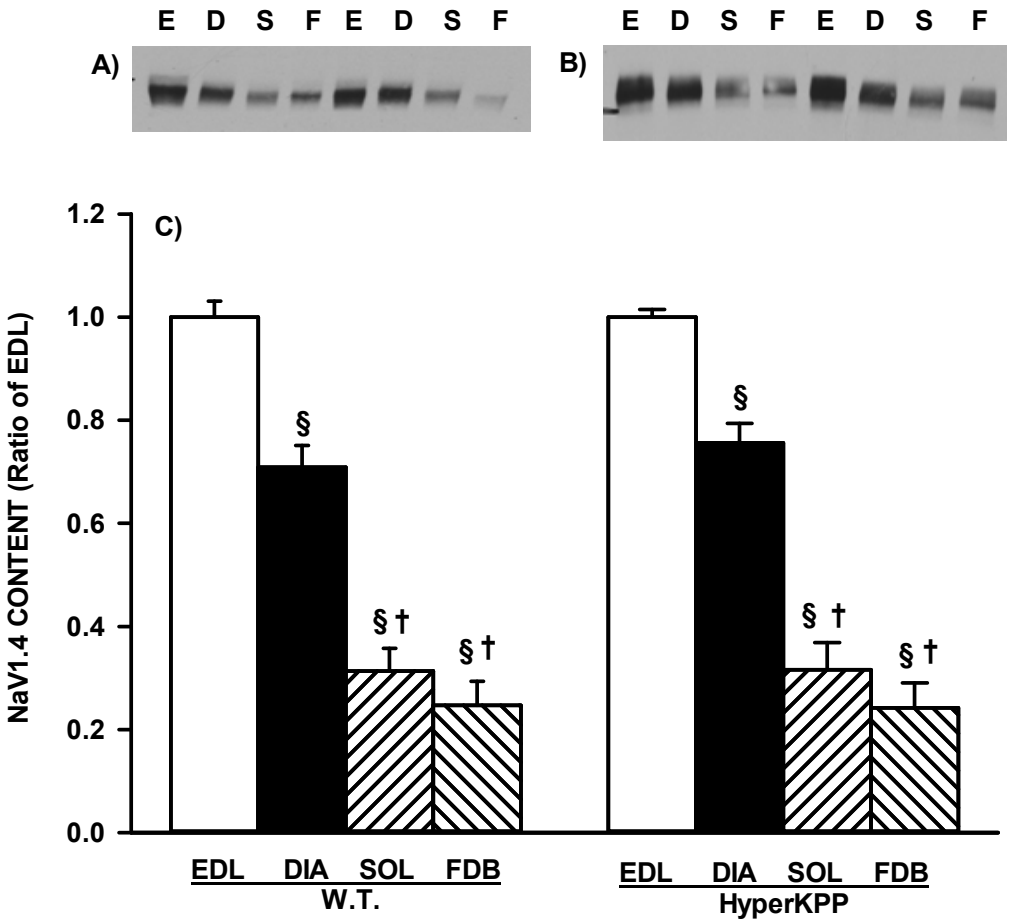

Figure 2.2. EDL had the largest while soleus and flexor digitorum brevis (FDB) had the lowest Nav1.4 channel protein content. Representative Western blots for wild-type (A) and HyperKPP (B) muscles. E, EDL; D, diaphragm; S, soleus; F, FDB. C: mean Nav1.4 channel protein content expressed as a ratio of the content in EDL. Vertical bars represent the SE of 7–8 muscles. DIA, diaphragm; SOL, soleus. §Significantly different from EDL; †significantly different from diaphragm, ANOVA, and LSD, $P < 0.05$.

the M1592V mutation might influence contractility in different muscles. For wild-type mice, diaphragm had the highest total Na^+ influx (i.e., no TTX) followed by EDL and soleus (Fig. 2.3). For these muscles, adding 500 nM TTX barely reduced Na^+ influx by $19-62$ nmol·g wet weight^{-1}·min^{-1}. Total Na^+ influxes were significantly greater in HyperKPP than in wild-type EDL, diaphragm, and soleus. Adding 500 nM TTX significantly reduced Na^+ influx in all three HyperKPP muscles to levels similar to those observed in TTX-exposed wild-type muscles. TTX-sensitive Na^+ influxes in HyperKPP diaphragm were 21% greater than in HyperKPP EDL and soleus. Interestingly, both total and TTX- sensitive Na^+ influxes were very small in HyperKPP FDB and were not significantly different from wild-type FDB. So, the order of the TTX-sensitive Na^+ influx in HyperKPP muscles is diaphragm > EDL ~ soleus >>> FDB which is quite different from the order for Nav1.4 channel content given above.

MUSCLE CONTRACTILITY

The large Na^+ influx in HyperKPP muscles is responsible for the membrane depolarization, and the force depression is due to the depolarization-induced Na^+ channel inactivation (Clausen *et al.*, 2011). Thus, the aim here was to measure the capacity of HyperKPP muscles to generate tetanic force in normal and at high $[K^+]_e$ and determine whether it correlates with the TTX-sensitive Na^+ influx. Skeletal muscles have different K^+ sensitivities. For example, the $[K^+]_e$ at which twitch and tetanic force start to decrease is lower in soleus than EDL (Cairns *et al.*, 1997; Yensen *et al.*, 2002). To determine the differences in K^+ sensitivity between wild-type and HyperKPP muscles, it was important to choose an $[K^+]_e$ for which the decrease in force was small in wild-type muscles, yet the force did not reach zero in HyperKPP muscles. Accordingly, the $[K^+]_e$ challenge was adjusted to cause similar decreases in tetanic

FIGURE 2.3

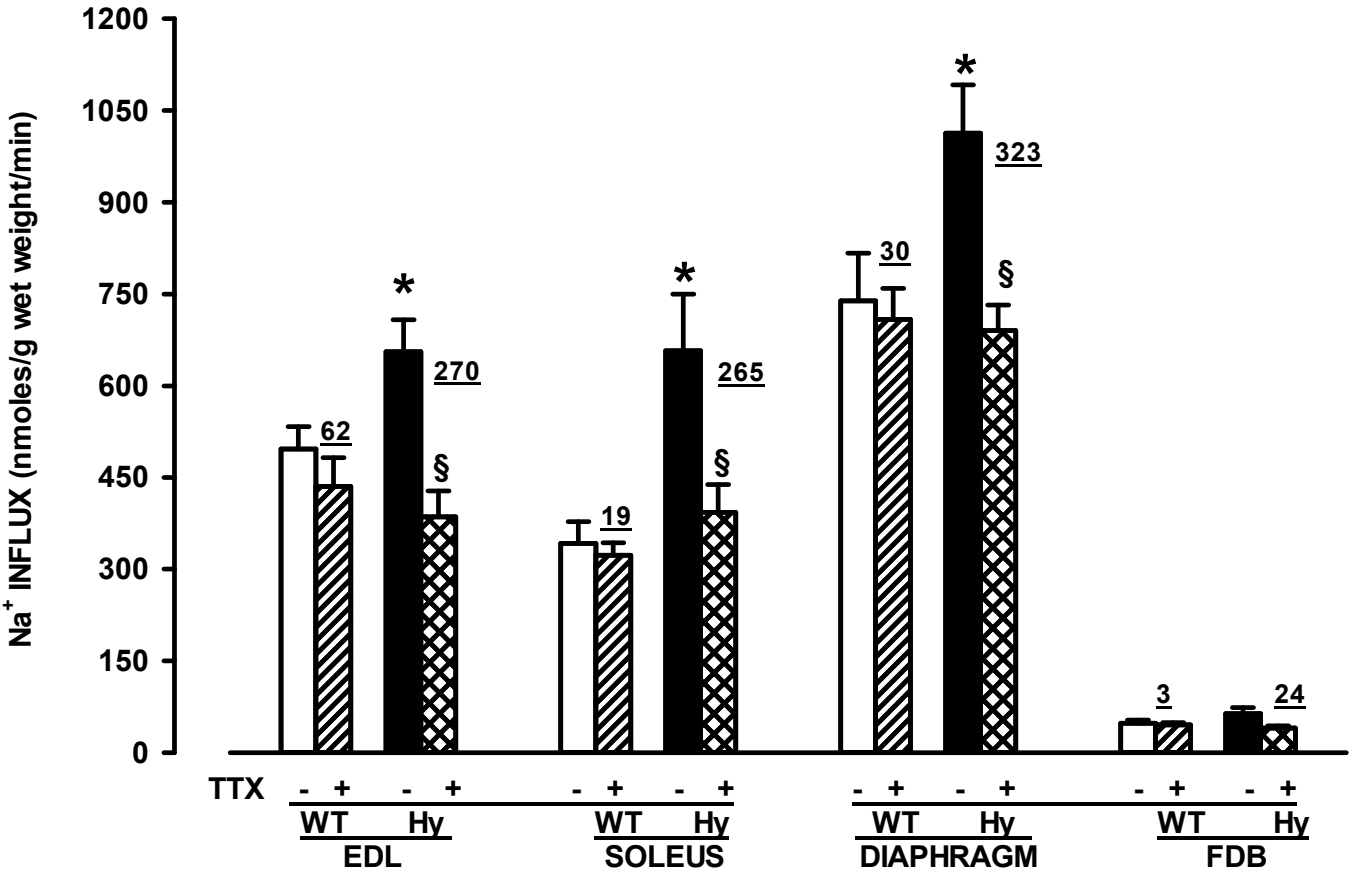

Figure 2.3. Tetrodotoxin (TTX)-sensitive $^{22}Na^+$ influx was the largest in HyperKPP diaphragm and the lowest in HyperKPP FDB, while those for HyperKPP EDL and soleus were slightly less than in diaphragm. We measured Na^+ influx by incubating muscles 10 min in the presence of 2 μCi of $^{22}Na^+$. When present (+), TTX concentration was 500 nM TTX. Numbers beside each open column represent the difference in mean $^{22}Na^+$ influx with and without TTX. Vertical bars represent the SE of 5 muscles. WT, wild type; Hy, HyperKPP. §Significantly different from 0 nM TTX; *significantly different from wild type, ANOVA, and LSD, $P < 0.05$.

force in all wild-type muscles (~30%). In this study, the $[K^+]_e$ challenge was 11 mM for EDL and FDB and 10 mM for soleus and diaphragm. Finally, since administration of calcium gluconate is known to alleviate symptoms in HyperKPP patients (Gamstorp *et al.*, 1957), we also characterized the effect of increased extracellular $[Ca^{2+}]$ ($[Ca^{2+}]_e$) on the contractility in HyperKPP muscles.

EDL. Peak tetanic forces were first measured immediately after muscle length adjustment while muscles were superfused with 4.7 mM K^+. At 1.3 mM Ca^{2+}, mean peak tetanic force of wild-type EDL was 30 N/cm^2, a value that is significantly greater than the 8 N/cm^2 generated by HyperKPP EDL (Fig. 2.4*A*). The decreases in mean peak tetanic force during the subsequent 30 min equilibrium period were on average 1 and 0.5 N/cm^2 for wild-type and HyperKPP EDL, respectively (i.e., the differences in forces between time 30 and 0 min). An increase in $[K^+]_e$ from 4.7 to 11 mM reduced mean peak tetanic force by 8 and 6 N/cm^2 in wild-type and HyperKPP EDL, respectively. While the absolute decreases are similar, on a relative scale they are 80% for HyperKPP compared with 27% for wild type. Furthermore, the difference in force between wild-type and HyperKPP EDL was 74% at 4.7 mM K^+ and increased to 93% at 11 mM K^+. Finally, mean peak tetanic force at 11 mM K^+ was down to just 1.5 N/cm^2 for HyperKPP EDL compared with 21 N/cm^2 for wild-type EDL.

At 2.4 mM Ca^{2+}, mean peak tetanic forces of wild-type EDL measured at 4 and 11 mM K^+ were not different to those measured at 1.3 mM Ca^{2+}. For HyperKPP EDL, a higher $[Ca^{2+}]_e$ significantly improved tetanic force as the force measured after the muscle length

FIGURE 2.4

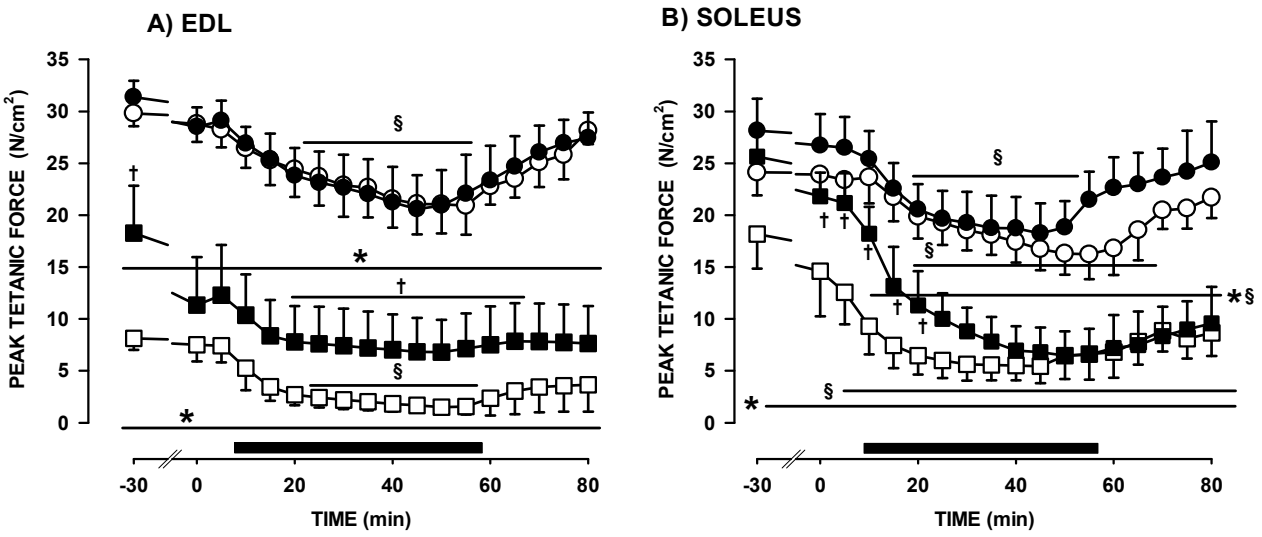

Figure 2.4 HyperKPP (A) EDL and (B) soleus developed less peak tetanic force than wild type muscles, especially at elevated $[K^+]_e$. Tetanic contractions were elicited with 200 msec train of pulses at 200 Hz for EDL and 140 Hz for soleus. In all experiments, muscle length was first adjusted to obtain maximum peak tetanic force, which is shown at time -30 min. Muscles were then allowed 30 min equilibrium before $[K^+]_e$ was increased. Symbols: ○, ●, wild type; □, ■, HyperKPP; ○, □, 1.3 mM Ca^{2+}; ●, ■, 2.4 mM Ca^{2+}; horizontal black bars represent the time muscles were exposed at 11 mM (EDL) and 10 mM (soleus, as explained in text); vertical lines represent the S.E. of 5 muscles. § Mean peak tetanic forces were significantly different from that at time 0 min,* All mean peak tetanic forces of HyperKPP EDL were significantly different from those of wild type, ANOVA and L.S.D., $P < 0.05$. † Mean peak tetanic force at 2.4 mM Ca^{2+} were significantly different from those at 1.3 mM, ANOVA and L.S.D., $P < 0.05$.

adjustment was 18 N/cm^2 at 2.4 mM Ca^{2+} compared with 8 N/cm^2 at 1.3 mM Ca^{2+}. Interestingly, during the 30 min equilibrium, the mean peak tetanic force of HyperKPP EDL decreased by 7 N/cm^2, representing the largest loss compared with wild-type EDL at 1.3 and 2.4 mM Ca^{2+} and HyperKPP EDL at 1.3 mM Ca^{2+}. The decrease in force following the increase in $[K^+]_e$ from 4.7 to 11 mM was slightly less at 2.4 mM Ca^{2+} (4.5 N/cm^2) than at 1.3 mM Ca^{2+} (6.0 N/cm^2). Therefore, in most cases, an increase in $[Ca^{2+}]_e$ from 1.3 to 2.4 mM improved the capacity of HyperKPP EDL to generate tetanic force while it had no impact on wild-type EDL.

Soleus. At 1.3 mM Ca^{2+} and after muscle length adjustment, wild-type soleus muscle generated 24 N/cm^2 compared with a slightly lower value of 19 N/cm^2 for HyperKPP soleus (Fig. 2.4*B*). In regard to maximum tetanic force, then, the differences between wild type and HyperKPP were smaller for soleus (5N/cm^2) than for EDL (22 N/cm^2). During the 30 min equilibrium, force in wild-type soleus decreased only slightly (1 N/cm^2) compared with the decrease for HyperKPP soleus (4 N/cm^2). Thus, prior to the increase in $[K^+]_e$, mean peak tetanic force of HyperKPP soleus became significantly less than that of wild-type soleus. An increase in $[K^+]_e$ from 4.7 to 10 mM K^+ decreased mean peak tetanic force by 8 N/cm^2 for both wild-type and HyperKPP soleus. Again, on a relative scale, the decreases were larger for HyperKPP (56%) than for wild type (32%). As observed for EDL, an increase in $[K^+]_e$ also augmented the difference in force between wild-type and Hyper- KPP soleus from 39 to 60%, which is less than for the EDL (74 to 93%).

At 2.4 mM Ca^{2+}, mean peak tetanic forces of wild-type and HyperKPP soleus were 4 and 6 N/cm^2, respectively, higher than those at 1.3 mM Ca^{2+}. Again, the decrease in force during

the 30 min equilibrium period was greater for HyperKPP than wild-type soleus muscle. Surprisingly, the decrease in force for HyperKPP soleus at 10 mM K^+ was large enough that the force generated was comparable to that of HyperKPP soleus kept at 1.3 mM Ca^{2+}.

Diaphragm. An increase in $[K^+]_e$ from 4.7 to 10 mM resulted in small decreases in peak tetanic force for all wild- type diaphragms and most (6 out of 8) HyperKPP diaphragms as shown with an example in Fig. 2.5*A*. There were, however, two HyperKPP diaphragms that generated a normal force at 4.7 mM K^+, while at 10 mM they lost all capacity to generate tetanic force upon stimulation within 5 min while developing a strong contracture (Fig. 2.5*B*). Upon a return to 4.7 mM K^+, diaphragm relaxed as the contracture force decreased back to zero, but there was no recovery to generate tetanic force upon stimulation. The mean peak tetanic force measurements of wild-type and HyperKPP diaphragms were, respectively, 11 and 7 N/cm^2 and were not significantly different (Fig. 2.5*C*). Raising $[K^+]_e$ to 10 mM reduced mean force of six of eight diaphragms by 2 N/cm^2 (21%), which was actually smaller than the 3 N/cm^2 (27%) for wild type (Fig. 2.5*C*). So, most HyperKPP diaphragms appeared less affected than EDL and soleus. The mean peak tetanic force of HyperKPP diaphragm exposed to $[Ca^{2+}]_e$ of 4 mM was *1*) significantly greater than at 1.3 mM Ca^{2+} and *2*) not appreciably different from the force of wild-type diaphragm also at 4 mM Ca^{2+}.

FDB. At 4.7 mM K^+, mean peak tetanic force of wild-type and HyperKPP FDB were, respectively, 28 and 32 N/cm^2 (Fig. 2.6*A*). HyperKPP FDB was the only muscle for which mean tetanic force was not lower than in wild type. At 1.3 mM Ca^{2+}, an increase in $[K^+]_e$ to 11 mM decreased force by 14 N/cm^2 (46%) in HyperKPP FDB and 9 N/cm^2 (32%) in wild-type

FIGURE 2.5

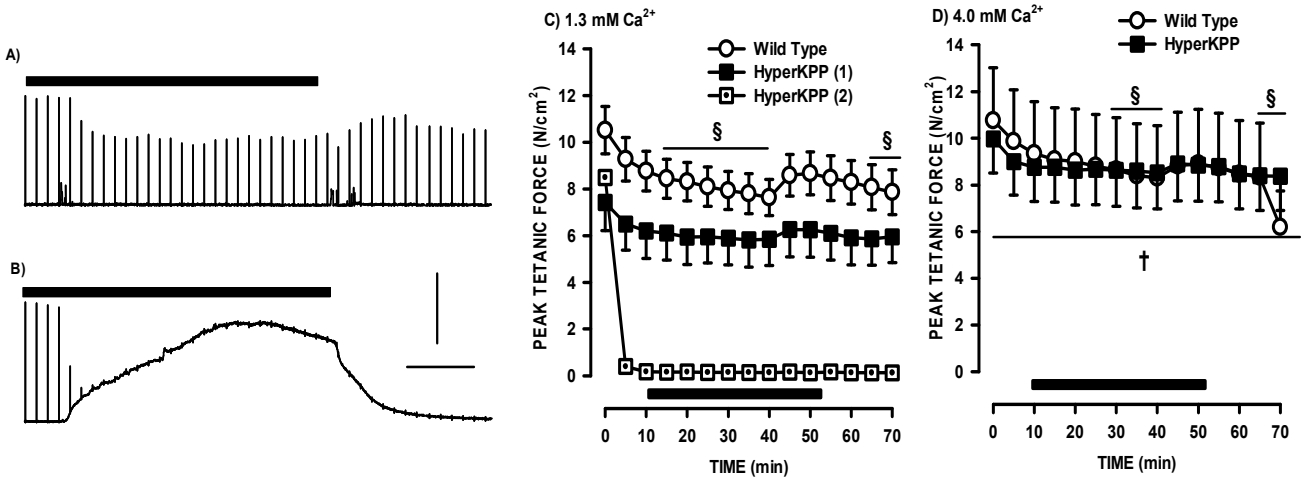

Figure 2.5. Variable effects of elevated $[K^+]_e$ in HyperKPP diaphragm. A-B) Representative chart recorder traces showing the effect of increasing $[K^+]_e$ from 4.7 to 10 mM K^+ when $[Ca^{2+}]_e$ was 1.3 mM. Effect of increasing $[K^+]_e$ from 4.7 to 10 mM while $[Ca^{2+}]_e$ was (C) 1.3 and (D) 4.0 mM. Tetanic contractions were elicited with 200 msec train of pulses at 140 Hz. Responses of HyperKPP diaphragms tested at 1.3 mM Ca^{2+} were divided into two groups: (1) those that behave as shown in A; (2) those that behave as shown in B (a situation never observed at 4.0 mM Ca^{2+}). Horizontal black bar represents the time at 10 mM K^+; vertical line in A, B represents 5 g; horizontal line 10 min. Vertical bars in C represent the S.E. of 5 wild type, and 6 HyperKPP(1) and 2 HyperKPP (2) diaphragms. There was no significant difference in mean peak tetanic force between wild type and HyperKPP diaphragm, ANOVA $P > 0.05$. §Mean peak tetanic forces were significantly different from that at time 0 min (observed only for wild type diaphragm), † Mean peak tetanic forces at 2.4 mM Ca^{2+} were significantly different from those at 1.3 mM Ca^{2+} (only for HyperKPP muscles) ANOVA and L.S.D., $P > 0.05$.

FDB, but the differences were not significant. Raising $[Ca^{2+}]_e$ to 4.0 mM had no effect (Fig. 2.6*B*). We obtain a large number of viable single fibers from FDB following a collagenase treatment. If HyperKPP FDB fibers are more depolarized than wild-type fibers as reported for soleus (Clausen *et al.*, 2011), then one should expect higher thresholds for contractions in HyperKPP fibers. This was not observed as wild-type and HyperKPP FDB single fibers had similar threshold values (Fig. 2.6*C*). We often observed with HyperKPP EDL and soleus sudden contractures possibly related to myotonic discharges (data not shown). Such contractures may then give rise to higher $[Ca^{2+}]_i$ and shorter sarcomere lengths in single FDB fibers. However, resting $[Ca^{2+}]_i$ and sarcomere lengths were not different between wild-type and HyperKPP single FDB fibers for $[K^+]_e$, ranging from 4.7 to 11 mM (Fig. 2.6, *D* and *E*). A similar situation was observed for $[Ca^{2+}]_i$ and sarcomere length during contractions.

FIBER TYPE COMPOSITION

It is known that HyperKPP muscles have more fibers expressing myosin IIA isoform than wild-type muscles (Hayward *et al.*, 2008). Here, the objective was to determine which muscles have significant changes in myosin isoform expression with an emphasis on whether HyperKPP muscles that had the smallest contractility defects in vitro (i.e., diaphragm and FDB) also had the smallest changes in myosin expression. Several muscle fibers express more than one myosin isoform; the numbers can be as high as 20–25% in EDL and soleus and 70% in FDB (Banas *et al.*, 2011). Therefore, for this study, we report our results in terms of the number of

FIGURE 2.6

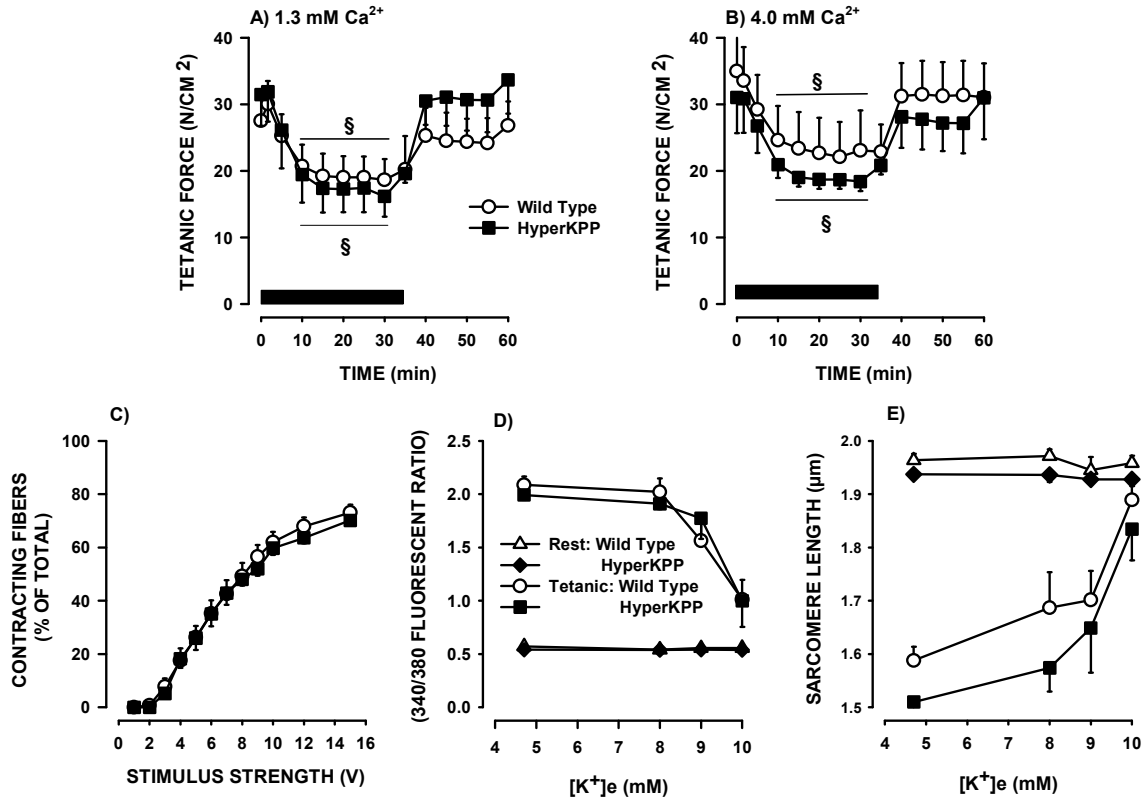

Figure 2.6. No evidence of abnormal contractility in FDB fibers from HyperKPP mice. Effects of 11 mM K^+ on tetanic force of small FDB muscle bundles at 1.3 (A) and 4.0 mM Ca^{2+} (B). Tetanic contractions were elicited with 200 msec train of pulses at 200 Hz. C: Number of contracting single FDB fibers at different stimulus strength expressed as a percent of the total number of fibers viewed under the microscope. D: Effects of K^+ on resting and tetanic myoplasmic Ca^{2+} in single FDB fibers. Fluorescence from fura-2 is expressed as a ratio of the fluorescence measured at 505 nm while the excitation wavelength was 340 nm divided by the fluorescence while excited at 380 nm. E: Effects of K^+ on sarcomere length of single FDB fibers at rest and during contraction. Horizontal black bar in A represents the time at 11 mM K^+. Number of samples: 5 bundles (A, B), 595 fibers from 8 wild type mice and 387 fibers from 5

mice (C), 5-8 fibers from 4 wild type and HyperKPP mice (D, E). There was no significant difference in mean peak tetanic force between wild type and HyperKPP FDB and between 1.3 and 4.0 mM Ca^{2+}, ANOVA, $P > 0.05$. § Mean peak tetanic forces were significantly different from that at time 0 min, ANOVA and L.S.D., $P > 0.05$.

fibers expressing each of the four myosin isoforms as opposed to the number of type I, IIA, IIB, and IIX fibers per se.

HyperKPP EDL muscles had the same number of fibers expressing myosin I and IIX compared with wild-type EDL (Fig. 2.7*A*). However, 49% of HyperKPP EDL fibers expressed myosin IIA, a percentage that was significantly greater than the 19% in wild-type EDL. The number of HyperKPP EDL fibers expressing myosin IIB was significantly lower by 15% compared with wild-type EDL. Significant differences in myosin expression were also observed for soleus (Fig. 2.7*B*). That is, the number of HyperKPP soleus fibers expressing myosin I was 9% greater and the number of those expressing myosin IIA was 8% lower compared with wild-type soleus. No significant difference was observed for diaphragm and FDB muscles (Fig.7, *C* and *D*).

EFFECT OF OUABAIN

Increasing the activity of the Na^+-K^+ pump activity helps restoring normal contractility in HyperKPP mouse muscle and in preventing paralytic attack in human patients (Wang & Clausen, 1976; Clausen *et al.*, 1980, 2011). We therefore tested how different HyperKPP muscles depend on the pump activity to sustain normal contractility compared with wild-type muscles. Addition of 10 μM ouabain had small effects on tetanic force of wild-type soleus, diaphragm, and FDB, causing 12–17% decrease in force within 30 min (Fig. 2.8*A*). Only wild-type EDL was largely affected, as ouabain caused a 61% decrease followed by a recovery when ouabain was washout out. Like its wild-type counterpart, HyperKPP FDB was not affected by the presence of ouabain (Fig. 2.8*B*). However, significant force losses were observed for HyperKPP EDL,

FIGURE 2.7

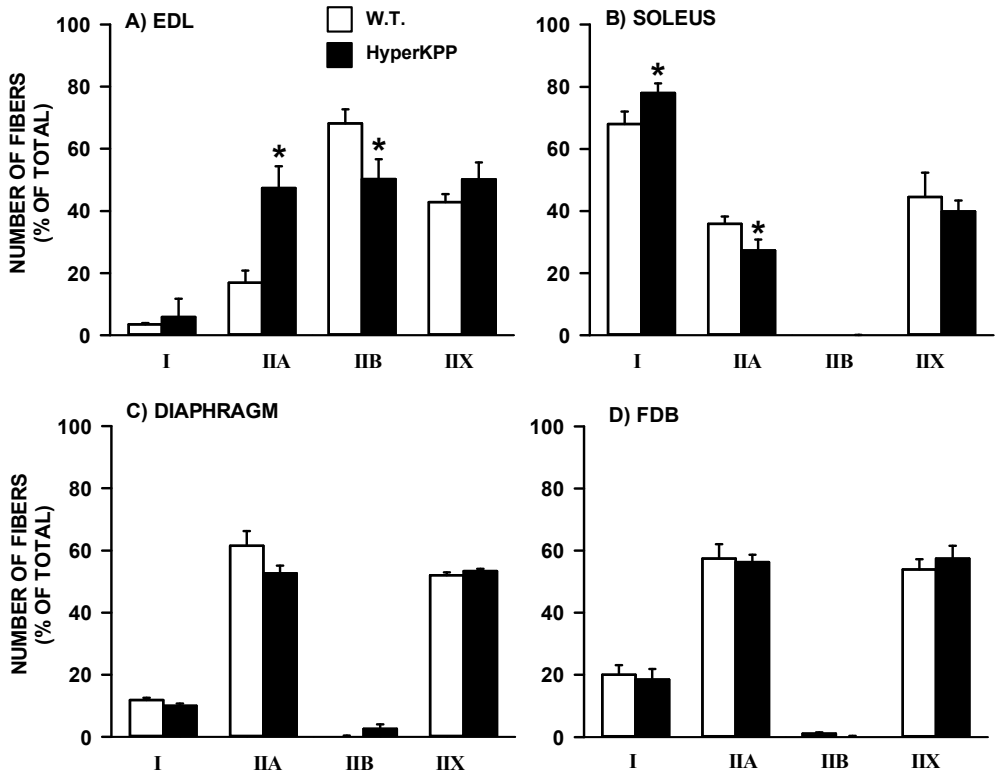

Figure 2.7. Significant changes in myosin expression occurred in HyperKPP EDL and soleus but not diaphragm and FDB. Many fibers expressed more than one myosin isoform. Here, the number of fibers represents how many fibers expressed each of the four myosin isoforms (and not the number of type I, IIA, IIB and IIX fibers). The numbers of fibers are expressed as a percent of the total number of fibers. Vertical bars represent the S.E. of 5 muscles. * Significantly different from wild type muscle.

FIGURE 2.8

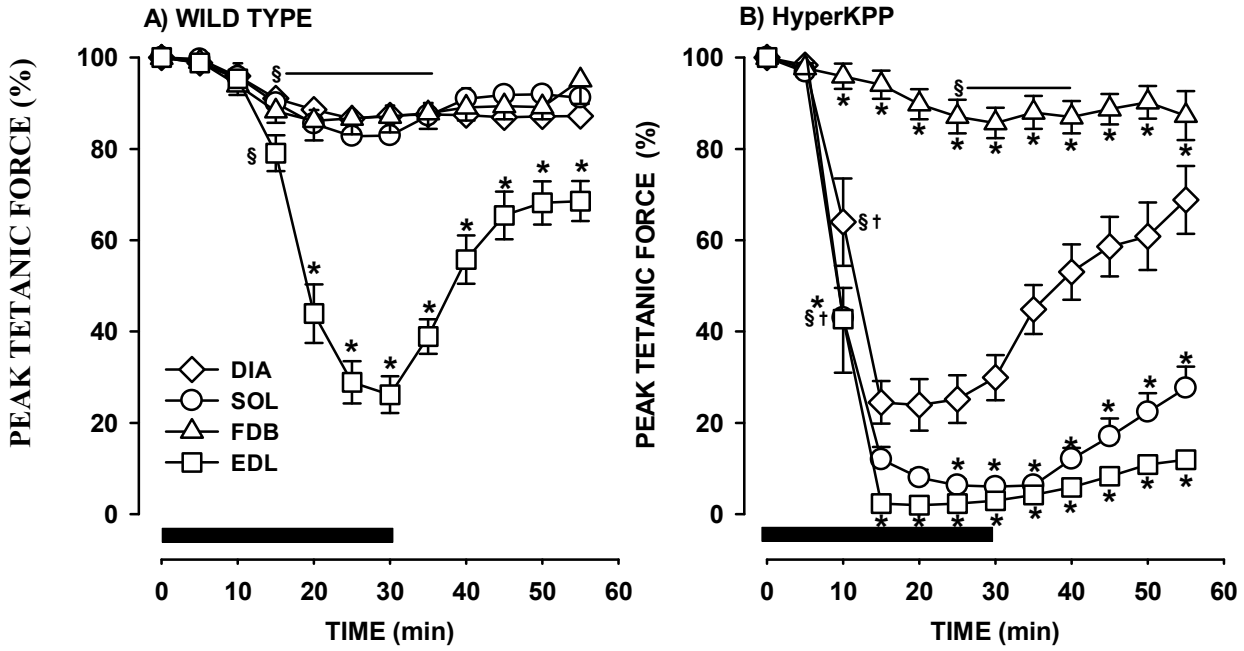

Figure 2.8. Ouabain depressed peak tetanic force in HyperKPP EDL, soleus, diaphragm and in wild type EDL while both wild type and HyperKPP FDB were unaffected. Peak tetanic force is expressed as a percent of the force at time 0 min. Horizontal black bar represents the time muscles were exposed to 10 μM ouabain. Vertical bars represent the S.E. of 5 muscles. * Mean peak tetanic force significantly different from that of diaphragm; § Indicate when the force depression became significant different from 100% until the 55th min or as indicated by the horizontal line; ✝ Indicate when the force of HyperKPP muscles became significantly different from the force in wild type muscles; in all cases the differences remained significant until the 55th min.

soleus and diaphragm, and the losses occurred while $[K^+]_e$ was kept at 4.7 mM. Peak tetanic force decreased to almost zero for HyperKPP EDL and soleus. HyperKPP diaphragm was less affected as the tetanic force decreased by 69%. Furthermore, upon removal of ouabain, only the diaphragm recovered substantial tetanic force, while HyperKPP EDL and soleus showed only minimal recovery.

EFFECTS OF Ni^{2+} AND BTP-2

The improvement of force generation by increases in $[Ca^{2+}]_e$ is not unique to HyperKPP muscles. It is also observed in wild-type muscles exposed to 10–11 mM K^+, except that $[Ca^{2+}]_e$ must be raised to 10 mM (Cairns *et al.*, 1998), while increases to 2.3–4.0 mM Ca^{2+} have no effect (this study). Both wild-type muscles at 10–11 mM K^+ and HyperKPP muscles at 4 mM K^+ exhibit significant membrane depolarization (Yensen *et al.*, 2002; Clausen *et al.*, 2011). Such depolarization reduces *1*) Ca^{2+} entry via L-type Ca^{2+} channels (Cav1.1 channels) during the initiation of muscle contraction and maintenance of the plateau phase during a tetanus (Cifelli *et al.*, 2008), and *2*) store operated Ca^{2+} entry (SOCE), which helps replenish Ca^{2+} sarcoplasmic reticulum content from extracellular source (Kurebayashi & Ogawa, 2001). We therefore tested the possibility that Ca^{2+} entry in HyperKPP muscles is increased via either pathway as a potential mechanism for the force increase by Ca^{2+}.

To test this possibility we first exposed wild-type and HyperKPP muscles to 5 mM Ni^{2+}, which blocks both pathways (Hobai *et al.*, 2000; Kurebayashi & Ogawa, 2001). The experimental protocol was as described by Thornton et al. (Thornton *et al.*, 2011), with an $[Ca^{2+}]_e$ of 2.4 mM. Exposing EDL to Ni^{2+} first caused a sudden increase in force followed by a decrease (Fig. 2.9*A*). Prior to the removal of Ni^{2+}, mean peak tetanic forces of wild-type and HyperKPP

EDL were, respectively, 71 and 52% of the mean force at time 0 min; the 19% difference being significant at $P = 0.06$. The sudden increase in tetanic force upon exposure and removal of Ni^{2+} was not observed with soleus, diaphragm and FDB. Ni^{2+} decreased peak force to a significantly greater extent in HyperKPP than in wild-type soleus as mean peak forces decreased to 63 and 40%, respectively (Fig. 2.9*B*). Ni^{2+} also reduced peak force in diaphragm and FDB, but with no significant difference between wild type and HyperKPP (Fig. 2.9, *C* and *D*).

Next, we tested the effects of 20 μM BTP-2, a known blocker of SOCE (Thornton *et al.*, 2011). For EDL, a sudden increase in force was also observed upon exposure to and removal of BTP-2 but to a lesser extent compared with the Ni^{2+} effect (Fig. 2. 10*A*). Interestingly, the subsequent decrease in peak force was significant in wild-type but not in HyperKPP EDL. BTP-2 caused decreases in peak force in soleus without any difference between wild type and HyperKPP (Fig. 2.10*B*). BTP-2 caused greater decreases in peak force in HyperKPP than in wild-type diaphragm and FDB, but significant differences were only observed for diaphragm (Fig. 2.10, *C* and *D*). Finally, contrary to the Ni^{2+} effects, removal of BTP-2 was not followed by an increase in force toward pre-exposure values.

FIGURE 2.9

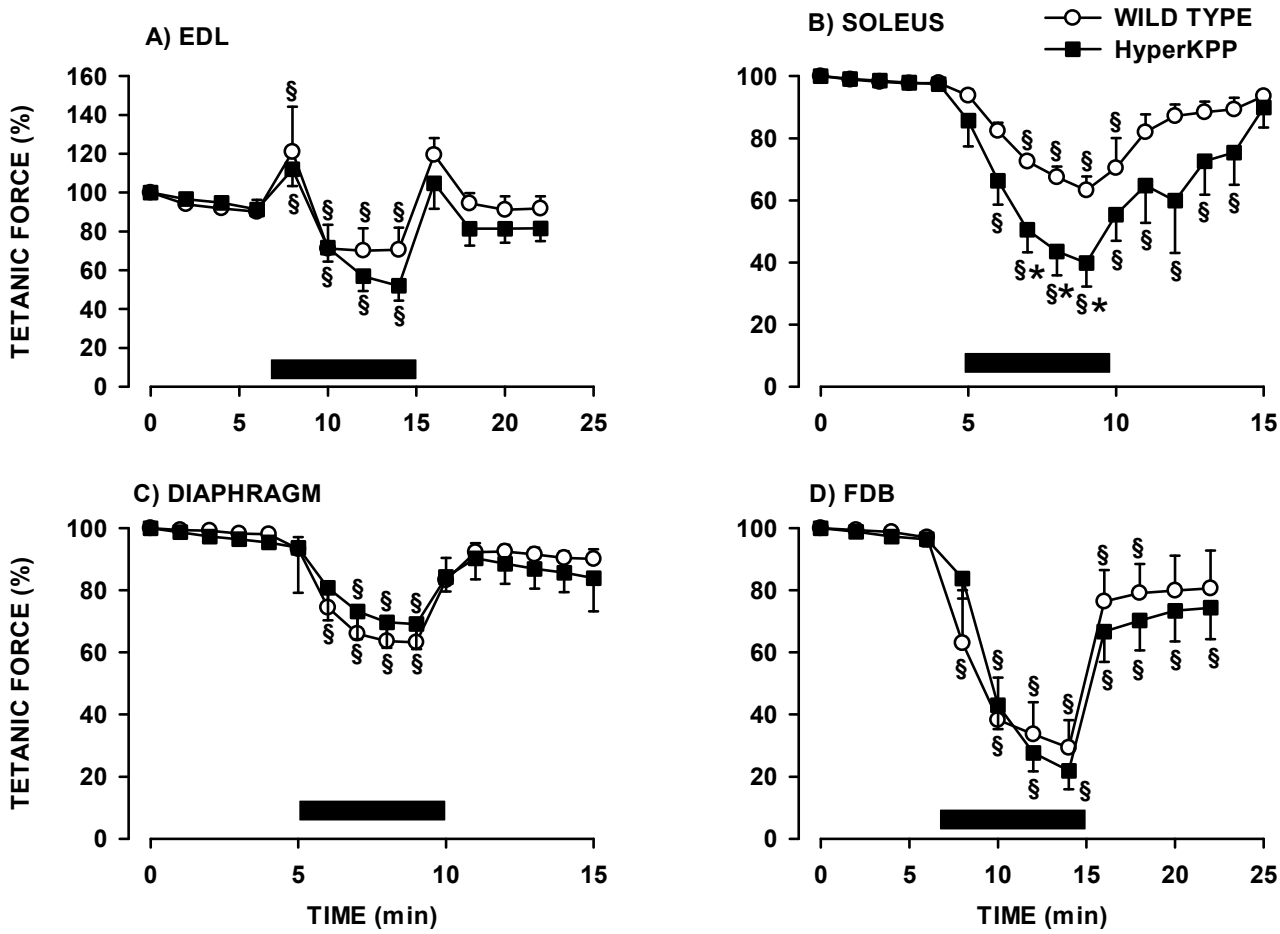

Figure 2.9. Ni^{2+} reduced peak tetanic force to a greater extent in HyperKPP than wild type EDL and soleus, while no difference was observed for diaphragm and FDB. EDL and FDB muscles were stimulated with train of pulses at 120 Hz every 2 min while soleus and diaphragm were stimulated with train of pulses at 100 Hz every min. $[Ca^{2+}]_e$ was 2.4 mM for all muscles. Horizontal black bars represent the time during which muscles were exposed to 5 mM Ni^{2+}. Vertical bars represent the S.E. of 5 muscles. § Mean peak tetanic force significantly different from Time 0 min.* Mean peak tetanic force of HyperKPP muscles significantly different from the mean value for wild type muscles, ANOVA, L.S.D., $P < 0.05$.

FIGURE 2.10

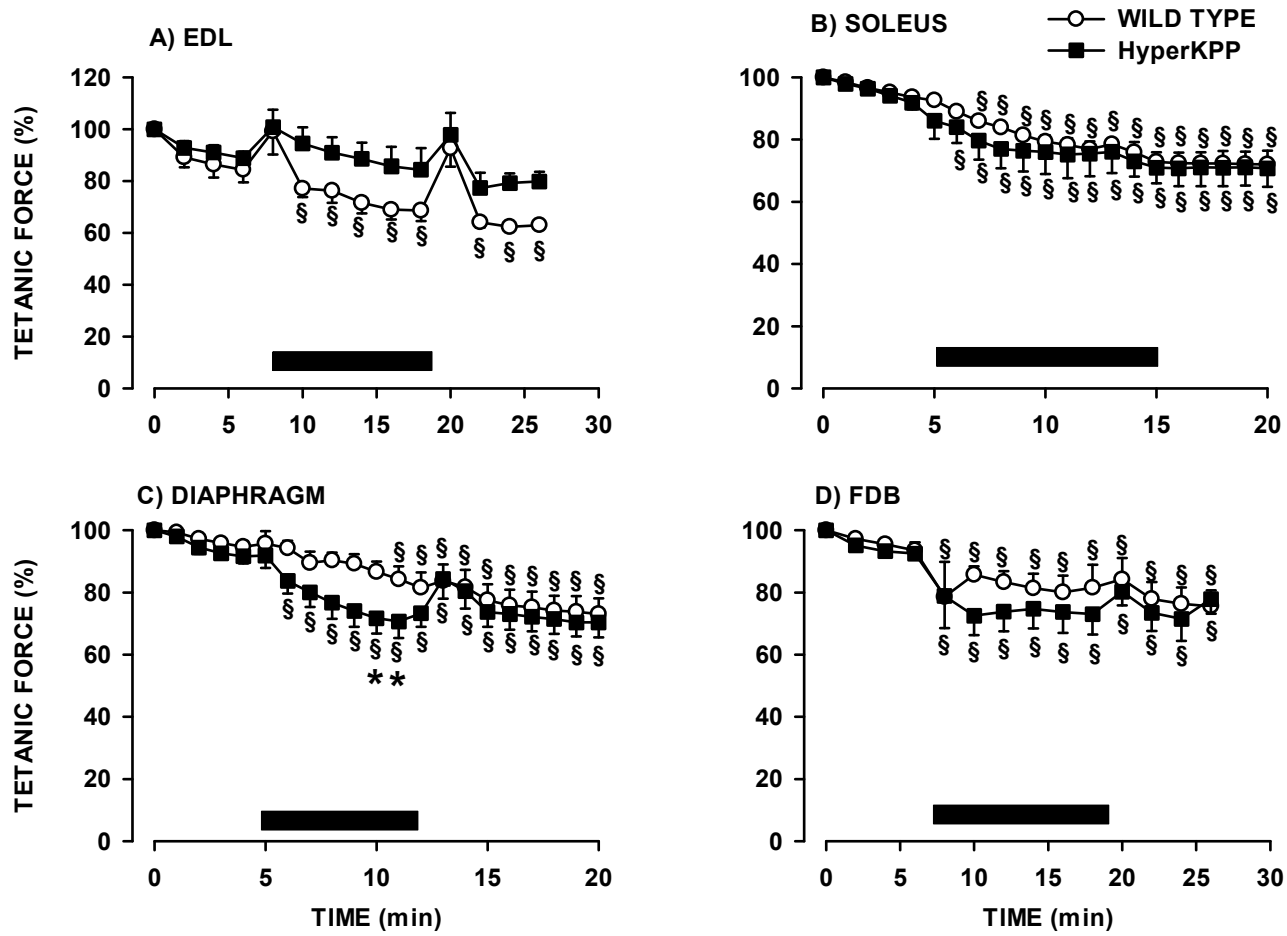

Figure 2.10. BTP-2 reduced peak tetanic force to a greater extent in HyperKPP than wild type diaphragm, while no difference was observed for EDL, soleus and FDB. EDL and FDB muscles were stimulated with train of pulses at 120 Hz every 2 min while soleus and diaphragm were stimulated with train of pulses at 100 Hz every min. $[Ca^{2+}]_e$ was 2.4 mM for all muscles. Horizontal black bars represent the time during which muscles were exposed to 20 μM BTP-2. Vertical bars represent the S.E. of 5 muscles. § Mean peak tetanic force significantly different from Time 0 min.* Mean peak tetanic force of HyperKPP muscles significantly different from the mean value for wild type muscles, ANOVA, L.S.D., $P < 0.05$.

DISCUSSION

The major findings of this study are: *1*) HyperKPP muscles contained fewer Nav1.4 channels than wild-type muscles; *2*) for HyperKPP, Nav1.4 channel protein content was in the order of EDL > diaphragm >> soleus ~ FDB muscles, *3*) whereas the TTX-sensitive Na^+ influx was in the order of diaphragm > EDL ~ soleus >>> FDB; 4) HyperKPP EDL and soleus had the largest contractile defects in vitro, while the defects were of smaller magnitude in most diaphragms and nonexistent in FDB; *5*) ouabain caused large decreases in force in HyperKPP EDL ~ soleus > diaphragm, but not in FDB; and *6*) significant changes in myosin isoform expression occurred in HyperKPP EDL and soleus, but none in diaphragm and FDB.

Nav1.4 CHANNEL CONTENT AND Na^+ INFLUX IN HYPERKPP MUSCLES

The relative differences in Nav1.4 channel protein content between wild-type EDL, diaphragm, and soleus, measured in this study, were similar to those reported in ^{3}H-labeled saxitoxin (a Na^+ channel blocker) binding studies (Bay & Strichartz, 1980). Furthermore, Na^+ current density near the motor end plate is greater in FDB than soleus, but away from the plate the current density is the same (Milton & Behforouz, 1995). Since the motor end plate comprises a very small part of the cell membrane, it is therefore not surprising that soleus and FDB had similar Nav1.4 channel content. So overall, while it was not possible to normalize the Nav1.4 channel content relative to that of β-actin because the expression of the latter differs between muscles, our Western blot analysis of Nav1.4 channel protein content in wild-type muscles is in agreement with previous studies. Similarly, the small TTX-sensitive Na^+ influxes in wild type were in agreement with the fact that TTX causes small membrane hyperpolarizations in EDL (Yensen *et al.*, 2002; Clausen *et al.*, 2011), while the greater Na^+ influx in HyperKPP than in wild-type EDL and soleus was as reported in a previous study (Clausen *et al.*, 2011).

A novel finding of this study is that the M1592V mutation significantly decreased the total Nav1.4 channel content in EDL, soleus, diaphragm and FDB compared with their wild-type counterparts, while it had no effect on the relative contents of the four muscles, which remained EDL > diaphragm > soleus > FDB. As previously shown, TTX-sensitive Na^+ influx was higher in HyperKPP than wild- type EDL and soleus (Clausen *et al.*, 2011). This study now reports that the same is observed for diaphragm but not for FDB, which had by far the lowest Na^+ influx. The Met1592Val mutant mRNA constitutes 42% of the total Nav1.4 mRNA in hindlimb muscles (Hayward *et al.*, 2008). Although we do not have tools at present to measure the relative amount of normal and mutant Nav1.4 proteins, if a corresponding protein ratio is maintained, then the large TTX-sensitive Na^+ influx in HyperKPP EDL may result from a Nav1.4 content only 23% of that Nav1.4 in wild-type EDL.

Importantly, the TTX-sensitive Na^+ influx did not simply correlate with the Nav1.4 channel content, as the HyperKPP diaphragm had the largest Na^+ influx despite having the second highest channel content, while the HyperKPP soleus had similar Na^+ influx as the EDL with only one-third of the channel content. Several possibilities may explain this observed lack of correlation between channel content and Na^+ influx. First, the normal and mutant Nav1.4 channels may be expressed on specific muscle membranes in varying ratios not related to mRNA ratio of the normal and mutant alleles. Second, the availability of Nav1.4 channels as reflected by their extent of inactivation may vary among different muscles. Third, other membrane components may contribute to the measured Na^+ influx in this complex system. From a physiological point of view, the extent of the resulting Na^+ influx should be a major determinant of the contractile abnormalities associated with the M1592V mutation. This leads to the

important additional question of whether the differences in Na^+ influx between HyperKPP muscles correlate with the differences in contractile abnormalities.

DIFFERENCES IN HYPERKPP SYMPTOMS AMONG MUSCLES

We used two approaches to document the extent of HyperKPP symptoms in various muscles. The first approach was a direct measurement of the contractile defects in vitro. For this approach, we measured the peak tetanic force at 4.7 mM (normal) and high $[K^+]_e$. The depression of force at elevated $[K^+]_e$ is due to a membrane depolarization that inactivates Nav1.4 channels. The relationship between force and resting membrane potential is the same between EDL and soleus muscles, but the extent of depolarization following an increase in $[K^+]_e$ is greater in soleus (Cairns *et al.*, 1997; Yensen *et al.*, 2002). This is why muscles have different sensitivity to the K^+-induced force depression. Consequently for this study, we chose a specific elevated $[K^+]_e$ of either 10 or 11 mM K^+, so the decreases in tetanic force were quite similar between various wild-type muscles (i.e., between 27 and 32%). While concentrations of 10–11 mM K^+ are much higher than the 6–8 mM plasma K^+ reported during paralytic attacks in human suffering from HyperKPP (Gamstorp *et al.*, 1957; Streeten *et al.*, 1971; Wang & Clausen, 1976), it is well established that interstitial $[K^+]_e$ during exercise is 4–5 mM above that of plasma $[K^+]_e$ (Nielsen *et al.*, 2004; McKenna *et al.*, 2008). Therefore, interstitial $[K^+]_e$ may reach 10 to 13 mM during the myotonic discharges that precede paralytic attacks.

The second approach was indirect by determining any changes in myosin isoform expression. The latter approach was based on the shift toward more fibers expressing myosin IIA in HyperKPP muscles (Hayward *et al.*, 2008). Periods of myotonic discharge are known to precede the paralytic attacks in individuals with HyperKPP (Miller *et al.*, 2004; Jurkat-Rott & Lehmann-Horn, 2007). Under anesthesia, myotonic discharges in muscles of HyperKPP mice

have also been reported, but only when the electromyography (EMG) needle is moved (Hayward *et al.*, 2008). We have also observed with EMG measurements greater electrical activity in muscles of fully awakened HyperKPP mice compared with those of wildtype muscles (D. DeJong and J.-M. Renaud, unpublished results). Such greater electrical activity in the HyperKPP mice is most likely caused by myotonic discharges, which over time would be expected to produce training effects that result in a shift toward more oxidative type IIA fibers. In this study, we observed a correlation between muscles with the most prominent shift in myosin isoform expression (e.g., EDL) and the greatest susceptibility to depressed peak tetanic force. As previously reported (Hayward *et al.*, 2008), major contractile defects and a major shift in myosin isoform expression were observed for mouse EDL and soleus in HyperKPP mice. Here, we observed that the situation is not the same for HyperKPP FDB and diaphragm muscles. For the FDB, we saw no evidence for any shift in myosin expression nor for a contractile defect in terms of stimulation threshold, tetanic $[Ca^{2+}]_i$, peak tetanic force and sarcomere length; i.e., it appears that the FDB muscle is resistant to the effects of mutant Nav1.4 in this mouse model of HyperKPP.

Most HyperKPP diaphragm had some contractile defects, but the extent was much less than for EDL and soleus. At 4.7 mM K, HyperKPP diaphragm generated 29% less force than wild-type diaphragm; a value that was smaller than for EDL (74%) and soleus (39%). When $[K^+]_e$ was increased, the differences in force between wild-type and HyperKPP increased in EDL (to 93%) and soleus (to 60%) while it actually decreased in diaphragm (to 23%). Also, there was no shift in myosin isoform expression in HyperKPP diaphragm, while there were significant ones in EDL and soleus. It thus appears that diaphragm is relatively spared from the

consequences of the HyperKPP mutation under baseline conditions compared with EDL and soleus.

There were two HyperKPP diaphragm muscles that became fully paralyzed at 11 mM K^+. It is noteworthy that this behavior is not specific to diaphragm, as we also occasionally observed sudden contractures and paralysis in EDL and soleus that could occur while $[K^+]_e$ was normal or elevated (data not shown). These findings are consistent with clinical observations indicating that most HyperKPP patients do not suffer respiratory distress, except for very few cases (Creutzfeldt *et al.*, 1963; Bradley *et al.*, 1990). Given that the myosin isoform expression did not differ between wild-type and HyperKPP diaphragm, this muscle expressing the mutant Nav1.4 channels may be less likely to develop myotonia and increases in $[K^+]_e$ that could otherwise trigger paralytic attacks.

ROLE OF Na^+ AND Na^+-K^+ PUMP IN THE DIFFERENCES IN HYPERKPP SYMPTOMS AMONG MUSCLES

Our major objective was to establish how the differences in HyperKPP symptoms between muscles may depend on Nav1.4 channel content and TTX-sensitive Na^+ influx. In regard to the FDB, it had the lowest Nav1.4 channel content and by far the lowest TTX-sensitive Na^+ influx of the four muscles tested. The most logical explanation for the lack of HyperKPP symptoms in this muscle is the very low Na^+ influx. However, the same explanation does not hold for EDL, soleus, and diaphragm.

As discussed above, the differences in tetanic force between wild-type and HyperKPP muscles at normal $[K^+]_e$ were greater in EDL compared with soleus (Fig. 2.4), which differs from a previous study performed at lower experimental temperature and stimulation frequencies (Clausen *et al.*, 2011). Furthermore, the shifts in myosin isoform expression were much larger

in EDL than in soleus. While the lower shift in soleus may in part be because most fibers already expressed myosin I and IIA, it may also be an indication of lower frequency of myotonic discharge. The greater impairment of contractility in HyperKPP EDL compared with soleus occurred despite the fact that these two muscles had similar TTX-sensitive Na^+ influx. Moreover, the HyperKPP diaphragm, which had the largest TTX-sensitive Na^+ influx, showed smaller contractile defects and no shift in myosin isoform expression. We therefore suggest that, while a large Na^+ influx is important in triggering myotonic discharges and eventually paralysis in HyperKPP muscles (likely via membrane depolarization), the diaphragm may express other membrane components that render it more resistant to depolarization and thereby contribute to protection from paralysis.

As a first step toward understanding the differential vulnerability of specific muscles to paralysis in this model, we determined the importance of the Na^+-K^+ pump for which increased activity can prevent paralytic attacks in HyperKPP patients (Wang & Clausen, 1976; Clausen *et al.*, 2011). For EDL and soleus harboring HyperKPP mutants, exposure to ouabain dramatically reduced tetanic force (Fig. 2.7). This suggests that the Na^+-K^+ pump plays a major role in maintaining membrane excitability in those two HyperKPP muscles and is also relevant, albeit to a lesser extent, in the wild-type EDL. In agreement with possible protective mechanisms noted above for the diaphragm, the loss of tetanic force was significantly less in HyperKPP diaphragm compared with the EDL and soleus. Furthermore, mutant diaphragm muscle demonstrated a more rapid recovery of force upon removal of ouabain than EDL and soleus.

Another consideration is that moderate exercise helps to prevent paralytic attacks by unknown mechanisms (Gamstorp *et al.*, 1957), and it is possible that continuous activity of the diaphragm may similarly contribute to protection. A final consideration is the diaphragm

dependency on extracellular Ca^{2+} for contraction. Removal of extracellular Ca^{2+} slightly reduces force generation in EDL and soleus, whereas it completely abolishes contractility in diaphragm within 15 min similarly to cardiac muscle for which contractility is abolished in 5 min (Viirès *et al.*, 1988; Zavecz *et al.*, 1991). Furthermore, there is evidence for a greater activity of the $Na^{+/}Ca^{2+}$ exchanger in diaphragm than in hindlimb muscles (Zavecz *et al.*, 1991; Zavecz & Anderson, 1992). When the sarcolemma depolarizes and generates smaller action potential amplitude, contractility may then be less affected in diaphragm than in EDL and soleus because of higher myoplasmic Ca^{2+} during contraction similar to the observation in cardiac muscle. Upon membrane depolarization of HyperKPP muscles with increased myoplasmic Na^{+} (Ricker *et al.*, 1989; Amarteifio *et al.*, 2012), the $Na^{+/}Ca^{2+}$ exchanger may operate in the reverse mode, increasing Ca^{2+} influx and force during contractions. Such mechanism could be relevant during the ouabain exposure, which likely caused an increase in myoplasmic Na^{+} in view of the large influx. Under conditions of strong membrane depolarization leading to action potential failure, of course, this mechanism would not be expected to improve diaphragm force. In this case, an excessive depolarization may have inactivated most Na^{+} channels, while activating L-type Ca^{2+} channels and triggering $Na^{+/}Ca^{2+}$ exchanger reverse mode, leading to high myoplasmic Ca^{2+} and thus the observed large contracture. Overall, these findings are consistent with the notion that other membrane components in the diaphragm play important role in modifying the effects of excess Na^{+} influx on excitability.

Ca^{2+} ENTRY IN HYPERKPP MUSCLES

Increasing $[Ca^{2+}]_e$ from 1.3 to 10 mM improves force generation in wild-type muscle exposed to elevated $[K^{+}]_e$ (Cairns *et al.*, 1998), while increases to 2.3–4.0 have no effect (this study). However, for HyperKPP muscles, similar increases in $[Ca^{2+}]_e$ (to 2.3 mM for EDL and

soleus, to 4.0 mM for diaphragm) improved force generation even when $[K^+]_e$ was 4 mM K^+, i.e., HyperKPP muscles depend more on extracellular Ca^{2+} than wild-type muscles. HyperKPP FDB was the only exception, possibly because it has no defective contractility and thus may have a lower Ca^{2+} sensitivity similar to wild-type muscles. Our results are also consistent with the fact that administration of calcium gluconate is known to alleviate symptoms in HyperKPP patients (Gamstorp *et al.*, 1957).

As mentioned in RESULTS, force improvement by Ca^{2+} in both wild-type and HyperKPP muscles are observed when the cell membrane is depolarized, a condition that can lower Ca^{2+} entry via Cav1.1 channels (blocked by Ni^{2+}) and SOCE (blocked by Ni^{2+} and BTP-2). In wild-type EDL, Ni^{2+} and BTP-2 reduced force to the same extent, suggesting that the force decrease in the presence of either Ni^{2+}or BTP-2 is related to a lower Ca^{2+} entry through SOCE as previously suggested (Thornton *et al.*, 2011). For wild-type soleus, the force depression was 15% greater in the presence of Ni^{2+} than in the presence of BTP-2, suggesting that Ca^{2+} entry via Cav1.1 channels is important to maintain tetanic force. The force reduction by BTP-2 was the same in wild-type and HyperKPP soleus, suggesting that SOCE is not affected in HyperKPP soleus. However, BTP-2 reduced force to a lower extent in wild-type than in HyperKPP EDL. Thornton et al. (2011) have reported that muscles from old mice are less affected by BTP-2 than muscles from young mice, and they demonstrated that it was because Ca^{2+} entry through SOCE was impaired with aging (Thornton *et al.*, 2011). We therefore proposed that contrary to soleus, SOCE is impaired in HyperKPP EDL. More importantly, if Ca^{2+} entry via SOCE is reduced in HyperKPP EDL, it is then an unlikely mechanism for the force increase by Ca^{2+}.

Force depression in HyperKPP soleus with Ni^{2+} was twice as large as with BTP-2. This suggests an important Ca^{2+} entry through Cav1.1 during tetanic contractions in HyperKPP soleus,

and more importantly this Ca^{2+} entry plays an important role in maintaining contractility over time. The same may be true for HyperKPP EDL because BTP-2 did not significantly reduce force whereas Ni^{2+} did, again supporting an important Ca^{2+} entry via Cav1.1 channels in HyperKPP EDL. On the basis of our results, we suggest that HyperKPP EDL and soleus depend more than their wild-type counterparts on Ca^{2+} entry via Cav1.1 channels, and it may be one mechanism responsible for the force increase by elevated Ca^{2+} because of greater Ca^{2+} influx allowing for higher myoplasmic Ca^{2+} during contractions.

Interestingly, our results do not support a similar mechanism for diaphragm and FDB. First, in wild-type diaphragm and especially in FDB, the magnitude of the Ni^{2+} effect was greater than for BTP-2. Therefore Ca^{2+} entry via both Cav1.1 and SOCE is important to maintain contractility. This is not surprising for diaphragm since it is already established that it depends on Ca^{2+} influx through Cav1.1 channels during contraction to a greater extent than hindlimb muscles (Viirès *et al.*, 1988; Zavecz *et al.*, 1991). However, this is the first time a study provides evidence for a similar pattern in FDB. Second, the Ni^{2+} effects were the same in wild-type and HyperKPP diaphragm and FDB, while the BTP-2 effects were slightly greater in HyperKPP muscles. It would thus appear that Ca^{2+} entry via SOCE is greater in HyperKPP than in diaphragm and FDB. It may also be a potential mechanism by which an increased $[Ca^{2+}]_e$ improved contractility in HyperKPP diaphragm.

In conclusion, this study demonstrates that the susceptibility to weakness in mouse muscles expressing HyperKPP mutant Na^+ channels was greatest for EDL > soleus >> diaphragm > FDB. The FDB, which appeared unaffected by HyperKPP, also showed the lowest Nav1.4 channel protein content and TTX-sensitive Na^+ influx. An unexpected finding is that the diaphragm, which is seldom affected by HyperKPP, expressed a high Nav1.4 channel protein

content and the largest increase in TTX-sensitive Na^+ influx compared with EDL and soleus. A reduction of Na^+-K^+-ATPase activity with ouabain completely abolishes the capacity of HyperKPP EDL and soleus to contract but only partially in diaphragm, suggesting that some other membrane components protect the latter muscle against HyperKPP symptoms. This study also showed that compared with wild-type muscles, HyperKPP EDL and soleus rely to a larger extent on Ca^{2+} entry via Cav1.1 channels, while diaphragm and FDB may rely more on SOCE, and potentially these dependencies may play a role in the improvement of muscle contractility

CHAPTER 3

UNDERSTANDING THE PHYSIOLOGY OF THE ASYMPTOMATIC DIAPHRAGM OF THE M1592V HYPERKALEMIC PERIODIC PARALYSIS MOUSE

by

Tarek Ammar[1], Wei Lin[1], Amanda Higgins[1], Lawrence J. Hayward[2] and Jean-Marc Renaud[1]

[1]Department of Cellular and Molecular Medicine, University of Ottawa, Ottawa, Ontario, Canada; and [2]Department of Neurology, University of Massachusetts Medical School, Worcester, Massachusetts

Journal of General Physiology 146: 509–525, 2015.

AUTHORS CONTRIBUTION

- Ammar: Fig 3.1, 3.2, 3.3, 3.4, 3.5, 3.6, 3.7, 3.8, 3.9, 3.10, 3.11, 3.12E and 3.13
- Lin: Fig. 3.12A-D and 3.13
- Higgins: 3.12A-D and 3.13

ABSTRACT

The diaphragm muscle of hyperkalemic periodic paralysis (HyperKPP) patients and of the M1592V HyperKPP mouse model rarely suffers of the myotonic and paralytic symptoms that occur in limb muscles. Enigmatically, HyperKPP diaphragm expresses the mutant Nav1.4 channel, and more importantly has an abnormally high Na^+ influx similar to that in EDL and soleus, two hindlimb muscles suffering of the robust HyperKPP abnormalities. The objective was to uncover the physiological mechanisms that render HyperKPP diaphragm asymptomatic. A first mechanism involves efficient maintenance of resting membrane polarization in HyperKPP diaphragm at various extracellular K^+ concentrations compared to larger membrane depolarizations in HyperKPP EDL and soleus. The improved resting membrane potential (EM) results from significantly increased Na^+ K^+ pump electrogenic activity, and not from an increased protein content. Action potential amplitude was greater in HyperKPP diaphragm than in HyperKPP soleus and EDL providing a second mechanism for the asymptomatic behavior of the HyperKPP diaphragm. One suggested mechanism for the greater action potential amplitude is lower intracellular Na^+ concentration because of greater Na^+ K^+ pump activity allowing better Na^+ current during the action potential depolarization phase. Finally, HyperKPP diaphragm had a greater capacity to generate force at depolarized EM compared to wild type diaphragm. Action potential amplitude was not different between wild type and HyperKPP diaphragm. There was also no evidence for an increased activity of the Na^+ Ca^{2+} exchanger working in the reverse mode in HyperKPP diaphragm compared to wild type diaphragm. So, a third mechanism remains to be elucidated to fully understand how HyperKPP diaphragm generates more force compared to wild type. Although the mechanism for the greater force at depolarized resting EM remains to be

determined, this study provides support for the modulation of the Na^+ K^+ pump as a component of therapy to alleviate weakness in HyperKPP.

INTRODUCTION

Hyperkalemic periodic paralysis (HyperKPP) is an autosomal dominant disease with nearly complete penetrance (Gamstorp *et al.*, 1957; Bradley *et al.*, 1990). The disease manifests with periods of myotonic discharge and episodic paralytic attacks (Lehmann-Horn *et al.*, 1983; Bradley *et al.*, 1990; Miller *et al.*, 2004). Weakness is prominent in the limbs and may completely incapacitate patients for hours at a time, with the frequency of paralytic attacks ranging from 3 to 28 per month (Miller *et al.*, 2004). A key hallmark of the disease is the precipitation of paralytic attacks following potassium ingestion (Gamstorp *et al.*, 1957; Poskanzer & Kerr, 1961; Streeten *et al.*, 1971; Wang & Clausen, 1976; Bradley *et al.*, 1990). Paralysis is in some cases associated with plasma [K^+] increasing from the normal 4 mM to 6-8 mM (Gamstorp *et al.*, 1957; Lehmann-Horn *et al.*, 1983; Miller *et al.*, 2004), whereas in other cases there is no increase (Poskanzer & Kerr, 1961; Rüdel & Ricker, 1985; Chinnery *et al.*, 2002). Most of the available treatments for HyperKPP are limited either by partial effectiveness or declining efficacy over time (Clausen *et al.*, 1980; Lehmann-Horn *et al.*, 1983).

HyperKPP is caused by missense mutations in the SCN4A gene that encodes for the α-subunit of the Nav1.4 sodium channel expressed in adult skeletal muscles (Cannon, 2006). Most HyperKPP cases (~66%) result from two mutations: threonine to methionine at residue 704 (T704M) or methionine to valine at residue 1592 (M1592V); the remaining cases are related to seven other mutations (Miller *et al.*, 2004). The mutations cause three primary functional defects in the Nav1.4 channel. First, the steady state activation curve shifts toward more negative membrane potentials (EMs, Rojas *et al.*, 1999), which lowers action potential threshold. Second, the steady state slow inactivation shifts toward less negative EMs (Hayward *et al.*, 1999). Third, mutant channels enter a non-inactivation mode upon membrane depolarization at elevated

extracellular K^+ concentration ($[K^+]_e$), an effect not observed in normal channels (Cannon *et al.*, 1991).

As a consequence of these defects, Nav1.4 channels open at greater frequency at rest resulting in large Na^+ influx (Clausen *et al.*, 2011; Lucas *et al.*, 2014), which then depolarizes the cell membrane (Lehmann-Horn *et al.*, 1983; Ricker *et al.*, 1989; Clausen *et al.*, 2011; Lucas *et al.*, 2014) . Myotonic discharges occur when the EM approaches a threshold for sustained firing. $[K^+]_e$ increases as several action potentials are generated. In normal muscles, increases in $[K^+]_e$ causes a membrane depolarization that inactivates Nav1.4 channels, thereby reducing action potential amplitude (Yensen *et al.*, 2002). As a consequence of lower action potential amplitude, less Ca^{2+} is released from the sarcoplasmic reticulum, resulting in decreased force or sarcomere shortening as $[Ca^{2+}]_i$ becomes sub-maximal (Zhu *et al.*, 2013; Lucas *et al.*, 2014). In HyperKPP limb muscles, the effects of increased K^+ on EM and force are greater than in normal muscles (Wang & Clausen, 1976; Lehmann-Horn *et al.*, 1983, 1987; Hayward *et al.*, 2008; Clausen *et al.*, 2011; Lucas *et al.*, 2014), often causing complete loss of membrane excitability. In fact, this sensitivity to elevated K^+ constitutes a key feature of HyperKPP.

HyperKPP patients primarily suffer from limb weakness or paralysis, but surprisingly only ~25% of patients experience respiratory distress (Charles *et al.*, 2013). In one study (Lucas *et al.*, 2014), only 2 of 8 tested diaphragms from the M1592V HyperKPP knock-in mouse model completely stopped contracting upon stimulation while developing a prolonged contracture (in the absence of stimulation) when $[K^+]_e$ was increased to 10 mM, whereas the remaining six HyperKPP diaphragms had similar tetanic force at 4.7 and 10 mM K^+ when compared to their wild type counterpart. Furthermore, in this study, neither a sudden loss in the ability to respond to stimuli nor a prolonged contracture were observed from the 44 tested HyperKPP diaphragms during an

experiment at any $[K^+]_e$, in the presence of ouabain to inhibit the Na^+ K^+ ATPase pump (NKA) or ORM-10103 to inhibit the Na^+ Ca^{2+} exchanger (NCX). Thus, the susceptibility to paralysis of HyperKPP diaphragm appears to be very low, at least in the context of the M1592V mutation. An asymptomatic diaphragm muscle is surprising for two reasons. First, diaphragm expresses the Nav1.4 channel protein at 75% of the level in extensor digitorum longus (EDL) and twice the level in soleus, being two muscles suffering of HyperKPP symptoms (Zhou & Hoffman, 1994; Lucas *et al.*, 2014). Second, the tetrodotoxin (TTX)-sensitive Na^+ influx in diaphragm is the largest of these three HyperKPP muscles (Lucas *et al.*, 2014). A better understanding of the mechanisms by which HyperKPP diaphragm maintains its force may help us develop better and more effective treatments for HyperKPP patients.

The objective of this study was to clarify the physiological mechanisms that render diaphragm muscle less vulnerable to the ionic perturbations produced by HyperKPP mutant Na channel expression. We compared how various $[K^+]_e$ affect the resting EM, action potential and tetanic force as well as the protein content and electrogenic contribution of the α1 and α2 isoforms of the NKA in EDL, soleus and diaphragm. The results showed that the HyperKPP diaphragm is resistant to weakness because (a) the NKA electrogenic contribution to resting EM was greater in HyperKPP than in wild type diaphragm, HyperKPP EDL and soleus; (b) at depolarized resting EM, HyperKPP diaphragm generated an action potential with greater amplitude than HyperKPP soleus and EDL and (c) it generated greater tetanic force than its wild-type counterpart.

MATERIALS AND METHODS

ANIMALS AND APPROVAL FOR ANIMAL STUDIES

HyperKPP mice (strain FVB.129S4(B6)-*Scn4a*$^{tm1.1Ljh}$/J) were generated by knocking in the equivalent of human missense mutation M1592V into the mouse genome; i.e., at position 1585 as previously described by Hayward et al. (2008). The FVB strain was used as wild-type mouse. All mice were 2-3 months old and weighed 20-25 g. The homozygous mutants generally do not survive beyond postnatal day five, so knock-in mice were maintained as heterozygotes by crossbreeding with FVB mice. Mice were fed ad libitum and housed according to the guidelines of the Canadian Council for Animal Care. The Animal Care Committee of the University of Ottawa approved all experimental procedures used in this study. Before muscle excision, 2-3-mo-old mice were anaesthetized with a single intraperitoneal injection of 2.2 mg ketamine/0.4 mg xylazine/0.22 mg acepromazine per 10 g of animal body weight, and sacrificed by cervical dislocation. EDL, soleus, FDB or diaphragm were then dissected out. For force measurements, 5-7 mm wide diaphragm strips were used.

GENOTYPING

A 2 mm tail piece was incubated overnight with 500 µl tail digestion buffer (0.2 mM Na_2EDTA and 25 mM NaOH, pH 12.3) and 50 µl Proteinase K (1mg/mL) at 56°C. DNA extraction involved the addition of 650 µl of 1:1 Phenol:CIA and centrifuged at 12000 g for 10 min. 650 µl of CIA was added twice to the pellet and centrifuged before suspending the resulting pellet in 750 µl of isopropyl alcohol. After 10 min, the solution was centrifuged 15 min at 15000 g. The alcohol was removed and the pellet suspended in 750 µl 70% ethanol and centrifuged. After removing the alcohol, the pellet was let to dry 30 min before thro addition of 200 µl TE buffer (10mM Tris, 1

mM EDTA, pH 8.0) and incubated at 65 °C for 2 hours. PCR was then completed using the previously extracted DNA and the following primers:

NC1F (forward): 5'-TGTCTAACTTCGCCTACGTCAA-3'

NC2R (reverse): 5'-GAGTCACCCAGTACCTCTTTGG-3'

PCR products were digested 6 h using the restriction digest enzyme *Nsp*I. The mutation that is knocked in to the HyperKPP mice causes the removal of one *Nsp*I cut site that is easily detected by agarose gel electrophoresis; two bands were visualized for wild-type mice, which carry the cut site on both alleles, and three bands were seen for heterozygous HyperKPP mice harboring one normal allele and one mutant allele.

WESTERN BLOTS OF Na^+ K^+ ATPase α-1 AND α2

Muscles were homogenized in buffer containing (mM): 50 Tris, 150 NaCl, 1% TritonX-100, 0.5% sodium deoxycholate, 0.1% SDS, protease inhibitor cocktail, and pH 8.0. Samples were rotated end-over-end for 1 h. Homogenates were centrifuged 30 min at 17500 g and 4°C. Protein concentration was determined in supernatants using the BCA assay method (Thermo Scientific). Forty µg of proteins aliquots of the muscle lysates was diluted with Laemmli sample buffer and heated for 20 min at 56°C. Proteins were separated on 8% of acrylamide gel at 100 V and transferred onto nitrocellulose membranes (Miniprotean 3 apparatus; Bio-Rad Laboratories). Equal protein loading was verified with Ponceau S (MP Biomedicals). Membranes were blocked overnight at 4°C with 5% skim milk powder in PBS containing 0.1% Tween, washed 3 times (10 min each) with PBS and incubated overnight with either rabbit anti-NKAα1 antibody (Cell Signaling Technology) diluted at 1:1000 in PBS containing 5% BSA or rabbit anti-NKAα2 antibody (EMD Millipore) diluted at 1:5000 in PBS containing 5% skim milk. Membranes were washed 3 times (10 min each) with PBS and incubated 1 h with Horseradish Peroxidase-conjugated

goat anti-rabbit antibody (Jackson ImmunoResearch Laboratories, Inc.) diluted at 1:10000 in PBS containing 5% skim milk. Bands were visualized by chemiluminescence using the ECL kit (PerkinElmer, Inc. MA, USA) on Cl-X Posure film (Thermo Scientific). Films (Cl-XPosure film, Thermo Fisher Scientific) were scanned (MP 600 Cannon PIXMA) and quantified using Image J (U. S. National Institutes of Health).

PHYSIOLOGICAL MEASUREMENTS

SOLUTIONS

Control solution contained (mM): 118.5 NaCl, 4.7 KCl, 1.3 $CaCl_2$, 3.1 $MgCl_2$, 25 $NaHCO_3$, 2 NaH_2PO_4, and 5.5 D-glucose. Solutions containing different K^+ concentrations were prepared by adding the appropriate amount of KCl. Solutions containing ouabain, a NKA inhibitor (Sigma-Aldrich) were prepared by dissolving ouabain directly in the control solution. Solutions containing 2-[(3,4-dihydro-2-phenyl-2H-1-benzopyran-6-yl)oxy]-5-nitro-pyridine (ORM-10103, an inhibitor of the Na^+ Ca^{2+} exchanger (NCX; Sigma-Aldrich) were prepared by first dissolving ORM-10103 in DMSO before it was added to the control solution. For the experiments involving ORM-10103, the final DMSO concentration was 0.1% (vol/vol) including the control solution. Solutions were continuously bubbled with 95% O_2–5% CO_2 to maintain a pH of 7.4. Experimental temperature was 37°C. Total flow of solutions in the muscle chamber was 15 ml/min being split just above and below the muscle in order to prevent any buildup of reactive oxygen species, which is quite large at 37°C (Edwards *et al.*, 2007).

FORCE MEASUREMENT

Muscle length was adjusted to give maximal tetanic force. Muscles were positioned horizontally in a Plexiglas chamber. One end of the muscle was fixed to a stationary hook, whereas the other end was attached to a force transducer (model # 400A, Aurora Scientific Canada). The transducer was connected to a data acquisition system (KCP13104, Keithley) and data were

recorded at 5 kHz. Tetanic force was defined as the force developed while muscles were electrically stimulated and was calculated as the difference between the maximum force during a contraction and the baseline force measured 5 ms before stimulation. Electrical stimulations were applied across two platinum wires (4 mm apart) located on opposite sides of the fibers. They were connected to a Grass S88 stimulator and a Grass SIU5 isolation unit (Grass Technologies). Tetanic contractions were elicited with 200-ms trains of 0.3 ms, 10-V (supramaximal voltage) pulses. Stimulation frequencies were set to give maximum tetanic force: being 140 Hz for soleus and 200 Hz for EDL and diaphragm. Tetanic contractions were elicited every 5 min.

RESTING EM AND ACTION POTENTIAL MEASUREMENTS

Resting EM and action potential were measured using glass microelectrodes. Microelectrodes tip resistances were 7~15 MΩ and that of the reference electrode ~1 MΩ. All electrodes were filled with 2 M K-citrate. A recording was rejected when the change in potential upon penetration was not a sharp drop or when the microelectrode potential did not return to zero upon withdrawal from the fiber. Single action potentials were elicited using fine platinum wires placed along the surface fibers using a single 10-V, 0.3-ms square pulse.

STATISTICS

Data are expressed as MEAN ± SEM (SEM). For statistical differences, two-way ANOVAs were used for Western blot measurements. Statistical comparisons between wild-type and HyperKPP muscles involved different mice and for such comparison force and EMs were independent from one another. Force and EMs were also measured at different $[K^+]_e$ or ouabain concentration using the same muscles; in this case the measurements are not independent from one another. As a consequence of the experimental design, we had two error terms: (1) the population error from the variability between mice when comparing wild-type and HyperKPP and (2) a within

muscle error when comparing the effects of K^+ and ouabain. So, statistical analyses were performed using spit-plot ANOVA designs as described by Steel and Torrie (1980). For this, the comparison between wild-type and HyperKPP was part of the whole plot, which used the population error, whereas the comparison for the K^+ and ouabain effect was part of the split plot, which used the within muscle error. Calculations were made using the General Linear Model procedures of the Statistical Analysis Software (version 9.3, SAS Institute Inc.). When a main effect or an interaction was significant, the least square difference (LSD) was used to locate the significant differences. The word "significant" refers only to a statistical difference ($P<0.05$).

RESULTS

$[K^+]_e$ EFFECTS ON TETANIC FORCE AND RESTING EM

As mentioned in the Introduction, the K^+-induced force depression starts with a membrane depolarization. So, we first analyzed the K^+ effects on tetanic force and resting EM to construct tetanic force-resting EM relationships to document how much of the force losses in HyperKPP muscles compared to wild type are related to membrane depolarization. At 4.7 mM K^+ (control), mean tetanic forces using the data from all tested HyperKPP soleus and EDL in this study were significantly lower than their wild type counterparts. Wild type and HyperKPP soleus respectively generated on average a tetanic force of 19.3 and 12.7 N/cm^2; i.e., mean tetanic force of HyperKPP soleus was 66% of the wild-type force (Fig. 3.1A). Wild-type and HyperKPP EDL respectively generated 29.8 and 22.7 N/cm^2 for a HyperKPP force being 76% of wild-type (Fig. 3.1B). For the diaphragm, however, there was no significant difference between wild-type and HyperKPP (Fig. 3.1C). The relative decreases in mean tetanic force of HyperKPP soleus and EDL at 9-11 mM K^+ were significantly greater in HyperKPP than wild-type EDL and soleus (Fig. 3.2A, B) but not in diaphragm as there was no difference between wild type and HyperKPP (Fig. 3.2C). Thus, HyperKPP diaphragms do not have a greater sensitivity to the K^+-induced force depression as observed with EDL and soleus.

HyperKPP muscle fibers are known to have less negative resting EM than normal fibers (Lehmann-Horn *et al.*, 1983, 1987; Ricker *et al.*, 1989; Clausen *et al.*, 2011). Furthermore, the K^+-induced force depression is caused by a depolarization of the cell membrane, which then causes an inactivation of $Na_V1.4$ channels (Renaud & Light, 1992; Cairns *et al.*, 1997; Yensen *et al.*, 2002). To better understand the importance of the membrane depolarization in the lower force

FIGURE 3.1

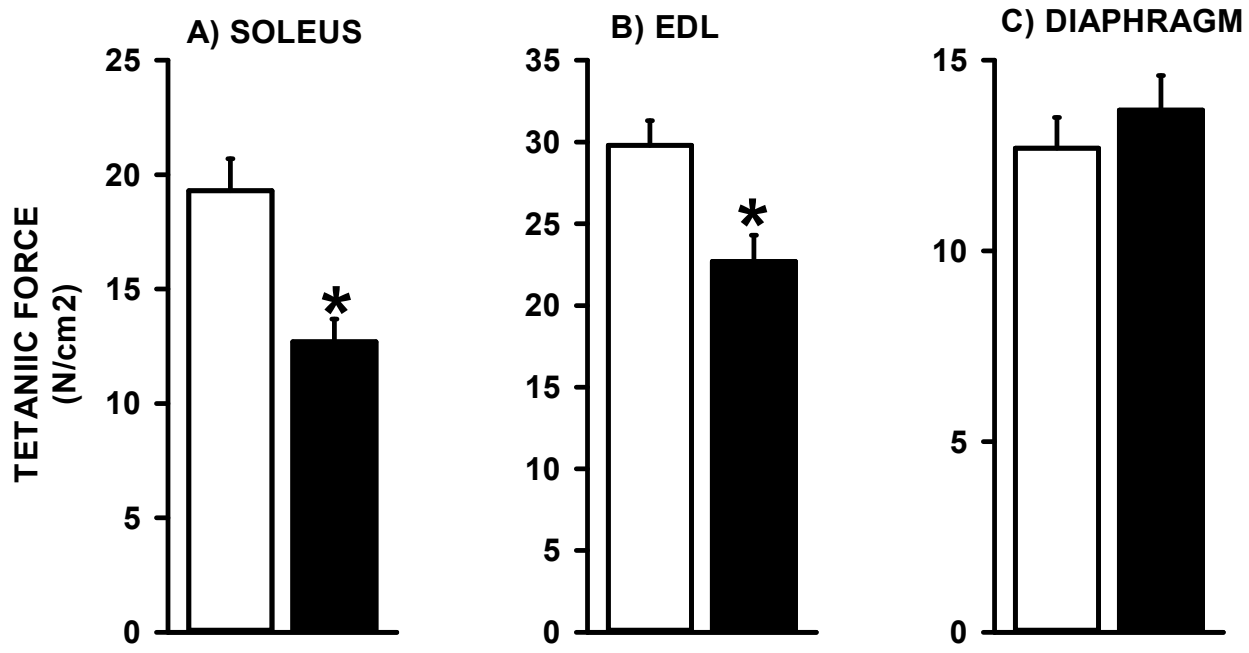

Figure 3.1. HyperKPP soleus and EDL but not diaphragm generated less tetanic force than their wild-type muscles(A-C). Tetanic force was elicited with 200-msec train of 0.3 msec, 10-V square pulses at 140 Hz for soleus and 200 Hz for EDL and diaphragm. Data were acquired immediately after adjusting the length for maximum force at the beginning of an experiment. The tetanic forces from every experiment including those for EM measurements were used to calculate mean tetanic force. Error bars represent the SEM of 24 solei, 34 EDL and 44 diaphragms. *, Mean tetanic force of HyperKPP muscles was significantly different from that of wild-type; ANOVA and L.S.D., $P < 0.05$.

FIGURE 3.2

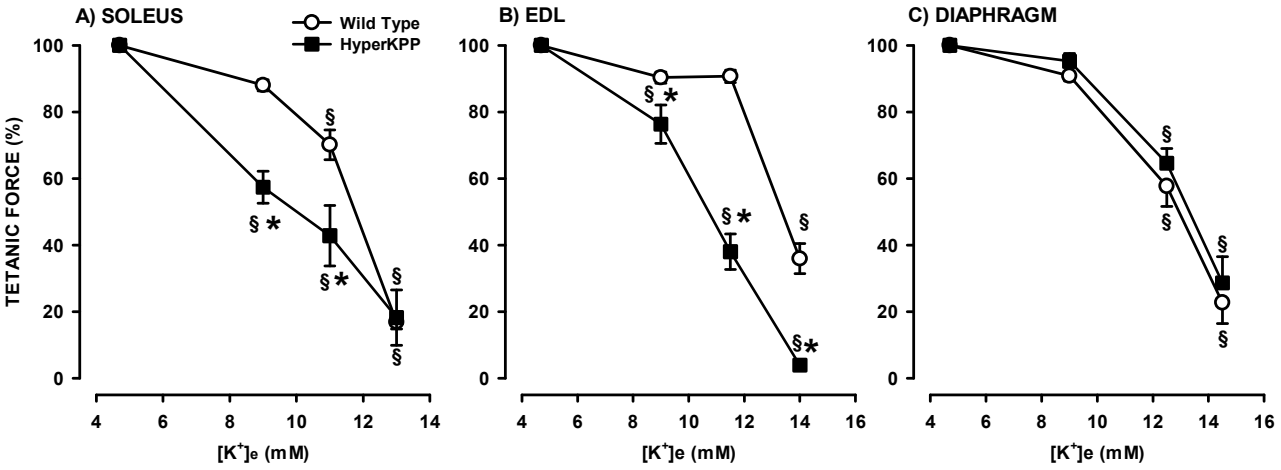

Figure 3.2. HyperKPP soleus and EDL but not diaphragm were more sensitive to the K^+-induced force depression (A-C). Each muscle was tested at only one elevated $[K^+]_e$. Tetanic force is expressed as a percentage of the force at 4.7 mM K^+. Error bars represent the SEM of five muscles. **§,** mean tetanic force was significantly different from the mean force at 4.7 mM K^+.***,** mean tetanic force of HyperKPP muscle was significantly different from the mean force of wild-type muscle; ANOVA and L.S.D. $P < 0.05$.

generated by HyperKPP EDL and soleus or the conservation of force for the diaphragm, we measured resting EM in 10-15 fibers chosen at random from the muscle surface at different $[K^+]_e$ (note here that action potentials were not measured to determine if a fiber was excitable or not). At 4.7 mM K^+, mean resting EM was 15 mV lower in HyperKPP than wild-type soleus, a difference that became smaller as $[K^+]_e$ was increased because the K^+-induced membrane depolarization per $[K^+]_e$ decade was smaller in HyperKPP soleus (Fig. 3.3A). For EDL, the difference in resting EM between wild-type and HyperKPP was smaller, being 5-9 mV among the different $[K^+]_e$ as the slopes of the membrane depolarization were not different between wild-type and HyperKPP (Fig. 3.3B). The smallest difference in resting EM between wild-type and HyperKPP was with the diaphragm, being only 2-4 mV and non-significant at all $[K^+]_e$ (Fig. 3.3C).

Resting EM varied tremendously among mammalian muscle fibers. Consequently, one cannot just use the mean resting EM to represent all fibers. The frequency distribution of resting EM was then documented by separating all measured values in bins of 5 mV. For soleus muscles, the frequency distribution for HyperKPP fibers was shifted toward less negative resting EM compared to wild-type fibers at both 4.7 and 13 mM K^+ (Fig. 3.4A, B). At 4.7 mM K^+, 69% of all wild-type soleus fibers had a resting EM above -70 mV compared to only 21% for HyperKPP fibers. Muscles with mean resting EM less than -55 mV lose their capacity to generate force (Renaud & Light, 1992; Cairns *et al.*, 1997). At 4.7 mM K^+, 27% of all HyperKPP soleus fibers had resting EM below -55 mV compared to less than 1% for wild-type fibers. The proportion of HyperKPP soleus fibers with resting EM below -55 mV increases to 78% at 13 mM K^+, whereas it increased only to 46% for wild type fibers. A similar shift toward less negative resting EM in HyperKPP EDL fibers was also observed at 4.7 and 14 mM K^+ (Fig. 3.4C, D). There were, however

FIGURE 3.3

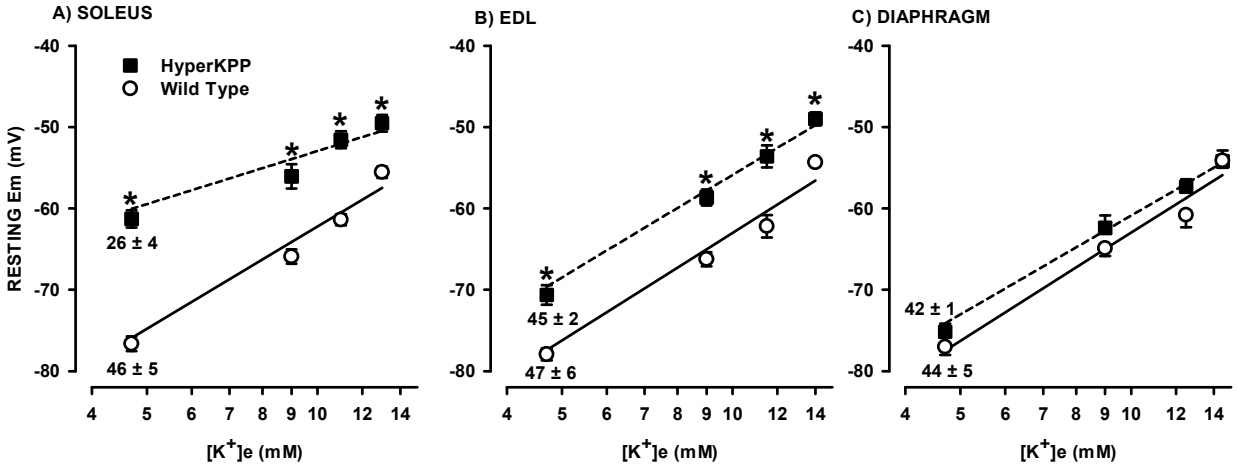

Figure 3.3. HyperKPP soleus and EDL but not diaphragm fibers were more depolarized than their wild-type fibers. Each muscle was tested at one or two elevated $[K^+]_e$. Resting EM was measured in several fibers in each muscle (A-C). An average resting EM was calculated for each muscle, and from the muscle averages a final mean was calculated. Error bars represent the SEM of 209-278 fibers/19 muscles at 4.7 mM K^+; 65-107 fibers/5-6 muscles at other $[K^+]_e$. Numbers below resting EM at 4.7 mM K^+ indicate the slope and SEM of the membrane depolarization (in mV/$[K^+]_e$ decade) using the mean resting EM versus log($[K^+]_e$); calculations were performed using the LINEST function of Excel 2013 (correlation coefficients of the analyses ranged from 0.973 to 0.999). *, mean resting EM of HyperKPP muscle was significantly different from the mean value of wild-type muscle; ANOVA and L.S.D. $P < 0.05$.

FIGURE 3.4

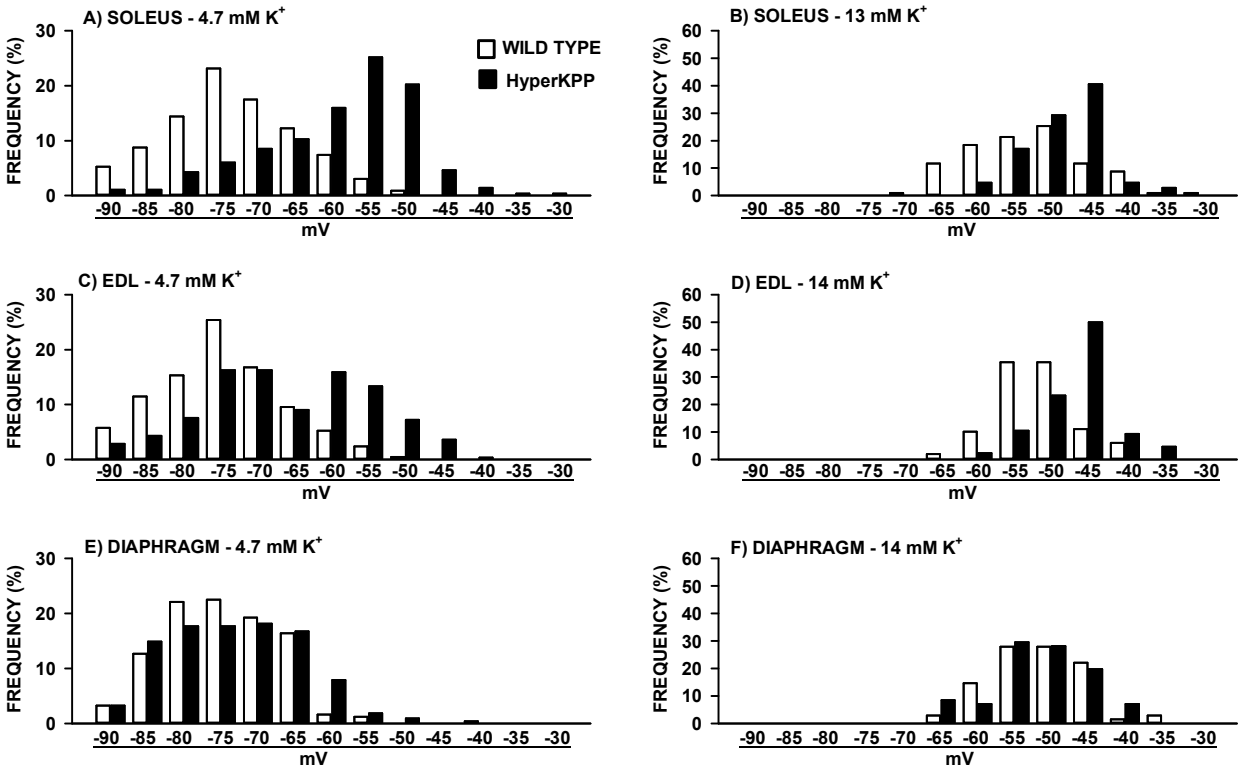

Figure 3.4. The frequency distribution of resting EM was shifted toward less negative resting EM in the HyperKPP soleus and EDL but not in the diaphragm when compared with wild-type muscles. Resting EM values were separated in bin of 5 mV, and the number of fibers in each bin is expressed as a percentage of the total number of tested fibers. The resting EM values under each pair of bars represent the upper bound of each bin. The total number of fibers were 209-278 (A, C and E) for 4.7 mM K^+ and 68-106 at the elevated $[K^+]_e$ (B, D and F).

two major differences between HyperKPP soleus and EDL: At 4.7 mM K^+, 47% of HyperKPP EDL fibers had a resting EM above -70 mV compared with only 21% for soleus fibers, whereas the proportion of fibers with resting EM below -55 mV was just 11% for EDL compared to 27% for soleus. Contrary to hindlimb muscles, there was no major shift in the frequency distribution of resting EM between wild-type and HyperKPP diaphragm (Fig. 3.4E, F). Only small differences were observed where the number of fibers with resting EM ranging between -65 and -75 mV was less in HyperKPP than in wild-type, whereas the number of fibers with resting EM between -55 and -60 mV was slightly higher in HyperKPP. These small differences explained the slightly less negative mean resting EM of HyperKPP fibers compared to wild type fibers in Fig. 3.3C.

Next we ascertained how much of the lower forces in HyperKPP EDL and soleus and the conservation of force in HyperKPP diaphragm are related to resting EM. To do this, we took into consideration that the tetanic force from a whole muscle is a function of the mean resting EM of all fibers as previously reported (Renaud & Light, 1992; Cairns *et al.*, 1997). To construct a tetanic force-resting EM relationship, we calculated all mean absolute forces at different $[K^+]_e$ as a percentage of the force generated by wild type muscles at 4.7 mM K^+. The force generated by HyperKPP soleus at 4.7 and 9 mM K^+ fell very close to the tetanic force-resting EM of wild-type soleus suggesting that the lower tetanic forces of HyperKPP soleus at those $[K^+]_e$ are largely caused by less negative mean resting EM (Fig. 3.5A). Interestingly, although tetanic force in wild-type soleus is expected to reach zero at -54 mV, HyperKPP soleus still generated some force between -55 and -49 mV.

The tetanic force of HyperKPP EDL at 4.7 and 9 mM fell below the expected force from the force-EM relationship of wild-type EDL (Fig. 3.5B). For example, HyperKPP EDL tetanic

FIGURE 3.5

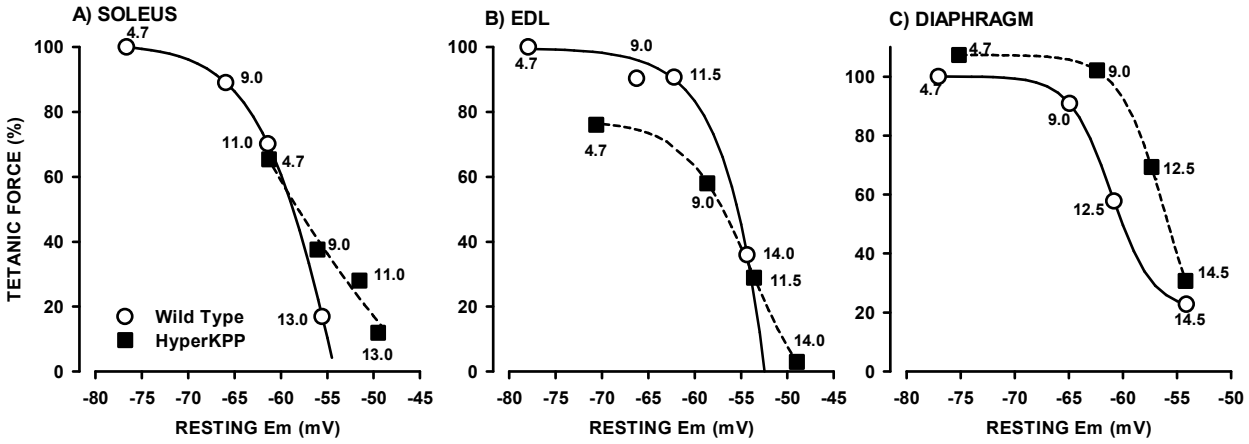

Figure 3.5. Tetanic force versus resting EM relationships. (A-C) Relationships were made by first expressing all mean tetanic forces of wild-type and HyperKPP muscles at various $[K^+]_e$ as a percentage of the mean tetanic force of wild-type muscles at 4.7 mM K^+ (taken as the normal maximum force these muscles can generate), and then plotting the relative values against the resting EM shown in Fig. 2. The numbers beside each symbol indicate the $[K^+]_e$ at which tetanic force and resting EM were measured. The curves were plotted after fitting the data points to the following sigmoidal relationship:

$$FORCE = c + \frac{a}{1 + e^{-(^{(Em-d)}/_{b})}}$$

where a, b, c and d are constants.

force at -71 mV (measured at 4.7 mM K^+) was 76%, whereas at that EM the expected tetanic force of wild-type EDL was 98%. It thus appears that the lower force in HyperKPP EDL is not just related to less negative resting EM. At resting EM smaller than -53 mV, HyperKPP EDL developed more force than wild-type. For example, HyperKPP EDL force at -48 mV (measured at 14 mM K^+) was 3%, whereas for wild type zero force was expected to occur at -52 mV. Remarkably, the tetanic force-resting EM was significantly shifted toward less negative resting EM in HyperKPP diaphragm (Fig. 3.5C). The largest difference was observed at -59 mV as the expected wild type force was 41% compared to 86% for HyperKPP, representing a 45% difference.

The results so far revealed two major features in this model of HyperKPP that spare the diaphragm from altered function compared to the robust abnormalities observed in EDL and soleus. The first one is smaller membrane depolarization in HyperKPP diaphragm (this study) despite the fact that it has the largest TTX-sensitive Na^+ influx of all three muscles (Lucas *et al.*, 2014). The second factor is a greater capacity of HyperKPP diaphragm to generate more force than wild type at depolarized resting EM. To further understand the lower membrane depolarization in HyperKPP diaphragm we determined how the content and electrogenic contribution of NKA differ between HyperKPP diaphragm, EDL and soleus. To further understand the capacity of HyperKPP diaphragm to generate more force at depolarized EM, we tested (a) the possibility that NCX works in the reverse mode when the membrane is depolarized as has been suggested previously for wild-type diaphragm (Zavecz & Anderson, 1992) and (b) whether the HyperKPP diaphragm fibers generate better action potentials than wild-type when the membrane is depolarized by K^+.

NKA

For the measurements of NKAα1 and NKAα2 protein content, we included the FDB because it is also an asymptomatic muscle, but contrary to diaphragm it has a very low TTX-

sensitive Na^+ influx even though its Nav1.4 channel protein content is comparable to that of soleus (Lucas *et al.*, 2014). Here, we first determined whether the NKA protein content is greater in HyperKPP than in wild-type diaphragm as it has been reported for HyperKPP EDL (Clausen *et al.*, 2011). HyperKPP EDL was the only muscle with significantly greater NKAα1 protein content than in the wild-type counterpart (Fig 3.6A). Next, we determined how the large increase in NKAα1 protein content in HyperKPP EDL affected the relative differences between muscles in wild-type and HyperKPP. Although wild-type EDL had two to three times less NKAα1 content compared to soleus, diaphragm and FDB, the NKAα1 content in HyperKPP EDL was no longer different from the other three muscles (Fig 3.6B). The situation was the same for the NKAα2 protein content. That is, HyperKPP EDL had a greater NKAα2 content than in wild type (Fig 3.7A). As a consequence of the increase, wild type diaphragm had similar NKAα2 protein content to wild type EDL, whereas for HyperKPP NKAα2, the content was less in diaphragm than EDL (Fig 3.7B). It was also noted that the 83% higher content in HyperKPP than in wild-type EDL as well as the 21% higher content in HyperKPP soleus were similar to the values reported from an ouabain binding studies (Clausen *et al.*, 2011).

Next, we assessed how inhibiting NKA activity with ouabain affected tetanic force and resting EM. We first used ouabain at a concentration of 1 μM, to reduce NKAα2 activity by 92% and that of NKAα1 by 6% according to the ouabain Ki values reported by Chibalin et al. (2012) that were measured from changes in rat diaphragm resting EM following exposure to various ouabain concentrations. At 4.7 mM K^+, 1 μM ouabain reduced mean tetanic force of wild-type soleus by 7%, whereas resting EM depolarized by 8 mV (Fig. 3.8A). The decrease in tetanic force for HyperKPP soleus was much larger at 42% despite a similar depolarization of 7 mV.

FIGURE 3.6

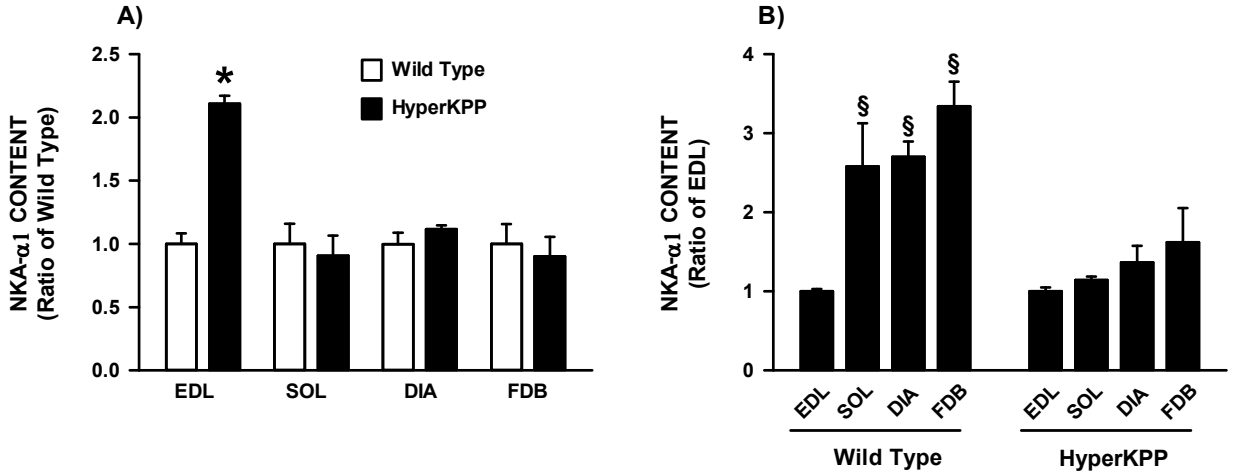

Figure 3.6. NKAα1 protein content was significantly higher in HyperKPP than in wild-type EDL, whereas there was no difference for soleus, diaphragm and FDB muscles. (A) For each muscle, NKAα1 contents were calculated as a ratio of the content in wild-type muscle. (B) For each of wild-type and HyperKPP, NKAα1 contents were calculated as a ratio of the EDL content. Error bars represent the SEM of five muscles. **§**, mean NKAα1, content significantly different from mean content in EDL; *****, mean NKAα1 content was significantly different from wild-type content, ANOVA and L.S.D., $P < 0.05$.

FIGURE 3.7

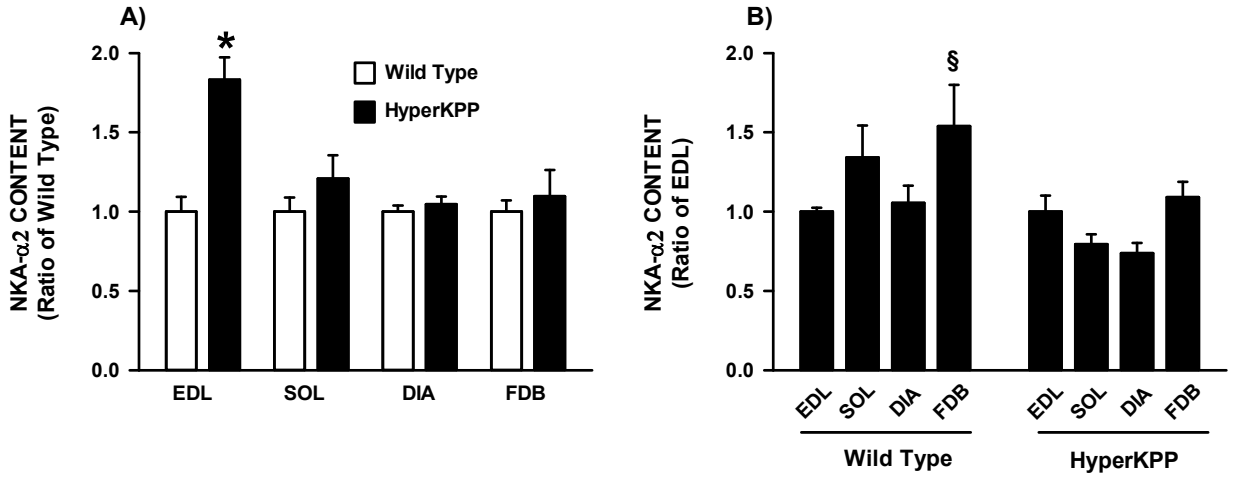

Figure 3.7. NKAα2 protein content was significantly higher in HyperKPP than in wild-type EDL, whereas there was no difference for soleus, diaphragm and FDB muscles. (A) For each muscle, NKAα2 contents were calculated as a ratio of the content in wild-type muscle. (B) For each of wild-type and HyperKPP, NKAα2 contents were calculated as a ratio of the EDL content. Error bars represent the SEM of 8-10 muscles. §, mean NKAα2 content significantly different from mean content in EDL; *, mean, NKAα2 content was significantly different from wild-type content, ANOVA and L.S.D., $P < 0.05$.

FIGURE 3.8

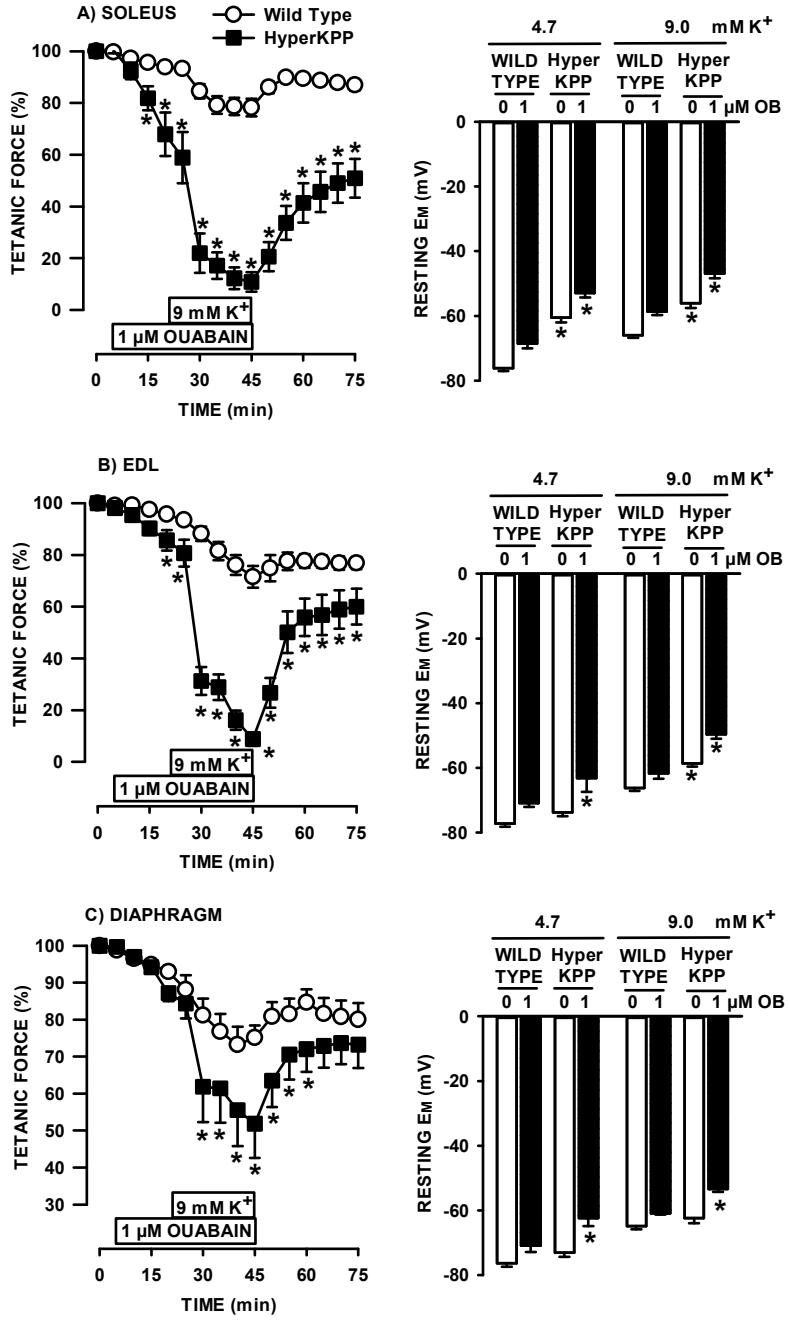

Figure 3.8. Ouabain caused greater loss of tetanic force and membrane depolarization in HyperKPP EDL and soleus than in diaphragm. (A-C) All muscles were allowed a 30-min equilibrium at 4.7 mM K^+ before any measurements or changes in $[K^+]_e$ or ouabain. For force measurements, muscles were exposed 20 min to ouabain while being exposed to 4.7 mM K^+ before

$[K^+]_e$ was increased to 9 mM, still in the presence of ouabain as indicated in the figures. A similar approach was used for resting EM with half the muscles; for the other half, muscles were exposed to ouabain only after $[K^+]_e$ had been raised to 9 mM K^+. The resting EM at 9 mM and 1 μM ouabain were not different between the two approaches, so the data were pooled. Error bars represent SEM; force of five muscles; resting EM: 70-93 fibers/9 muscles at 4.7 mM K^+ and 39-80 fibers/6 muscles for all other conditions. ***** mean tetanic force or resting EM of HyperKPP muscle was significantly different from the mean values of wild-type muscle, ANOVA and L.S.D., $P < 0.05$.

Ouabain also caused greater decrease in force at 9 mM K^+ in HyperKPP soleus even though the ouabain-induced membrane depolarization was 7 mV in wild-type and 9 mV in HyperKPP. The apparent greater ouabain effect on HyperKPP soleus force despite similar extent of depolarizations was because in the absence of ouabain resting EM at 4.7 mM K^+ was -75 and -60 mV in wild-type and HyperKPP soleus, respectively. As per the tetanic force-resting EM curve (Fig. 3.5A), small 7-9 mV depolarization is expected to have small effects on wild-type force, whereas in HyperKPP soleus the effects were greater because the starting resting EM was in the steepest portion of the curve. The ouabain and K^+ effects in EDL (Fig. 3.8B) resembled those of soleus.

The situation was very different with diaphragm (Fig. 3.8C). First, the decrease in force upon exposure to 1 μM ouabain at 4.7 mM K^+ was not different between wild type and HyperKPP diaphragm because resting EM in the presence of ouabain did not decrease below -72 mV for wild-type and -63 mV for HyperKPP; i.e., resting EM remained in a range for which there is little effect on tetanic force (Fig. 3.5C). Second, although the decrease in tetanic force in wild-type diaphragm upon raising $[K^+]_e$ to 9 mM at 1 μM ouabain was similar to that of wild-type soleus and EDL, the decrease in HyperKPP diaphragm was only 42% compared to 89-91% in soleus and EDL. For a complete loss of force in HyperKPP diaphragm at 9 mM K^+, HyperKPP diaphragm had to be exposed to 10 μM ouabain (Fig. 3.9A), which fully inhibits NKAα2 and NKAα1 by 37% (Chibalin *et al.*, 2012). The large decrease in force in that condition was related to a membrane depolarization to -50 mV (Fig. 3.9B), an EM at which tetanic force is expected to be zero in HyperKPP diaphragm (Fig. 3.5C).

At 100 μM ouabain, both NKAα1 and NKAα2 are fully inhibited (Chibalin *et al.*, 2012). At 4.7 mM K^+, 100 μM ouabain reduced tetanic force of the HyperKPP diaphragm by 84% (Fig.

FIGURE 3.9

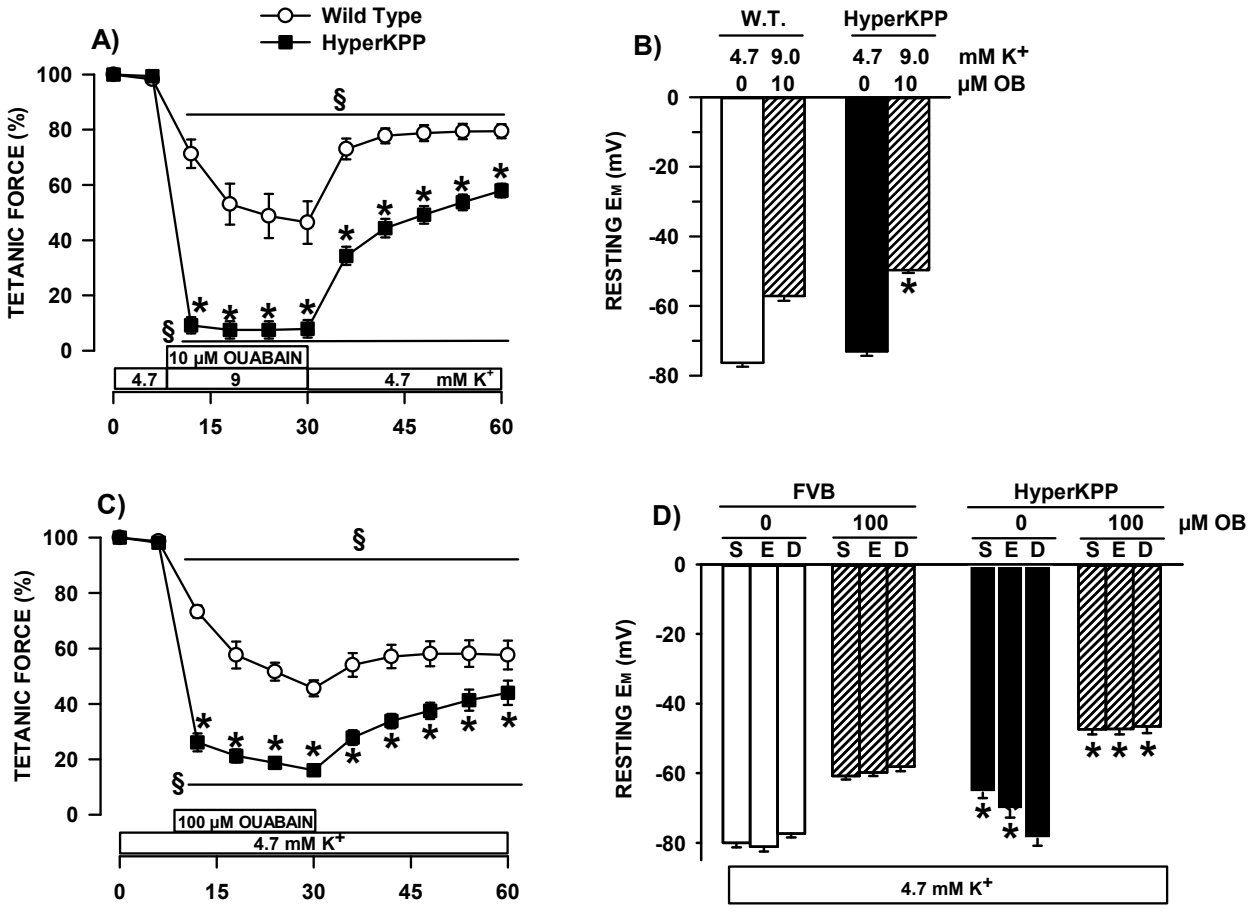

Figure 3.9. Effect of 10 µM ouabain at 9 mM K^+ and 100 µM ouabain at 4.7 mM K^+. Effects of 10 µM ouabain added as $[K^+]_e$ was increased to 9 mM on (A) tetanic force and (B) resting EM of diaphragm. Effects of 100 µM ouabain at 4.7 mM K^+ on (C) tetanic force and (D) resting EM of soleus (S), EDL (E) and diaphragm (D). Error bars represent the SEM of 5 muscles (A, B), 86-177 fibers/5 muscles (C, D). ***,** mean tetanic force or resting EM of HyperKPP muscle was significantly different from the mean values of wild-type muscle, ANOVA and L.S.D., $P < 0.05$.

3.9C; similar experiments were not carried out with EDL and soleus because 10 μM ouabain is sufficient to completely abolished tetanic force in HyperKPP EDL and soleus; Lucas *et al.*, 2014). Although the HyperKPP diaphragm had the most negative and HyperKPP soleus the least negative resting EM at 4.7 mM K^+, an exposure to 100 μM ouabain depolarized the membrane to the same level in all three muscles; i.e., -47 mV (Fig. 3.9D).

The total electrogenic contribution of NKAα1 and NKAα2, calculated from the differences in resting EM in the absence and presence of 100 μM ouabain, was 19-21 mV in wild-type muscles and was no significantly different from the 18-23 mV contribution in HyperKPP soleus and EDL (Fig. 3.10A). In HyperKPP diaphragm, however, the total NKA contribution was significantly greater at 32 mV compared to only 19 mV in wild-type diaphragm. The NKAα2 electrogenic contribution, calculated from the depolarization caused by 1 μM ouabain, was similar in wild-type and HyperKPP soleus and higher in HyperKPP EDL and diaphragm than in their wild-type counterparts, even though the differences were not significant (Fig. 3.10B). The NKAα1 electrogenic contribution, or the difference between total and NKAα2 contribution, was not different between wild-type and HyperKPP EDL and soleus, whereas it was significantly greater in HyperKPP than in wild-type diaphragm (Fig. 3.10C).

NCX

Increasing $[Ca^{2+}]_e$ improves force generation of HyperKPP muscles (Creutzfeldt *et al.*, 1963; Lucas *et al.*, 2014). Furthermore, contrary to wild type EDL and soleus, diaphragm depends on Ca^{2+} influx to maintain twitch force (Viirès *et al.*, 1988), and there is evidence that NCX plays a role in diaphragm contractility (Zavecz *et al.*, 1991; Zavecz & Anderson, 1992). In cardiac muscle, membrane depolarization and increases in $[Na^+]_i$ are two mechanisms by which $[Ca^{2+}]_i$ is

FIGURE 3.10

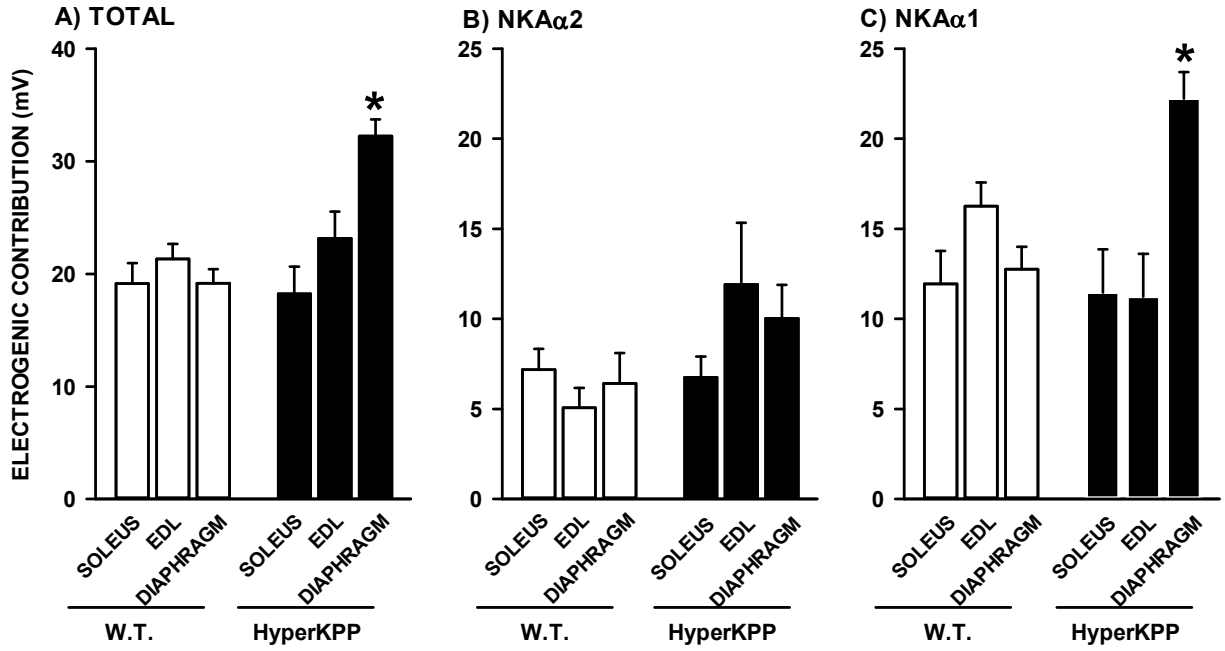

Figure 3.10. The NKA electrogenic contribution at 4.7 mM K^+ was significantly greater in HyperKPP diaphragm than in EDL and soleus. (A) Total NKA electrogenic contribution calculated from the difference in resting EM in the absence and presence of 100 μM ouabain, which fully inhibits NKAα1 and NKAα2 activity. (B) NKAα2 electrogenic contribution calculated from the difference in resting EM in the absence and presence of 1 μM ouabain, which reduced the activity of NKAα2 by 92% and that of NKAα1 by 6%. (C) NKAα1 electrogenic contribution calculated from the difference in total and NKAα2 electrogenic contribution. Error bars represent the SEM for the number of fibers and muscles given in Fig.8. * mean electrogenic contribution in HyperKPP was significantly different from the mean value for wild type; ANOVA and L.S.D., $P < 0.05$.

elevated during contraction as NCX works in the reverse mode (Janvier & Boyett, 1996) and a similar mechanism has been proposed for diaphragm (Zavecz & Anderson, 1992). We therefore investigated whether the greater force in HyperKPP diaphragm at less negative resting EM involves higher NCX activity in the reverse mode. To test this, we measure tetanic force while exposing muscles to 3 μM ORM-10103, a NCX inhibitor (Jost *et al.*, 2013).

The effects of ORM-10103 were first tested in wild-type EDL as this muscle is the least dependent on extracellular Ca^{2+} (Viirès *et al.*, 1988) and for which there is no evidence for a role of NCX during contractions (Blaustein & Lederer, 1999). As expected, ORM-10103 had no effect on tetanic force of that muscle at 4.7 and 12.5 mM K^+ (Fig. 3.11A). ORM-10103 had no effect on HyperKPP EDL while exposed to 4.7 mM K^+, but the force loss at 11 mM K^+ was greater in the presence of ORM-10103 (Fig. 3.11B). Similarly, the decrease in tetanic force in wild-type and HyperKPP diaphragm at 12.5 mM K^+ was greater in the presence than in the absence of ORM-10103 (Fig. 3.11C, D). However, the difference in force in the absence and presence of ORM-10103 at 12.5 mM K^+ was the same for wild type and HyperKPP diaphragm suggesting that an increased NCX activity in the reverse mode is not a mechanism that can explain the greater force in HyperKPP diaphragm at depolarized resting EM (Fig. 3.5C).

ACTION POTENTIAL – RESTING EM RELATIONSHIP

Next, we measured action potentials in soleus, EDL and diaphragm fibers. In general, at 4.7 mM K^+, action potentials were easily triggered in wild type muscles, for which >95% of fibers generated an action potential upon stimulation. The situation was very different in HyperKPP soleus and EDL. At 4.7 mM K^+, 30% of HyperKPP soleus fibers failed to generate an action potential upon stimulation, while 27% of HyperKPP EDL did the same. Among the excitable

FIGURE 3.11

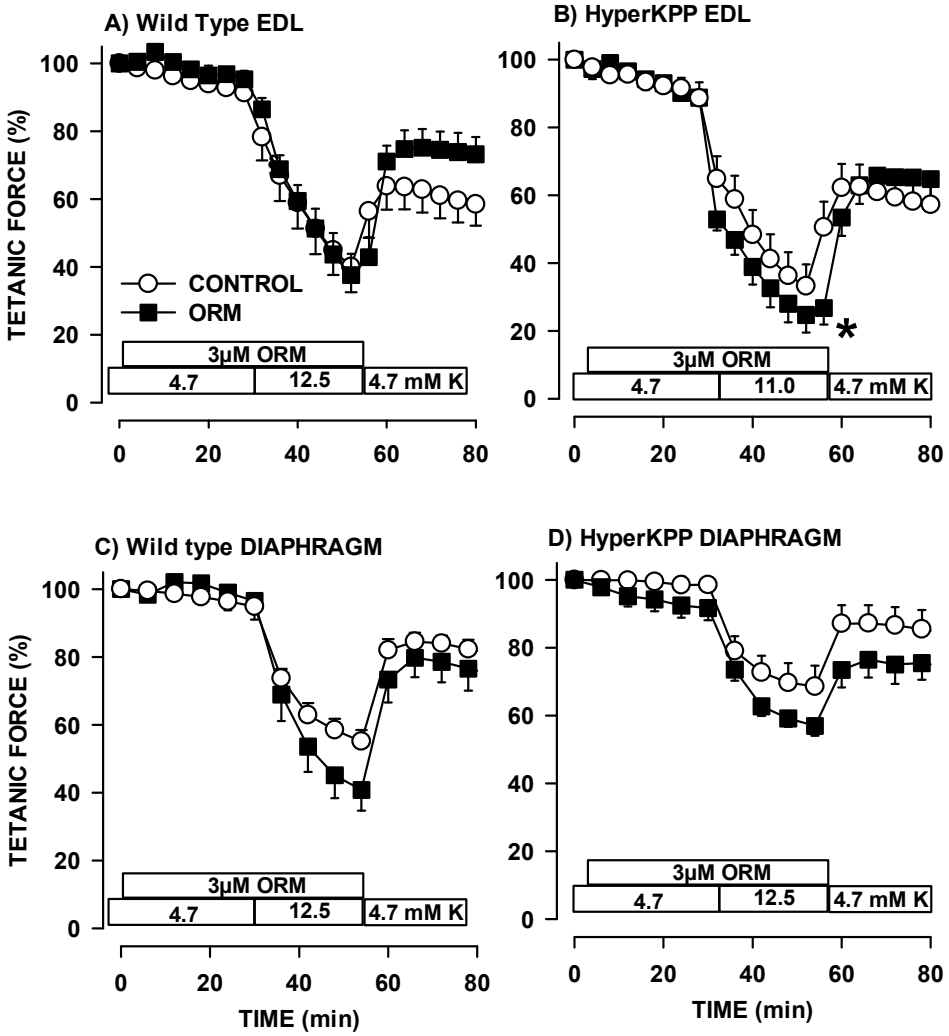

Figure 3.11. ORM-10103 caused small decreases in tetanic force in wild-type diaphragm, HyperKPP EDL and diaphragm, but not in wild-type EDL. (A-D) Muscles were first exposed to 3 μM ORM-10103, an NCX inhibitor, while being exposed to 4.7 mM K^+. The increased in $[K^+]_e$ was to 12.5 mM for all muscles, except for the HyperKPP EDL for which the increase was to 11 mM K^+ as this muscle was more sensitive to the K^+-induced force depression. Error bars represent the SEM of 5 muscles. *, mean tetanic force of ORM-10103-exposed muscles was significantly less than the mean value of control, ANOVA and L.S.D. $P < 0.05$.

fibers, action potential shapes were quite similar between wild-type and HyperKPP EDL fibers when resting EM was greater than -80 mV (measured at 4.7 mM K^+, Fig. 3.12A, B). At less negative resting EM such as between -55 and -75 mV (8-10 mM K^+), HyperKPP EDL fibers had action potentials with lower amplitude than their wild-type counterparts. Very few fibers generated action potential below a resting EM of -55 mV (12-15 mM K^+) and for those that did the amplitude was very small.

A major aim here was to test whether the shift in the tetanic force versus resting EM relationship in HyperKPP diaphragm versus wild-type (Fig. 3.5) can be explained by action potentials with greater amplitude in HyperKPP than wild-type diaphragm at depolarized resting EM. To do this, we first took into consideration the large variability in resting EM (Fig, 4). That is, action potentials were measured in several fibers while being exposed at $[K^+]_e$ varying between 4.7 and 14.5 mM. Fibers were then separated according to their resting EM in bins of 5 mV. For each bin, mean resting EM, action potential amplitude and peak were averaged to construct action potential amplitude versus resting EM relationship.

For soleus and EDL, mean action potential amplitudes were similar between wild-type and HyperKPP at resting EM above -70 mV (Fig. 12C, D). At resting EM less negative than -70 mV, action potential amplitude became smaller in HyperKPP soleus and EDL compared their wild-type counterpart. Contrary to the situation with soleus and EDL, mean action potential amplitudes at various resting EM were not different between wild-type and HyperKPP diaphragm (Fig. 3.12E). We then compared the action potential amplitude versus resting EM between muscles for each of wild-type and HyperKPP. For wild-type, mean action potential amplitudes were lower in soleus and EDL compared with the diaphragm, with significant differences at depolarized resting EM

FIGURE 3.12

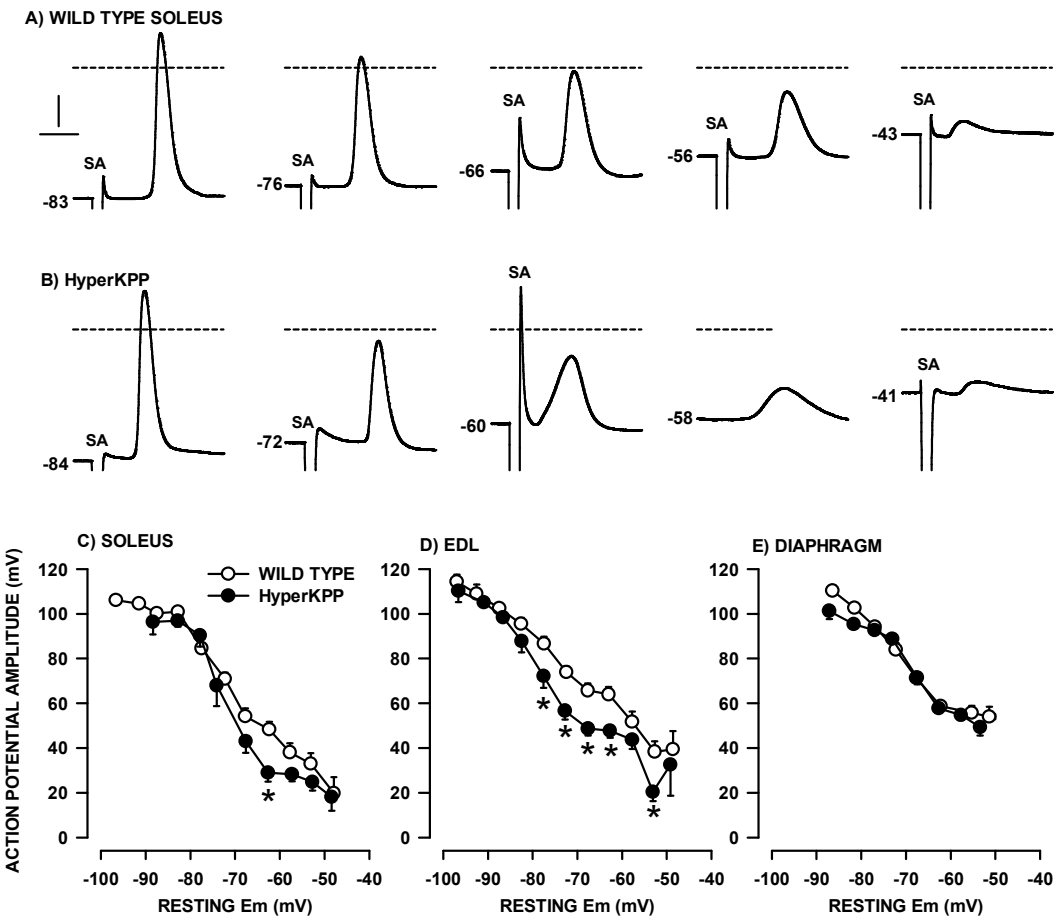

Figure 3.12. Action potential amplitudes were lower in HyperKPP than in wild-type soleus and EDL but not diaphragm. Examples of action potential traces from (A) wild-type and (B) HyperKPP EDL. Numbers at the start of each trace represent the starting resting EM. SA is for the 0.3 msec long stimulus artifact. Dashed horizontal lines represent 0 mV. Vertical and horizontal bars represent 20 mV and 1 msec, respectively. (C-E) Resting EM and action potentials were measured from fibers located at the muscle surface. Each muscle was tested at 2 or 3 $[K^+]_e$. Data from all fibers were pooled together and separated according to their resting EM in bin of 5 mV. For each bin, resting EM and action potential amplitudes were averaged. Vertical and horizontal

bars represent the SEM of action potential amplitude and resting EM, respectively (not shown if smaller than symbol). The total number of samples varied between 158 and 385 fibers from 5 to 11 muscles. *, mean action potential amplitude from HyperKPP fibers was significantly different from that of wild-type; ANOVA and L.S.D. $P < 0.05$.

(Fig. 3.13A). The differences between diaphragm and hindlimb muscles were more pronounced in HyperKPP (Fig. 3.13B). Similar analyses for action potential peak versus resting EM relationships gave rise to similar differences between wild-type and HyperKPP and between EDL, soleus and diaphragm to those observed for the action potential amplitude vs. resting EM relationships (not depicted).

FIGURE 3.13

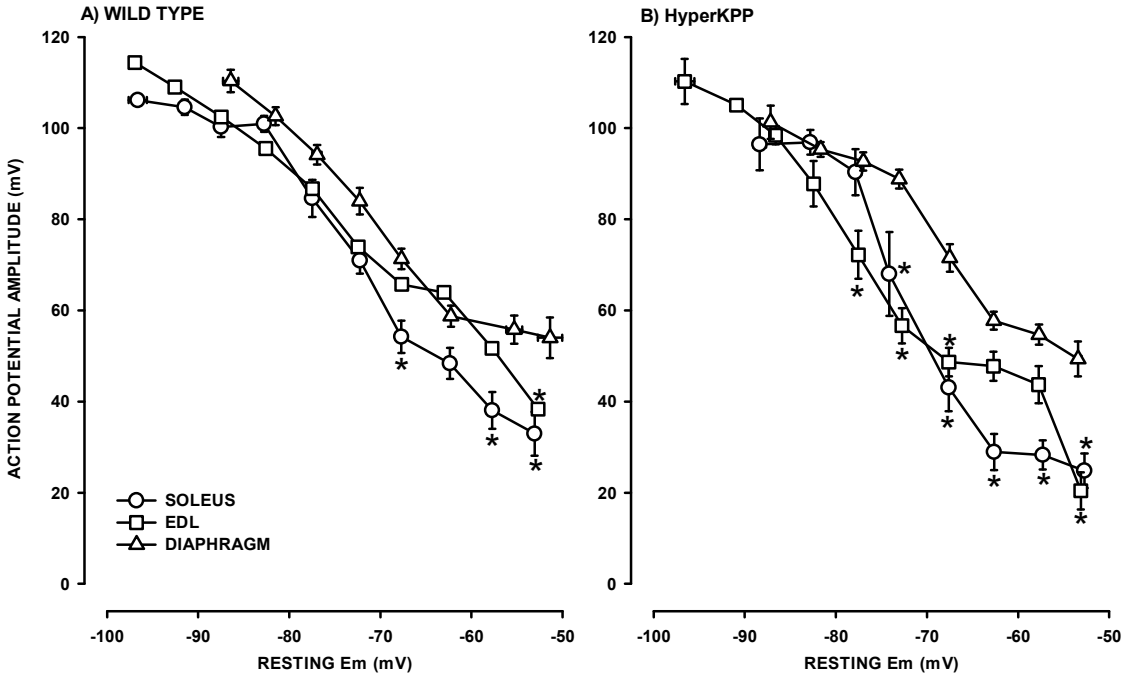

Figure 3.13. At depolarized resting EM, action potential amplitude becomes significantly less in soleus than EDL than in diaphragm, especially for HyperKPP. (A and B) The data are the same as in Fig. 12 but replotted to show differences between muscles. *, mean action potential amplitude from EDL or soleus fibers was significantly different from that of diaphragm fibers; ANOVA and L.S.D. $P < 0.05$.

DISCUSSION

Individuals with HyperKPP rarely suffer from respiratory distress, though this can occur more frequently following procedures or exposure to anesthetic agents (Charles *et al.*, 2013). In two of our studies (this study and Lucas et al., 2014), only 2 of the 52 tested diaphragm muscles from the M1592V HyperKPP mouse model suddenly stopped contracting upon stimulation as if they had become paralyzed in the course of an in vitro experiment. The objective of this study was to identify physiological mechanisms that render HyperKPP diaphragm resistant to weakness triggered by elevated $[K^+]_e$. The major findings of this study were: (a) contrary to HyperKPP soleus and EDL fibers which were highly depolarized compared to their wild-type counterparts, there was no significant difference in mean or in the frequency distribution of resting EM between diaphragm fibers from HyperKPP compared to wild type; (b) the entire tetanic force-resting EM relationship of HyperKPP diaphragm was shifted to less negative resting EM when compared with the wild-type relationship, whereas only a partial shift was observed for HyperKPP soleus and EDL; (c) NKAα1 and NKAα2 protein content was the same in wild-type and HyperKPP diaphragm; (d) the NKA electrogenic contribution, especially the α1 subunit, was greater in HyperKPP diaphragm, whereas for soleus and EDL the total NKAα1 and NKAα2 electrogenic contribution was not different between wild type and HyperKPP; (e) the action potential amplitude versus resting EM relationship of HyperKPP diaphragm was similar to that of wild-type diaphragm whereas it was shifted toward more depolarized resting EM when compared to HyperKPP soleus and EDL.

PROTECTION OF RESTING EM BY NKA AS ONE MECHANISM

It is well known that resting EM is more depolarized in HyperKPP muscles from both mouse and patients, which likely is a major contributor to muscle weakness (Lehmann-Horn *et al.*,

1983, 1987; Ricker *et al.*, 1989; Clausen *et al.*, 2011). The importance of less polarization of the resting EM contributing to the lower force is further confirmed in this study from three points of view. First, there was a major shift in the frequency distribution of resting EM toward lower EM values in HyperKPP soleus and EDL (Fig. 3.4A, B). Second, many fibers had resting EM lower than -55 mV, an EM below which muscles failed to generate force (Renaud & Light, 1992; Cairns *et al.*, 1997). In that regard, 30% of HyperKPP soleus fibers failed to generate an action potential upon stimulation, a value that was close to the 27% of fibers with a resting EM below -55 mV. Third, the tetanic force generated at 4.7 and 9 mM K^+ by HyperKPP soleus was very close to the expected force from the tetanic force versus resting EM relationship of wild-type soleus.

At 4.7 mM K^+ the relative difference in tetanic force between wild-type and HyperKPP was less for EDL (24%) than soleus (34%). We can again demonstrate that the difference between the two muscles is in part related to differences in resting EM. That is, HyperKPP EDL had a greater mean resting EM because of a larger proportion of fibers having resting EM above -70 mV and less below -55 mV than in HyperKPP soleus. However, contrary to HyperKPP soleus, the tetanic forces generated by HyperKPP EDL at 4.7 and 9 mM K^+ was less than the expected forces from the mean resting EM and the tetanic force versus resting EM relationship of wild-type EDL suggesting that perhaps other factors are involved in lowering force in HyperKPP EDL as discussed in the section entitled 'Importance of stronger action potential'.

The situation in HyperKPP diaphragm was completely different to that of hindlimb muscles. The differences in mean resting EM between wild-type and HyperKPP at various $[K^+]_e$ ranged between 2 and 4 mV in diaphragm compared to 6-15 mV in soleus and 5-9 mV in EDL. Furthermore, contrary to HyperKPP soleus and EDL, there were only small differences in the frequency distribution of resting EM between wild-type and HyperKPP diaphragm. The

importance of better resting EM in HyperKPP diaphragm than in soleus and EDL especially at high $[K^+]_e$ can be illustrated as follows. For HyperKPP soleus at 9 mM K^+, resting EM was -56 mV and tetanic force 40% of wild-type force at 4.7 mM K^+ (used as the maximum force normal muscle can generate, Fig. 3.5). At the same $[K^+]_e$, resting EM of HyperKPP diaphragm was -62 mV and tetanic force was 96% of maximum force, representing a 56% difference in force between HyperKPP soleus and diaphragm. If, on the other hand, HyperKPP diaphragm had depolarized to -56 mV, then according to the tetanic force-resting EM relationship in Fig. 3.5C tetanic force would have only been 50%, representing just a 10% difference with soleus. When similar calculations are carried out for EDL, the differences in tetanic force at 9 mM K^+ with HyperKPP diaphragm is 39%, being reduced to 21% if the diaphragm resting EM had depolarized to -59 mV as observed in EDL instead of the measured -62 mV. Thus, a better maintenance of resting EM (this study) despite large Na^+ influx (Lucas *et al.*, 2014) is one important mechanism that protects HyperKPP diaphragm from the robust symptoms observed in HyperKPP soleus and EDL.

This study now provides evidence for an increased electrogenic contribution of NKA, primarily its α1 isoform, to the resting EM of HyperKPP diaphragm. We suggest that the increase in NKA electrogenic contribution is related to greater NKA activity in HyperKPP than in wild-type diaphragm as we did not observe a difference in the NKAα1 or NKAα2 protein content between wild-type and HyperKPP diaphragm. In fact, it appears that changes in NKA content does very little as the NKA electrogenic contribution in HyperKPP EDL was similar to that in wild type EDL despite a 1.5- to 2.0-fold greater NKAα1 and NKAα2 content in HyperKPP (Figs. 3.6A, 7A; Clausen et al., 2011). Also, an increased electrogenic contribution was observed only in the HyperKPP diaphragm despite the fact that the NKA content was no longer different between HyperKPP soleus, EDL and diaphragm as it was for wild type muscles (Figs. 3.6B, 3.7B). A

possible mechanism for the difference in NKA activity between diaphragm and limb muscles is the fact that the former is constantly active. Reducing the time interval between contractions to 1 min not only acutely increases NKA activity in wild-type and HyperKPP muscles, but it also allows for an increase in tetanic force in HyperKPP soleus toward the wild-type level (Overgaard *et al.*, 1999; Clausen *et al.*, 2011). This is in agreement with the fact that HyperKPP patients sometimes can avoid a weakness or paralytic attack with mild exercise (Poskanzer & Kerr, 1961).

An activation of NKA by the β-adrenergic agonist salbutamol has been shown to eliminate muscle weakness in hindlimb muscles of patients and mice suffering of HyperKPP (Wang & Clausen, 1976; Clausen *et al.*, 2011). Altogether it would appear that a salbutamol treatment would help in keeping a higher NKA activity in hindlimb muscles and thus prevents weakness. Unfortunately, the efficacy of salbutamol decreases over time in human patients (Clausen *et al.*, 1980). The loss of effectiveness over time suggests that there is a fundamental difference in the regulation of NKA activity between HyperKPP hindlimb and diaphragm muscles, and a better understanding of this regulation in future studies will help us develop more effective and sustained pharmacological strategies to treat HyperKPP patients.

IMPORTANCE OF STRONGER ACTION POTENTIAL

As discussed above, the mean tetanic forces generated by HyperKPP soleus at resting EM between -55 and -60 mV (or at 4.7 or 9 mM K^+) were close to our expectation from the tetanic force versus resting EM relationship of wild-type soleus. In EDL, on the other hand, the mean tetanic forces between -60 and -70 mV were less than the expectation. One possible reason for this difference may be in the generation of action potentials. HyperKPP soleus fibers generated action potentials of similar amplitude than their wild-type counterpart when resting EM was greater than -70 mV with just a small tendency for lower amplitude below -70 mV. For EDL, the

differences between wild-type and HyperKPP were more pronounced and started when resting EM was less than -80 mV. Considering the shift in the resting EM frequency distribution toward lower potential, we suggest that even at 4.7 mM K^+ HyperKPP EDL have many fibers with resting EM at which they generate lower action potential amplitude than wild type, which then most likely results in lower Ca^{2+} release and force generation. This difference between HyperKPP soleus and EDL cannot be explained from our results. Lower action potential amplitude can be related to higher $[Na^+]_i$ which are known to be higher in HyperKPP muscles (Lehmann-Horn *et al.*, 1987; Ricker *et al.*, 1989; Amarteifio *et al.*, 2012). Higher $[Na^+]_i$ then lowers action potential amplitude as the decreased Na^+ concentration gradient is reduced (Cairns *et al.*, 2003). However, this explanation is questionable if we consider the lack of any significant difference in NKA electrogenic contribution (Fig.3.10) and Na^+ influx between HyperKPP soleus and EDL (Lucas *et al.*, 2014). Another possibility is the difference in ClC-1 Cl^- channel activity between these two muscles and varying this channel activity at elevated $[K^+]_e$ significantly impact on the capacity of muscle to generate action potentials and force (Pedersen *et al.*, 2005, 2009*a*, 2009*b*).

Interestingly, HyperKPP EDL and soleus still generated small amount of force when resting EM became below -55 mV, a potential at which no more force was generated by wild-type muscles as previously reported (Renaud & Light, 1992; Cairns *et al.*, 1997). At those resting EM, action potential measurements became very difficult because of a very large number of unexcitable fibers. Furthermore, although many fibers failed to generate single action potentials, the situation may be different during a tetanic stimulation train during which a few action potentials may eventually be generated considering that the steady state slow inactivation never reaches zero (Hayward *et al.*, 1999) and that K^+ at a concentration as low as 10 mM provokes a non-inactivation mode in the mutant Nav1.4 channel (Cannon *et al.*, 1991). So, at resting EM below -55 mV few

action potentials are generated by mutant Nav1.4 channels during a tetanus giving rise to small force development.

The situation was again different with diaphragm. Contrary to soleus and EDL, HyperKPP diaphragm was slightly less sensitive to the K^+-induced force depression than wild-type diaphragm; although the effect was not significant it was constantly observed in all experiments. The lower sensitivity to K^+ was not accompanied by smaller membrane depolarizations when $[K^+]_e$ was increased. In fact, the reverse was observed as mean resting EM were slightly lower in HyperKPP than in wild-type diaphragm. Moreover, there was little difference in the resting EM frequency distribution. As a consequence of this situation, the tetanic force versus mean resting EM was significantly shifted toward less negative resting EM so that at depolarized EM HyperKPP diaphragm generated greater tetanic force than wild-type diaphragm.

The shift cannot be explained by the generation of action potential with greater amplitude in HyperKPP than in wild-type because there was no difference in the action potential amplitude versus resting EM relationship, at least in regards to the generation of single action potentials. Another possibility is greater increases in $[Ca^{2+}]_i$ during a contraction in HyperKPP diaphragm fibers in the absence of any difference in action potential amplitude. An NCX inhibition resulted in lower force in both wild-type and HyperKPP diaphragm at 12.5 mM K^+ (Fig. 3.11) supporting a role for NCX working in the reverse mode to increase $[Ca^{2+}]_i$ during contraction, which is in agreement with previous studies (Zavecz *et al.*, 1991; Zavecz & Anderson, 1992; Blaustein & Lederer, 1999). However, the force reduction upon NCX inhibition was the same in wild-type and HyperKPP. So, if there is a greater $[Ca^{2+}]_i$ during contraction in the HyperKPP diaphragm, it is unlikely that the mechanism involves NCX. Another possibility is a greater Ca^{2+} entry via the store operated Ca^{2+} entry to maintain high Ca^{2+} content in the sarcoplasmic reticulum as previously

reported (Lucas *et al.*, 2014) or greater Ca^{2+} release by the sarcoplasmic reticulum when Cav1.1 and RyR1 channels are activated by action potentials.

Although there was no difference in the action potential amplitude versus resting EM between wild-type and HyperKPP diaphragm, we observed that this relationship in diaphragm was shifted toward less negative resting EM when compared to EDL and soleus. The shift was small with few significant differences for wild-type muscles when resting EM was less than -70 mV. For HyperKPP muscles, on the other hand, the differences were much greater and became significant when resting EM was less than -80 mV. It thus appears that HyperKPP diaphragm has a better capacity of generating normal action potentials than HyperKPP hindlimb muscles. One possible mechanism for the improved action potential amplitude is lower $[Na^+]_i$ than in hindlimb muscles because of greater NKA activity. The better action potentials also constitute a second mechanism that renders HyperKPP diaphragm asymptomatic.

In conclusion, we provide evidence here that compared to HyperKPP soleus and EDL (a) HyperKPP diaphragm muscle better maintains its resting EM at various $[K^+]_e$ despite very large Na^+ influx through defective Nav1.4 channels and (b) generates larger action potentials at depolarized EM, providing two essential mechanisms that minimize weakness in HyperKPP diaphragm. The improved resting EM is related to significant increases in the electrogenic contribution (or activity) of the NKAα1 isoform rather than an increase in NKA protein content. The improved capacity of HyperKPP diaphragm to generate action potentials may also be due to the higher NKA activity that maintains low $[Na^+]_i$. Finally, compared with wild-type, the HyperKPP diaphragm generated more force at depolarized resting EM. The mechanism for this improved force generation could not be discerned here as it was not related to the generation of stronger action potentials compared to wild-type nor to a greater contribution of NCX working in

the reverse mode to the increase in $[Ca^{2+}]_i$ during contraction. Future studies will be necessary to understand the mechanisms responsible for the higher NKA activity in HyperKPP diaphragm and to examine whether facilitating these pathways in hindlimb muscles could improve function for HyperKPP patients.

CHAPTER 4

INVESTIGATING THE EFFECT OF MODULATING PKA/PKC ON THE ASYMPTOMATIC BEHAVIOR OF HYPERKPP DIAPHRAGM

Tarek Ammar and Jean-Marc Renaud

Department of Cellular and Molecular Medicine, University of Ottawa, Ottawa, Ontario, Canada

ABSTRACT

HyperKPP diaphragm is asymptomatic despite having high TTX-sensitive Na^+ influx as EDL and soleus which are severely affected by the disease. The asymptomatic behavior of the HyperKPP diaphragm is due a greater electrogenic contribution of NKA pump than EDL and soleus allowing a better maintenance of resting EM and AP amplitude in HyperKPP diaphragm. Protein kinase A (PKA) and protein kinase C (PKC) are known to increase NKA pump activity by phospholemman (PLM) phosphorylation. So, one of the objectives of this study was to investigate whether an inhibition of PKA or PKC renders the HyperKPP diaphragm symptomatic. The decrease in force at 12.5 mM K^+ was augmented in HyperKPP diaphragm when exposed to 90 nM staurosporin, a PKA/PKC inhibitor. GF109203X, a PKC inhibitor, at 1 μM had no effect on tetanic force at 4.7 and 12.5 mM K^+ suggesting that PKC is not involved. Inhibition of PKA by H89 resulted in greater force loss at 12 .5 mM K^+ in HyperKPP diaphragm and to a lesser extent in WT diaphragm. Another PKA inhibitor KT5720 had similar effect on tetanic force at 12.5 mM K^+ but the extent of decrease was smaller than with H89. A second objective was to test whether an activation of PKC in HyperKPP soleus can alleviate symptoms; i.e., reduce the extent of force loss at 12.5 mM K^+. Exposing WT and HyperKPP soleus to 100 and 300 nM PMA resulted in progressive loss of tetanic force at 4.7 mM K^+; i.e., it worsened the muscle weakness at normal $[K^+]_e$. It is concluded that i) PKA activity may be involved in the asymptomatic behavior of the diaphragm and ii) an activation of PKC is not a feasible therapeutic approach to treat HyperKPP.

INTRODUCTION

Despite the fact that human diaphragm expresses the Nav1.4 channel mRNA, only 26% of HyperKPP patients report breathing problems (Charles *et al.*, 2013) which would be expected if diaphragm suffers of myotonia and weakness/paralysis like the limb muscles. Moreover, patients from a family with Met1592Val mutation never reported any breathing difficulties (Poskanzer & Kerr, 1961; Chinnery *et al.*, 2002). Chapters 2 and 3 provided strong evidence that the diaphragm of HyperKPP M1592V mouse is mostly asymptomatic. That is, while it expresses Nav1.4 channel and has a resting TTX-sensitive Na^+ influx as high as in HyperKPP soleus and EDL, it suffers none of the symptoms downstream of the Na^+ influx (Fig. 1.14). One major mechanism that renders the diaphragm asymptomatic is a better maintenance of resting EM because of higher electrogenic contribution of NKA pump, a situation that does not occur in soleus and EDL. HyperKPP diaphragm also generates better AP amplitude than HyperKPP EDL and soleus possibly because of lower $[Na^+]_i$ maintained by the higher NKA pump activity (Chapter 3). Finally, at resting EM less negative than -60 mV, HyperKPP diaphragm generated more force than WT even though AP amplitudes are the same in HyperKPP and WT raising the possibility that there is greater Ca^{2+} release during contraction in HyperKPP diaphragm.

Phospholemman (PLM) is a protein that regulates NKA pump. It associates with the NKA pump α subunit and decreases its activity by lowering both internal Na^+ and external K^+ affinities(Crambert *et al.*, 2002). This inhibition is relieved upon PLM phosphorylation by PKC and PKA (Silverman *et al.*, 2005; Despa *et al.*, 2005; Han *et al.*, 2006; Bibert *et al.*, 2008; Pavlovic *et al.*, 2013*b*). Furthermore, the β_2-adrenergic agonist salbutamol increases force of HyperKPP soleus exposed to 10 mM $[K^+]_e$ to levels similar to the WT (Clausen *et al.*, 2011). β-adrenergic agonists activates NKA pump via the PKA pathway (Clausen, 2003; Shattock, 2009; Clausen *et*

al., 2011; Pavlovic *et al.*, 2013*a*). β-adrenergic agonists also increase Ca^{2+} release during a contraction as the ryanodine receptor, the sarcoplasmic reticulum Ca^{2+} release is phosphorylated by PKA (Cairns *et al.*, 1993; Ha *et al.*, 1999; Reiken *et al.*, 2003; Rudolf *et al.*, 2006). So a mechanism by which HyperKPP diaphragm is asymptomatic may involve greater PKA or PKC activity than in hindlimb muscles maintaining higher NKA pump activity and Ca^{2+} release with greater force generation as an end result.

Ongoing work in the laboratory has provided evidence that concomitant activation of K_{ATP} channels and inhibition of ClC-1 Cl^- channels improve force in HyperKPP soleus and EDL at high $[K^+]_e$ (Lin and Renaud, unpublished results). In regard to K_{ATP} channels, the proposed mechanism involves resting EM hyperpolarization (Zhu *et al.*, 2014) as G_K is increased. The hyperpolarization then reduces the extent of Nav1.4 inactivation increasing the number of excitable fibers, AP amplitude and thus force. As discussed in the General Introduction, a decrease in G_{Cl} in WT improves force at high $[K^+]_e$ by increasing the number of excitable fibers and AP amplitude (Pedersen *et al.*, 2005) and by hyperpolarizing resting EM (Higgins MSc thesis, 2014). In expression systems such as HEK293 cells and COS-1 cells PKA activates K_{ATP} channels, made of Kir6.2/SUR2A subunits that are expressed in skeletal muscles (Béguin *et al.*, 1999; Lin *et al.*, 2000). In skeletal muscles, phosphorylation of ClC-1 channel by PKC reduces its activity (Tricarico *et al.*, 1991; Rosenbohm *et al.*, 1999; Pierno *et al.*, 2007; Pedersen *et al.*, 2009*a*). Thus, another possible mechanism by which HyperKPP diaphragm is asymptomatic may involve higher PKA/PKC activity not only stimulating NKA pump and Ca^{2+} release but also activating K_{ATP} channels while lowering ClC-1 channels activity.

As of now there are PKA/PKC activators that have been used in clinical trials such as forskolin for PKA for treatment of bronchial asthma PKA (Gonzalez-Sanchez *et al.*, 2006; Huerta

et al., 2010) and bryostatin for PKC for melanoma and myeloma (Propper *et al.*, 1998; Varterasian *et al.*, 2001). Thus, documenting whether PKA or PKC play a role in the asymptomatic diaphragm can eventually lead to a new pharmaceutical strategy to treat HyperKPP. So, the initial objective here was to test the hypothesis that blocking PKA and PKC activity will render HyperKPP diaphragm symptomatic; that is increase its sensitivity to K^+-induced force loss. However, it soon became evident that the so called PKA/PKC inhibitors either had no effect or were not specific enough to obtain clear conclusions. So, a second objective was to test the hypothesis that activating PKA/PKC in HyperKPP soleus will reduce the extent of symptoms in HyperKPP hindlimb muscles. In regard to the second objective, data for the PKC activation are presented in this chapter while those for PKA are in the next chapter.

MATERIALS AND METHODS

ANIMALS AND APPROVAL FOR ANIMAL STUDIES

HyperKPP mice (strain FVB.129S4(B6)-*Scn4a*$^{tm1.1Ljh}$/J) were generated by knocking in the equivalent of human missense mutation M1592V into the mouse genome; i.e., at position 1585 as previously described by Hayward et al. (2008). The FVB strain was used as wild-type mouse. All mice were 2-3 months old and weighed 20-30 g. The homozygous mutants generally do not survive beyond postnatal day five, so knock-in mice were maintained as heterozygotes by crossbreeding with FVB mice. Mice were fed ad libitum and housed according to the guidelines of the Canadian Council for Animal Care. The Animal Care Committee of the University of Ottawa approved all experimental procedures used in this study. Before muscle excision, 2-3-months old mice were anaesthetized with a single intraperitoneal injection of 2.2 mg ketamine/0.4 mg xylazine/0.22 mg acepromazine per 10 g of animal body weight, and sacrificed by cervical dislocation. Diaphragm strips (5-7 mm wide) and soleus muscles were then dissected out.

GENOTYPING

A 2 mm tail piece was incubated overnight with 500 µl tail digestion buffer (0.2 mM Na_2EDTA and 25 mM NaOH, pH 12.3) and 50 µl Proteinase K (1mg/mL) at 56 °C. DNA extraction involved the addition of 650 µl of 1:1 Phenol:CIA and centrifuged at 12000 g for 10 min. 650 µl of CIA was added twice to the pellet and centrifuged before suspending the resulting pellet in 750 µl of isopropyl alcohol. After 10 min, the solution was centrifuged 15 min at 15000 g. The alcohol was removed and the pellet suspended in 750 µl 70% ethanol and centrifuged. After removing the alcohol, the pellet was let to dry 30 min before the addition of 200 µl TE buffer (10mM Tris, 1 mM EDTA, pH 8.0) and incubated at 65 °C for 2 hours. PCR was then completed using the previously extracted DNA and the following primers:

NC1F (forward): 5'-TGTCTAACTTCGCCTACGTCAA-3'

NC2R (reverse): 5'-GAGTCACCCAGTACCTCTTTGG-3'

PCR products were digested 6 hr using the restriction digest enzyme *Nsp*I. The mutation that is knocked in to the HyperKPP mice causes the removal of one *Nsp*I cut site that is easily detected by agarose gel electrophoresis; two bands were visualized for wild-type mice, which carry the cut site on both alleles, and three bands were seen for heterozygous HyperKPP mice harboring one normal allele and one mutant allele.

SOLUTIONS

Control solution contained in (mM): 118.5 NaCl, 4.7 KCl, 1.3 $CaCl_2$, 3.1 $MgCl_2$, 25 $NaHCO_3$, 2 NaH_2PO_4, and 5.5 D-glucose. Solutions containing different K^+ concentrations were prepared by adding the appropriate amount of KCl. Staurosporin, GF109203X, H89, KT5720, and PMA were prepared by first dissolving them in DMSO before being added to the control solution. For all solutions including control, the final DMSO concentration was 0.1% (vol/vol). Solutions were continuously bubbled with 95% O_2–5% CO_2 to maintain a pH of 7.4. Experimental temperature was 37°C. Total flow of solutions in the muscle chamber was 15 ml/min being split just above and below the muscle in order to prevent any buildup of reactive oxygen species, which is quite large at 37°C and deleterious (Edwards *et al.*, 2007).

FORCE MEASUREMENT

Muscles were positioned horizontally in a Plexiglas chamber. One end of the muscle was fixed to a stationary hook, whereas the other end was attached to a force transducer (model # 400A, Aurora Scientific Canada). The transducer was connected to a data acquisition system (KCP13104, Keithley) and data were recorded at 5 kHz. Electrical pulses were applied across two platinum wires (4 mm apart) located on opposite sides of the fibers. The wires were connected to a Grass S88 stimulator and a Grass SIU5 isolation unit (Grass Technologies). Tetanic contractions were

elicited with 200-ms trains of 0.3 ms, 10-V (supramaximal voltage) pulses. Stimulation frequencies were set to give maximum tetanic force: being 200 Hz for diaphragm and 140 Hz for soleus. Tetanic contractions were elicited every 2 min. Muscle length was adjusted to give maximal tetanic force and muscles were then allowed to equilibrate for 30 min at 4.7 mM K^+ before any change in [K^+] or drug addition. Tetanic force was defined as the force developed while muscles were electrically stimulated and was calculated as the difference between the maximum force during a contraction and the baseline force measured 5 ms before stimulation.

STATISTICS

Data are presented as means ± SE. ANOVA was used to determine significant differences. Split plot ANOVA designs were used when muscles were tested at all-time levels. ANOVA calculations were made with version 9.2 General Linear Model procedures of the Statistical Analysis Software (SAS Institute, Cary, NC). When a main effect or an interaction was significant, the least square difference was used to locate the significant differences (Steel & Torrie, 1980). The word "significant" refers only to a statistical difference ($P < 0.05$).

RESULTS AND DISCUSSION

In an attempt to test the hypothesis that higher PKA or PKC activity in HyperKPP diaphragm is involved in its asymptomatic behavior, diaphragm strips were first exposed to 90 nM staurosporin, a PKC/PKA inhibitor (Meyer *et al.*, 1989). Staurosporin had no effect on tetanic force at 4.7 mM K^+ but caused a greater decreases in force at 12.5 mM K^+ (Fig. 4.1). A specific PKC inhibitor, GF109203X, at a concentration of 1 μM, a concentration large enough to prevent the large decrease in ClC-1 channel activity induced by PKC in skeletal muscles (Toullec *et al.*, 1991; Pedersen *et al.*, 2009*a*), had no effect on force at 4.7 and 12.5 mM K^+ (Fig. 4.2). The results suggest that PKC is not involved in sparing HyperKPP diaphragm from symptoms.

Next, HyperKPP diaphragm was exposed to 2 μM of H89, a PKA inhibitor (Lochner & Moolman, 2006). H89 had no effect on force at 4.7 mM K^+ but caused significantly greater decrease in tetanic force than in control condition when $[K^+]_e$ was increased to 12.5 mM (Fig. 4.3A). H89 also caused greater decrease in force in WT at 12.5 mM K^+, albeit to a smaller extent than in HyperKPP diaphragm (Fig. 4.3B). To further confirm that the effect of H89 were due to a PKA inhibition, a second inhibitor, KT5720 was used at a concentration of 1 and 3 μM (Kase *et al.*, 1987). Both concentrations caused greater force loss at 12.5 mM K^+ (Fig. 4.4), but the effects were much smaller than with H89 and were not significant.

Although H89 and KT5729 are widely used to specifically inhibit PKA they also inhibit other kinases such as mitogen- and stress-activated protein kinase, p70 ribosomal protein S6 kinase and Rho-dependent protein kinase at the concentrations used in this study (Davies *et al.*, 2000; Murray, 2008). Furthermore, considering the variability in the effects of two PKA inhibitors, these experiments alone do not allow us to reach a clear conclusion that PKA is an important factor in protecting diaphragm from HyperKPP symptoms.

FIGURE 4.1

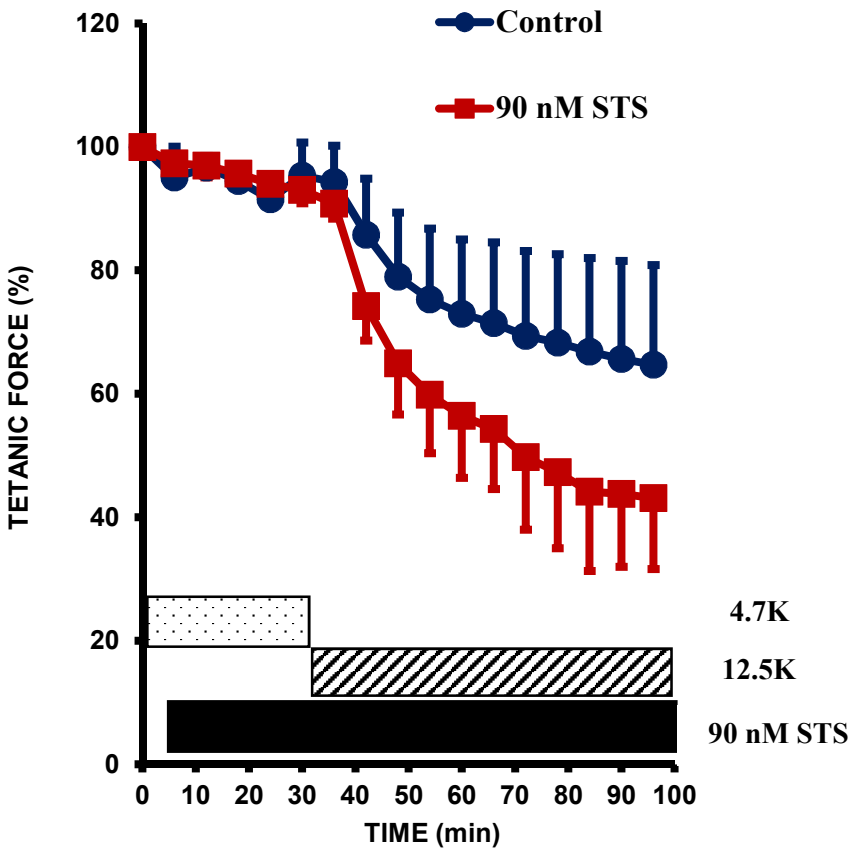

Figure 4.1. Inhibiting PKA/PKC with 90 nM staurosporin (STS) increased the extent of force loss in HyperKPP diaphragm at 12.5 mM K^+. Peak tetanic force is expressed as a percent of the force at time 0 min. Tetanic contractions were elicited with 200 ms train of pulses at 200 Hz every 2 min. Muscles were allowed 30 min of equilibrium at 4.7 mM K^+ (not shown in the figure) before adding STS at 6 min. Symbols:●, control group (no STS); ■, STS treated group. Vertical bars represent the S.E. of 3 muscles. ANOVA and L.S.D. $P < 0.05$.

FIGURE 4.2

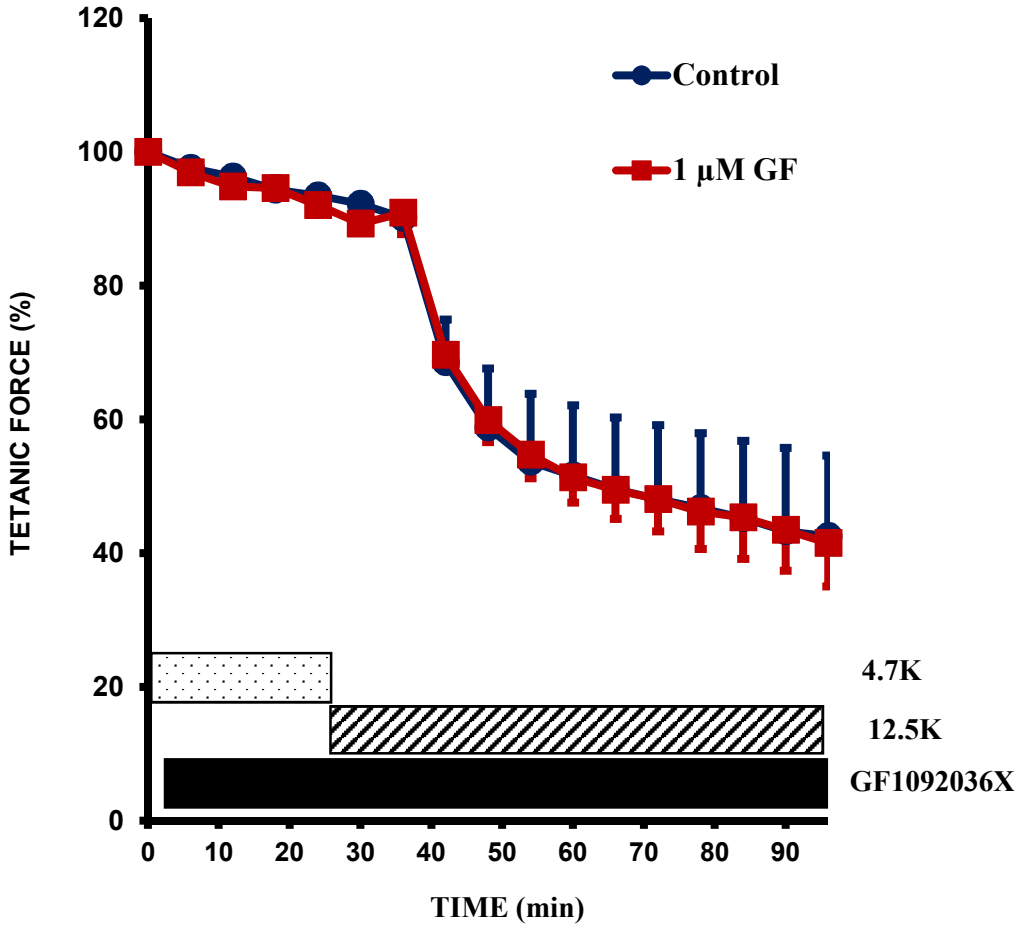

Figure 4.2. Inhibiting PKC with 1 µM GF109203X did not affect tetanic force at 4.7 and 12.5 mM K^+ in HyperKPP diaphragm. Peak tetanic force is expressed as a percent of the force at time 0 min. Tetanic contractions were elicited with 200 ms train of pulses at 200 Hz every 2 min. Muscles were allowed 30 min of equilibrium at 4.7 mM K^+ (not shown in the figure) before adding GF1092036X at 6 min. Symbols:●, control group (No GF109203X); ■, GF109203X treated group. Vertical bars represent the S.E. of 3 muscles. ANOVA and L.S.D. $P < 0.05$.

FIGURE 4.3

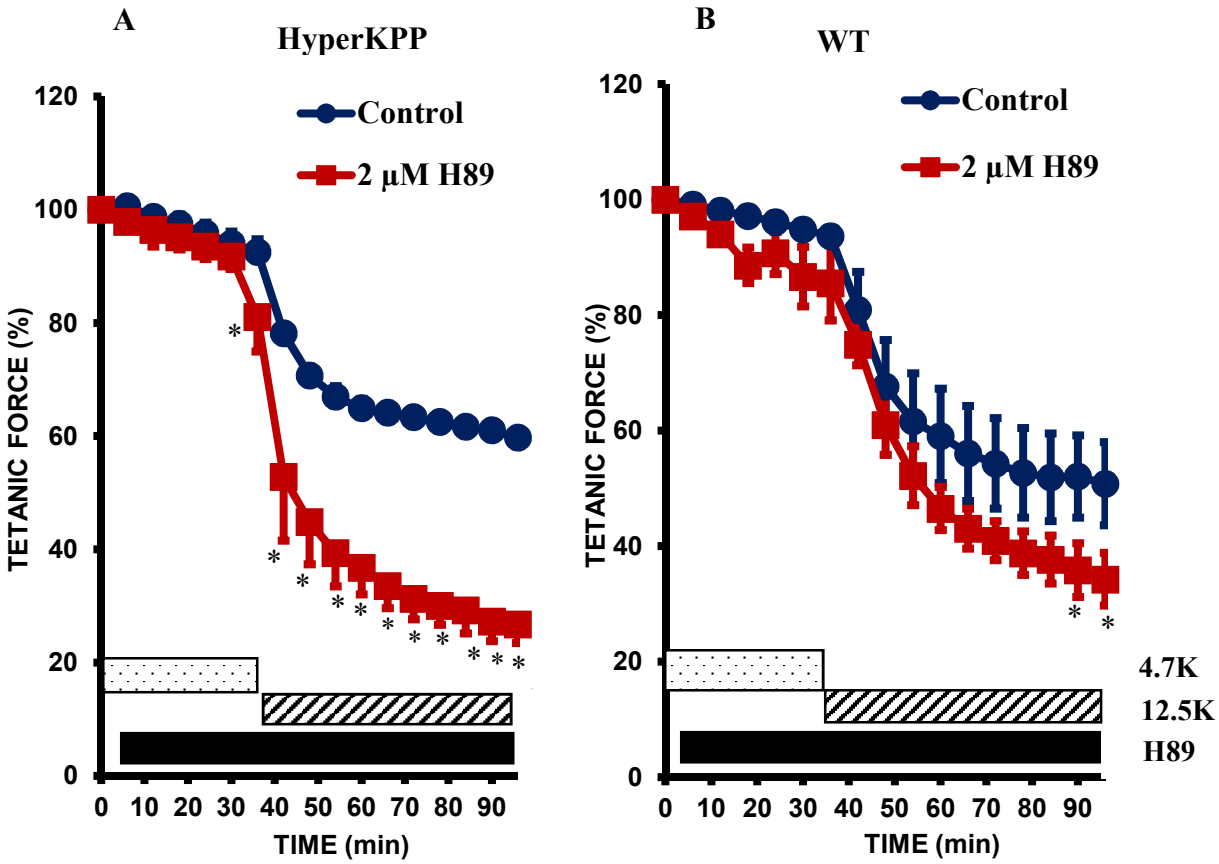

Figure 4.3. Inhibiting PKA with 2 µM H89 caused greater force loss in HyperKPP than WT diaphragm at 12.5 mM K^+. Peak tetanic force is expressed as a percent of the force at time 0 min. Tetanic contractions were elicited with 200 ms train of pulses at 200 Hz every 2 min. Muscles were allowed 30 min of equilibrium at 4.7 mM K^+ (not shown in the figure) before adding H89 at 6 min. A) HyperKPP, B) WT. Symbols:●, control group (No H89); ■, H89 treated group. Vertical bars represent the S.E. of 3 muscles. *, Mean tetanic force of HyperKPP or WT muscles in presence of H89 was significantly different from that of control; ANOVA and L.S.D., $P < 0.05$.

FIGURE 4.4

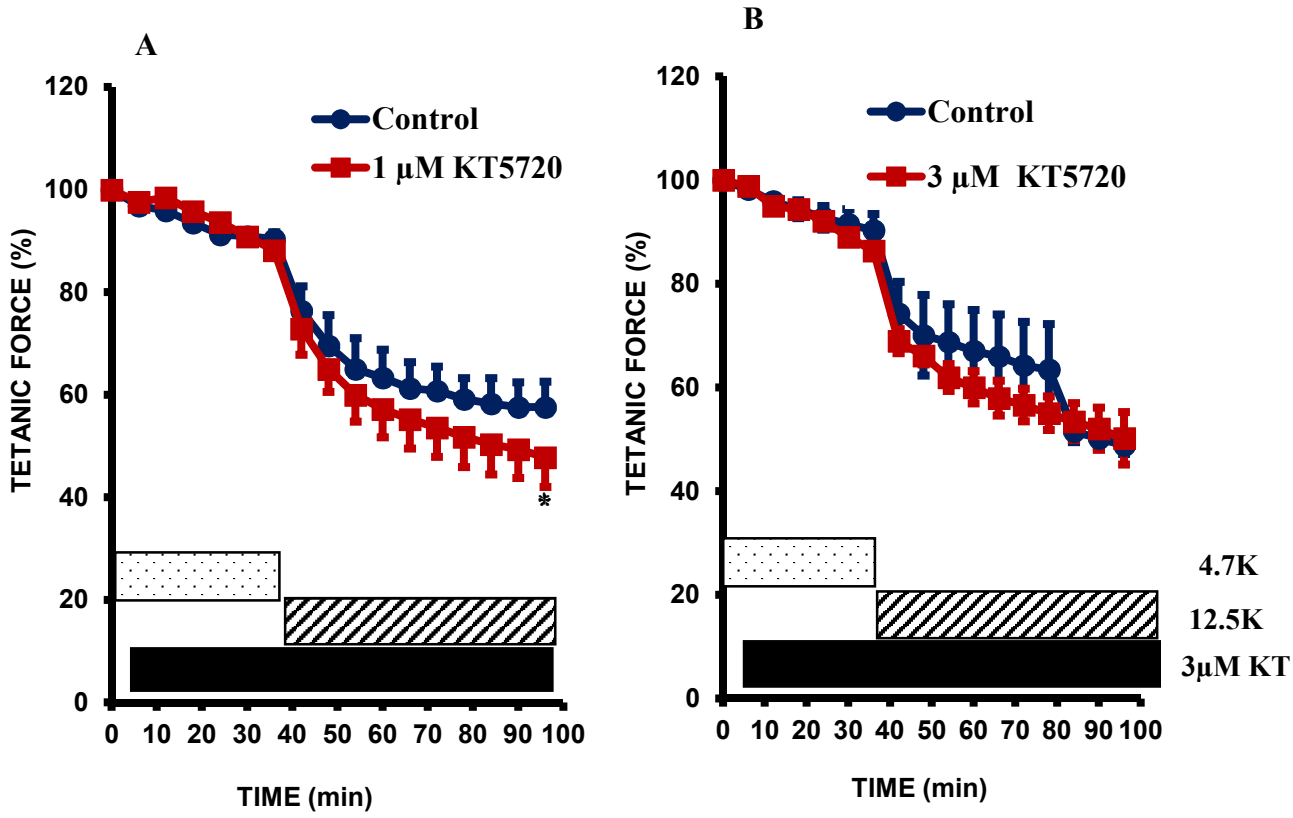

Figure 4.4. Inhibiting PKA with KT5720 increases the extent of force loss in HyperKPP diaphragm at 12.5 mM K^+. Peak tetanic force is expressed as a percent of the force at time 0 min. Tetanic contractions were elicited with 200 ms train of pulses at 200 Hz every 2 min. Muscles were allowed 30 min of equilibrium at 4.7 mM K^+ (not shown in the figure) before adding KT5729 at 6 min. A) 1 µM KT5729, B) 3 µM KT5729. Symbols:●, control group (No KT5720); ■, KT5720 treatment group. Vertical bars represent the S.E. of 3 muscles. *, Mean tetanic force of HyperKPP muscles in presence of KT5720 was significantly different from that of control; ANOVA and L.S.D., $P < 0.05$.

As mentioned in the Introduction the second objective was to test the potential of activating PKC (this chapter) and PKA (chapter 5) in HyperKPP soleus in alleviating HyperKPP symptoms. PMA, a known PKC activator, was first tested at 300 nM based on previous studies that showed an increase in NKA activity (Gao *et al.*, 1999). However, at that concentration PMA significantly worsened the capacity to generate force even at 4.7 mM K^+ (Fig. 4.5A). Reducing PMA concentration to 100 nM (Juel *et al.*, 2014) still worsened force generation (Fig. 4.5B).

In conclusion, this study did not provide evidence that PKC is involved in the asymptomatic behavior of HyperKPP diaphragm because inhibiting PKC by GF109203X did not affect tetanic force production. In regards to a potential role of PKA, the results were inconclusive because the PKA inhibitors tested in this study had effects with different magnitude and lacked the specificity. Finally, the results do not support an activation of PKC as a potential therapy to alleviate HyperKPP symptoms in hindlimb muscles.

FIGURE 4.5

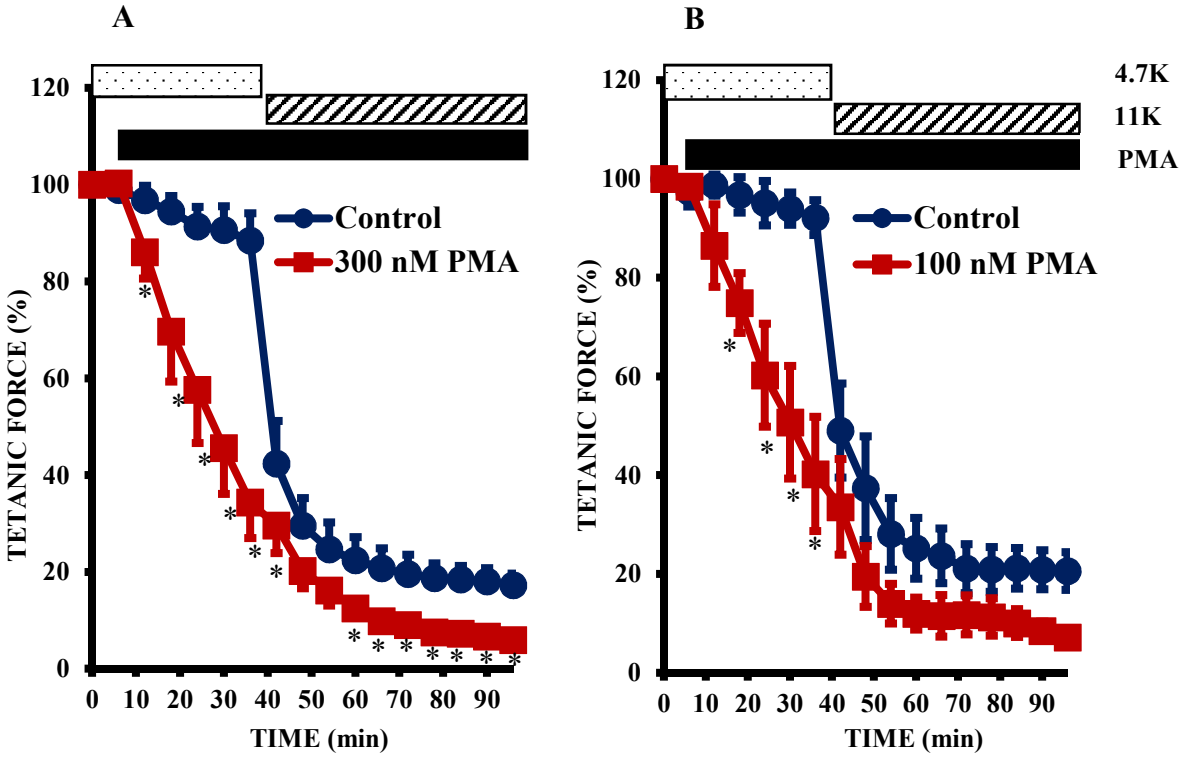

Figure 4.5. Activating PKC with PMA causes significant force loss in HyperKPP soleus at 4.7 mM K^+. Peak tetanic force is expressed as a percent of the force at time 0 min. Tetanic contractions were elicited with 200 ms train of pulses at 140 Hz every 2 min. Muscles were allowed 30 min of equilibrium at 4.7 mM K^+ (not shown in the figure) before adding PMA at 6 min. A) Muscles were first tested with 300 nM PMA B) Considering the effect is small in (A) a lower dose of 100 nM PMA was tested. Symbols:●, control group (No PMA); ■ PMA treated group. Vertical bars represent the S.E. of 3 muscles. *, Mean tetanic force of HyperKPP muscles in presence of PMA was significantly different from that of control; ANOVA and L.S.D., $P < 0.05$.

CHAPTER 5

INVESTIGATING THE IMPACT OF ACTIVATING PKA AS A POTENTIAL THERAPEUTIC APPROACH TO TREAT HYPERKALEMIC PERIODIC PARALYSIS

Tarek Ammar and Jean-Marc Renaud

Department of Cellular and Molecular Medicine, University of Ottawa, Ottawa, Ontario, Canada

ABSTRACT

HyperKPP treatments are not fully effective or lose effectiveness over time. Salbutamol, a β_2-adrenergic agonist, can prevent paralysis in HyperKPP patients and fully restores force generation in skeletal muscles of a HyperKPP mouse model. One mechanism of action of salbutamol is the activation of NKA pump via the cAMP/PKA pathway. More importantly, NKA pump is an important cell membrane component that contributes to the asymptomatic behavior of HyperKPP diaphragm. However, salbutamol loses effectiveness over time in some HyperKPP patients. The aim of this study was to investigate a different approach to activate PKA for a new a therapy to treat HyperKPP. First the effects of forskolin, an adenylate cyclase activator, were tested. Tetanic force of HyperKPP soleus increased in the presence of forskolin while $[K^+]_e$ was 4.7 mM. However, when $[K^+]_e$ was increased to 8 mM, the force loss was greater in the presence than in the absence of forskolin. Probenecid a multidrug resistance protein (MRP) inhibitor had no effect on how forksolin modulated force at 4.7 mM K^+, but reduced the extent of force loss at 8 mM K^+. Forskolin did not significantly affect resting EM, AP peak and the number of excitable fibers. PKA is also known to phosphorylate K_{ATP} channels and increase their activity. However, glibenclamide, a K_{ATP} channel blocker, did not modify the forksolin effects on tetanic force. So pinacidil, a K_{ATP} channel opener, was tested. It increased force production, hyperpolarized resting EM, improved AP peak and increased the number of excitable fibers in HyperKPP soleus. Exposing soleus to both forksolin and pinacidil did not result in greater force improvement and membrane excitability compared to pinacidil alone. It was noted that the efficiency of forskolin at improving tetanic force was less than previously reported with salbutamol. Here, it is shown that salbutamol fully restores the tetanic force of HyperKPP soleus at 8 mM K^+ to level similar to that of WT force whether salbutamol was added while HyperKPP soleus was at 4.7 mM K^+ before

switching to 8 mM K^+ or after 30 min exposure to 8 mM K^+. It is concluded that forskolin is less effective than salbutamol in alleviating HyperKPP symptoms and that activation of K_{ATP} channels should be considered as another potential approach to treat HyperKPP patients.

INTRODUCTION

Salbutamol, a β_2-adrenergic agonist, has been used to treat HyperKPP patients, as it prevents paralytic attack after a K^+ ingestion or exercise (Clausen & Flatman, 1977; Clausen *et al.*, 1980). Salbutamol restores force of HyperKPP soleus almost completely to WT levels even after force had been depressed by 10 mM K^+ (Clausen *et al.*, 2011). The mechanism of action of β_2-adrenergic receptor activation involves an activation of NKA pump (Wang & Clausen, 1976; Clausen & Flatman, 1977; Buchanan *et al.*, 2002; Clausen *et al.*, 2011) reducing $[Na^+]_i$ and $[K^+]_e$ while hyperpolarizing resting EM; all events that help restoring membrane excitability at high $[K^+]_e$. It also increases $[Ca^{2+}]_i$ during a contraction (Cairns *et al.*, 1993; Ha *et al.*, 1999; Rudolf *et al.*, 2006) which can help compensate if membrane excitability is not fully restored.

Salbutamol is a Food and Drug Administration (FDA) approved drug that is acutely used during bronchial asthma. However, chronic use over time leads to loss of effectiveness (Sears, 2002; Cazzola *et al.*, 2012). Chronic administration of salbutamol for 2 weeks also resulted in 22% reduction in β_2-adrenergic receptor density (Hayes *et al.*, 1996). Loss of effectiveness has been reported with chronic use in HyperKPP patients too. For example, over a period of 2-3 years, 3 out of 10 HyperKPP patients are no longer alleviated from the symptoms by salbutamol (Wang & Clausen, 1976; Clausen *et al.*, 1980). So, the use of salbutamol on a chronic basis is not feasible as a treatment for HyperKPP.

β_2-adrenergic receptors are Gs protein coupled receptors and together they activate adenylyl cyclase and increase cAMP levels. The binding of cAMP to PKA increases the activity of the latter (Johnson, 1998; Cazzola *et al.*, 2012). PKA phosphorylation of PLM allows for an increased NKA pump activity via an increase in Na^+ affinity (Bibert *et al.*, 2008; Shattock, 2009; Pavlovic *et al.*, 2013*a*; Pirkmajer & Chibalin, 2016). PKA also phosphorylate ryanodine receptors

allowing for an increase in $[Ca^{2+}]_i$ (Reiken *et al.*, 2003; Rudolf *et al.*, 2006; Cairns & Borrani, 2015). Skeletal muscle K_{ATP} channels are composed Kir6.2 and SUR2A (Ashcroft, 2000). PKA phosphorylation of these subunits, increases the channel activity (Béguin *et al.*, 1999; Lin *et al.*, 2000). More importantly, as activation of K_{ATP} channel hyperpolarizes resting EM in WT muscles (Zhu *et al.*, 2014). It is therefore expected to help restore resting EM in HyperKPP muscles. So, an activation of PKA maybe another strategy to treat HyperKPP patients.

One approach to activate PKA can involve a stimulation of adenylate cyclase with forskolin to increase cAMP levels. Forskolin is a commercially available supplement. It is also being tested in clinical trials to treat asthma (Gonzalez-Sanchez *et al.*, 2006; Huerta *et al.*, 2010). So, the objective of this study was to test the hypothesis that "exposing HyperKPP muscles to forskolin will improve membrane excitability and force generation to level similar to that of WT as observed with salbutamol".

MATERIALS AND METHODS

ANIMALS AND APPROVAL FOR ANIMAL STUDIES

HyperKPP mice (strain FVB.129S4(B6)-*Scn4a*$^{tm1.1Ljh}$/J) were generated by knocking in the equivalent of human missense mutation M1592V into the mouse genome; i.e., at position 1585 as previously described by Hayward et al. (2008). The FVB strain was used as wild-type mouse. All mice were 2-3 months old and weighed 20-30 g. The homozygous mutants generally do not survive beyond postnatal day five, so knock-in mice were maintained as heterozygotes by crossbreeding with FVB mice. Mice were fed ad libitum and housed according to the guidelines of the Canadian Council for Animal Care. The Animal Care Committee of the University of Ottawa approved all experimental procedures used in this study. Before muscle excision, 2-3 months old mice were anaesthetized with a single intraperitoneal injection of 2.2 mg ketamine/0.4 mg xylazine/0.22 mg acepromazine per 10 g of animal body weight, and sacrificed by cervical dislocation. Soleus muscles were then dissected out.

GENOTYPING

A 2 mm tail piece was incubated overnight with 500 µl tail digestion buffer (0.2 mM Na_2EDTA and 25 mM NaOH, pH 12.3) and 50 µl Proteinase K (1mg/mL) at 56 °C. DNA extraction involved the addition of 650 µl of 1:1 Phenol:CIA and centrifuged at 12000 g for 10 min. 650 µl of CIA was added twice to the pellet and centrifuged before suspending the resulting pellet in 750 µl of isopropyl alcohol. After 10 min, the solution was centrifuged 15 min at 15000 g. The alcohol was removed and the pellet suspended in 750 µl 70% ethanol and centrifuged. After removing the alcohol, the pellet was let to dry 30 min before the addition of 200 µl TE buffer (10mM Tris, 1 mM EDTA, pH 8.0) and incubated at 65 °C for 2 hours. PCR was then completed using the previously extracted DNA and the following primers:

NC1F (forward): 5'-TGTCTAACTTCGCCTACGTCAA-3'

NC2R (reverse): 5'-GAGTCACCCAGTACCTCTTTGG-3'

PCR products were digested 6 h using the restriction digest enzyme *Nsp*I. The mutation that is knocked in to the HyperKPP mice causes the removal of one *Nsp*I cut site that is easily detected by agarose gel electrophoresis; two bands were visualized for wild-type mice, which carry the cut site on both alleles, and three bands were seen for heterozygous HyperKPP mice harboring one normal allele and one mutant allele.

SOLUTIONS

Control solution contained in (mM): 118.5 NaCl, 4.7 KCl, 1.3 $CaCl_2$, 3.1 $MgCl_2$, 25 $NaHCO_3$, 2 NaH_2PO_4 and 5.5 D-glucose. Solutions containing different K^+ concentrations were prepared by adding the appropriate amount of KCl. All drug used in this study were prepared by first dissolving them in DMSO before being added to the control solution. For all solutions including control, the final DMSO concentration was 0.1% (vol/vol). Solutions were continuously bubbled with 95% O_2–5% CO_2 to maintain a pH of 7.4. Experimental temperature was 37°C. Total flow of solutions in the muscle chamber was 15 ml/min being split just above and below the muscle in order to prevent any buildup of reactive oxygen species, which is quite large at 37°C and deleterious (Edwards *et al.*, 2007).

FORCE MEASUREMENT

Muscles were positioned horizontally in a Plexiglas chamber. One end of the muscle was fixed to a stationary hook, whereas the other end was attached to a force transducer (model # 400A, Aurora Scientific Canada). The transducer was connected to a data acquisition system (KCP13104, Keithley) and data were recorded at 5 kHz. Electrical pulses were applied across two platinum wires (4 mm apart) located on opposite sides of the fibers. The wires were connected to a Grass S88 stimulator and a Grass SIU5 isolation unit (Grass Technologies). Tetanic contractions were

elicited with 200-ms trains of 0.3 ms, 10-V (supramaximal voltage) pulses. Stimulation frequencies were set to give maximum tetanic force: being 140 Hz for soleus. Tetanic contractions were elicited every 2 or 5 min as indicated in the legend. Muscle length was adjusted to give maximal tetanic force and muscles were then allowed to equilibrate for 30 min at 4.7 mM K^+ before any change in [K^+] or drug addition. Tetanic force was defined as the force developed while muscles were electrically stimulated and was calculated as the difference between the maximum force during a contraction and the baseline force measured 5 ms before stimulation.

RESTING EM AND ACTION POTENTIAL MEASUREMENTS

Resting EM and action potential were measured using glass microelectrodes. Microelectrodes tip resistances were 7~15 MΩ and that of the reference electrode were ~1 MΩ. All electrodes were filled with 3 M KCL. A recording was rejected when the change in potential upon penetration was not a sharp drop or when the microelectrode potential did not return to zero upon withdrawal from the fiber. Single action potentials were elicited using fine platinum wires placed along the surface fibers using a single 10-V, 0.3-ms square pulse. For each muscle, measurements were done in 10-15 fibers and a mean value was then calculated for each muscle.

STATISTICS

Data are presented as means ± SE. ANOVA was used to determine significant differences. Split plot ANOVA designs were used when muscles were tested at all-time levels. ANOVA calculations were made with version 9.2 General Linear Model procedures of the Statistical Analysis Software (SAS Institute, Cary, NC). When a main effect or an interaction was significant, the least square difference was used to locate the significant differences (Steel & Torrie, 1980). The word "significant" refers only to a statistical difference ($P < 0.05$).

RESULTS

EFFECT OF FORSKOLIN ON FORCE

A 30 min exposure to 10 μM forskolin at 4.7 mM K^+ increased tetanic force of HyperKPP soleus by 24% (Fig. 5.1A), i.e. from 20 N/cm^2 to 25 N/cm^2. While this effect alleviated muscle weakness, it did not allow for an increase in force to levels measured in WT soleus, which on average generated 34 N/cm^2. Surprisingly, when $[K^+]_e$ was increased to 11 mM force decreased from 124% to 25% which was greater than the force loss from 89% to 17% in the absence of forskolin. Even more unexpected was the effect of forskolin in WT soleus, while it had no effect at 4.7 mM K^+ it caused a greater force depression at 11 mM K^+ in WT soleus as force decreased by 40% and 67% in the absence and presence of forskolin, respectively (Fig. 5.1B).

Recent studies have shown that any manipulations that cause an increase in cAMP levels, such as exposure to β_2-adrenergic agonists and forskolin, result in a transient increase in twitch force in WT mouse diaphragm; the rising phase lasting 30 minutes (Duarte *et al.*, 2012). The initial increase in force is associated with increases in $[Ca^{2+}]_i$ during contractions as PKA phosphorylates ryanodine receptor, the sarcoplasmic reticulum Ca^{2+} release channels (Reiken *et al.*, 2003; Rudolf *et al.*, 2006; Lynch & Ryall, 2008). The subsequent force decline is due to a cAMP efflux as it is transported by MRP. cAMP is then metabolized to adenosine, which acts on its receptors to inhibit adenylyl cyclase resulting in a decreased cAMP production counteracting the β-adrenergic agonist and forskolin effect (Godinho & Costa, 2003; Chiavegatti *et al.*, 2008; Duarte *et al.*, 2012). Considering that soleus was exposed to 11 mM K^+ 30 min after an exposure to forskolin, it is then possible that the force decrease may not only be due to the K^+-induced force depression but also due an increase in extracellular cAMP ($[cAMP]_e$) and adenosine. Probenecid is an

FIGURE 5.1

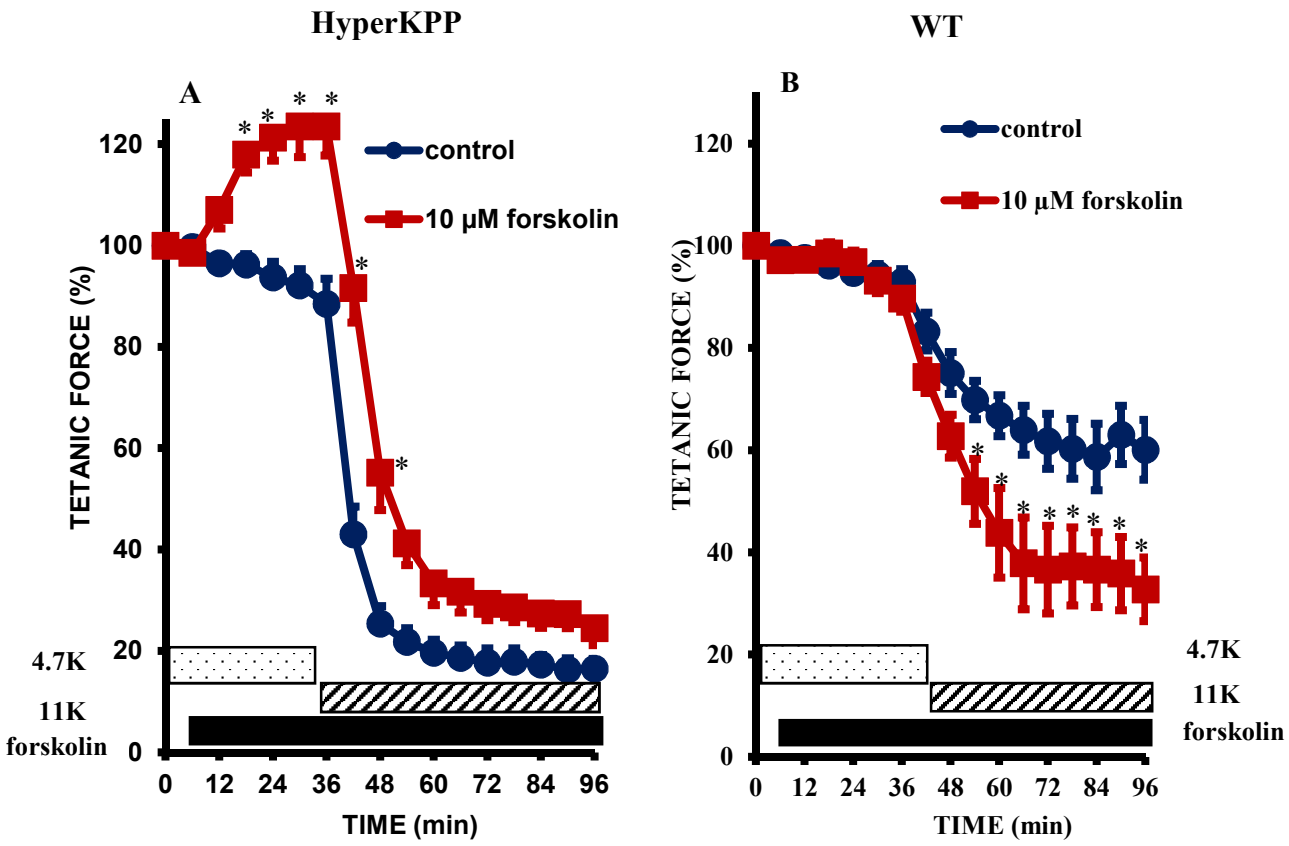

Figure 5.1. Forskolin improved force generation in at 4.7 mM K^+ in HyperKPP soleus but caused a greater depression at 11 mM K^+ in both HyperKPP and WT soleus. Tetanic contractions were elicited with 200 ms train of pulses at 140 Hz every 2 min. Peak tetanic force is expressed as a percent of the force at time 0 min. Muscles were allowed 30 min of equilibrium at 4.7 mM K^+ (not shown in the figure) before adding forskolin at time 6 min. A) HyperKPP and B) WT soleus. Symbols:●, control (No forskolin); ■, 10 µM forskolin. Vertical bars represent the S.E. of 3 HyperKPP muscles and 5 WT muscles. *, Mean tetanic force of HyperKPP or WT muscles in presence of forskolin was significantly different from that of control; ANOVA and L.S.D., $P < 0.05$.

MRP inhibitor and has been shown to prevent the subsequent force decrease observed with β_2-adrenergic receptor agonists by reducing cAMP efflux and the subsequent adenosine production (Chiavegatti *et al.*, 2008; Duarte *et al.*, 2012). So, next we tested whether probenecid can prevent the large decrease in tetanic force when $[K^+]_e$ was increased.

For the rest of the study a new protocol was used. First, the duration for which soleus was exposed to any drug while at 4.7 mM K^+ was increased from 30 min to 2 hr to better understand how stable force is in the presence of forskolin before increasing $[K^+]_e$; i.e. to determine if there is any major decrease in tetanic force after 30 min exposure to forskolin as it occurs for the twitch force in WT mouse diaphragm. Second, tetanic force, resting EM and AP were concomitantly measured using paired muscles form the same mouse. One soleus was used for force measurement, the other for resting EM and AP. This approach was used to better relate how change in membrane excitability by forskolin and forskolin + probenecid affects force production. Third, the elevated $[K^+]_e$ was reduced from 11 to 8 mM because at 11 mM too many HyperKPP fibers depolarize beyond -55 mV, an EM at which AP are no longer generated (Chapter 3).

Addition of forskolin increased force to 110% after 30 min (Fig. 5.2), then force started to decrease gradually reaching 95% of initial force after 2 hr, while for control HyperKPP tetanic force was significantly less at 71%. When $[K^+]_e$ was increased to 8 mM, tetanic force decreased to 41% within 15 min for control HyperKPP, changing very little thereafter. In the presence of forskolin, the force decrease was slower but still greater than in control as observed with 11 mM K^+. That is, it decreased from 94% to 49% for a net decrease of 45% compared to 33% in control condition after 1 hr. The decrease with forskolin was, however slower, occurring over 50 min compared to only 15 min in the absence of forskolin. The initial force increase and the subsequent

FIGURE 5.2

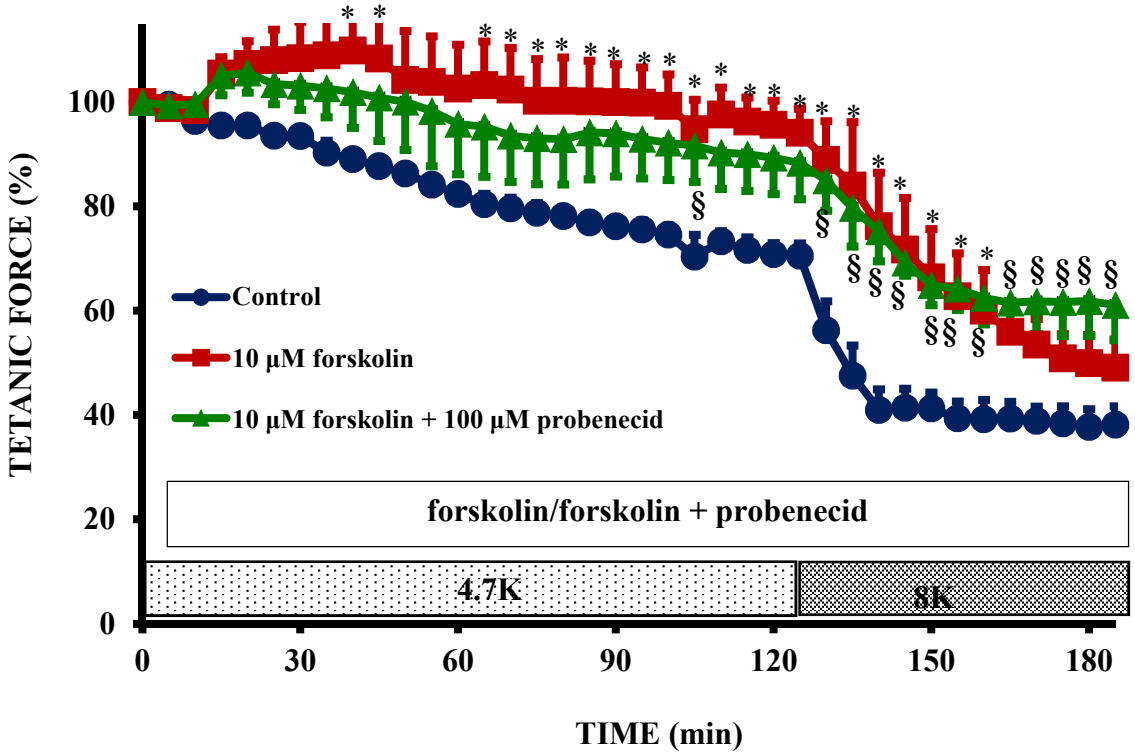

Figure 5.2. Forskolin + probenecid reduced force loss at 8 mM K^+ in HyperKPP soleus. Tetanic contractions were elicited with 200 ms train of pulses at 140 Hz every 5 min. Peak tetanic force is expressed as a percent of the force at time 0 min. Muscles were allowed 30 min of equilibrium at 4.7 mM K^+ (not shown in the figure). Forskolin with or without probenecid was added at time 5 min. Symbols:●, control; ■, 10 µM forskolin; ▲ 10 µM forskolin + 100 µM probenecid. Vertical bars represent the S.E. of 5 muscles. *, Mean tetanic force of HyperKPP muscles in presence of forskolin; §, mean tetanic force of HyperKPP muscles in presence of forskolin and probenecid; were significantly different from that of control; ANOVA and L.S.D., $P < 0.05$.

decrease upon the addition of forskolin at 4.7 mM K^+ was not significantly affected by the concomitant addition of probenecid. The major effect of adding both forskolin and probenecid was at 8 mM K^+ as the loss of tetanic force was smaller. That is, in the presence of probenecid and forskolin the decrease in force after 60 min was 27% compared to 45% in the presence of forskolin alone.

For 4.7 mM K^+, resting EM measurements were carried out at 30 min, the time at which force was at its maximum, and at 90 min before switching to 8 mM K^+. Mean resting EM here was significantly less negative in HyperKPP control, being -65 mV compared to WT for which the mean was -77mV (Fig. 5.3A). Exposure to forskolin did not improve resting EM after 30 and 90 min as mean resting EM were at -65 and -63 mV, respectively. Concomitant exposure to forskolin and probenecid also failed to improve resting EM. Increasing $[K^+]_e$ to 8 mM K^+ depolarized mean resting EM to -68 mV in WT and to -59 mV in HyperKPP control. Again addition of forskolin or forskolin + probenecid did not improve resting EM.

After 30 min at 4.7 mM K^+, mean AP peak of WT was 17 mV in WT soleus fibers compared to -12 mV in HyperKPP control fibers (Fig. 5.3B). After 90 min, mean AP peak was lower in control HyperKPP, being -22 mV, a similar decrease did not occur with either forskolin or forskolin + probenecid. At 8 mM K^+, mean AP peak decreased to -2 mV in WT and to -33 mV in control HyperKPP. Forskolin did not significantly affect mean AP peak while the decrease in mean AP peak was less with forskolin + probenecid, albeit the difference with forskolin alone was not significant.

The number of fibers that generated an AP upon stimulation represented 85% of the tested fibers in WT at 4.7 mM K^+ while it was 60% in control HyperKPP at 30 min (Fig 3.C),

FIGURE 5.3

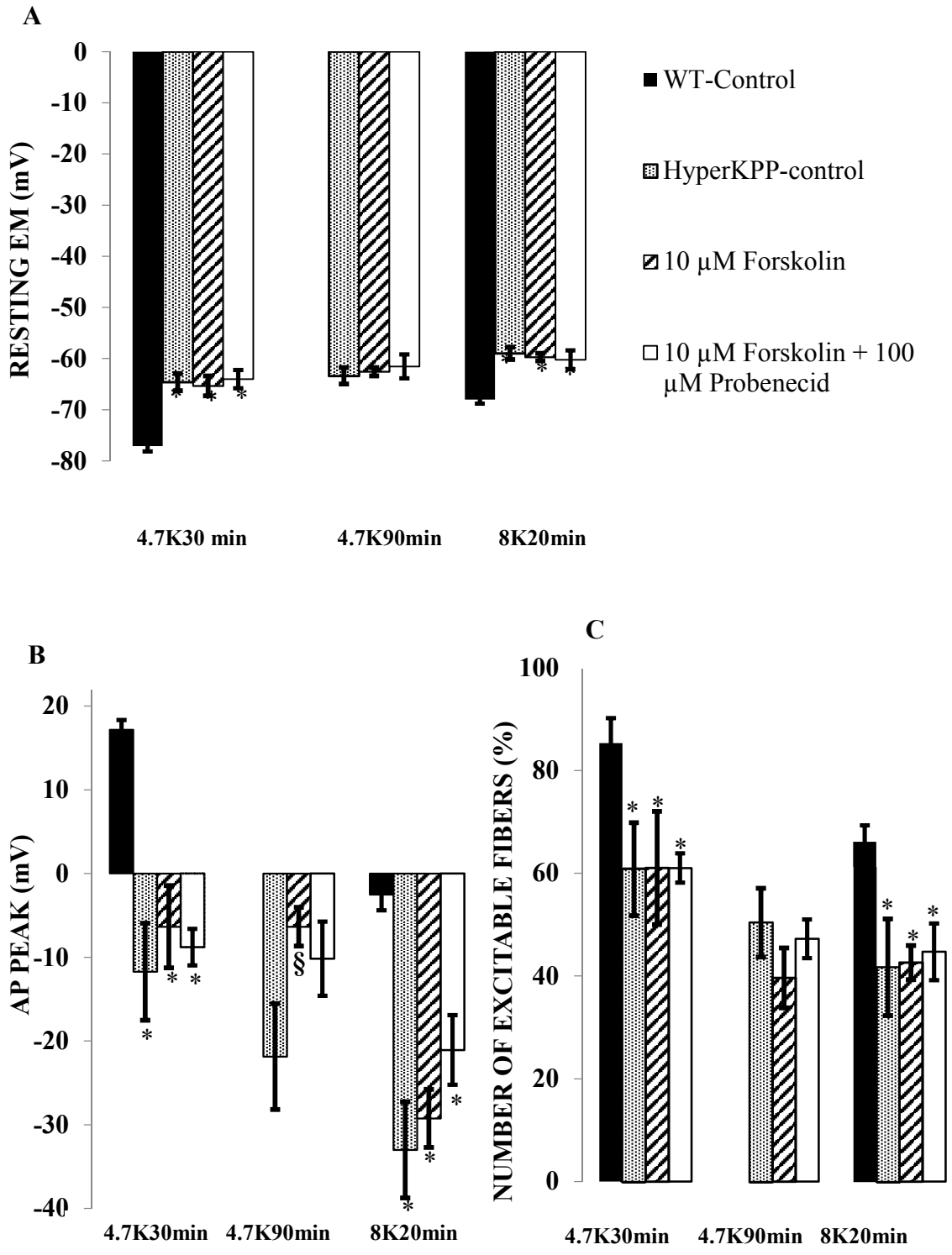

Figure 5.3. Forskolin and forskolin + probenecid slightly improved AP peak while it did not improve excitability and resting EM in HyperKPP soleus. A) resting EM, B) AP peak and C)

number of excitable fibers percentage. At 4.7 mM K^+, resting EM was measured between 25 and 35 min (labelled 30 min) and 85 and 95 min (labelled 90 min). At 8 mM K^+, resting EM was measured between 15 and 25 min (labelled 20 min). The total number of fibers tested ranged from 82-123 for each condition. Vertical bars represent the S.E. of 5 muscles. *, Mean values of HyperKPP muscles were significantly different from that of WT; §, Mean values of HyperKPP muscles in presence of forskolin and forskolin + probenecid were significantly different from HyperKPP control; ANOVA and L.S.D., $P < 0.05$.

becoming even lower to 50% after 90 min (Fig. 5.3C). At 8 mM K^+, the number of excitable fibers in WT decreased to 60% while it decreased to 42% in control HyperKPP. Forskolin and forskolin + probenecid failed to improve the number of excitable fibers at 4.7 or 8 mM K^+.

FORSKOLIN AND K_{ATP} CHANNEL

The absence of any hyperpolarization by forskolin suggests that neither the activity of NKA pumps and K_{ATP} channels was increased. To confirm that K_{ATP} channels were not activated, muscles were exposed to forskolin in the presence and absence of 10 μM glibenclamide, a K_{ATP} channel inhibitor. The increase in force and the slow decrease thereafter observed with forskolin was not affected by the presence of glibenclamide (Fig. 5.4), further supporting the notion that the increase in force with forskolin does not involve an increase in K_{ATP} channel activity.

Since there is no evidence for the activation of K_{ATP} channels by forskolin, the next question was whether a combination of pinacidil, a K_{ATP} channel opener, and forskolin can better alleviate HyperKPP symptoms. At 4.7 mM K^+, pinacidil alone increased mean tetanic force by 27% in 15 min (Fig. 5.5), which was greater than the 10% increase by forskolin. Thereafter, tetanic force in the presence of pinacidil decreased reaching 116% after 2 hr. Concomitant exposure to forskolin and pinacidil did not significantly increase tetanic force above that of pinacidil alone and did not affect the subsequent decrease. When $[K^+]_e$ was increased to 8 mM for 60 min in presence of pinacidil, tetanic force decreased only by 7% of the initial force at the start of an experiment compared to 51% in presence of forskolin alone. Notably, concomitant exposure to pinacidil and forskolin resulted in greater decrease force, i.e.16%, when compared with pinacidil alone but still less than the control, which was 62%.

After 30 min at 4.7 mM K^+ in presence of pinacidil, mean resting EM was 4 mV more

FIGURE 5.4

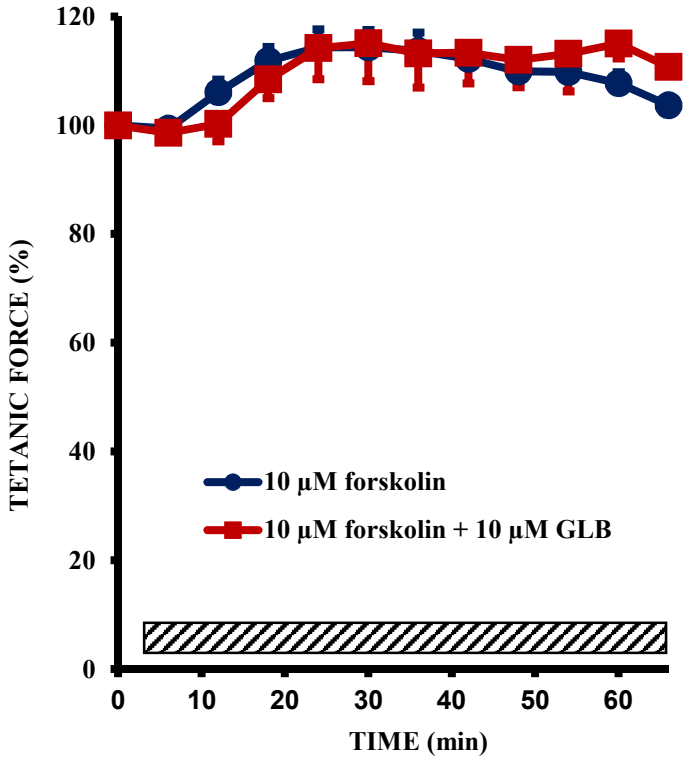

Figure 5.4. Inhibiting K_{ATP} channel with glibenclamide did not affect how forskolin modulates force in HyperKPP soleus. Tetanic contractions were elicited with 200 ms train of pulses at 140 Hz every 2 min. Peak tetanic force is expressed as a percent of the force at time 0 min. Muscles were allowed 30 min of equilibrium at 4.7 mM K^+ (not shown in the figure) before adding forskolin or forskolin + glibenclamide at time 6 min. Symbols: ●, 10 µM forskolin; ■, 10 µM forskolin + 10 µM glibenclamide. Vertical bars represent the S.E. of 3 muscles. ANOVA and L.S.D., $P < 0.05$.

FIGURE 5.5

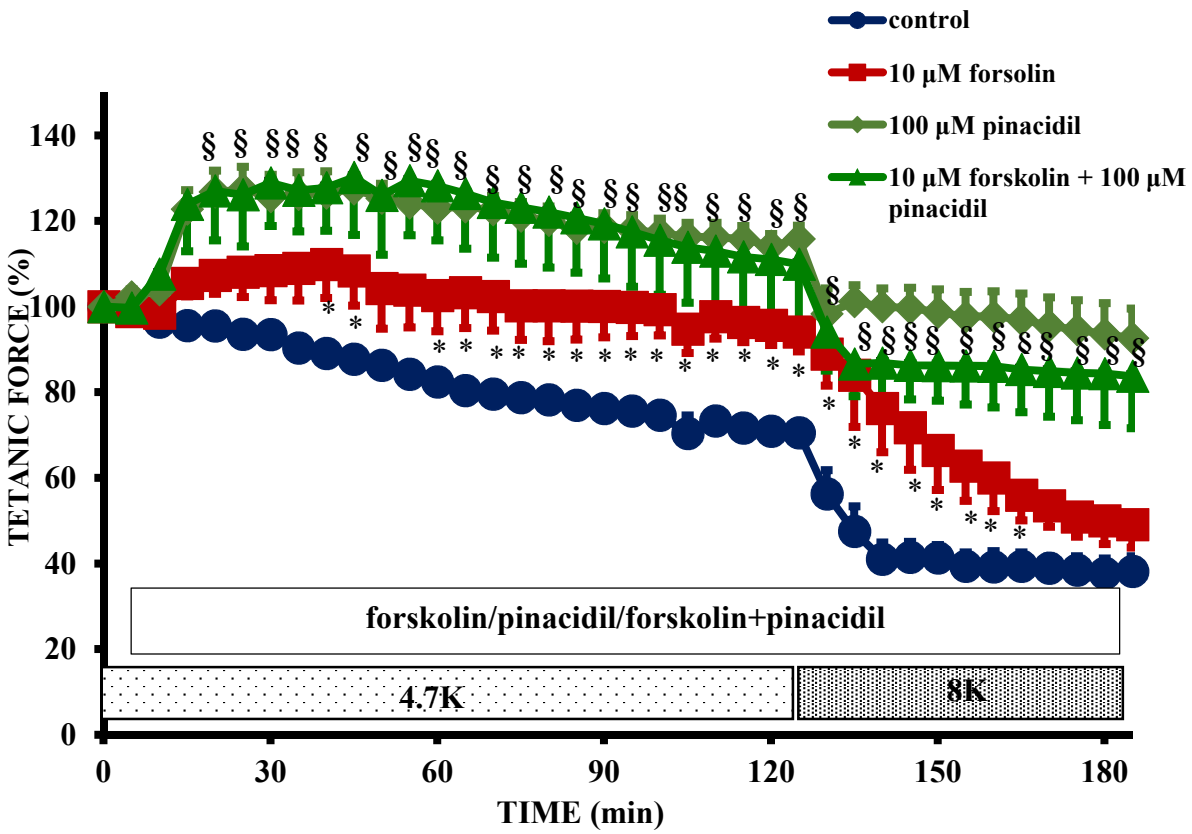

Figure 5.5. Pinacidil increases force production at 4.7 mM K^+ and 8 mM K^+ in HyperKPP soleus. Tetanic contractions were elicited with 200 ms train of pulses at 140 Hz every 5 min. Peak tetanic force is expressed as a percent of the force at time 0 min. Muscles were allowed 30 min of equilibrium at 4.7 mM K^+ (not shown in the figure). Forskolin, pinacidil and pinacidil + forskolin were added at time 6 min. Note that control and forskolin group are the same ones as in Fig. 5.2. Symbols: ●, control; ■, 10 µM forskolin; ◆, 100 µM pinacidil; ▲, 100 µM pinacidil + 10 µM forskolin. Vertical bars represent the S.E. of 5 muscles. *, Mean tetanic force of HyperKPP muscles in presence of forskolin; §, mean tetanic force of HyperKPP muscles in presence of pinacidil and forskolin + pinacidil; were significantly different from that of control; ANOVA and L.S.D., $P < 0.05$.

negative compared to that of control condition (Fig. 5.6A). The difference in resting EM was still present at 90 min. Despite this, mean resting EM in presence of pinacidil (-69 mV) was significantly lower than in WT fibers for which mean resting EM was at -77 mV. At 8 mM K^+, mean resting EM was 3 mV more negative in the presence than in the absence of pinacidil. Addition of forskolin to pinacidil did not further improve mean resting EM compared to pinacidil alone.

The most striking effect for pinacidil was a significant improvement of mean AP peak. After 30 min at 4.7 mM K^+, mean AP peak was 2 mV in the presence of pinacidil compared to -12 mV in the control fibers (Fig. 5.6B). At 90 min, mean AP peak was 6 and -22 mV in the presence and absence of pinacidil, respectively. At 8 mM K^+, pinacidil also improved mean AP peak being -20 mV with pinacidil compared to -33 mV in control. Mean AP was not different between pinacidil and pinacidil + forskolin after 30 min at 4.7 mM K^+ and at 8 mM K^+.

The number of excitable fibers after 30 min at 4.7 mM K^+ was 75% in presence of pinacidil compared to 61% in the control and in presence of forsklin (Fig. 5.6C). After 90 min, the mean number of excitable fibers decreased to 68% in presence in pinacidil while it was 50% in control and 40% with forskolin. At 8 mM K^+, the number of excitable fibers decreased to 55% in the presence of pinacidil a value that was greater than 42% and 43% in control and in presence of forskolin, respectively. Concomitant addition of pinacidil and forskolin did not cause a further improvements compared to pinacidil alone.

SALBUTAMOL

Restoration of membrane excitability and force in HyperKPP soleus (this study) was much less than when compared to full restoration by salbutamol in a previous study

FIGURE 5.6

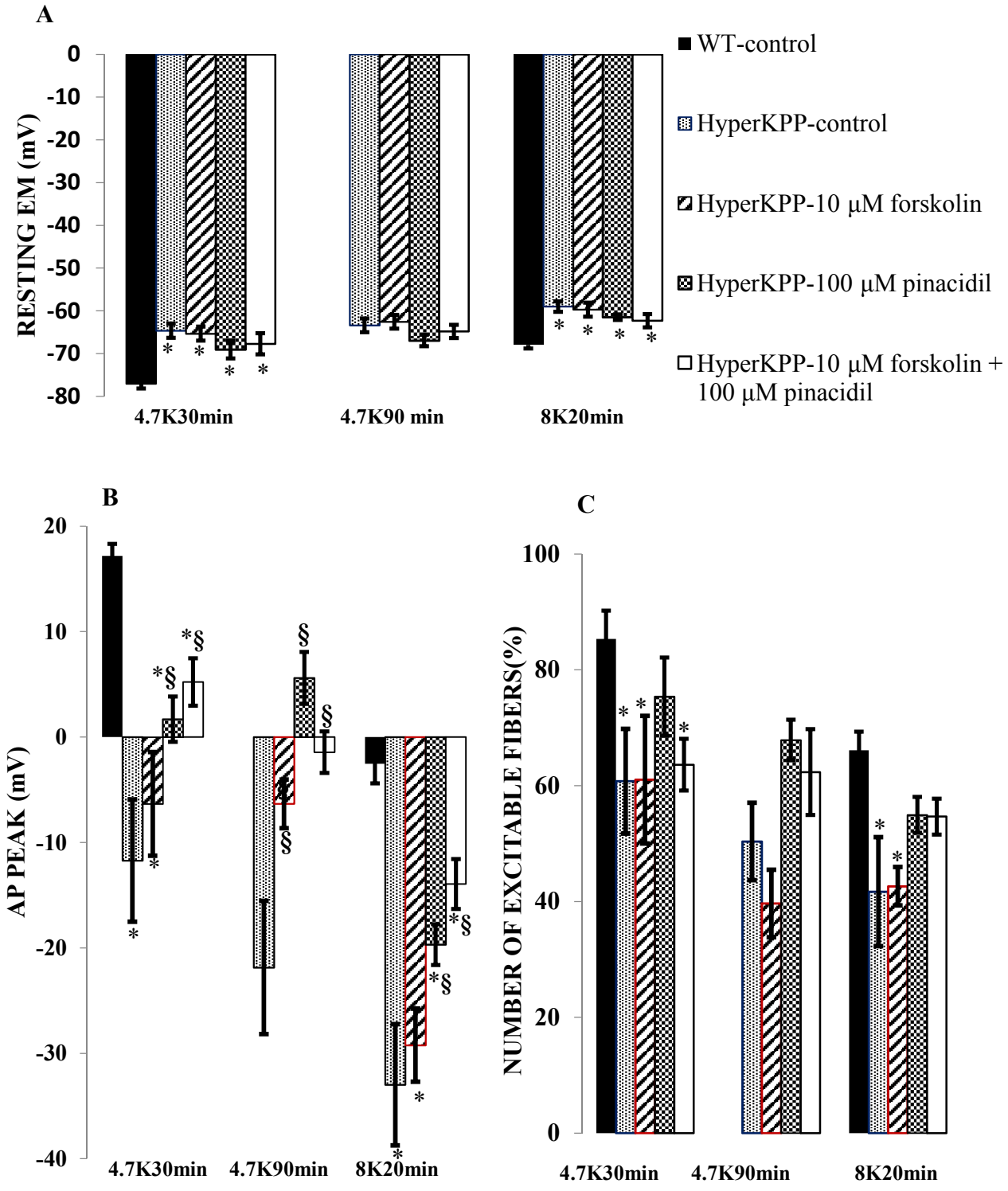

Figure 5.6. Pinacidil improves membrane excitability in HyperKPP soleus. A) resting EM, B) AP peak and C) number of excitable fibers percentage. At 4.7 mM K^+, resting EM was measured

between 25 and 35 min (labelled 30 min) and 85 and 95 min (labelled 90 min). At 8 mM K^+, resting EM was measured between 15 and 25 min (labelled 20 min). Note that control and forskolin group are the same ones as in Fig. 5.3. The total number of fibers tested ranged from 82-127 for each condition. Vertical bars represent the S.E. of 5 muscles. *, Mean values of HyperKPP muscles were significantly different from that of WT; §, Mean values of HyperKPP muscles in presence of forskolin, pinacidil and pinacidil + forskolin were significantly different from HyperKPP control; ANOVA and L.S.D., $P < 0.05$.

(Clausen *et al.*, 2011). Two main differences exist between our study and that of Clausen et al. The first difference is the time when muscles are exposed to drugs. Clausen et al. added salbutamol only after increasing $[K^+]_e$ to 10 mM, while in this study muscles were exposed to forskolin while still exposed to 4.7 mM K^+. Considering that the eventual increase in $[cAMP]_e$ and adenosine associated with β_2-adrenergic agonists and forskolin causes force depression (Godinho & Costa, 2003; Chiavegatti *et al.*, 2008; Duarte *et al.*, 2012), it is then possible that salbutamol may be less effective at improving force at high $[K^+]_e$ if also added while muscles are exposed to 4.7 mM K^+. The second difference is the experimental temperature, which was 37°C in our study and 30°C in the Clausen et al. study. Such difference in temperature may have a large impact on the cAMP transport rate as it has been shown for NKA pump (Pedersen *et al.*, 2003) which may lead to a greater rate of cAMP transport and greater adenosine production at 37°C. So, in a final experiment we compared the effects of adding either salbutamol while $[K^+]_e$ is at 4.7 mM before switching to 8 mM K^+ versus adding salbutamol after the switch to 8 mM K^+.

Addition of 1 μM salbutamol at 4.7 mM K^+ first increased tetanic force by 29% in 10 min (Fig. 5.7). Then raising $[K^+]_e$ to 8 mM K^+ in presence of salbutamol only caused a small decrease in tetanic force from 122% to 106%. Adding salbutamol after a 1 hr exposure to 8 mM K^+ significantly increased force from 58% to 132% within 10 min.

So far, the data has been presented as a percentage of the force measured at the start of an experiment (i.e. time 0) for each individual group to best compare the effect of various drug applications without the complication of the variability of the initial tetanic force. However, to better understand how effective a drug condition is at improving tetanic force of HyperKPP soleus

FIGURE 5.7

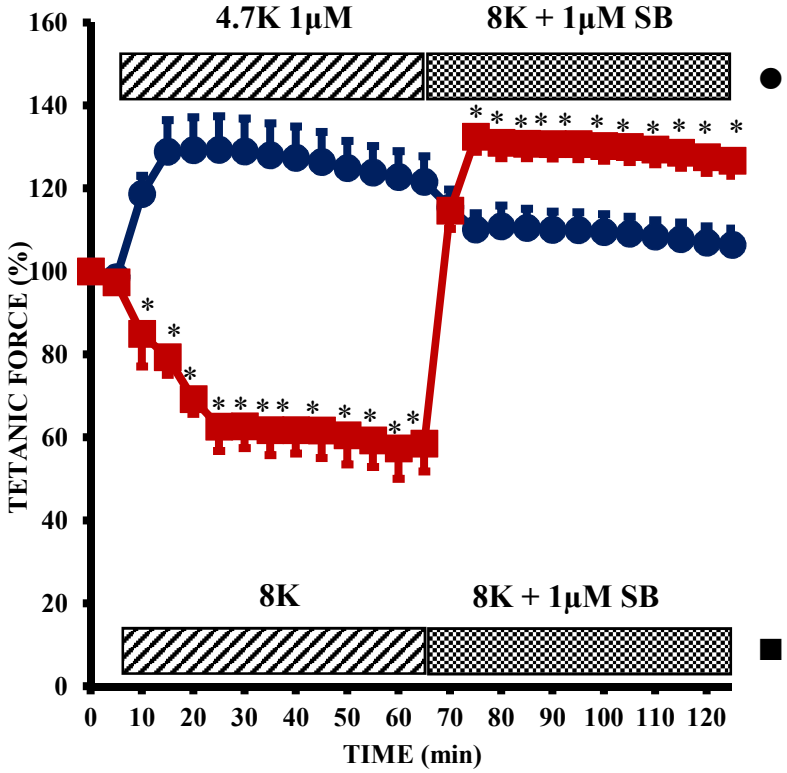

Figure 5.7. Salbutamol increases force in HyperKPP soleus. Tetanic contractions were elicited with 200 ms train of pulses at 140 Hz every 5 min. Peak tetanic force is expressed as a percent of the force at time 0 min. Muscles were allowed 30 min of equilibrium at 4.7 mM K^+ (not shown in the figure). Salbutamol or 8 mM K^+ were added at time 6 min. Symbols:●, 1 µM salbutamol was added at 4.7 mM K^+ for 1 hr then followed by 1 µM salbutamol at 8 mM K^+ for 1 hr; ■, 8K is perfused first for 1 hr then 1 µM salbutamol was added at 8 mM K^+ for 1 hr. Vertical bars represent the S.E. of 4 muscles for salbutamol added at 4.7 mM K^+ group and 5 muscles for salbutamol added at 8 mM K^+ group. *, Mean tetanic force of HyperKPP muscles were significantly different between the two groups; ANOVA and L.S.D., $P < 0.05$.

to that of WT, one must also look at the absolute forces. The mean tetanic force at the start of an experiment was 26.5 N/cm^2 for WT soleus (Table 5.1). Mean tetanic force of HyperKPP soleus was quite variable between experiments; which is typical of the disease as muscles of patients can be normal at one time with intermittent muscle weakness. For this study however, mean tetanic force of HyperKPP soleus varied between 13.5 and 19.4 N/cm^2, all being significantly less than the force in WT soleus. At 4.7 mM K^+, the efficacy of improving force in HyperKPP soleus was in the order of salbutamol ≈ pinacidil > forskolin. At 8 mM K^+, the efficacy was in the order of salbutamol added at 8 mM K^+ > pinacidil ≈ salbutamol added at 4.7 mM K^+ > forskolin. It is important to note here that the time at which salbutamol was added was also very important as its addition after an exposure to 8 mM K^+ was the most effective time to apply salbutamol.

TABLE 5.1

Mouse	Condition	No drug treament		Drug treatment	
		4.7 mM K^+	**8 mM K^+**	**4.7 mM K^+**	**8 mM K^+**
WT	**Control**	26.5 ± 2.4	20.8 ± 2.3		
HyperKPP	**Control**	15.7 ± 1.0*	6.0 ± 0.6*		
	Forskolin	17.3 ± 2.1*		19.0 ± 2.5*	8.6 ± 1.5*
	Pinacidil	19.4 ± 2.1*		24.5 ± 2.6	17.8 ± 2.0
	Salbutamol added at 4.7 mM K^+	13.5 ± 0.5*		17.6 ± 1.6*	14.4 ± 0.8
	Salbutamol added at 8 mM K^+	18.6 ± 2.0*			23.7 ± 2.9

Table 5.1. Salbutamol is the most effective treatment that fully restored force at 8 mM K^+ to level similar to WT. Absolute force is given in N/cm^2. Tetanic force at 4.7 mM K^+ with no drug treatment represents the absolute force measured at the start of each experiment (the force at time 0 in Fig. 5.2, 5.5 and 5.7) before application of any drug. For each drug treatment at 4.7 mM K^+, the values reported represent the maximum values reached at 35, 40 and 20 min for forskolin, pinacidil and salbutamol, respectively. Values at 8 mM K^+ represent the values after 60 min at 8 mM K^+. Values are presented as mean ± SE. *, Mean tetanic force of HyperKPP muscles was significantly different from WT at the same $[K^+]_e$; ANOVA and L.S.D., $P < 0.05$.

DISCUSSION

The major findings of this study were: 1) forskolin improved force of HyperKPP soleus at 4.7 mM K^+ but enhanced the force loss at 8 and 11 mM K^+, 2) addition of probenecid did not affect the modulation of force by forskolin at 4.7 mM K^+ but reduced the extent of force loss at 8 mM K^+ when compared to the decrease in presence of forskolin alone, 3) activation of K_{ATP} channels with pinacidil increased force production at 4.7 mM K^+ and reduced the extent of force loss at 8 mM K^+ 4) pinacidil but not forskolin induced a hyperpolarization of resting EM, increased number of excitable fibers and improved AP peak at 4.7 and 8 mM K^+, 5) salbutamol was more effective at improving tetanic force generation than forksolin and pinacidil.

PKA AS A THERAPEUTIC TARGET IN HYPERKPP SOLEUS

Exposing HyperKPP soleus to forskolin improved tetanic force at 4.7 mM K^+. Thisresult was expected because activation of adenylyl cyclase by forskolin increases cAMP, which then activates PKA. PLM phosphorylation by PKA increases NKA pump activity (Bibert *et al.*, 2008; Shattock, 2009; Pavlovic *et al.*, 2013*a*; Pirkmajer & Chibalin, 2016), which then contributes to the hyperpolarization of resting EM leading to better AP and fiber excitability (Clausen & Flatman, 1977; Hicks & McComas, 1989; Buchanan *et al.*, 2002). Force is also expected to increase as PKA phosphorylates ryanodine receptor resulting in greater Ca^{2+} release during contraction as the open probability of the channel increases (Reiken *et al.*, 2003; Rudolf *et al.*, 2006; Cairns & Borrani, 2015). However, contrary to our expectations, resting EM and the number of excitable fibers did not improve after 30 and 90 min of forskolin exposure even though tetanic force had increased. Such results then suggest that the increase in force in the presence of forskolin at 4.7 mM K^+ can only involve an increase in Ca^{2+} release.

One possible reason for the lack of improvement in membrane excitability is that PKA activation of NKA pump is not properly functioning in HyperKPP soleus. However, salbutamol which acts via the PKA pathway, not only improves force but also activates NKA pump in HyperKPP soleus (Clausen *et al.*, 2011). So, an improper activation is an unlikely reason for the lack of improvement of membrane excitability by forskolin. The next reason for a lack of resting EM improvement is the production of adenosine from cAMP transported out of the fiber by MRP. In WT mouse diaphragm, β_2-adrenergic agonists and forskolin cause transient increases in twitch force (Duarte *et al.*, 2012). The initial force increase, which lasts 30 min is due to an increase in $[Ca^{2+}]_i$ (Reiken *et al.*, 2003; Rudolf *et al.*, 2006) while the subsequent decrease is due a buildup of $[cAMP]_e$ which is then metabolized to adenosine. Adenosine then suppresses force by exerting a negative feedback inhibition on adenylyl cyclase thus reducing cAMP generation (Godinho & Costa, 2003; Chiavegatti *et al.*, 2008; Duarte *et al.*, 2012). The decline returns twitch force back to either the force prior to drug exposure or even lower. Using tetanic contraction in this study, the decrease in force was much less with forskolin in HyperKPP soleus. The most likely explanation for the discrepancy between twitch and tetanic force is that AP are generated during a tetanus allowing for a more sustained $[Ca^{2+}]_i$ than with twitch.

While the increase in twitch force occurs over 30 min in WT mouse diaphragm, the time at which the force decline starts is expected to occur sooner in fibers located at the muscle surface than those in the middle core. Accordingly, improvement in membrane excitability in HyperKPP soleus should occur sooner in surface fibers as well as the subsequent decline; i.e. it is more than likely that the decline in membrane excitability started before the 30 min exposure to forskolin, the time at which resting EM and AP potentials were measured. Future studies will therefore be

necessary to determine if forskolin improves membrane excitability during the first 10 min of exposure.

Another unexpected finding was the decrease in tetanic force at 8 mM K^+ which was greater in the presence than in the absence of forskolin in both WT and HyperKPP soleus. This finding can again be explained by a higher production of adenosine from $[cAMP]_e$ which then depresses the force, except that at high $[K^+]_e$ the effect maybe more prominent because of an already reduced membrane excitability by K^+. Further support for this explanation comes from the fact that adding probenecid, an inhibitor of cAMP efflux via MRP (Chiavegatti *et al.*, 2008; Duarte *et al.*, 2012), reduced the extent of the force decrease at 8 mM K^+ in the presence of forskolin.

SALBUTAMOL VERSUS FORSKOLIN

HyperKPP patients can prevent paralytic attacks induced by K^+ ingestion or exercise with salbutamol (Wang & Clausen, 1976; Clausen *et al.*, 1980). Also, tetanic force is fully restored to WT levels when HyperKPP mouse soleus is exposed to salbutamol at 10 mM K^+ (Clausen *et al.*, 2011). The comparison of the effects of forskolin and salbutamol (Fig. 5.7 and Table 5.1) clearly demonstrated that salbutamol is more effective at alleviating HyperKPP symptoms whether it was added while HyperKPP soleus was exposed to 4.7 mM K^+ or after an exposure to 8 mM K^+.

The increase in cAMP levels are up to 4-fold greater with forskolin than with the β-adrenergic agonist isporenaline in WT rat EDL (Chiavegatti *et al.*, 2008). Low concentrations of clenbuterol and fenoterol, two other β_2-adrenergic receptors agonists, increase twitch force in WT mouse diaphragm without the subsequent force decline observed at higher concentrations of the same β_2-adrenergic agonists (Duarte *et al.*, 2012). It is then possible that forksolin is less effective at improving membrane excitability and force in WT and HyperKPP soleus because the increase

in $[cAMP]_i$ and $[cAMP]_e$ is much higher than with salbutamol resulting in greater adenosine production which then lowers force and membrane excitability.

Another possible reason that forskolin is less effective maybe related to the fact that not all the effects of β_2-adrenergic receptors are PKA dependent. For example, β_2-adrenergic receptors in both cardiac and smooth muscles cells activate ion channels via Gs protein dependent but cAMP independent pathways (Yatani *et al.*, 1987, 1988; Kume *et al.*, 1994). One of these channels is the Ca^{2+} sensitive K^+ channels (BK). So, if salbutamol also activates K^+ channel via a Gs pathway independent of cAMP/PKA pathway, then it could be another reason as to why salbutamol is more effective than forskolin as discussed for K_{ATP} channel in the next section

K_{ATP} CHANNEL AS A THERAPEUTIC TARGET IN HYPERKPP SOLEUS

In expression systems, PKA activates K_{ATP} channels made of the Kir6.2 and SUR2A subunits, the same subunits that constitute the channels in skeletal muscles (Béguin *et al.*, 1999; Lin *et al.*, 2000). Increasing G_K by activating K_{ATP} channels hyperpolarizes resting EM in WT (Zhu *et al.*, 2014) as it approaches more easily the more negative E_K. The absence of a hyperpolarization of resting EM in the presence of forskolin and the failure of K_{ATP} channel inhibitor glibenclamide to affect the force increase by forskolin indicates that K_{ATP} channels were not activated in the presence of forskolin in HyperKPP soleus.

So, next we tested whether an activation of K_{ATP} channels in the absence and the presence of forskolin can improve membrane excitability and force production. Addition of pinacidil alone resulted in force increase at 4.7 and 8 mM K^+. Pinacidil improvement of force was associated with hyperpolarization of resting EM, an increase in AP peak and in the number of excitable fibers. It is notably important that the increase in AP peak occurs despite the fact that an increase in K_{ATP} channel activity normally reduces AP peak in WT as it provided an outward K^+ current during the

depolarization phase (Gong *et al.*, 2003). The net improvement observed here suggests that opening of K_{ATP} channels hyperpolarizes resting EM (Fig 5.6A) to the extent that a reduction in Nav1.4 channel inactivation improves AP amplitude to a greater extent than the decrease expected from the K^+ outward current through K_{ATP} channel. A combination of pinacidil and forskolin did not offer further improvement than pinacidil alone.

In conclusion, this study shows that a) forskolin increases force production in HyperKPP soleus at 4.7 mM K^+ but not at 8 or 11 mM K^+, b) salbutamol is more effective than forskolin at alleviating HyperKPP symptoms regardless of the time muscles are exposed to salbutamol. c) pinacidil increases force production at 4.7 and 8 mM K^+ as the activation of K_{ATP} channel hyperpolarizes resting EM increasing AP peak and the number of excitable fibers. Thus, this study provides evidence that an activation of K_{ATP} channel is another potential strategy for a new treatment to alleviate HyperKPP symptoms.

CHAPTER 6 - GENERAL DISCUSSION

HyperKPP is a channelopathy that results in muscle stiffness due to spontaneous AP generation, muscle weakness and paralytic attacks. As of now, there is no treatment that fully alleviates the symptoms and some of the available treatments lose effectiveness with time (Clausen *et al.*, 1980; Miller *et al.*, 2004). In most patients (85%), HyperKPP primarily affects limb muscles (Charles *et al.*, 2013). Notably, only 26% of patients report breathing difficulties. Patients carrying the M1592V mutation never complain from any respiratory distress (Poskanzer & Kerr, 1961; Chinnery *et al.*, 2002). This is surprising because the human diaphragm expresses the Nav1.4 channels mRNA (Zhou & Hoffman, 1994). So, the overall objective of this PhD study was to understand the mechanism(s) that spares the diaphragm from HyperKPP symptoms compared to hindlimb muscles. The importance of such understanding is crucial for developing new long lasting therapeutic approaches to treat the disease.

Using the M1592V HyperKPP mouse model, the major findings of this thesis were: 1) HyperKPP diaphragm expressed the mutant Nav1.4 channels as shown by western blotting and had a TTX-sensitive Na^+ influx similar to that observed in the symptomatic EDL and soleus muscles, an influx that was higher than WT muscles. 2) HyperKPP diaphragm is however mostly asymptomatic as it had no defect in membrane excitability and contractility such as those observed in EDL and soleus i.e., it had comparable resting EM and sensitivity to the K^+-induced force depression to that of WT diaphragm. 3) Three mechanisms responsible for the asymptomatic behavior of the diaphragm were elucidated: i) a better maintenance of resting EM due to a higher electrogenic contribution of NKA pump, ii) better AP amplitude compared to HyperKPP EDL and soleus, and iii) greater force generation at depolarized resting EM when compared to WT diaphragm. 4) The potential of activating PKA or PKC to treat the disease was tested using

HyperKPP soleus. Activation of PKC with PMA worsened the symptoms while exposing soleus to forskolin (an adenylyl cyclase activator) to increase cAMP and activate PKA improved force generation at 4.7 mM K^+ but not at 8 or 11 mM K^+. Exposure to salbutamol, a β_2-adrenergic receptor agonist, that also increases PKA activity was more effective than forskolin at both 4.7 and 8 mM K^+ in soleus. 5) Finally, the potential of activating K_{ATP} channels with pinacidil was tested in HyperKPP soleus. In this regard, activating K_{ATP} channels hyperpolarized resting EM resulting in better AP amplitude and force.

PATHOPHYSIOLOGY OF HyperKPP

HyperKPP mutations in Nav1.4 channels result in three major defects, First, the steady state activation curve is shifted toward more negative EM (Rojas *et al.*, 1999). Secondly, the steady state slow inactivation curve is shifted toward less negative EM and recovery from slow activation is accelerated (Hayward *et al.*, 1997). Third, mutant channels, also enter a non-inactivation mode upon membrane depolarization at elevated $[K^+]_e$ (Cannon *et al.*, 1991). One consequence of the first two defects is greater Nav1.4 channel open probability at rest, resulting in higher TTX-sensitive Na^+ influx in HyperKPP soleus and EDL that is 14 and 4 times greater than WT muscles, respectively. As consequence of this Na^+ influx resting EM is largely depolarized (Fig 6.1), this is based on the fact that exposing HyperKPP soleus to TTX allows the resting EM to return to levels similar to WT (Clausen *et al.*, 2011; Khogali *et al.*, 2015, Chapters 2 and 3). The depolarization then increases the probability of spontaneously generating AP because i) the hyperpolarized shift of the steady state activation curve lowers AP threshold and ii) the depolarized shift of the steady state slow inactivation curve results in lower extent of Nav1.4 channel slow inactivation.

Khogali et al. (2015) reported that the gastrocnemius muscle of HyperKPP free moving

FIGURE 6.1

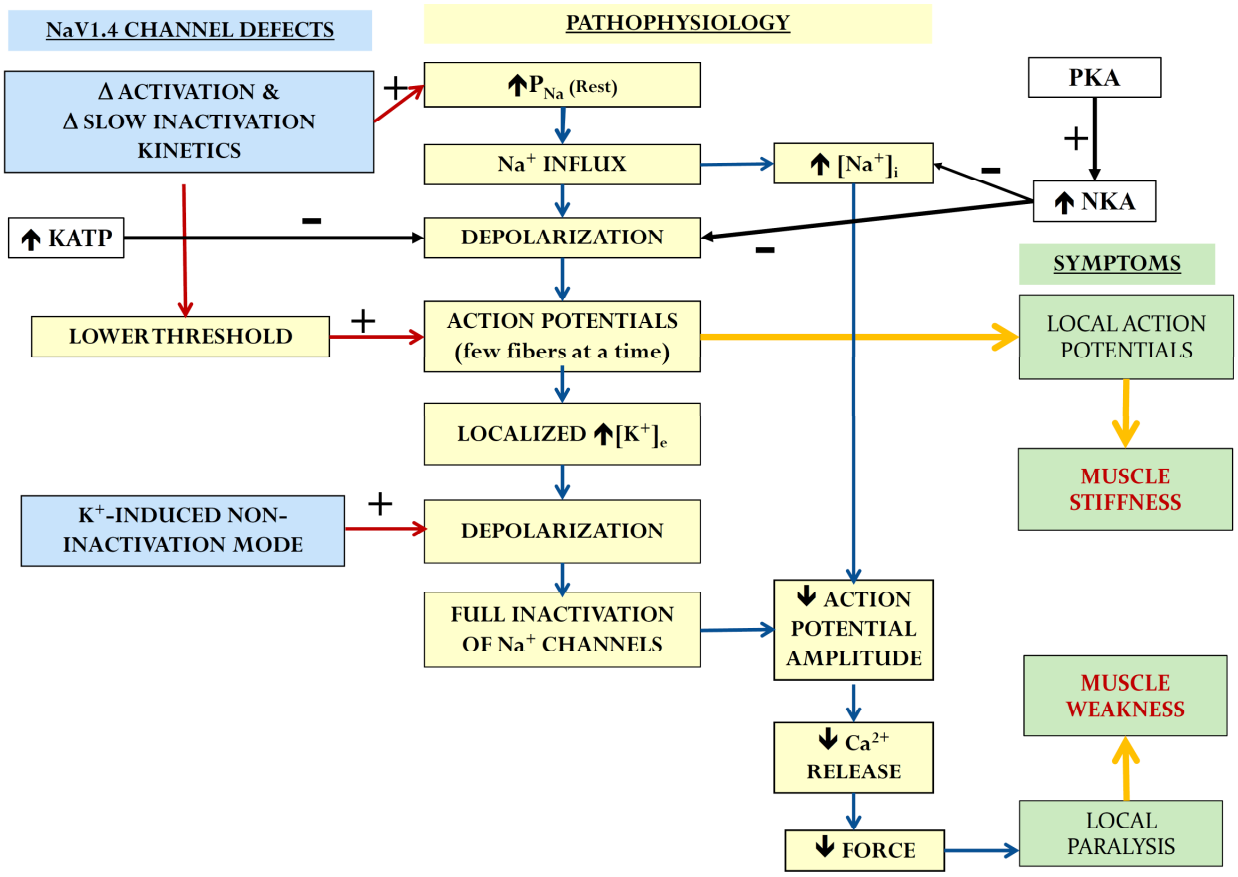

Figure 6.1. Diagram showing the mechanism by which activation of NKA pump and K_{ATP} channels can counteract the HyperKPP defects.

mice had greater EMG activity than WT. However, they failed to observe any myotonic discharge consisting of a series of EMG peaks as observed when the EMG electrode is moved (Hayward *et al.*, 2008). They also reported sudden contractions while muscles were at rest. The lack of myotonic discharge, except when EMG electrodes were moved in M1592V HyperKPP mouse is similar to the symptoms reported by members of a family carrying the same mutation (Poskanzer & Kerr, 1961; Chinnery *et al.*, 2002); that is, they suffer of muscle stiffness without any sign of myotonia, except upon the penetration of EMG electrodes. Khogali et al. (2015) suggested that for the M1592V mutation, muscles fibers are hyperexcitable generating APs at random in the absence of external neural stimulation resulting in stiffness rather than myotonia which is clinically defined as sustained burst of AP originating from muscle fiber and persisting for several seconds after neural stimulation has stopped (Cannon, 2006); one major support for this proposal is that spontaneous AP generation occurs in HyperKPP even when fibers are at rest.

Another feature from patients with M1592V mutations is muscle weakness lasting 3-4 days and on rare occasions full paralysis (1-3 times per year) (Poskanzer & Kerr, 1961; Chinnery *et al.*, 2002). HyperKPP mouse EDL and soleus produced lower force than WT controls even at the normal 4.7 mM K^+ (Hayward *et al.*, 2008; Clausen *et al.*, 2011; Khogali *et al.*, 2015, Chapters 2 and 3). This study showed that the lower force at 4.7 mM K^+ was associated with a mean resting EM that was depolarized by 7 mV in EDL and 16 mV in soleus compared to WT controls. This is because the frequency of distribution of resting EM in HyperKPP EDL and soleus fibers was shifted to depolarized resting EM. More importantly, 27% of all HyperKPP soleus fibers had a resting EM below -55 mV compared to <1% for WT fibers (Chapter 3) while for HyperKPP EDL only 11% of fibers had a resting EM below -55 mV. Force-resting EM relationship showed that force for HyperKPP and WT soleus and EDL falls drastically to zero between resting EM of -60

and -55 mV regardless of the $[K^+]_e$ (Fig. 3.5), which is in agreement with a pervious report (Cairns *et al.*, 1997). This is because below -55 mV fibers were unexcitable and AP could no longer be generated. HyperKPP muscles has long been known to have a higher K^+ sensitivity. Force resting EM relationship was not largely different between WT and HyperKPP muscles especially for soleus (Chapter 3). The main difference between WT and HyperKPP muscles was that at normal $[K^+]_e$ mean resting EM was already depolarized in HyperKPP muscles with large number of fibers with resting EM below -55 mV so that small increases in $[K^+]_e$ in HyperKPP muscles increase the number of fibers entering the EM range that will make them unexcitable causing force to decrease drastically compared to WT. To explain the muscle weakness in HyperKPP patients it is now proposed that few fibers become hyperexictable at a time with AP generation resulting in local increase in $[K^+]_e$ rather than in the whole muscle. Only fibers exposed to the high $[K^+]_e$ depolarize to the EM range of force loss resulting in muscle weakness rather than full paralysis.

MECHANISMS RENDERING HyperKPP DIAPHRAGM ASYMPTOMATIC

Evidence of an asymptomatic HyperKPP diaphragm first comes from the absence of an increased K^+ sensitivity to the K^+-induced force depression as seen in EDL and soleus. The lack of a higher K^+ sensitivity was because resting EM in HyperKPP diaphragm fibers was not different from that of WT diaphragm at all $[K^+]_e$, as observed for EDL and soleus (Chapter 3). Further evidence for the lack of symptoms in diaphragm is the lack of fiber type changes (Chapter 2). In affected muscles, there are major shifts toward myosin type IIA in tibialis anterior and EDL and a shift toward myosin type I in soleus (Hayward *et al.*, 2008; Khogali *et al.*, 2015, Chapter 2). It has been suggested that the fiber type change is a consequence of chronic muscular activity associated with spontaneous AP generation and stiffness, which mimics muscular activity during exercise training (Bassel-Duby & Olson, 2006; Hayward *et al.*, 2008). A similar shift was not observed in

diaphragm suggesting that spontaneous AP generation and/or stiffness are either rare or non-existent for that muscle.

The lack of any large number of strongly depolarized fibers in HyperKPP diaphragm was most interesting as the TTX-sensitive Na^+ influx in HyperKPP diaphragm was as high as observed in EDL and soleus. A novel finding of this study was the strength of NKA pump electrogenic contribution in counteracting the Na^+ induced membrane depolarization to resting EM. The electrogenic contribution of NKA pump was 13 mV greater in HyperKPP than WT diaphragm (Chapter 3). If a similar increase in NKA pump electrogenic contribution would occur in HyperKPP soleus and EDL, their mean resting EM would be -74 and -84 mV, respectively; i.e. similar to that of WT. Further evidence for the importance of NKA pump activity is the effect of fully inhibiting α2 subunit and a 37% inhibition of α1 subunit with 10 μM ouabain at 4.7 mM K^+. Ouabain basically abolished the capacity of HyperKPP EDL and soleus to generate tetanic force while that of the diaphragm was reduced only by 75% (Chapter 2). This was possible because most of the increase in NKA pump electrogenic contribution was from α1 subunit (Chapter 3) which was only inhibited by 37% at 10 μM oubain (Chibalin *et al.*, 2012). Furthermore, upon removal of ouabain, force started to recover rapidly in HyperKPP diaphragm but not in EDL or soleus. A greater electrogenic contribution also suggests that NKA pump is more active and most likely resulting in lower $[Na^+]_i$ in HyperKPP diaphragm than in EDL and soleus. Lower $[Na^+]_i$ may then explain the better AP amplitude observed in the HyperKPP diaphragm compared to EDL and soleus (Chapter 3) since the decrease in $[Na^+]$ gradient lower AP amplitude and depress tetanic force (Overgaard *et al.*, 1999; Cairns *et al.*, 2003).

The better maintenance of resting EM in the HyperKPP diaphragm was not due to an increased NKA pump protein content of either α1 or α2 subunits as their content did not show any

difference compared to WT diaphragm. It was therefore surprising that HyperKPP EDL did not have greater NKA pump electrogenic contribution considering that it had twice the protein content of α1 and α2 compared to WT EDL. PLM is a protein that associates with NKA pump and decreases the pump activity by decreasing internal Na^+ affinity (Crambert *et al.*, 2002). This inhibition is relieved upon PLM phosphorylation by PKA and PKC (Silverman *et al.*, 2005; Despa *et al.*, 2005; Han *et al.*, 2006; Bibert *et al.*, 2008; Pavlovic *et al.*, 2013*b*). Muscle exercise is known to prevent an upcoming limb paralytic attack in HyperKPP patients (Clausen *et al.*, 1980). Skeletal muscle activity increases NKA pump activity, its electrogenic contribution and PLM phosphorylation (Hicks & McComas, 1989; Nielsen & Clausen, 1997; Thomassen *et al.*, 2010, 2011; Benziane *et al.*, 2011). For example, repetitive stimulation of soleus increases the NKA pump electrogenic contribution hyperpolarizing resting EM by 10 mV leading to an increase in action potential amplitude by 15 mV (Hicks & McComas, 1989). So, one possible mechanism by which HyperKPP diaphragm is asymptomatic is higher NKA pump activity via increased PLM phosphorylation as the muscle is continuously active.

Another possible explanation is that while total increase in NKA pump total protein content is higher in HyperKPP EDL than WT, it may not be in the plasma membrane. It is now well established that not all NKA pumps are located in the plasma membrane. A proportion is stored in intracellular vesicles, and their translocation to plasma membrane is stimulated by insulin and during muscle activity (Chibalin *et al.*, 2001; Benziane & Chibalin, 2008). Many studies have shown that short bouts of exercise stimulate the translocation of NKA α1 and α2 pump from internal stores to the plasma membrane (Tsakiridis *et al.*, 1996; Juel *et al.*, 2000, 2001; Sandiford *et al.*, 2005). So, again the continued activity of the diaphragm may result in a greater proportion

of NKA pump in the cell membrane while for the least active EDL, which is active only 5% of the time (Hennig & Lømo, 1985), has most of its pump in intracellular stores.

Regardless of the mechanisms as to why NKA pumps are more active in HyperKPP diaphragm and not in EDL, the common feature is that the level of muscular activity being constant in diaphragm and sporadic in EDL resulting in greater NKA pump activity in HyperKPP diaphragm than WT or than HyperKPP EDL and soleus. Another mechanism that helped the HyperKPP diaphragm improve force production is the generation of greater force than WT at depolarized resting EM (Fig. 3.5). This higher force was observed while AP amplitude were similar between WT and HyperKPP diaphragm suggesting that a mechanism downstream of AP is involved. It is thus possible that there is greater Ca^{2+} release in HyperKPP diaphragm than WT especially at depolarized resting EM. PKA phosphorylation of ryanodine receptor, the SR Ca^{2+} release channel, increases Ca^{2+} release (Reiken *et al.*, 2003; Rudolf *et al.*, 2006).

Then, the possibility that the higher NKA activity in HyperKPP diaphragm was linked to higher PKA or PKC activity was tested. The results from this thesis did not provide evidence for a role of PKC as its inhibition by GF109203X had no effect on HyperKPP diaphragm force (Chapter 4). Inhibition of PKA with staurosporin, H89 and KT5720 did increase the extent of force loss at high $[K^+]_e$ in HyperKPP diaphragm. These findings support the idea that a greater PKA activity in diaphragm plays a role in the asymptomatic mechanism. However, the extent of force loss was quite variable among different inhibitors and a lack of PKA specificity for these drugs (Davies *et al.*, 2000; Murray, 2008) does not allow for a strong conclusion regarding the potential role of PKA in the asymptomatic feature of HyperKPP diaphragm. As discussed in Chapter 4 more studies will be necessary to fully understand the role of PKA in the asymptomatic behavior of HyperKPP diaphragm.

PKA AND K_{ATP} CHANNEL AS POTENTIAL THERAPEUTIC TARGETS

A last aim of this study was to determine the potential of activating PKA as a new therapy using HyperKPP soleus, the most affected muscle. Activation of β_2-adrenergic receptors can fully prevent a paralytic attack induced by K^+ ingestion (Wang & Clausen, 1976) as well as increase tetanic force of mouse HyperKPP soleus back to levels similar to WT even at high $[K^+]_e$ (Clausen *et al.*, 2011, Table 5.1). However, when β_2-adrenergic agonists are used chronically they lose effectiveness in some HyperKPP patients (Clausen *et al.*, 1980). Since one of the mechanisms of actions involves an activation of PKA (Clausen, 2003, 2013), a different approach was tested in which forskolin was used to activate adenylyl cyclase to increase cAMP levels which then activate PKA. Compared to salbutamol, forskolin was less effective at improving force at 4.7 and especially at 8 or 11 mM K^+. Remarkably and contrary to expectations, the improvement did not involve better resting EM or AP amplitude. As discussed in chapter 5, the lower effectiveness of forskolin may in part be related to cAMP exiting the myoplasm and being transformed to adenosine which reduces force (Godinho & Costa, 2003; Chiavegatti *et al.*, 2008; Duarte *et al.*, 2012). Then, this effect would become exaggerated the longer the muscles are exposed to forskolin and especially when membrane excitability was reduced at high $[K^+]_e$. This possibility is supported by the fact that forskolin improvement of force effects are greatly reduced at high $[K^+]_e$ as observed in this study. Furthermore, inhibiting cAMP efflux by inhibiting MRP with probenecid reduces the extent of force loss with forskolin at high $[K^+]_e$. The greater effects of salbutamol than forskolin may also be related to the fact that activation of the β-adrenergic receptor may be related to lower production of cAMP and adenosine as discussed in chapter 5.

Although PKA phosphorylation of Kir6.2 and SUR2A, the two subunits making K_{ATP} channel in skeletal muscles, increases the channel activity (Béguin *et al.*, 1999; Ashcroft, 2000;

Lin *et al.*, 2000), Chapter 5 provided no evidence for activation of K_{ATP} channels in the presence of forskolin as glibenclamide did not prevent the force improvement by forskolin. Activation of K_{ATP} channels with pinacidil improved force production in HyperKPP soleus mainly by hyperpolarizing resting EM which then increases the number of excitable fibers and AP amplitude. Notably, concomitant exposure to forskolin and pinacidil did not improve force or membrane excitability above that of pinacidil alone. This is either because of a production of adenosine counteracts any further increase in force and excitability or because the effects of both drugs are not additive.

In conclusion, this thesis provided strong evidence that a new therapy for HyperKPP should concentrate on increasing NKA pump and K_{ATP} channel activity because both can help in counteracting the Na^+ induced depolarization associated with large Na^+ influx through mutant Nav1.4 channels (Fig 6.1). This study also supports the feasibility of using an approach in which PKA is activated. However, future studies will be necessary to better understand why forskolin is not as effective as salbutamol. One possibility is an activation of PKA by a lower forskolin concentration is needed to lower cAMP and adenosine production in order to prevent the negative feedback on the β-adrenergic receptor.

REFERENCES

Adelman WJ & Palti Y (1969). The effects of external potassium and long duration voltage conditioning on the amplitude of sodium currents in the giant axon of the squid, Loligo pealei. *J Gen Physiol* **54,** 589–606.

Adrian RH & Bryant SH (1974). On the repetitive discharge in myotonic muscle fibres. *J Physiol* **240,** 505–515.

Aickin CC, Betz WJ & Harris GL (1989). Intracellular chloride and the mechanism for its accumulation in rat lumbrical muscle. *J Physiol* **411,** 437–455.

Allard B & Lazdunski M (1992). Nucleotide diphosphates activate the ATP-sensitive potassium channel in mouse skeletal muscle. *Pflugers Arch Eur J Physiol* **422,** 185–192.

Amarteifio E, Nagel AM, Weber M, Jurkat-Rott K & Lehmann-horn F (2012). Hyperkalemic Periodic Paralysis and Permanent Weakness : 3-T MR Imaging Depicts Intracellular 23Na Overload — Initial Results. *Radiology* **264,** 154–163.

Arimura K, Arimura Y, Ng AR, Sakoda S-I & Higuchi I (2007). Muscle membrane excitability after exercise in thyrotoxic periodic paralysis and thyrotoxicosis without periodic paralysis. *Muscle Nerve* **36,** 784–788.

Armstrong CM (1977). Inactivation of the sodium channel. II. Gating current experiments. *J Gen Physiol* **70,** 567–590.

Ashcroft FM (2000). *Ion Channels and Disease*. Elsevier.

Balser JR, Nuss HB, Chiamvimonvat N, Pérez-García MT, Marban E & Tomaselli GF (1996). External pore residue mediates slow inactivation in mu 1 rat skeletal muscle sodium channels. *J Physiol* **494,** 431–442.

Banas K, Clow C, Jasmin BJ & Renaud J-M (2011). The KATP channel Kir6.2 subunit content is

higher in glycolytic than oxidative skeletal muscle fibers. *Am J Physiol Regul Integr Comp Physiol* **301,** R916-25.

Barchi RL (1995). Molecular pathology of the skeletal muscle sodium channel. *Annu Rev Physiol* **57,** 355–385.

Bassel-Duby RR & Olson ENEN (2006). Signaling pathways in skeletal muscle remodeling. *Biochemistry* **75,** 19–37.

Bay CM & Strichartz GR (1980). Saxitoxin binding to sodium channels of rat skeletal muscles. *J Physiol* **300,** 89–103.

Béguin P, Nagashima K, Nishimura M, Gonoi T & Seino S (1999). PKA-mediated phosphorylation of the human K(ATP) channel: Separate roles of Kir6.2 and SUR1 subunit phosphorylation. *EMBO J* **18,** 4722–4732.

Bendahhou S, Fournier E, Sternberg D, Bassez G, Furby A, Sereni C, Donaldson MR, Larroque M-M, Fontaine B & Barhanin J (2005). In vivo and in vitro functional characterization of Andersen's syndrome mutations. *J Physiol* **565,** 731–741.

Bennetts B, Rychkov GY, Ng H-L, Morton CJ, Stapleton D, Parker MW & Cromer B a (2005). Cytoplasmic ATP-sensing domains regulate gating of skeletal muscle ClC-1 chloride channels. *J Biol Chem* **280,** 32452–32458.

Benziane B & Chibalin A V (2008). Frontiers: skeletal muscle sodium pump regulation: a translocation paradigm. *Am J Physiol Endocrinol Metab* **295,** E553-8.

Benziane B, Widegren U, Pirkmajer S, Henriksson J, Stepto NK & Chibalin A V (2011). Effect of exercise and training on phospholemman phosphorylation in human skeletal muscle. *Am J Physiol Endocrinol Metab* **301,** E456-66.

Bibert S, Roy S, Schaer D, Horisberger J-D & Geering K (2008). Phosphorylation of

phospholemman (FXYD1) by protein kinases A and C modulates distinct Na,K-ATPase isozymes. *J Biol Chem* **283,** 476–486.

Blanco G (2005). Na,K-ATPase subunit heterogeneity as a mechanism for tissue-specific ion regulation. *Semin Nephrol* **25,** 292–303.

Blaustein MP & Lederer WJ (1999). Sodium/Calcium Exchange: Its Physiological Implications. *Physiol Rev* **79,** 763–854.

Bollensdorff C, Knopp A, Biskup C, Zimmer T & Benndorf K (2004). Na(+) current through KATP channels: consequences for Na(+) and K(+) fluxes during early myocardial ischemia. *Am J Physiol Heart Circ Physiol* **286,** H283-95.

Bradley WG, Taylor R, Rice DR, Hausmanowa-Petruzewicz I, Adelman LS, Jenkison M, Jedrzejowska H, Drac H & Pendlebury WW (1990). Progressive Myopathy in Hyperkalemic Periodic Paralysis. *Arch Neurol* **47,** 1013–1017.

Buchanan R, Nielsen OB & Clausen T (2002). Excitation- and β2-agonist-induced activation of the Na+-K+ pump in rat soleus muscle. *J Physiol* **545,** 229–240.

Cairns SP & Borrani F (2015). β-Adrenergic modulation of skeletal muscle contraction: key role of excitation-contraction coupling. *J Physiol* **593,** 4713–4727.

Cairns SP, Buller SJ, Loiselle DS & Renaud J-M (2003). Changes of action potentials and force at lowered [Na+]o in mouse skeletal muscle: implications for fatigue. *Am J Physiol Cell Physiol* **285,** C1131-41.

Cairns SP, Flatman JA & Clausen T (1995). Relation between extracellular [K+], membrane potential and contraction in rat soleus muscle: modulation by the Na+-K+ pump. *Pflügers Arch Eur J Physiol* **430,** 909–915.

Cairns SP, Hing WA, Slack JR, Mills RG & Loiselle DS (1997). Different effects of raised [K+]o

on membrane potential and contraction in mouse fast- and slow-twitch muscle. *Am J Physiol* **273,** C598–C611.

Cairns SP, Hing WA, Slack JR, Mills RG & Loiselle DS (1998). Role of extracellular [Ca2+] in fatigue of isolated mammalian skeletal muscle. *J Appl Physiol* **84,** 1395–1406.

Cairns SP, Ruzhynsky V & Renaud J-M (2004). Protective role of extracellular chloride in fatigue of isolated mammalian skeletal muscle. *Am J Physiol Cell Physiol* **287,** C762-70.

Cairns SP, Westerblad H & Allen DG (1993). Changes of tension and [Ca2+]i during beta-adrenoceptor activation of single, intact fibres from mouse skeletal muscle. *Pflugers Arch* **425,** 150–155.

Cannon SC (2006). Pathomechanisms in channelopathies of skeletal muscle and brain. *Annu Rev Neurosci* **29,** 387–415.

Cannon SC (2010). Voltage-sensor mutations in channelopathies of skeletal muscle. *J Physiol* **588,** 1887–1895.

Cannon SC (2015). Channelopathies of skeletal muscle excitability. *Compr Physiol* **5,** 761–790.

Cannon SC, Brown RH & Corey DP (1991). A sodium channel defect in hyperkalemic periodic paralysis: potassium-induced failure of inactivation. *Neuron* **6,** 619–626.

Catterall WA (2014). Structure and function of voltage-gated sodium channels at atomic resolution. *Exp Physiol* **99,** 35–51.

Catterall WA & Swanson TM (2015). Structural Basis for Pharmacology of Voltage-Gated Sodium and Calcium Channels. *Mol Pharmacol* **88,** 141–150.

Cazzola M, Page CP, Calzetta L & Matera MG (2012). Pharmacology and therapeutics of bronchodilators. *Pharmacol Rev* **64,** 450–504.

Chahine M, Deschene I, Chen LQ & Kallen G (1996). Electrophysiological characteristics of

cloned skeletal and cardiac muscle sodium channels. *Am J Physiol* **271,** 498–506.

Charles G, Zheng C, Lehmann-Horn F, Jurkat-Rott K & Levitt J (2013). Characterization of hyperkalemic periodic paralysis: a survey of genetically diagnosed individuals. *J Neurol* **260,** 2606–2613.

Chen Y, Yu FH, Surmeier DJ, Scheuer T & Catterall WA (2006). Neuromodulation of Na+ channel slow inactivation via cAMP-dependent protein kinase and protein kinase C. *Neuron* **49,** 409–420.

Cheng C-J, Lin S-H, Lo Y-F, Yang S-S, Hsu Y-J, Cannon SC & Huang C-L (2011). Identification and functional characterization of Kir2.6 mutations associated with non-familial hypokalemic periodic paralysis. *J Biol Chem* **286,** 27425–27435.

Chiavegatti T, Costa VL, Araújo MS & Godinho RO (2008). Skeletal muscle expresses the extracellular cyclic AMP-adenosine pathway. *Br J Pharmacol* **153,** 1331–1340.

Chibalin A V, Heiny J a, Benziane B, Prokofiev A V, Vasiliev A V, Kravtsova V V & Krivoi II (2012). Chronic nicotine modifies skeletal muscle Na,K-ATPase activity through its interaction with the nicotinic acetylcholine receptor and phospholemman. *PLoS One* **7,** e33719.

Chibalin A V, Kovalenko M V, Ryder JW, Féraille E, Wallberg-Henriksson H & Zierath JR (2001). Insulin- and glucose-induced phosphorylation of the Na(+),K(+)-adenosine triphosphatase alpha-subunits in rat skeletal muscle. *Endocrinology* **142,** 3474–3482.

Chin ER, Olson EN, Richardson JA, Yang Q, Humphries C, Shelton JM, Wu H, Zhu W, Bassel-Duby R & Williams RS (1998). A calcineurin-dependent transcriptional pathway controls skeletal muscle fiber type. *Genes Dev* **12,** 2499–2509.

Chinnery PF, Walls TJ, Hanna MG, Bates D & Fawcett PRW (2002). Normokalemic periodic

paralysis revisited: does it exist? *Ann Neurol* **52,** 251–252.

Cifelli C, Boudreault L, Gong B, Bercier J-P & Renaud J-M (2008). Contractile dysfunctions in ATP-dependent K+ channel-deficient mouse muscle during fatigue involve excessive depolarization and Ca2+ influx through L-type Ca2+ channels. *Exp Physiol* **93,** 1126–1138.

Cifelli C, Bourassa F, Gariépy L, Banas K, Benkhalti M & Renaud J-M (2007). KATP channel deficiency in mouse flexor digitorum brevis causes fibre damage and impairs Ca2+ release and force development during fatigue in vitro. *J Physiol* **582,** 843–857.

Clausen T (2003). Na+-K+ pump regulation and skeletal muscle contractility. *Physiol Rev* **83,** 1269–1324.

Clausen T (2013). Quantification of Na+,K+ pumps and their transport rate in skeletal muscle: functional significance. *J Gen Physiol* **142,** 327–345.

Clausen T & Flatman JA (1977). The effect of catecholamines on Na-K transport and membrane potential in rat soleus muscle. *J Physiol* **270,** 383–414.

Clausen T, Nielsen OB, Clausen JD, Pedersen TH & Hayward LJ (2011). Na+,K+-pump stimulation improves contractility in isolated muscles of mice with hyperkalemic periodic paralysis. *J Gen Physiol* **138,** 117–130.

Clausen T, Wang P, Orskov H & Kristensen O (1980). Hyperkalemic periodic paralysis. Relationships between changes in plasma water, electrolytes, insulin and catecholamines during attacks. *Scand J Clin Lab Invest* **40,** 211–220.

Clement JPI, Kunjilwar K, Gonzalez G, Schwanstecher M, Panten U, Aguilar-Bryan L & Bryan J (1997). Association and stoichiometry of K ATP channel subunits. *Neuron* **18,** 827–838.

Crambert G, Fuzesi M, Garty H, Karlish S & Geering K (2002). Phospholemman (FXYD1) associates with Na,K-ATPase and regulates its transport properties. *Proc Natl Acad Sci U S*

A **99,** 11476–11481.

Creutzfeldt OD, Abbott BC, Fowler WM & Pearson CM (1963). Muscle membrane potentials in episodic adynamia. *Electroencephalogr Clin Neurophysiol* **15,** 508–519.

Cummins TR, Zhou J, Sigworth FJ, Ukomadu C, Stephan M, Ptácek LJ & Agnew WS (1993). Functional consequences of a Na+ channel mutation causing hyperkalemic periodic paralysis. *Neuron* **10,** 667–678.

Davies NP et al. (2005). Andersen-Tawil syndrome: new potassium channel mutations and possible phenotypic variation. *Neurology* **65,** 1083–1089.

Davies NW (1990). Modulation of ATP-sensitive K+ channels in skeletal muscle by intracellular protons. *Nature* **343,** 375–377.

Davies SP, Reddy H, Caivano M & Cohen P (2000). Specificity and mechanism of action of some commonly used protein kinase inhibitors. *Biochem J* **351,** 95–105.

Despa S, Bossuyt J, Han F, Ginsburg KS, Jia L-G, Kutchai H, Tucker AL & Bers DM (2005). Phospholemman-phosphorylation mediates the beta-adrenergic effects on Na/K pump function in cardiac myocytes. *Circ Res* **97,** 252–259.

Dhamoon AS, Pandit S V., Sarmast F, Parisian KR, Guha P, Li Y, Bagwe S, Taffet SM & Anumonwo JMB (2004). Unique Kir2.x properties determine regional and species differences in the cardiac inward rectifier K+ current. *Circ Res* **94,** 1332–1339.

DiFranco M, Hakimjavadi H, Lingrel JB & Heiny JA (2015*a*). Na,K-ATPase 2 activity in mammalian skeletal muscle T-tubules is acutely stimulated by extracellular K+. *J Gen Physiol* **146,** 281–294.

DiFranco M, Herrera A & Vergara JL (2011). Chloride currents from the transverse tubular system in adult mammalian skeletal muscle fibers. *J Gen Physiol* **137,** 21–41.

DiFranco M, Quinonez M & Vergara JL (2012). The delayed rectifier potassium conductance in the sarcolemma and the transverse tubular system membranes of mammalian skeletal muscle fibers. *J Gen Physiol* **140,** 109–137.

DiFranco M, Yu C, Quiñonez M & Vergara JL (2015*b*). Inward rectifier potassium currents in mammalian skeletal muscle fibres. *J Physiol* **593,** 1213–1238.

Drost G, Blok JH, Stegeman DF, van Dijk JP, van Engelen BG & Zwarts MJ (2001). Propagation disturbance of motor unit action potentials during transient paresis in generalized myotonia: a high-density surface EMG study. *Brain* **124,** 352–360.

Duarte T, Menezes-Rodrigues FS & Godinho RO (2012). Contribution of the extracellular cAMP-adenosine pathway to dual coupling of β2-adrenoceptors to Gs and Gi proteins in mouse skeletal muscle. *J Pharmacol Exp Ther* **341,** 820–828.

Dulhunty A (1978). The dependence of membrane potential on extracellular chloride concentration in mammalian skeletal muscle fibres. *J Physiol* **276,** 67–82.

Dunn SE, Burns JL & Michel RN (1999). Calcineurin is required for skeletal muscle hypertrophy. *J Biol Chem* **274,** 21908–21912.

Edwards JN, Macdonald WA, van der Poel C & Stephenson DG (2007). O2($^{\bullet-}$) production at 37 degrees C plays a critical role in depressing tetanic force of isolated rat and mouse skeletal muscle. *Am J Physiol Cell Physiol* **293,** C650-60.

Fahlke C & Rüdel R (1995). Chloride currents across the membrane of mammalian skeletal muscle fibres. *J Physiol* **484 (Pt 2,** 355–368.

Fahlke C, Rüdel R, Mitrovic N, Zhou M & George AL (1995). An aspartic acid residue important for voltage-dependent gating of human muscle chloride channels. *Neuron* **15,** 463–472.

Featherstone DE, Richmond JE & Ruben PC (1996). Interaction between fast and slow inactivation

in Skm1 sodium channels. *Biophys J* **71,** 3098–3109.

Flagg TP, Enkvetchakul D, Koster JC & Nichols CG (2010). Muscle KATP channels: recent insights to energy sensing and myoprotection. *Physiol Rev* **90,** 799–829.

Fontaine B (2008). Periodic paralysis. *Adv Genet* **63,** 3–23.

Fontaine B, Khurana TS, Hoffman EP, Bruns GA, Haines JL, Trofatter JA, Hanson MP, Rich J, McFarlane H & Yasek DM (1990). Hyperkalemic periodic paralysis and the adult muscle sodium channel alpha-subunit gene. *Science* **250,** 1000–1002.

Fournier E, Arzel M, Sternberg D, Vicart S, Laforet P, Eymard B, Willer J-C, Tabti N & Fontaine B (2004). Electromyography guides toward subgroups of mutations in muscle channelopathies. *Ann Neurol* **56,** 650–661.

Furman RE & Barchi RL (1978). The pathophysiology of myotonia produced by aromatic carboxylic acids. *Ann Neurol* **4,** 357–365.

Gamstorp I, Hauge M, Helwelglarsen HF, Mjones H & Sagild U (1957). Adynamia episodica hereditaria: a disease clinically resembling familial periodic paralysis but characterized by increasing serum potassium during the paralytic attacks. *Am J Med* **23,** 385–390.

Gao J, Mathias RT, Cohen IS, Wang Y, Sun X & Baldo GJ (1999). Activation of PKC increases Na+-K+ pump current in ventricular myocytes from guinea pig heart. *Pflugers Arch* **437,** 643–651.

Godinho RO & Costa VL (2003). Regulation of intracellular cyclic AMP in skeletal muscle cells involves the efflux of cyclic nucleotide to the extracellular compartment. *Br J Pharmacol* **138,** 995–1003.

Goldin AL (2001). Resurgence of sodium channel research. *Annu Rev Physiol* **63,** 871–894.

Goldin AL, Barchi RL, Caldwell JH, Hofmann F, Howe JR, Hunter JC, Kallen RG, Mandel G,

Meisler MH, Netter YB, Noda M, Tamkun MM, Waxman SG, Wood JN & Catterall WA (2000). Nomenclature of voltage-gated sodium channels. *Neuron* **28,** 365–368.

Gong B, Legault D, Miki T, Seino S & Renaud JM (2003). KATP channels depress force by reducing action potential amplitude in mouse EDL and soleus muscle. *Am J Physiol Cell Physiol* **285,** C1464-74.

Gonzalez-Sanchez R, Trujillo X, Trujillo-Hernandez B, Vasquez C, Huerta M & Elizalde A (2006). Forskolin versus Sodium Cromoglycate for Prevention of Asthma Attacks: A Single-blinded Clinical Trial. *J Int Med Res* **34,** 200–207.

Gurnett CA, Kahl SD, Anderson RD & Campbell KP (1995). Absence of the skeletal muscle sarcolemma chloride channel ClC-1 in myotonic mice. *J Biol Chem* **270,** 9035–9038.

Ha TN, Posterino GS & Fryer MW (1999). Effects of terbutaline on force and intracellular calcium in slow-twitch skeletal muscle fibres of the rat. *Br J Pharmacol* **126,** 1717–1724.

Han F, Bossuyt J, Despa S, Tucker AL & Bers DM (2006). Phospholemman phosphorylation mediates the protein kinase C-dependent effects on Na+/K+ pump function in cardiac myocytes. *Circ Res* **99,** 1376–1383.

Hayes MJ, Qing F, Rhodes CG, Rahman SU, Ind PW, Sriskandan S, Jones T & Hughes JM (1996). In vivo quantification of human pulmonary beta-adrenoceptors: effect of beta-agonist therapy. *Am J Respir Crit Care Med* **154,** 1277–1283.

Hayward LJ, Brown RH & Cannon SC (1996). Inactivation defects caused by myotonia-associated mutations in the sodium channel III-IV linker. *J Gen Physiol* **107,** 559–576.

Hayward LJ, Brown RH & Cannon SC (1997). Slow inactivation differs among mutant Na channels associated with myotonia and periodic paralysis. *Biophys J* **72,** 1204–1219.

Hayward LJ, Kim JS, Lee M-Y, Zhou H, Kim JW, Misra K, Salajegheh M, Wu F, Matsuda C,

Reid V, Cros D, Hoffman EP, Renaud J-M, Cannon SC & Brown RH (2008). Targeted mutation of mouse skeletal muscle sodium channel produces myotonia and potassium-sensitive weakness. *J Clin Invest* **118,** 1437–1449.

Hayward LJ, Sandoval GM & Cannon SC (1999). Defective slow inactivation of sodium channels contributes to familial periodic paralysis. *Neurology* **52,** 1447–1453.

He S, Shelly DA, Moseley AE, James PF, James JH, Paul RJ & Lingrel JB (2001). The alpha(1)- and alpha(2)-isoforms of Na-K-ATPase play different roles in skeletal muscle contractility. *Am J Physiol Regul Integr Comp Physiol* **281,** R917–R925.

Heine R, Pika U & Lehmann-Horn F (1993). A novel SCN4A mutation causing myotonia aggravated by cold and potassium. *Hum Mol Genet* **2,** 1349–1353.

Heinemann S, Terlau H, Stühmer W, Imoto K & Numa S (1992). Calcium channel characteristics conferred on the sodium channel by single mutations. *Nature* **356,** 441–443.

Heiny JA, Valle JR & Bryant SH (1990). Optical evidence for a chloride conductance in the T-system of frog skeletal muscle. *Pflugers Arch Eur J Physiol* **416,** 288–295.

Hennig R & Lømo T (1985). Firing patterns of motor units in normal rats. *Nature* **314,** 164–166.

Hibino H, Inanobe A, Furutani K, Murakami S, Findlay I & Kurachi Y (2010). Inwardly Rectifying Potassium Channels: Their Structure, Function, and Physiological Roles. *Physiol Rev* **90,** 291–366.

Hicks A & McComas AJ (1989). Increased sodium pump activity following repetitive stimulation of rat soleus muscles. *J Physiol* **414,** 337–349.

Higgins A (2014). A moderate reduction in skeletal muscle chloride conductance improves contractile force generation in wildtype, but not in hyperkalemic periodic paralysis. *MSc Thesis, uOttawa*.

Hilber K, Sandtner W, Zarrabi T, Zebedin E, Kudlacek O, Fozzard HA & Todt H (2005). Selectivity filter residues contribute unequally to pore stabilization in voltage-gated sodium channels. *Biochemistry* **44,** 13874–13882.

Hobai IA, Hancox JC & Levi AJ (2000). Inhibition by nickel of the L-type Ca channel in guinea pig ventricular myocytes and effect of internal cAMP. *Am J Physiol Heart Circ Physiol* **279,** H692-701.

Hodgkin AL & Huxley AF (1952*a*). A quantitative description of membrane current and its application to conduction and excitation in nerve. *J Physiol* **117,** 500–544.

Hodgkin AL & Huxley AF (1952*b*). The dual effect of membrane potential on sodium conductance in the giant axon of Loligo. *J Physiol* **116,** 497–506.

Huerta M, Urzua Z, Trujillo X, Gonzalez-Sanchez R & Trujillo-Hernandez B (2010). Forskolin Compared with Beclomethasone for Prevention of Asthma Attacks: A Single-Blind Clinical Trial. *J Int Med Res* **38,** 661–668.

Hundal HS, Maxwell DL, Ahmed A, Darakhshan F, Mitsumoto Y & Klip A (1994). Subcellular distribution and immunocytochemical localization of Na,K- ATPase subunit isoforms in human skeletal muscle. *MolMembrBiol* **11,** 255–262.

Janvier NC & Boyett MR (1996). The role of Na-Ca exchange current in the cardiac action potential. *Cardiovasc Res* **32,** 69–84.

Johnson M (1998). The β-adrenoceptor. In *American Journal of Respiratory and Critical Care Medicine*, pp. S146-53.

Jost N, Nagy N, Corici C, Kohajda Z, Horváth a, Acsai K, Biliczki P, Levijoki J, Pollesello P, Koskelainen T, Otsomaa L, Tóth a, Papp JG, Varró a & Virág L (2013). ORM-10103, a novel specific inhibitor of the Na+/Ca2+ exchanger, decreases early and delayed

afterdepolarizations in the canine heart. *Br J Pharmacol* **170,** 768–778.

Juel C (1986). Potassium and sodium shifts during in vitro isometric muscle contraction, and the time course of the ion-gradient recovery. *Pflugers Arch* **406,** 458–463.

Juel C, Grunnet L, Holse M, Kenworthy S, Sommer V & Wulff T (2001). Reversibility of exercise-induced translocation of Na+-K+ pump subunits to the plasma membrane in rat skeletal muscle. *Pflügers Arch Eur J Physiol* **443,** 212–217.

Juel C, Nielsen JJ & Bangsbo J (2000). Exercise-induced translocation of Na(+)-K(+) pump subunits to the plasma membrane in human skeletal muscle. *Am J Physiol Regul Integr Comp Physiol* **278,** R1107-10.

Juel C, Nordsborg NB & Bangsbo J (2014). Purinergic effects on Na,K-ATPase activity differ in rat and human skeletal muscle. *PLoS One* **9,** e91175.

Jurkat-Rott K & Lehmann-Horn F (2007). Genotype-phenotype correlation and therapeutic rationale in hyperkalemic periodic paralysis. *Neurotherapeutics* **4,** 216–224.

Kase H, Iwahashi K, Nakanishi S, Matsuda Y, Yamada K, Takahashi M, Murakata C, Sato A & Kaneko M (1987). K-252 compounds, novel and potent inhibitors of protein kinase C and cyclic nucleotide-dependent protein kinases. *Biochem Biophys Res Commun* **142,** 436–440.

Khogali S, Lucas B, Ammar T, Dejong D, Barbalinardo M, Hayward LJ & Renaud J (2015). Physiological basis for muscle stiffness and weakness in a knock-in M1592V mouse model of hyperkalemic periodic paralysis. *Physiol Rep* **3,** e12656.

Koch MC, Steinmeyer K, Lorenz C, Ricker K, Wolf F, Otto M, Zoll B, Lehmann-Horn F, Grzeschik KH & Jentsch TJ (1992). The skeletal muscle chloride channel in dominant and recessive human myotonia. *Science* **257,** 797–800.

Kraner SD, Tanaka JC & Barchi RL (1985). Purification and functional reconstitution of the

voltage-sensitive sodium channel from rabbit T-tubular membranes. *J Biol Chem* **260,** 6341–6347.

Kristensen M, Hansen T & Juel C (2006). Membrane proteins involved in potassium shifts during muscle activity and fatigue. *Am J Physiol Regul Integr Comp Physiol* **290,** R766-72.

Kubisch C, Schmidt-Rose T, Fontaine B, Bretag AH & Jentsch TJ (1998). ClC-1 chloride channel mutations in myotonia congenita: variable penetrance of mutations shifting the voltage dependence. *Hum Mol Genet* **7,** 1753–1760.

Kume H, Hall IP, Washabau RJ, Takagi K & Kotlikoff MI (1994). β-Adrenergic agonists regulate KCa channels in airway smooth muscle by cAMP-dependent and -independent mechanisms. *J Clin Invest* **93,** 371–379.

Kurebayashi N & Ogawa Y (2001). Depletion of Ca2+ in the sarcoplasmic reticulum stimulates Ca2+ entry into mouse skeletal muscle fibres. *J Physiol* **533,** 185–199.

Leech C & Stanfield P (1981). Inward rectification in frog skeletal muscle fibres and its dependence on membrane potential and external potassium. *J Physiol* **319,** 295–309.

Lehmann-Horn F, Küther G, Ricker K, Grafe P, Ballanyi K & Rüdel R (1987). Adynamia episodica hereditaria with myotonia: a non-inactivating sodium current and the effect of extracellular pH. *Muscle Nerve* **10,** 363–374.

Lehmann-Horn F, Rüdel R, Dengler R, Lorković H, Haass A & Ricker K (1981). Membrane defects in paramyotonia congenita with and without myotonia in a warm environment. *Muscle Nerve* **4,** 396–406.

Lehmann-Horn F, Rüdel R, Ricker K, Lorković H, Dengler R & Hopf HC (1983). *Two cases of adynamia episodica hereditaria: in vitro investigation of muscle cell membrane and contraction parameters.*

Light PE, Comtois AS & Renaud JM (1994). The effect of glibenclamide on frog skeletal muscle: evidence for K+ATP channel activation during fatigue. *J Physiol* **475,** 495–507.

Lin YF, Jan YN & Jan LY (2000). Regulation of ATP-sensitive potassium channel function by protein kinase A-mediated phosphorylation in transfected HEK293 cells. *EMBO J* **19,** 942–955.

Lindinger MI, Hawke TJ, Vickery L, Bradford L & Lipskie SL (2001). An integrative, in situ approach to examining K^+ flux in resting skeletal muscle. *Can J Physiol Pharmacol* **79,** 996–1006.

Links TP, Zwarts MJ, Wilmink JT, Molenaar WM & Oosterhuis HJGH (1990). Permanent muscle weakness in familial hypokalaemic periodic paralysis: Clinical, radiological and pathological aspects. *Brain* **113,** 1873–1889.

Lipicky RJ, Bryant SH & Salmon JH (1971). Cable parameters, sodium, potassium, chloride, and water content, and potassium efflux in isolated external intercostal muscle of normal volunteers and patients with myotonia congenita. *J Clin Invest* **50,** 2091–2103.

Lipkind GM & Fozzard HA (2008). Voltage-gated Na channel selectivity: the role of the conserved domain III lysine residue. *J Gen Physiol* **131,** 523–529.

Lochner A & Moolman JA (2006). The Many Faces of H89: A Review. *Cardiovasc Drug Rev* **24,** 261–274.

Lopatin AN, Makhina EN & Nichols CG (1994). Potassium channel block by cytoplasmic polyamines as the mechanism of intrinsic rectification. *Nature* **372,** 366–369.

Lossin C & George AL (2008). Myotonia congenita. *Adv Genet* **63,** 25–55.

Lucas B, Ammar T, Khogali S, DeJong D, Barbalinardo M, Nishi C, Hayward LJ & Renaud J-M (2014). Contractile abnormalities of mouse muscles expressing hyperkalemic periodic

paralysis mutant NaV1.4 channels do not correlate with Na+ influx or channel content. *Physiol Genomics* **46,** 385–397.

Lueck JD, Rossi AE, Thornton C a, Campbell KP & Dirksen RT (2010). Sarcolemmal-restricted localization of functional ClC-1 channels in mouse skeletal muscle. *J Gen Physiol* **136,** 597–613.

Lynch GS & Ryall JG (2008). Role of beta-adrenoceptor signaling in skeletal muscle: implications for muscle wasting and disease. *Physiol Rev* **88,** 729–767.

MacIntosh BR, Holash RJ & Renaud J-M (2012). Skeletal muscle fatigue--regulation of excitation-contraction coupling to avoid metabolic catastrophe. *J Cell Sci* **125,** 2105–2114.

Matar W, Lunde JA, Jasmin BJ & Renaud JM (2001). Denervation enhances the physiological effects of the K(ATP) channel during fatigue in EDL and soleus muscle. *Am J Physiol Regul Integr Comp Physiol* **281,** R56–R65.

Matsuda H, Saigusa A & Irisawa H (1987). Ohmic conductance through the inwardly rectifying K channel and blocking by internal Mg2+. *Nature* **325,** 156–159.

Matthews E, Labrum R, Sweeney MG, Sud R, Haworth A, Chinnery PF, Meola G, Schorge S, Kullmann DM, Davis MB & Hanna MG (2009). Voltage sensor charge loss accounts for most cases of hypokalemic periodic paralysis. *Neurology* **72,** 1544–1547.

McKenna MJ, Bangsbo J & Renaud J-M (2008). Muscle K+, Na+, and Cl disturbances and Na+-K+ pump inactivation: implications for fatigue. *J Appl Physiol* **104,** 288–95.

Meyer T, Regenass U, Fabbro D, Alteri E, Rösel J, Müller M, Caravatti G & Matter A (1989). A derivative of staurosporine (CGP 41 251) shows selectivity for protein kinase C inhibition and in vitro anti-proliferative as well as in vivo anti-tumor activity. *Int J Cancer* **43,** 851–856.

Miller TM, Dias da Silva MR, Miller H a, Kwiecinski H, Mendell JR, Tawil R, McManis P, Griggs

RC, Angelini C, Servidei S, Petajan J, Dalakas MC, Ranum LPW, Fu YH & Ptácek LJ (2004). Correlating phenotype and genotype in the periodic paralyses. *Neurology* **63,** 1647–1655.

Milton RL & Behforouz M a (1995). Na channel density in extrajunctional sarcolemma of fast and slow twitch mouse skeletal muscle fibres: functional implications and plasticity after fast motoneuron transplantation on to a slow muscle. *J Muscle Res Cell Motil* **16,** 430–439.

Mohr M, Nordsborg N, Nielsen JJ, Pedersen LD, Fischer C, Krustrup P & Bangsbo J (2004). Potassium kinetics in human muscle interstitium during repeated intense exercise in relation to fatigue. *Pflugers Arch* **448,** 452–456.

Murphy KT, Macdonald WA, McKenna MJ & Clausen T (2006). Ionic mechanisms of excitation-induced regulation of Na+-K+-ATPase mRNA expression in isolated rat EDL muscle. *Am J Physiol Regul Integr Comp Physiol* **290,** R1397-406.

Murray AJ (2008). Pharmacological PKA inhibition: all may not be what it seems. *Sci Signal* **1,** re4.

Nielsen JJ, Kristensen M, Hellsten Y, Bangsbo J & Juel C (2003). Localization and function of ATP-sensitive potassium channels in human skeletal muscle. *Am J Physiol Regul Integr Comp Physiol* **284,** R558-63.

Nielsen JJ, Mohr M, Klarskov C, Kristensen M, Krustrup P, Juel C & Bangsbo J (2004). Effects of high-intensity intermittent training on potassium kinetics and performance in human skeletal muscle. *J Physiol* **554,** 857–870.

Nielsen OB & Clausen T (1997). Regulation of Na(+)-K+ pump activity in contracting rat muscle. *J Physiol* **503 (Pt 3,** 571–581.

Noda M, Suzuki H, Numa S & Stühmer W (1989). A single point mutation confers tetrodotoxin and saxitoxin insensitivity on the sodium channel II. *FEBS Lett* **259,** 213–216.

Noma A (1983). ATP-regulated K+ channels in cardiac muscle. *Nature* **305,** 147–148.

O'Reilly JP, Wang SY & Wang GK (2001). Residue-specific effects on slow inactivation at V787 in D2-S6 of Na(v)1.4 sodium channels. *Biophys J* **81,** 2100–2111.

Ober KP (1992). Thyrotoxic periodic paralysis in the United States. Report of 7 cases and review of the literature. *Medicine (Baltimore)* **71,** 109–120.

Overgaard K, Nielsen OB, Flatman JA & Clausen T (1999). Relations between excitability and contractility in rat soleus muscle: role of the Na+-K+ pump and Na+/K+ gradients. *J Physiol* **518,** 215–225.

de Paoli FV, Broch-Lips M, Pedersen TH & Nielsen OB (2013). Relationship between membrane Cl- conductance and contractile endurance in isolated rat muscles. *J Physiol* **591,** 531–545.

de Paoli FV, Ørtenblad N, Pedersen TH, Jørgensen R & Nielsen OB (2010). Lactate per se improves the excitability of depolarized rat skeletal muscle by reducing the Cl- conductance. *J Physiol* **588,** 4785–4794.

Papponen H, Nissinen M, Kaisto T, Myllylä V V, Myllylä R & Metsikkö K (2008). F413C and A531V but not R894X myotonia congenita mutations cause defective endoplasmic reticulum export of the muscle-specific chloride channel CLC-1. *Muscle Nerve* **371,** 317–325.

Pavlovic D, Fuller W & Shattock MJ (2013*a*). Novel regulation of cardiac Na pump via phospholemman. *J Mol Cell Cardiol* **61,** 83–93.

Pavlovic D, Hall AR, Kennington EJ, Aughton K, Boguslavskyi A, Fuller W, Despa S, Bers DM & Shattock MJ (2013*b*). Nitric oxide regulates cardiac intracellular Na^+ and Ca^{2+} by modulating Na/K ATPase via PKCε and phospholemman-dependent mechanism. *J Mol Cell Cardiol* **61,** 164–171.

Payandeh J, Gamal El-Din TM, Scheuer T, Zheng N & Catterall WA (2012). Crystal structure of

a voltage-gated sodium channel in two potentially inactivated states. *Nature* **486,** 135–139.

Pearson CM (1964). the Periodic Paralyses: Differential Features and Pathological Observations in Permanent Myopathic Weakness. *Brain* **87,** 341–354.

Pedersen TH, Clausen T & Nielsen OB (2003). Loss of force induced by high extracellular [K+] in rat muscle: effect of temperature, lactic acid and beta2-agonist. *J Physiol* **551,** 277–286.

Pedersen TH, Macdonald WA, de Paoli FV, Gurung IS & Nielsen OB (2009*a*). Comparison of regulated passive membrane conductance in action potential-firing fast- and slow-twitch muscle. *J Gen Physiol* **134,** 323–337.

Pedersen TH, de Paoli F & Nielsen OB (2005). Increased excitability of acidified skeletal muscle: role of chloride conductance. *J Gen Physiol* **125,** 237–246.

Pedersen TH, de Paoli FV, de Paoli FV, Flatman J a & Nielsen OB (2009*b*). Regulation of ClC-1 and KATP channels in action potential-firing fast-twitch muscle fibers. *J Gen Physiol* **134,** 309–322.

Pedersen TH, Riisager A, de Paoli FV, Chen T-Y & Nielsen OB (2016). Role of physiological ClC-1 Cl- ion channel regulation for the excitability and function of working skeletal muscle. *J Gen Physiol* **147,** 291–308.

Pierno S, Desaphy J-F, Liantonio A, De Luca A, Zarrilli A, Mastrofrancesco L, Procino G, Valenti G & Conte Camerino D (2007). Disuse of rat muscle in vivo reduces protein kinase C activity controlling the sarcolemma chloride conductance. *J Physiol* **584,** 983–995.

Pirkmajer S & Chibalin A V (2016). Na,K-ATPase regulation in skeletal muscle. *Am J Physiol Endocrinol Metab*ajpendo.00539.2015.

Plaster NM et al. (2001). Mutations in Kir2.1 cause the developmental and episodic electrical phenotypes of Andersen's syndrome. *Cell* **105,** 511–519.

Poskanzer DC & Kerr DN (1961). A third type of periodic paralysis, with normokalemia and favourable response to sodium chloride. *Am J Med* **31,** 328–342.

Propper DJ, Macaulay V, O'byrne KJ, Braybrooke JP, Wilner SM, Ganesan TS, Harris AL & Talbot DC (1998). A phase II study of bryostatin 1 in metastatic malignant melanoma. *Br J CancerPropper, D J, Macaulay, V, O'byrne, K J, Braybrooke, J P, Wilner, S M, Ganesan, T S, ... Talbot, D C (1998) A phase II study bryostatin 1 metastatic Malig melanoma Br J Cancer, 78(10), 1337–1341 Retrieved from http/* **78,** 1337–1341.

Pusch M (2002). Myotonia caused by mutations in the muscle chloride channel gene CLCN1. *Hum Mutat* **19,** 423–434.

Pusch M, Noda M, Stuhmer W, Numa S & Conti F (1991). Single point mutations of the sodium channel drastically reduce the pore permeability without preventing its gating. *Eur Biophys J* **20,** 127–133.

Pusch M, Steinmeyer K, Koch MC & Jentsch TJ (1995). Mutations in dominant human myotonia congenita drastically alter the voltage dependence of the CIC-1 chloride channel. *Neuron* **15,** 1455–1463.

Puwanant A & Ruff RL (2010). INa and IKir are reduced in Type 1 hypokalemic and thyrotoxic periodic paralysis. *Muscle Nerve* **42,** 315–327.

Radzyukevich TL, Moseley AE, Shelly DA, Redden GA, Behbehani MM, Lingrel JB, Paul RJ & Heiny JA (2004). The Na(+)-K(+)-ATPase alpha2-subunit isoform modulates contractility in the perinatal mouse diaphragm. *Am J Physiol Cell Physiol* **287,** C1300–C1310.

Radzyukevich TL, Neumann JC, Rindler TN, Oshiro N, Goldhamer DJ, Lingrel JB & Heiny J a (2013). Tissue-specific role of the Na,K-ATPase α2 isozyme in skeletal muscle. *J Biol Chem* **288,** 1226–1237.

Reiken S, Lacampagne A, Zhou H, Kherani A, Lehnart SE, Ward C, Huang F, Gaburjakova M, Gaburjakova J, Rosemblit N, Warren MS, He K-L, Yi G-H, Wang J, Burkhoff D, Vassort G & Marks AR (2003). PKA phosphorylation activates the calcium release channel (ryanodine receptor) in skeletal muscle: defective regulation in heart failure. *J Cell Biol* **160,** 919–928.

Renaud JM & Light P (1992). Effects of K+ on the twitch and tetanic contraction in the sartorius muscle of the frog, Rana pipiens. Implication for fatigue in vivo. *Can J Physiol Pharmacol* **70,** 1236–1246.

Ricker K, Camacho LM, Grafe P, Lehmann-Horn F & Rüdel R (1989). Adynamia episodica hereditaria: what causes the weakness? *Muscle Nerve* **12,** 883–891.

Roberts R & Barchi R (1987). The voltage-sensitive sodium channel from rabbit skeletal muscle. Chemical characterization of subunits. *J Biol Chem* **262,** 2298–2303.

Rojas C V, Neely A, Velasco-Loyden G, Palma V & Kukuljan M (1999). Hyperkalemic periodic paralysis M1592V mutation modifies activation in human skeletal muscle Na+ channel. *Am J Physiol* **276,** C259–C266.

Rojas C V, Wang JZ, Schwartz LS, Hoffman EP, Powell BR & Brown RH (1991). A Met-to-Val mutation in the skeletal muscle Na+ channel alpha-subunit in hyperkalaemic periodic paralysis. *Nature* **354,** 387–389.

Rosenbohm A, Rüdel R & Fahlke C (1999). Regulation of the human skeletal muscle chloride channel hClC-1 by protein kinase C. *J Physiol* **514,** 677–685.

Rüdel R & Ricker K (1985). The primary periodic paralyses. *Trends Neurosci* **8,** 467–470.

Rudolf R, Magalhães PJ & Pozzan T (2006). Direct in vivo monitoring of sarcoplasmic reticulum Ca2+ and cytosolic cAMP dynamics in mouse skeletal muscle. *J Cell Biol* **173,** 187–193.

Rudy B (1978). Slow inactivation of the sodium conductance in squid giant axons. Pronase

resistance. *J Physiol* **283,** 1–21.

Ruff RL (1999). Insulin acts in hypokalemic periodic paralysis by reducing inward rectifier K+ current. *Neurology* **53,** 1556–1563.

Ruff RL, Simoncini L & Stühmer W (1988). Slow sodium channel inactivation in mammalian muscle: a possible role in regulating excitability. *Muscle Nerve* **11,** 502–510.

Ryan DP, da Silva MRD, Soong TW, Fontaine B, Donaldson MR, Kung AWC, Jongjaroenprasert W, Liang MC, Khoo DHC, Cheah JS, Ho SC, Bernstein HS, Maciel RMB, Brown RH & Ptácek LJ (2010). Mutations in potassium channel Kir2.6 cause susceptibility to thyrotoxic hypokalemic periodic paralysis. *Cell* **140,** 88–98.

Sacconi S, Simkin D, Arrighi N, Chapon F, Larroque MM, Vicart S, Sternberg D, Fontaine B, Barhanin J, Desnuelle C & Bendahhou S (2009). Mechanisms underlying Andersen's syndrome pathology in skeletal muscle are revealed in human myotubes. *Am J Physiol Cell Physiol* **297,** C876-85.

Sandiford SDE, Green HJ & Ouyang J (2005). Mechanisms underlying increases in rat soleus Na+-K+-ATPase activity by induced contractions. *J Appl Physiol* **99,** 2222–2232.

Sansone V, Griggs RC, Meola G, Ptácek LJ, Barohn R, Iannaccone S, Bryan W, Baker N, Janas SJ, Scott W, Ririe D & Tawil R (1997). Andersen's syndrome: a distinct periodic paralysis. *Ann Neurol* **42,** 305–312.

Sears MR (2002). Adverse effects of β-agonists. *J Allergy Clin Immunol* **110,** S322–S328.

Shattock MJ (2009). Phospholemman: its role in normal cardiac physiology and potential as a druggable target in disease. *Curr Opin Pharmacol* **9,** 160–166.

Sheets MF & Hanck D a (1999). Gating of skeletal and cardiac muscle sodium channels in mammalian cells. *J Physiol* **514,** 425–436.

Silverman B d Z, Fuller W, Eaton P, Deng J, Moorman JR, Cheung JY, James AF & Shattock MJ (2005). Serine 68 phosphorylation of phospholemman: acute isoform-specific activation of cardiac Na/K ATPase. *Cardiovasc Res* **65,** 93–103.

Simoncini L & Stühmer W (1987). Slow sodium channel inactivation in rat fast-twitch muscle. *J Physiol* **383,** 327–337.

Sjøgaard G, Adams RP & Saltin B (1985). Water and ion shifts in skeletal muscle of humans with intense dynamic knee extension. *Am J Physiol* **248,** R190–R196.

Standen NB, Pettit AI, Davies NW & Stanfield PR (1992). Activation of ATP-dependent K+ currents in intact skeletal muscle fibres by reduced intracellular pH. *Proc R Soc B Biol Sci* **247,** 195–198.

Steel RG & Torrie JH (1980). Principles and procedures of statistics: a biometrical approach. *Newyork McGraw-Hill Book, 1980*.

Steinmeyer K, Ortland C & Jentsch TJ (1991). Primary structure and functional expression of a developmentally regulated skeletal muscle chloride channel. *Nature* **354,** 301–304.

Sternberg D, Maisonobe T, Jurkat-Rott K, Nicole S, Launay E, Chauveau D, Tabti N, Lehmann-Horn F, Hainque B & Fontaine B (2001). Hypokalaemic periodic paralysis type 2 caused by mutations at codon 672 in the muscle sodium channel gene SCN4A. *Brain* **124,** 1091–1099.

Street D, Nielsen J-J, Bangsbo J & Juel C (2005). Metabolic alkalosis reduces exercise-induced acidosis and potassium accumulation in human skeletal muscle interstitium. *J Physiol* **566,** 481–489.

Streeten DH, Dalakos TG & Fellerman H (1971). Studies on hyperkalemic periodic paralysis. Evidence of changes in plasma Na and Cl and induction of paralysis by adrenal glucocorticoids. *J Clin Invest* **50,** 142–155.

Struyk AF & Cannon SC (2008). Paradoxical depolarization of BA2+- treated muscle exposed to low extracellular K+: insights into resting potential abnormalities in hypokalemic paralysis. *Muscle Nerve* **37,** 326–337.

Stühmer W, Conti F, Suzuki H, Wang XD, Noda M, Yahagi N, Kubo H & Numa S (1989). Structural parts involved in activation and inactivation of the sodium channel. *Nature* **339,** 597–603.

Tawil R, Ptacek LJ, Pavlakis SG, DeVivo DC, Penn AS, Ozdemir C & Griggs RC (1994). Andersen's syndrome: potassium-sensitive periodic paralysis, ventricular ectopy, and dysmorphic features. *Ann Neurol* **35,** 326–330.

Terlau H, Heinemann SH, Stühmer W, Pusch M, Conti F, Imoto K & Numa S (1991). Mapping the site of block by tetrodotoxin and saxitoxin of sodium channel II. *FEBS Lett* **293,** 93–96.

Thabet M, Miki T, Seino S & Renaud J-M (2005). Treadmill running causes significant fiber damage in skeletal muscle of KATP channel-deficient mice. *Physiol Genomics* **22,** 204–212.

Thomassen M, Christensen PM, Gunnarsson TP, Nybo L & Bangsbo J (2010). Effect of 2-wk intensified training and inactivity on muscle Na+-K+ pump expression, phospholemman (FXYD1) phosphorylation, and performance in soccer players. *J Appl Physiol* **108,** 898–905.

Thomassen M, Rose AJ, Jensen TE, Maarbjerg SJ, Bune L, Leitges M, Richter EA, Bangsbo J & Nordsborg NB (2011). Protein kinase Cα activity is important for contraction-induced FXYD1 phosphorylation in skeletal muscle. *Am J Physiol Regul Integr Comp Physiol* **301,** R1808-14.

Thornton AM, Zhao X, Weisleder N, Brotto LS, Bougoin S, Nosek TM, Reid M, Hardin B, Pan Z, Ma J, Parness J & Brotto M (2011). Store-operated Ca(2+) entry (SOCE) contributes to normal skeletal muscle contractility in young but not in aged skeletal muscle. *Aging (Albany*

NY) **3,** 621–634.

Todt H, Dudley SC, Kyle JW, French RJ & Fozzard HA (1999). Ultra-slow inactivation in mu1 Na+ channels is produced by a structural rearrangement of the outer vestibule. *Biophys J* **76,** 1335–1345.

Toullec D, Pianetti P, Coste H, Bellevergue P, Grand-Perret T, Ajakane M, Baudet V, Boissin P, Boursier E & Loriolle F (1991). The bisindolylmaleimide GF 109203X is a potent and selective inhibitor of protein kinase C. *J Biol Chem* **266,** 15771–15781.

Tricarico D, Conte Camerino D, Govoni S & Bryant SH (1991). Modulation of rat skeletal muscle chloride channels by activators and inhibitors of protein kinase C. *Pflugers Arch Eur J Physiol* **418,** 500–503.

Tricarico D, Servidei S, Tonali P, Jurkat-Rott K & Conte Camerino D (1999). Impairment of skeletal muscle adenosine triphosphate-sensitive K+ channels in patients with hypokalemic periodic paralysis. *J Clin Invest* **103,** 675–682.

Tristani-Firouzi M, Jensen JL, Donaldson MR, Sansone V, Meola G, Hahn A, Bendahhou S, Kwiecinski H, Fidzianska A, Plaster N, Fu Y-H, Ptacek LJ & Tawil R (2002). Functional and clinical characterization of KCNJ2 mutations associated with LQT7 (Andersen syndrome). *J Clin Invest* **110,** 381–388.

Trivedi JR, Bundy B, Statland J, Salajegheh M, Rayan DR, Venance SL, Wang Y, Fialho D, Matthews E, Cleland J, Gorham N, Herbelin L, Cannon S, Amato A, Griggs RC, Hanna MG & Barohn RJ (2013). Non-dystrophic myotonia: prospective study of objective and patient reported outcomes. *Brain* **136,** 2189–2200.

Tsakiridis T, Wong PP, Liu Z, Rodgers CD, Vranic M & Klip A (1996). Exercise increases the plasma membrane content of the Na+ -K+ pump and its mRNA in rat skeletal muscles. *J Appl*

Physiol **80,** 699–705.

Varterasian ML, Pemberton PA, Hulburd K, Rodriguez DH, Murgo A & Al-Katib AM (2001). Phase II study of bryostatin 1 in patients with relapsed multiple myeloma. *Invest New Drugs* **19,** 245–247.

Vassilev PM, Scheuer T & Catterall WA (1988). Identification of an intracellular peptide segment involved in sodium channel inactivation. *Science* **241,** 1658–1661.

Viirès N, Murciano D, Seta JP, Dureuil B, Pariente R & Aubier M (1988). Effects of Ca2+ withdrawal on diaphragmatic fiber tension generation. *J Appl Physiol* **64,** 26–30.

Vilin YY, Fujimoto E & Ruben PC (2001). A single residue differentiates between human cardiac and skeletal muscle Na+ channel slow inactivation. *Biophys J* **80,** 2221–2230.

Vivaudou MB, Arnoult C & Villaz M (1991). Skeletal muscle ATP-sensitive K+ channels recorded from sarcolemmal blebs of split fibers: ATP inhibition is reduced by magnesium and ADP. *J Membr Biol* **122,** 165–175.

Wallinga W, Meijer SL, Alberink MJ, Vliek M, Wienk ED & Ypey DL (1999). Modelling action potentials and membrane currents of mammalian skeletal muscle fibres in coherence with potassium concentration changes in the T-tubular system. *Eur Biophys J* **28,** 317–329.

Wang P & Clausen T (1976). Treatment of attacks in hyperkalaemic familial periodic paralysis by inhalation of salbutamol. *Lancet* **1,** 221–223.

West JW, Patton DE, Scheuer T, Wang Y, Goldin AL & Catterall WA (1992). A cluster of hydrophobic amino acid residues required for fast Na(+)-channel inactivation. *Proc Natl Acad Sci U S A* **89,** 10910–10914.

Williams MW, Resneck WG, Kaysser T, Ursitti JA, Birkenmeier CS, Barker JE & Bloch RJ (2001). Na,K-ATPase in skeletal muscle: two populations of beta-spectrin control

localization in the sarcolemma but not partitioning between the sarcolemma and the transverse tubules. *J Cell Sci* **114,** 751–762.

Wu F, Mi W, Burns DK, Fu Y, Gray HF, Struyk AF & Cannon SC (2011). A sodium channel knockin mutant (NaV1.4-R669H) mouse model of hypokalemic periodic paralysis. *J Clin Invest* **121,** 4082–4094.

Wu F, Mi W, Hernández-Ochoa EO, Burns DK, Fu Y, Gray HF, Struyk AF, Schneider MF & Cannon SC (2012). A calcium channel mutant mouse model of hypokalemic periodic paralysis. *J Clin Invest* **122,** 4580–4591.

Wulff H, Castle NA & Pardo LA (2009). Voltage-gated potassium channels as therapeutic targets. *Nat Rev Drug Discov* **8,** 982–1001.

Yang N, Ji S, Zhou M, Ptácek LJ, Barchi RL, Horn R & George AL (1994). Sodium channel mutations in paramyotonia congenita exhibit similar biophysical phenotypes in vitro. *Proc Natl Acad Sci U S A* **91,** 12785–12789.

Yatani A, Codina J, Reeves JP & Brown AM (1987). G Protein Directly Regulates Mammalian Cardiac. *Science (80-)* **238,** 1288–1292.

Yatani A, Imoto Y, Codina J, Hamilton SL, Brown AM & Birnbaumer L (1988). The stimulatory G protein of adenylyl cyclase, G(s), also stimulates dihydropyridine-sensitive Ca2+ channels. Evidence for direct regulation independent of phosphorylation by cAMP-dependent protein kinase or stimulation by a dihydropyridine agonist. *J Biol Chem* **263,** 9887–9895.

Yensen C, Matar W & Renaud J-M (2002). K+-induced twitch potentiation is not due to longer action potential. *Am J Physiol Cell Physiol* **283,** C169-77.

Zavecz JH & Anderson WM (1992). Role of extracellular Ca2+ in diaphragmatic contraction: effects of ouabain, monensin, and ryanodine. *J Appl Physiol* **73,** 30–35.

Zavecz JH, Anderson WM & Adams B (1991). Effect of amiloride on diaphragmatic contractility: evidence of a role for Na(+)-Ca2+ exchange. *J Appl Physiol* **70,** 1309–1314.

Zhao Y, Yarov-Yarovoy V, Scheuer T & Catterall WA (2004). A Gating Hinge in Na+ Channels. *Neuron* **41,** 859–865.

Zhou J & Hoffman E (1994). Pathophysiology of sodium channelopathies. Studies of sodium channel expression by quantitative multiplex fluorescence polymerase chain reaction. *J Biol Chem* **269,** 18563–71.

Zhu Z, Sierra A, Burnett CM-L, Chen B, Subbotina E, Koganti SRK, Gao Z, Wu Y, Anderson ME, Song L-S, Goldhamer DJ, Coetzee WA, Hodgson-Zingman DM & Zingman L V (2014). Sarcolemmal ATP-sensitive potassium channels modulate skeletal muscle function under low-intensity workloads. *J Gen Physiol* **143,** 119–134.

Zhu Z, Sierra A, Burnett CM-L, Chen B, Subbotina E, Koganti SRK, Gao Z, Wu Y, Anderson ME, Song L-S, Goldhamer DJ, Coetzee WA, Hodgson-Zingman DM & Zingman L V. (2013). Sarcolemmal ATP-sensitive potassium channels modulate skeletal muscle function under low-intensity workloads. *J Gen Physiol* **143,** 119–134.

APPENDIX

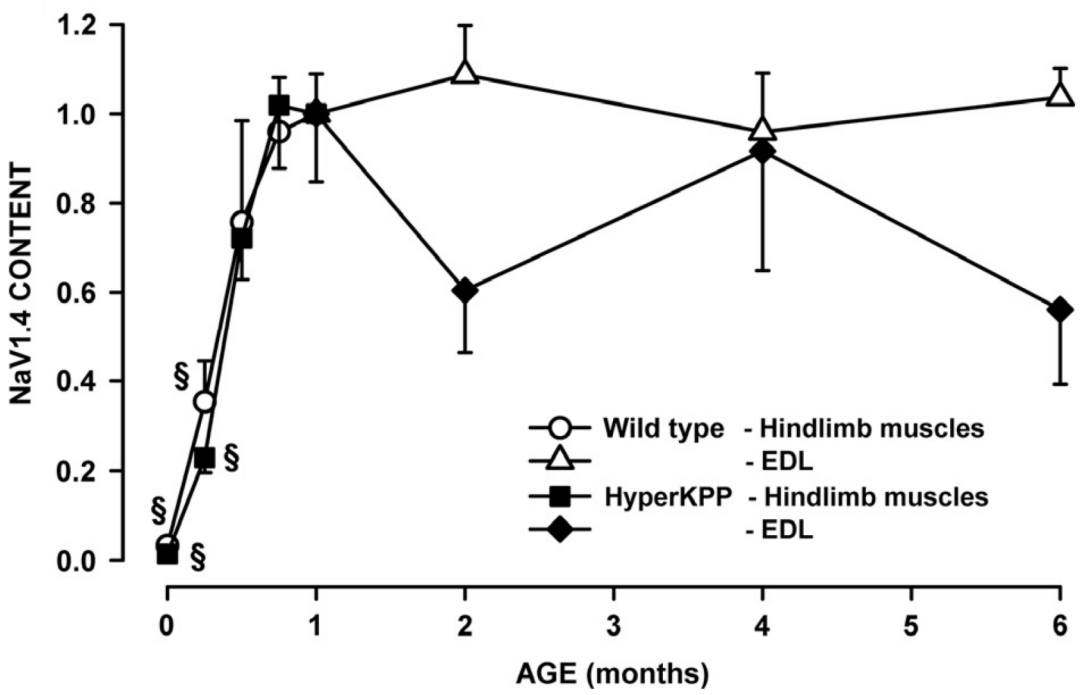

Appendix 1. The total Nav1.4 protein content reached adult level by 3 weeks of age in both wild type and HyperKPP muscles. For the ages of 0–4 weeks, Nav1.4 protein content was determined using all hindlimb muscles to have sufficient proteins for Western Blot. For the ages from 1- to 6-month old, Nav1.4 channel content was determined only in the symptomatic EDL. Nav1.4 content was first expressed as a ratio of β-actin content before being converted as a ratio of the data at 1 month. Vertical bars represent the SE of five muscles (age 0–4 weeks), five wild type, and 8–9 HyperKPP EDL (age 1–6 months). There was no significant difference between wild type and HyperKPP (ANOVA, $P > 0.05$). §Mean Nav1.4 content was significantly different from the mean content at 1 month, ANOVA, and LSD $P < 0.05$. LSD (data generated by T Ammar, published in Khogali et al., 2015).